

**Some Properties of the Silent Pool
of Synaptic Vesicles and Further
Characterisation of the Mode of
Vesicular Exocytosis**

By

Tae Guen Kuan (B.Sc.)

A thesis submitted in partial fulfilment for the requirements for the
degree of Doctor of Philosophy at the University of Central
Lancashire

July, 2020

STUDENT DECLARATION FORM

Concurrent registration for two or more academic awards

I declare that while registered as a candidate for the research degree, I have not been a registered candidate or enrolled student for another award of the University or other academic or professional institution

Material submitted for another award

I declare that no material contained in the thesis has been used in any other submission for an academic award and is solely my own work

Signature of Candidate



Tae Guen Kuan

Type of Award

Doctorate of Philosophy, PhD

School

School of Pharmacy and Biomedical Sciences,
University of Central Lancashire

Abstract

Synaptic communication involves action potentials (AP) being generated and travelling along the axon such that they depolarise the presynaptic nerve terminal to induce synaptic vesicles (SVs) to exocytose and release their neurotransmitter. Changes in the properties of the synapse is the basis of synaptic plasticity and memory and defects in this process can lead to neuronal dysfunction. However, a full molecular description of synaptic transmission is lacking and this means that our understanding of many neuronal diseases is incomplete.

The research reported in this thesis concerns the properties of three distinct pools of SVs that are present within nerve terminals. Normally, both the readily releasable pool (RRP) and the reserve pool (RP) can contribute to release during strong stimulation. However, the third pool, silent pool (SP), of vesicles does not normally get released and so this has not been very well characterised. Herein, we have successfully managed to evoke the release of the SP of glutamate (GLU) containing SVs. This was achieved using Roscovitine, a Cdk5 inhibitor. We have established that this drug truly can allow the evoked release of the SP as such release is not due to the RRP and RP recycling and re-releasing. Some properties of the SP were: (i) it has very specific Ca^{2+} requirements and it is inhibited if one reduces Ca^{2+} entry through any of three VDCCs: P/Q, N or L type; (ii) it is perturbed by activation of PKCs or inhibition of protein phosphatase 2; (iii) it can still be released if the actin cytoskeleton is stabilised by treating nerve terminals with Jasplakinolide (JASP) or non-muscle myosin 2 (NM-II) activity is blocked by Blebbistatin. Synapsin 1 (Syn 1) is a phospho-protein which has been suggested to regulate the SP. Using western blotting of synaptosomes that had been stimulated under various conditions, preliminary experiments were performed to ascertain whether changes in specific phosphorylation sites on Syn 1 correlated with SP release: the Cdk5 phosphorylated site at Ser-553 seemed to have reduced phosphorylation whilst the CaMKII phosphorylated site Ser-603 seemed to have an increase in phosphorylation.

Very intriguingly, an antidepressant drug, Fluoxetine, can also allow the evoked release of the SP of GLU containing SVs and this drug works on the same pool as Roscovitine and there is no additivity in SP release if both drugs are employed.

Previously, it was found that using High Potassium (HK5C) or Ionomycin (ION5C) the RRP is released by a Kiss-and-Run exocytotic mechanism (KR) whilst the RP is released by a full fusion (FF) mechanism. Furthermore, it was discovered that ION5C acts on a dynamin (Dyn) dependent KR pathway whilst HK5C works through a NM-II dependent KR pathway. Herein, some further properties of these 2 distinct pathways have been deduced. Some properties of the Dyn dependent KR pathway dissected, herein, were: (i) utilises Dyn already located on a membrane compartment for the closure of the fusion pore. This was ascertained by the fact that MITMAB – a drug that prevents Dyn binding to membranes – failed to perturb this KR process whereas this is switched to FF by the drug Dynasore that inhibits the GTPase activity of Dyn; (ii) requires the activity of endogenous PKA because this mode is switched to FF when PKAs are blocked by the drug KT 5720; (iii) regulated specifically by P/Q VDCCs because blockade of these channels, but not others, switched this KR mode to FF; (iv) requires intact actin microfilaments for the closure of the fusion pore because disassembly of these cytoskeletal components by Latrunculin (LAT) switches this mode to FF and this drug action is not perturbed by blockade of PKCs with Go 6983; (v) stabilisation of actin microfilaments with JASP does not perturb this KR. Additionally, the NM-II dependent KR shows some distinct properties from the Dyn dependent KR: (i) it is not switched to FF following inhibition of PKAs; (ii) L-type VDCCs blockers switched this mode to FF but blockers of other VDCCs did not; (iii) LAT treatment seems to switch this KR mode but further investigation suggests that this treatment may perturb the action of the stimulus itself (HK5C) rather than the mode and it would appear that LAT may activate PKCs that induce the apparent effect since this is blocked by Go 6983.

The RP of GLU containing SVs evoked by both ION5C or HK5C is also dependent on the actin microfilaments because LAT induced disassembly blocks its release although JASP does not. As the RP is blocked by LAT, the effect of actin microfilament disassembly on the release of the SP could not be studied.

In conclusion, some properties of the SP of GLU containing SVs have been characterized whilst there were further differences determined between the Dyn dependent and the NM-II dependent KR modes. These latter findings suggest that rather than one common KR mechanism that can be regulated by either Dyn or NM-II, there is probably two distinct KR mechanisms that get activated by different stimulation conditions.

Contents

Declaration.....	I
Abstract.....	II
Contents.....	IV
List of Figures.....	X
List of Abbreviations and Acronyms.....	XVII
Acknowledgements.....	XX
<u>Chapter 1: Introduction.....</u>	1
1.1 Synaptic Transmission.....	2
1.2 SV pools.....	2
1.3 The Silent Pool (SP).....	6
1.4 Roscovitine.....	8
1.5 Cdk 5 Phosphorylation targets.....	9
1.5.1 Dynamin 1.....	9
1.5.2 Myosin 2.....	10
1.5.3 Synapsin I.....	10
1.5.4 α-Synuclein.....	15
1.6 Fluoxetine.....	16
1.7 SV cycling.....	17
1.8 Kiss-and-Run.....	20
1.9 Aims.....	25
<u>Chapter 2: Materials and Methods.....</u>	27
2.1 Materials.....	28
2.1.1 Buffering reagents.....	28
2.1.2 Stimulation solutions.....	28
2.1.3 Drug employed and their final concentrations.....	29
2.1.4 Other drugs employed.....	30
2.1.5 Measuring Instruments.....	30
2.1.6 Antibodies used for western blotting.....	31
2.2 Preparation of Synaptosomes.....	31
2.3 Glutamate release assay.....	32
2.4 FM 2-10 Styryl Dye release assay.....	34
2.5 Fura-2 assay.....	35
2.5.1 Background.....	35
2.5.2 Procedure.....	36
2.6 Data analysis.....	38
2.7 Western blotting.....	39
2.7.1 Sample Preparation.....	39

2.7.2	Bradford assay.....	39
2.7.3	Electrophoresis and Transfer.....	39
2.7.4	Probing and Chemiluminescence.....	40
2.7.5	Quantification of bands.....	40
2.8	Bioenergetic measurement with Seahorse XFp machine.....	41
2.8.1	Background.....	41
2.8.2	Method.....	43
Chapter 3: Roscovitine and the Silent Pool.....		45
3.1	SP SVs release by HK5C or ION5C following Roscovitine treatment.....	46
3.1.1	100 μ M Roscovitine induced maximum HK5C evoked GLU release.....	46
3.1.2	ION5C also releases the SP following 100 μ M Roscovitine treatment.....	48
3.1.3	The effect of Roscovitine on HK5C and ION5C induced changes in $[Ca^{2+}]_i$ in synaptosomes.....	49
3.2	Roscovitine did not induce recycling and re-release of the RRP and the RP.....	50
3.3	Roscovitine induces the HK5C evoked release of the SP of SVs independently of NM-II activity.....	53
3.4	Calcium dependency of Roscovitine induced SP release.....	54
3.4.1	Higher $[Ca^{2+}]_e$ did not support the SP release.....	55
3.4.2	Regulation of PKC activity can inhibit the SP release evoked in Roscovitine treated synaptosomes.....	60
3.4.3	Inhibition of Ca^{2+} entry through N-, P/Q-, and L-type Ca^{2+} channels inhibit the release of the SP.....	66
3.5	The role of actin microfilament in the SP exocytosis.....	75
3.5.1	The SP cannot studied following disassembly of actin microfilaments as the RP is perturbed.....	76
3.5.2	RRP, RP, and SP SVs release normally when actin microfilament is stabilised.....	77
3.6	Antagonism between Cdk5 and PP2B.....	79
3.6.1	Inhibition of PP2B and Cdk5 with Cys A and Roscovitine inhibited the SP exocytosis.....	79
3.6.2	The SP exocytosis in disturbed following Cys A plus Roscovitine treatment because of reduction in the HK5C evoked $\Delta [Ca^{2+}]_i$	81
3.7	Measurement of the bioenergetics of synaptosomes following various drug treatments.....	83
3.7.1	100 μ M Roscovitine.....	85
3.7.2	Dynasore.....	87

3.7.3	Blebbistatin.....	90
3.7.4	PMA.....	92
3.7.5	PMA with Roscovitine.....	94
3.7.6	Go6983.....	96
3.7.7	Go6983 with Roscovitine.....	98
3.7.8	JASP plus Roscovitine.....	100
3.7.9	Cys A plus Roscovitine.....	102
3.8	Phosphorylation of Syn I following Roscovitine treatment.....	104
3.8.1	Results.....	104
3.8.2	Phosphorylation of Syn I Ser-553 <i>in vivo</i>	105
3.8.3	Phosphorylation of Syn I Ser-9 in synaptosomes.....	109
3.8.4	Phosphorylation of Syn I Ser-603 in nerve terminals.....	113
3.9	Discussion.....	118
3.9.1	Roscovitine effect on the SP release.....	118
3.9.2	Phosphorylation of Syn I following Roscovitine treatment.....	121
3.10	Future research.....	124
3.10.1	Reversibility of Roscovitine.....	125
3.10.2	PKA dependency of SP release.....	125
3.10.3	Repeat for western blot experiment.....	126
3.11	Conclusion.....	126
<u>Chapter 4: Fluoxetine and the Silent Pool</u>		128
4.1	Introduction.....	129
4.2	Establish optimum condition for Fluoxetine to allow HK5C evoked SP release.....	130
4.2.1	5 min incubation with various doses of Fluoxetine.....	130
4.2.2	20 min incubation with various doses of Fluoxetine.....	134
4.2.3	Dual treatment of Fluoxetine with Roscovitine.....	141
4.3	The effect of Fluoxetine on HK5C evoked $\Delta [Ca^{2+}]_i$	143
4.4	Fluoxetine did not induce recycling and re-release of the RRP and RP.....	144
4.5	ION5C evoked SP release.....	146
4.5.1	40 nM supports ION5C evoked SP release.....	146
4.5.2	Fluoxetine did not induce recycling and re-release of the RRP and RP under ION5C stimulation.....	147
4.6	Bioenergetics results.....	150
4.6.1	5 min incubation with 1 μ M Fluoxetine.....	150
4.6.2	20 min incubation with 1 μ M Fluoxetine.....	153
4.7	Discussion.....	156
4.7.1	Glutamate assay.....	156
4.7.2	Fura-2 assay.....	157
4.7.3	Bioenergetics.....	158

4.8 Future studies.....	159
4.8.1 Mechanism of Fluoxetine induced SP release.....	159
4.8.2 Ca ²⁺ dependency of Fluoxetine induce SP release.....	160
4.8.3 Reversibility of Fluoxetine.....	161
4.8.4 Phosphorylation.....	162
4.9 Conclusion.....	162
<u>Chapter 5: Mode of Release: Role of Dynamin, PKA, and Calcium Channels.....</u>	163
5.1 Introduction.....	164
5.2 The effect of the Dyn inhibitor MITMAB on the mode of release.....	166
5.2.1 MITMAB does not change the HK5C, ION5C, 4AP5C evoked GLU release.....	167
5.2.2 MITMAB does not interfere with Dyn dependent KR pathway.....	169
5.2.3 MITMAB does not perturb calcium entry evoked by HK5C or ION5C.....	170
5.3 Inhibition of endogenous PKA perturbs the Dyn dependent KR mechanism for the RRP SVs but not the NM-II dependent KR pathway.....	172
5.3.1 PKA inhibition with KT5720 does not affect GLU release evoked by either stimuli.....	173
5.3.2 KT5720 treatment switches 4AP5C and ION5C induced release to FF but HK5C induced mode of the release remains unchanged	175
5.4 Conditions under which HK5C evokes Dyn dependent KR of the RRP depends upon active endogenous PKA.....	179
5.4.1 KT5720 has no effect on HK5C evoked GLU release in Go6983 treated synaptosomes.....	179
5.4.2 HK5C evoked FM dye release switch to FF in terminals co- treated with Go6983 and KT5720.....	180
5.5 The effect of calcium channel blockers on NM-II and Dyn dependent regulation of RRP SV mode.....	181
5.5.1 HK5C evoked $\Delta[Ca^{2+}]_i$ is reduced by specific calcium channel blockers in Go6983 treated terminals.....	184
5.5.2 Calcium channel inhibition did not affect the HK5C evoked GLU release in Go6983 treated terminals.....	186
5.5.3 P/Q type calcium channel inhibition changed Dyn dependent HK5C evoked from KR mode to FF.....	188
5.5.4 Go6983 treatment does not interfere with switching of the RRP mode.....	190
5.6 Bioenergetics.....	193
5.6.1 MTMAB.....	194

5.6.2	KT5720.....	196
5.6.3	Go6983 plus KT5720.....	198
5.6.4	Go6983 plus AGA.....	200
5.6.5	Go6983 plus NIF.....	202
5.6.6	OA.....	204
5.6.7	Go6983 plus OA.....	206
5.7	Discussion.....	209
5.7.1	MITMAB.....	209
5.7.2	PKA.....	210
5.7.3	Calcium channel dependency of KR.....	211
5.7.4	Bioenergetics.....	212
5.8	Conclusion.....	212
<u>Chapter 6: The effect of actin cytoskeleton disassembly and stabilisation on the mode of SV release.....</u>		
6.1	Introduction.....	215
6.2	The effect of disassembly of actin cytoskeleton on the evoked release and mode of exocytosis.....	217
6.2.1	LAT inhibits the release of the RP but not the RRP.....	217
6.2.2	LAT does not inhibit the FM dye release relative to control.....	219
6.2.3	The action of LAT on evoked $\Delta[Ca^{2+}]_i$	221
6.2.4	Higher $[Ca^{2+}]_e$ did not rescue the Lat induced inhibition of evoked RP exocytosis.....	223
6.2.5	PKC inhibition reversed LAT effect on HK5C evoked release.....	224
6.3	Stabilisation of Actin.....	227
6.3.1	Actin stabilisation does not affect evoked GLU and FM dye release, nor evoked $\Delta[Ca^{2+}]_i$	228
6.3.2	JASP treatment reverse Lat's action.....	232
6.3.3	LAT does not perturb the HK5C evoked calcium entry in the presence of JASP.....	233
6.3.4	JASP treatment prevents LAT action on evoked FM dye release.....	235
6.4	Bioenergetics.....	240
6.4.1	LAT.....	240
6.4.2	Go6983 with LAT.....	242
6.4.3	JASP.....	244
6.4.4	JASP with LAT.....	246
6.4.5	LAT with JASP with OA.....	248
6.5	Discussion.....	251
6.5.1	Effect of actin disassembly.....	251

6.5.2	Effect of actin stabilisation.....	253
6.5.3	Bioenergetics.....	254
6.6	Conclusion.....	254
Chapter 7:	Discussion.....	256
7.1	Results.....	257
7.1.1	Roscovitine.....	257
7.1.2	Fluoxetine.....	261
7.1.3	Effect of PKA and calcium channel on regulation of SV releasing modes.....	262
7.1.4	Effect of actin cytoskeleton on the releasing mode.....	264
7.2	Future studies.....	267
Chapter 8:	References and Appendix.....	272
8.1	References.....	273
8.2	Appendix 1.....	291
8.3	Appendix 2.....	313
8.4	Appendix 3.....	315

List of Figures

Figure 1.1: Vesicle pools and size.....	4
Figure 1.2: Three-pool model of SV pools.....	5
Figure 1.3: Phosphorylation sites in Syn I.....	12
Figure 1.4: Overview of KR, CME, UE, ADBE.....	18
Figure 2.1: Antibodies employed for western blotting.....	31
Figure 2.2: Key parameters of mitochondrial respiration measured by the machine..	42
Figure 2.3: Complexes in electron transport chain that each modulators targets.....	42
Figure 3.1: Increasing Roscovitine concentration induced greater HK5C evoked GLU release relative to non-drug treated control.....	47
Figure 3.2: HK5C evoked GLU release following treatment with 100 μ M and 200 μ M Roscovitine.....	47
Figure 3.3: ION5C evoked GLU release following 100 μ M Roscovitine pre- treatment.....	48
Figure 3.4: $\Delta[\text{Ca}^{2+}]_i$ induced by HK5C in control and 100 μ M Roscovitine treated terminals.....	49
Figure 3.5: $\Delta[\text{Ca}^{2+}]_i$ induced by ION5C in control and 100 μ M Roscovitine treated terminals.....	50
Figure 3.6: HK5C evoked release in control and in terminals treated with 100 μ M Roscovitine plus Dynasore or Pitstop2 TM	52
Figure 3.7: HK5C evoked GLU release with 50 μ M Blebbistatin with 100 μ M Roscovitine.....	53
Figure 3.8: GLU release evoked by HK5C and HK10C or HK20C.....	57
Figure 3.9: GLU release evoked by HK5C and HK10C or HK20C with 100 μ M Roscovitine.....	58
Figure 3.10: Change in $\Delta [\text{Ca}^{2+}]_i$ induce by HK10C in control and 100 μ M Roscovitine treated synaptosomes.....	59
Figure 3.11: Change in $\Delta [\text{Ca}^{2+}]_i$ induced by HK20C in control and 100 μ M Roscovitine treated terminals.....	59
Figure 3.12: HK5C evoked GLU release in non-drug treated control and 1 μ M PMA plus 100 μ M Roscovitine.....	61
Figure 3.13: ION5C evoked GLU release in control and 1 μ M PMA treated terminal and 1 μ M PMA plus 100 μ M Roscovitine.....	62
Figure 3.14: HK5C evoked $\Delta [\text{Ca}^{2+}]_i$ comparing Roscovitine alone and 1 μ M PMA plus 100 μ M Roscovitine.....	63
Figure 3.15: ION5C evoked $\Delta[\text{Ca}^{2+}]_i$ in Roscovitine plus 1 μ M PMA and Roscovitine treated terminals.....	63

Figure 3.16: HK5C evoked GLU release in control and a) 1 μ M Go6983 and 1 μ M Go6983 + 100 μ M Roscovitine.....	65
Figure 3.17: HK5C evoked GLU release in control and 1 μ M CONO plus 100 μ M Roscovitine.....	67
Figure 3.18: HK5C evoked changes in Δ $[Ca^{2+}]_i$ in control and 1 μ M CONO treated synaptosomes.....	68
Figure 3.19: HK5C evoked Δ $[Ca^{2+}]_i$ in control and 1 μ M CONO plus 100 μ M Roscovitine treated terminals	69
Figure 3.20: HK5C evoked GLU release comparing control with AGA plus 100 μ M Roscovitine.....	70
Figure 3.21: HK5C evoked changes in Δ $[Ca^{2+}]_i$ comparing Roscovitine with AGA.....	71
Figure 3.22: HK5C evoked GLU release comparing Roscovitine with NIF.....	73
Figure 3.23: HK5C evoked changes in Δ $[Ca^{2+}]_i$ comparing Roscovitine with NIF.....	74
Figure 3.24: HK5C evoked GLU release from terminals treated with or without Roscovitine plus JASP.....	78
Figure 3.25: HK5C evoked GLU release from Roscovitine or Roscovitine plus JASP treated synaptosomes.....	78
Figure 3.26: HK5C evoked GLU release in terminal treated with Roscovitine and Cys A.....	80
Figure 3.27: HK5C evoked Δ $[Ca^{2+}]_i$ in terminal treated with Roscovitine and Cys A.....	82
Figure 3.28: The effect of 100 μ M Roscovitine treatment on the bioenergetics of synaptosomes.....	85
Figure 3.29: The effect of 100 μ M Roscovitine treatment on various bioenergetics parameters.....	86
Figure 3.30: The effect of 160 μ M Dynasore treatment on the bioenergetics of synaptosomes.....	87
Figure 3.31: The effect of 160 μ M Dynasore treatment on various bioenergetics parameters.....	88
Figure 3.32: The effect of 50 μ M Blebbistatin treatment on the bioenergetics of synaptosomes.....	90
Figure 3.33: The effect of 50 μ M Blebbistatin treatment on various bioenergetics parameters.....	91
Figure 3.34: The effect of 1 μ M PMA treatment on the bioenergetics of synaptosomes.....	92
Figure 3.35: The effect of 1 μ M PMA treatment on various bioenergetics parameters.....	93

Figure 3.36: The effect of 1 μ M PMA plus 100 μ M Roscovitine treatment on the bioenergetics of synaptosomes.....	94
Figure 3.37: The effect of 1 μ M PMA plus 100 μ M Roscovitine treatment on various bioenergetics parameters.....	95
Figure 3.38: The effect of 1 μ M Go6983 treatment on the bioenergetics of synaptosomes.....	96
Figure 3.39: The effect of 1 μ M Go6983 treatment on various bioenergetics parameters.....	97
Figure 3.40: The effect of 1 μ M Go6983 plus 100 μ M Roscovitine treatment on the bioenergetics of synaptosomes.....	98
Figure 3.41: The effect of 1 μ M Go6983 plus 100 μ M Roscovitine treatment on various bioenergetics parameters.....	99
Figure 3.42: The effect of 2.5 μ M JASP plus 100 μ M Roscovitine treatment on the bioenergetics of synaptosomes.....	100
Figure 3.43: The effect of 2.5 μ M JASP plus 100 μ M Roscovitine treatment on various bioenergetics parameters.....	101
Figure 3.44: The effect of 1 μ M Cys A plus 100 μ M Roscovitine treatment on the bioenergetics of synaptosomes.....	102
Figure 3.45: The effect of 1 μ M Cys A plus 100 μ M Roscovitine treatment on various bioenergetics parameters.....	103
Figure 3.46: Phosphorylation of Syn I on the Ser-553.....	106
Figure 3.47: Semi-quantitative analysis of Syn I phospho-Ser-553.....	108
Figure 3.48: Phosphorylation of Syn I on the Ser-9 at 2 sec and 15 sec stimulations.....	110
Figure 3.49: Phosphorylation of Syn I on the Ser 9 at 30 sec and 120 sec stimulations.....	110
Figure 3.50: Semi-quantitative analysis of Syn I phospho-Ser-9.....	112
Figure 3.51: Phosphorylation of Syn I on the Ser-603 at 2 sec and 15 sec stimulations.....	114
Figure 3.52: Phosphorylation of Syn I on the Ser-603 at 30 sec and 120 sec stimulations.....	114
Figure 3.53: Semi-quantitative analysis of Syn I phospho-Ser-603.....	116
Figure 3.54: Summary of the findings in chapter 3.....	117
Figure 4.1: HK5C evoked GLU release in terminals treated with 1 μ M Fluoxetine....	131
Figure 4.2: 200 nM Fluoxetine.....	132
Figure 4.3: 100 nM Fluoxetine.....	133
Figure 4.4: 50 nM Fluoxetine.....	133
Figure 4.5: HK5C evoked GLU release following an extended 20 min incubation at 37°C with 1 μ M Fluoxetine.....	134

Figure 4.6: 200 nM Fluoxetine	135
Figure 4.7: 100 nM Fluoxetine.....	136
Figure 4.8: 60 nM Fluoxetine.....	137
Figure 4.9: 40 nM Fluoxetine.....	138
Figure 4.10: 20 nM Fluoxetine.....	138
Figure 4.11: HK5C evoked GLU release following 20 nM Fluoxetine and 40 nM Fluoxetine incubation for 20 min.....	139
Figure 4.12: 5 nM Fluoxetine.....	139
Figure 4.13: HK5C evoked GLU release following 5 min pre-treated terminals with 100 μ M Roscovitine or 40 nM Fluoxetine treatment for 20 min.....	140
Figure 4.14: HK5C evoked GLU release in terminals treated with Roscovitine and Fluoxetine plus Roscovitine.....	142
Figure 4.15: The $[Ca^{2+}]_i$ changes in induce by HK5C comparing control and 1 μ M Fluoxetine.....	143
Figure 4.16: GLU release in control and terminal with Dyansore plus Fluoxetine and Pitstop2 TM plus Fluoxetine.....	145
Figure 4.17: ION5C evoked GLU release in 40 nM Fluoxetine pre-treated terminal...	146
Figure 4.18: ION5C evoked GLU release in Dynasore plus Fluoxetine.....	148
Figure 4.19: ION5C evoked GLU release in Pitstop2 TM plus Fluoxetine.....	149
Figure 4.20: The effect of 5 min incubation with 1 μ M Fluoxetine treatment on the bioenergetics of synaptosomes.....	151
Figure 4.21: The effect of 5 min incubation with 1 μ M Fluoxetine treatment on various bioenergetics parameters.....	152
Figure 4.22: The effect of 20 min incubation with 1 μ M Fluoxetine treatment on the bioenergetics of synaptosomes.....	153
Figure 4.23: The effect of 20 min incubation with 1 μ M Fluoxetine treatment on various bioenergetics parameters.....	154
Figure 4.24: Summary of the findings in chapter 4.....	155
Figure 5.1: Evoked GLU release induced by 4AP5C, HK5C, ION5C in MITMAB treated terminals.....	168
Figure 5.2: FM 2-10 dye release evoked by HK5C and ION5C in the presence or absence of MITMAB	170
Figure 5.3: $\Delta[Ca^{2+}]_i$ induce by HK5C on 30 μ M MITMAB treated terminals.....	171
Figure 5.4: $\Delta[Ca^{2+}]_i$ induced by ION5C in 30 μ M MITMAB treated terminals	171
Figure 5.5: GLU release evoked by 4AP5C, HK5C, ION5C in KT5720 treated terminals.....	174
Figure 5.6: FM dye evoked by each stimulus in the presence or absence of KT5720....	176
Figure 5.7: Effect of Dynasore on HK5C, ION5C, and 4AP5C evoked GLU and FM dye.....	178

Figure 5.8: HK5C evoked GLU release from Go6983 plus KT5720 treated terminals...	180
Figure 5.9: HK5C evoked FM dye release from Go6983 plus KT5720 treated terminals.....	181
Figure 5.10: Effect of different calcium blockers on various releasing parameters evoked by HK5C	183
Figure 5.11: HK5C evoked $\Delta [Ca^{2+}]_i$ in terminals treated with Go6983 and calcium blockers.....	185
Figure 5.12: HK5C evoked GLU release in terminals treated with Go6983 and calcium blockers.....	187
Figure 5.13: HK5C evoked FM dye release in terminals treated with Go6983 and calcium blockers.....	189
Figure 5.14: HK5C evoked FM dye release in terminal treated with Go6983 plus OA...	191
Figure 5.15: HK5C evoked FM dye release in terminal treated with Go6983 plus OA plus CONO.....	191
Figure 5.16: HK5C evoked FM dye release in terminal treated with Go6983 plus OA plus NIF.....	192
Figure 5.17: HK5C evoked FM dye release in terminal treated with Go6983 plus OA plus AGA.....	192
Figure 5.18: The effect of 30 μ M MITMAB treatment on the bioenergetics of synaptosomes.....	194
Figure 5.19: The effect of 30 μ M MITMAB treatment on various bioenergetics parameters.....	195
Figure 5.20: The effect of KT5720 treatment on the bioenergetics of synaptosomes....	196
Figure 5.21: The effect of KT5720 treatment on various bioenergetics parameters.....	197
Figure 5.22: The effect of 1 μ M Go6983 plus 2 μ M KT5720 treatment on the bioenergetics of synaptosomes.....	198
Figure 5.23: The effect of 1 μ M Go6983 plus 2 μ M KT5720 treatment on various bioenergetics parameters.....	199
Figure 5.24: The effect of 1 μ M Go6983 plus 50 nM AGA treatment on the bioenergetics of synaptosomes.....	200
Figure 5.25: The effect of 1 μ M Go6983 plus 50 nM AGA treatment on various bioenergetics parameters.....	201
Figure 5.26: The effect of 1 μ M Go6983 plus 1 μ M NIF treatment on the bioenergetics of synaptosomes.....	202
Figure 5.27: The effect of 1 μ M Go6983 plus 1 μ M NIF treatment on various bioenergetics parameters.....	203
Figure 5.28: The effect of OA treatment on the bioenergetics of synaptosomes.....	204
Figure 5.29: The effect of OA treatment on various bioenergetics parameters.....	205

Figure 5.30: The effect of 1 μM Go6983 plus 0.8 μM OA treatment on the bioenergetics of synaptosomes.....	206
Figure 5.31: The effect of 1 μM Go6983 plus 0.8 μM OA treatment on various bioenergetics parameters.....	207
Figure 5.32: Summary of the findings in chapter 5.....	208
Figure 6.1: GLU release evoked by various stimuli in LAT treated terminals.....	218
Figure 6.2: FM dye release evoked by various stimuli in LAT treated terminals.....	220
Figure 6.3: HK5C evoked FM dye release in LAT plus OA treated synaptosomes.....	221
Figure 6.4: Change in $\Delta[\text{Ca}^{2+}]_i$ induce by HK5C in LAT treated terminals.....	222
Figure 6.5: Change in $\Delta[\text{Ca}^{2+}]_i$ induce by ION5C in LAT treated terminals.....	222
Figure 6.6: HK20C evoked GLU release in LAT treated terminals.....	223
Figure 6.7: HK5C evoked GLU release in Go6983 plus LAT treated terminals.....	225
Figure 6.8: HK5C evoked FM dye release in Go6983 plus LAT treated terminals.....	225
Figure 6.9: HK5C evoked Change in $\Delta[\text{Ca}^{2+}]_i$ release in Go6983 plus LAT treated terminals.....	226
Figure 6.10: ION5C evoked GLU release in Go6983 plus LAT treated terminals.....	227
Figure 6.11: HK5C evoked GLU release in JASP treated terminals.....	228
Figure 6.12: HK5C evoked FM dye in JASP treated terminals	229
Figure 6.13: Change in $\Delta[\text{Ca}^{2+}]_i$ in JASP treated terminals.....	229
Figure 6.14: ION5C evoked GLU release in JASP treated terminals.....	230
Figure 6.15: ION5C evoked FM dye in JASP treated terminals.....	231
Figure 6.16: ION5C evoked change in $\Delta[\text{Ca}^{2+}]_i$ in JASP treated terminals.....	231
Figure 6.17: HK5C evoked GLU release in JASP plus LAT treated terminals.....	232
Figure 6.18: ION5C evoked GLU release in JASP plus LAT treated terminals.....	233
Figure 6.19: HK5C evoked $\Delta[\text{Ca}^{2+}]_i$ in JASP plus LAT treated terminals.....	234
Figure 6.20: HK5C evoked FM dye release in JASP plus LAT treated terminals.....	235
Figure 6.21: ION5C evoked FM dye release in JASP plus LAT treated terminals.....	236
Figure 6.22: HK5C evoked FM dye release in JASP plus LAT plus OA treated terminals.....	238
Figure 6.23: ION5C evoked FM dye release in JASP plus LAT plus OA treated terminals.....	239
Figure 6.24: The effect of 15 μM LAT treatment on the bioenergetics of synaptosomes.....	240
Figure 6.25: The effect of 15 μM LAT treatment on various bioenergetics parameters..	241
Figure 6.26: The effect of Go6983 with LAT treatment on the bioenergetics of synaptosomes.....	242
Figure 6.27: The effect of Go6983 with LAT treatment on various bioenergetics parameters.....	243

Figure 6.28: The effect of 2.5 μ M JASP treatment on the bioenergetics of synaptosomes.....	244
Figure 6.29: The effect of 2.5 μ M JASP treatment on various bioenergetics parameters.....	245
Figure 6.30: The effect of 2.5 μ M JASP plus LAT treatment on the bioenergetics of synaptosomes.....	246
Figure 6.31: The effect of 2.5 μ M JASP plus LAT treatment on various bioenergetics parameters.....	247
Figure 6.32: The effect of 2.5 μ M JASP plus 15 μ M LAT plus 0.8 μ M OA treatment on the bioenergetics of synaptosomes.....	248
Figure 6.33: The effect of 2.5 μ M JASP plus 15 μ M LAT plus 0.8 μ M OA treatment on various bioenergetics parameters.....	249
Figure 6.34: Summary of the findings in chapter 6.....	250

List of Abbreviations and Acromnys

- [Ca²⁺]_e – Extracellular Ca²⁺
[Ca²⁺]_i – Intracellular Ca²⁺
Abp 1 – F-actin binding protein
ADBE – Activity dependent bulk endocytosis
AGA – ω-Agatoxin TK
AP – Action potential
ATP – Adenosine triphosphate
AZ – Active zone
α-syn – α-synuclein
BPB – bromophenol blue
cAMP – Cyclic adenosine monophosphate
cBIMP – Sp-5,6-dichloro-cBIMPS
CaMK II – Ca²⁺/calmodulin-dependent protein kinase II
CN – Calciuneurin
Cdk5 – Cyclin-dependent kinase 5
CME – Clathrin mediated endocytosis
CNS – Central nervous system
CONO – ω-Conotoxin GVIA
Cys A - Cyclosporine A
DAG – Diacylglycerol
DTT – Dithiothereitol
Dyn – Dynamin
EM – Electron microscopy
ETC – Electron transport chain
F-actin – Filamentous actin
FCCP – Carbonyl cyanide-4 (trifluoromethoxy) phenylhydrazone
FF – Full fusion
FP – Fusion pore
Fura-2-AM – Fura-2-acetoxymethly ester
GDH – Glutamate dehydrogenase type-II
GLU – Glutamate

GSK3 – Glycogen synthase kinase 3
GTP – Guanosine triphosphate
Gsn – gelsolin
JASP – Jasplakinolide
KO – Knockout
KR – Kiss and run
LAT – Latrunculin
LDS – Lithium dodecyl sulfate
MDD – Major depressive disorder
MITMAB – Myristyl trimethyl ammonium bromide
Mito-stress – Mitochondrial stress
MLCK – Myosin light chain kinase
mUnits – Milli-Units
NADP – Nicotinamide adenine dinucleotide phosphate
NIF – Nifedipine
NM-II – non-muscle myosin II
NMJ – Neuromuscular junction
NT – Neurotransmitter
OA – Okadaic acid
OCR – Oxygen consumption rate
PH – Pleckstrin-homology
PKA – Protein kinase A
PKC – Protein kinase C
PM – Plasma membrane
PMA – Phorbol 12-myristate 13-acetate
PP2B – Protein phosphatase 2B
PVDF – Polyvinylidene fluoride
RP – Reserve pool
RRP – Readily releasable pool
RT – Room temperature
S.E.M – Standard error of mean
Ser – Serine
SP – Silent pool
SSRI – Selective serotonin reuptake inhibitor

SVs – Synaptic vesicles

Syn I – Synapsin I

Syt – Synaptotagmin

TBS – Tris Buffered Saline

UE – Ultrafast endocytosis

VGCC – Voltage gated calcium channel

VAMP-2 – Vesicle-associated membrane protein 2

vGlut-1 – Vesicular glutamate transporter 1

Acknowledgement

Special thanks to my supervisor, Dr. Anthony Ashton. Without your help and commitment, it would have been impossible to finish this thesis, so I am very thankful to have you as my supervisor. I would also like to thank my friends in the lab, Adam Rostron and Stephen Gilbody. I am very grateful that I had you guys as my seniors who could guide me through the lab techniques which made it much easier to adapt to the lab environment. Dami, I don't know how many times I have called you seeking for your wisdom, but I don't remember a single moment you have picked up a phone negatively, that is very special thing for me and I am really thankful about it. For my mates outside the lab, Tyler and Luke. Without you boys, living in Preston would have been so dull. I won't forget the memories we have shared together. In few months of time, we might not be able to see each other as often as we used to, but lads, please remember that I will still be your friend and as we have said before, let's meet up at somewhere else again. It is fair to say that past three months were one of the toughest times I went through in my life. To complete this thesis, I had to remain focused and committed, thus I was continuously under the pressures and often became mentally vulnerable.

Lastly, special mention has to go to family. My mom, my dad, and my sister, even though, I am abroad on my own. I rarely feel that I am alone because I know that you are all praying for me and your love keeps me stable. Thank you so much for that.

Chapter 1:

Introduction

1.1. Synaptic Transmission

Synaptic transmission is the basis of neuronal communication and disturbance of this process is linked to the pathophysiology of numerous neuronal and psychiatric disorders (e.g. Parkinson disease, Alzheimer's disease, and others). Therefore, it is imperative to elucidate the molecular mechanism of synaptic vesicle (SV) exocytosis. In synaptic transmission, action potentials (AP) travelling along axons induce the depolarisation of presynaptic nerve terminals, this leads to the opening of voltage gated Ca^{2+} channels (VGCC), with a consequent increase in Ca^{2+} entry and an increase in intracellular Ca^{2+} ($[\text{Ca}^{2+}]_i$). This $[\text{Ca}^{2+}]_i$ increase promotes fusion between SV membranes and the presynaptic plasma membrane (PM), with the initial production of a fusion pore (FP). Following the creation of FPs, SVs undergo exocytosis and release their neurotransmitter (NT) content. Such released NTs then diffuse across the synaptic cleft, and bind to postsynaptic receptors leading to either excitation or inhibition of the postsynaptic neuron. The exocytosed SV proteins and lipids are then recovered from the PM via endocytosis. After the endocytosis and the reformation of the SVs, these are re-acidified and re-filled with NT so that they are prepared for subsequent rounds of release. This whole process is referred to as SV recycling. The limited number of SVs contained in the neurons means that a highly efficient and fast recycling process is required to allow maintenance of neurotransmission in response to various stimulation intensities (Sudhof, 2004; Becherer and Rettig, 2006; Di Maio, 2008; Alabi and Tsien, 2012).

1.2 SV pools

The development of the electron microscope (EM) in the early 1950s enabled the discovery of synaptic vesicles (SVs). During this period, Bernard Katz, with Jose del Castillo and Paul Fatt, had proposed the quantal theory of transmitter release in which NT molecules were released in discrete packages. This theory, alongside the first EM images of the synapse, led to the development of the vesicular hypothesis of neurotransmission.

In this hypothesis, transmitter is stored in SVs and its release from the vesicle interior following vesicular exocytosis forms the structural basis of quantal neurotransmission. Clearly, SVs are important structural features of presynaptic terminals and the disruption of their normal function is related to various neurological or psychiatric diseases (Alabi and Tsien, 2012).

Many studies have highlighted that neurons contain three distinct pools of SVs: the Readily Releasable Pool (RRP), the Reserve Pool (RP; also known as Recycling pool), and the Silent Pool (SP; also known as Resting pool and Reserve pool) (Denker and Rizzoli, 2010; Alabi and Tsien, 2012; Crawford and Kavalali, 2015; Fowler and Staras, 2015). High frequency repetitive stimulation of nerve terminals induces dramatic drops in NT release and this eventually leads to lower steady-state level of neurotransmission. This phenomenon of synaptic depression represents the depletion of SVs from the RRP. RRP are replenished by their recycling or by recruitment of the SVs from the RP. These two pools, which participate in exo- and endocytosis under prolonged stimulation, are jointly referred to as the total recycling pool. In cultured hippocampal cells, it was estimated that the total recycling pool contained ~21-25 vesicles per terminal, with ~4-8 vesicles in the RRP and ~17-20 vesicles in the RP (Fig 1.1). Considering the total amount of SVs in the terminal are >200, these values are strikingly low, suggesting that there is a large group of SVs in a distinct pool other than the RRP and RP exists, and this is the SP (Sudhof, 2004).

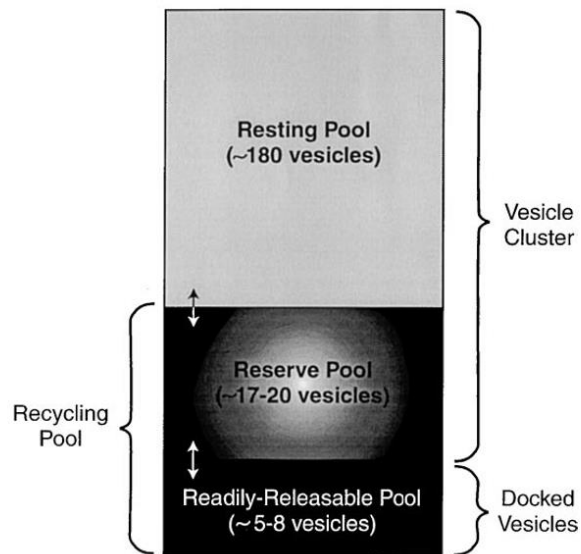


Figure 1.1. Vesicle pools and size (From Sudhof, 2000).

Rizzoli and Betz (2005) have proposed a three-pool model consisting of the RRP, RP, and SP organised in the order of their release. The model suggests that when stimulation arrives in the nerve terminal, the RRP, which are already docked at the active zone (AZ), release first, and the RP replenishes the RRP in the case of repetitive stimulation and any release, but that the SP is only released under extremely intense non-physiological stimulations conditions (Fig 1.2).

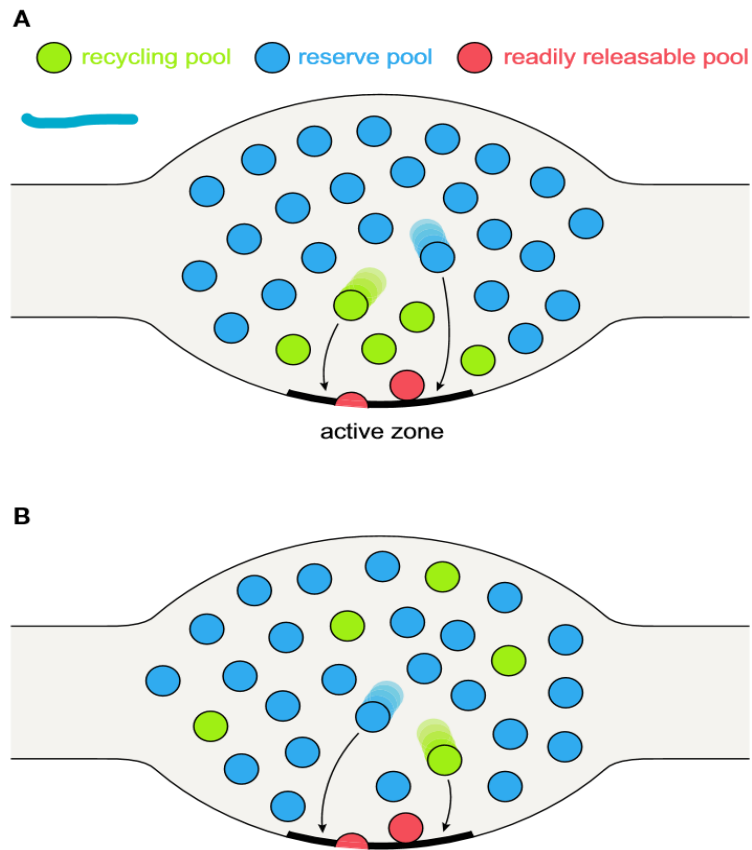


Figure 1.2. Three-pool model of SV pools (From Denker and Rizzoli, 2010).

This three-pool model fits in quite well with data produced utilising pHluorin experiments. Fernandez-Alfonso and Ryan (2008) showed that for three main SVs components (vGlut-1, VAMP-2, and Synaptotagmin 1 all linked to pHluorin molecules), around half of the tagged proteins appeared in the recycling pool that respond readily to prolonged stimulation by mobilising and fusing with the PM so these underwent exocytosis and endocytosis as detected by the pH sensitive pHluorin linked to these vesicular proteins. However, half of the labelled vesicles were targeted to a non-recycling, acidic compartment. The fraction of recycling and SPs varies across boutons within an individual axons, from 100% silent to 100% recycling. However, morphological studies on localisation of these pools shows strong evidence of intermixing between the SP and the recycling pools. Whilst RRP, that are understood to release first following the stimulation, may be docked at the AZ release sites, all other vesicles are positioned throughout the

synapse. Indeed, not all SVs docked at the AZ are necessarily releasing first. Moreover, in a study at frog neuromuscular junctions (NMJs), it was found that AZs were largely occupied by vesicles that do not normally release during physiological stimulation (Rizzoli and Betz, 2004; Denker and Rizzoli, 2010).

The properties of the RRP and RP have been well characterised. Currently one major debate is what mode of vesicle exocytosis occurs under particular stimulation conditions (Richards, 2009, 2010; Zhang *et al*, 2009; Alabi and Tsien, 2013). Ashton's group has shown that under strong stimulation-conditions, the RRP and the RP SVs are found to undergo different modes of fusion to release their NT contents. The RP SVs undergo a full fusion mode (FF), where during vesicular membrane fusion with the PM the FP opens, transmitter is released, but concurrently the FP continues to expand and the vesicle membrane collapses and fully integrates into the PM. Subsequently, the SV membrane is recovered via a clathrin- and dynamin (Dyn)-dependent process or via a Dyn-dependent process alone. Intriguingly, under strong stimulation conditions Ashton's group (Bhuva, 2015; Singh, 2017) have shown that the RRP SV undergoes a Kiss-and-run (KR) mode in which the FP opens, but rather than fully expanding and causing vesicle membrane collapse into the PM, it recloses via a process independent of clathrin. Research by Ashton and colleagues has discovered that these modes of exocytosis can switch and this depends upon changes in intracellular calcium levels and in protein phosphorylation/dephosphorylation (Ashton and Ushkaryov, 2005; Ashton *et al*, 2009, 2011, 2013).

1.3 The Silent Pool (SP)

There are many challenges in order for one to study the third pool, the SP. Studies on synapses have shown that this pool can contain up to 80% of all terminal SVs, but that under normal physiological conditions these SVs are not released. Why such a large number of SVs do not normally release remains an enigma. Some studies have suggested

that the SP may act as a buffer for proteins involved in SV recycling (Denker *et al*, 2011). The SP has been investigated at the neuromuscular junction (NMJ) of *Drosophila melanogaster* through various manipulations to this model. Particularly, it was determined that in flies carrying the temperature sensitive mutation of Shibire^{TS}, which is a homologue to the mammalian Dyn protein, extra release due to the SP SVs undergoing exocytosis was found under non-permissive raised temperatures. This is because at such increased temperature Dyn was inactive so that the RRP and the RP cannot recycle and this, therefore, allowed the SP to participate in the release. Subsequent reduction of the temperature back to a permissive temperature, Dyn became active again and allowed the recovery of all pools of SVs, and such results indicate that the SP is localised at a specific position within the SV aggregates (Kuromi and Kidokoro, 1998). This model further revealed that the SP vesicles share distinct biochemical properties with vesicles from the other two pools and they were released under normal physiological condition, and they could be involved in exocytosis under high frequency stimulation in this model (Kuromi and Kidokoro, 2005). Equivalent studies have not been made in mammalian nerve terminals because whilst there are Dyn knockout animals (Ferguson *et al*, 2007; Raimondi *et al*, 2011), there are no temperature sensitive Dyn mutations that might allow the SP to come on line and release following the release of the RRP and the RP.

Afuwape *et al* (2017) investigated the stability of recycling SVs via performing an extended incubation of FM 1-43 labelled terminals prior to a stimulation. They subsequently triggered the dye release from the hippocampal culture cells after incubation of FM labelled terminals at physiological temperature for 6 hours. It was found that vesicles in the SP are highly reluctant to intermix with the labelled recycling pool because the kinetics of FM dye release were the same after this extended incubation as after only a 10 min resting period following initial loading (Afuwape *et al*, 2017).

Molecular mechanisms underpinning the SP are mainly unknown. In contrast to the RRP that is known to dock at the AZ membrane, the RP and SP are identified to be highly

intermixed at the presynaptic terminal (Denker and Rizzoli, 2010). Despite this intermix, the fact that SVs are still capable of releasing in organised sequence means it is highly likely that there are unknown molecular tags that partition the SVs. It is possible that the SP has distinctive morphological features, such as size or shape of the vesicle that could distinguish this group of pool from others, but, ultrastructural studies have failed to discover significant morphological parameters that one could refer to when classifying each pool (Rizzoli & Betz, 2005). As over 400 different proteins are found on SVs (Takamori *et al*, 2006), it could be that variation in these proteins could provide the diversity in these vesicle pools. Thus, a combination of certain proteins on vesicle surface could explain how vesicles within the same presynaptic terminal have varying functional characteristics (Chamberland and Toth, 2015).

One of the possibilities is that there are molecular tags that associate with SV membrane that specify their identity and direct them to one pool or the other (Guarnieri, 2017). Synapsin I (Syn I) is a SV associated protein, and it is also a molecular marker of the RP, restricting SVs from this pool participating in neurotransmission (Denker *et al*, 2011). Thus, it could also contribute to restrict the mobilisation of the SP, justifying Syn I as one of the likely candidates to regulate the SP organisation. Another study has also suggested that the presence of vesicular zinc could be a possible hallmark of the SP. This study showed that zinc predominantly exists in a subpopulation of SVs and that such zinc-containing SVs only preferentially release during high frequency stimulation, an indication that these SVs may be derived from the SP (Lavoie *et al*, 2011).

1.4 Roscovitine

Recently Kim & Ryan (2010) used a small molecule inhibitor of Cdk5 [a proline-directed Ser/Thr kinase that is characterised to be implicated in cytoskeleton assembly and its organisation during axonal growth (Maccioni *et al*, 2001) and in many other processes such as SV recycling (Evans and Cousins, 2007)], called Roscovitine, and successfully

released SVs that were previously in a silent state from mammalian hippocampal cell cultures, i.e. part of the SP. The study reported that following Roscovitine treatment, stimulation with 100 action potentials (APs) was able to evoke 80%-90% of the entire vesicle pool in the terminal. The fact that a small stimulation like 100 AP, can drive exocytosis of virtually all of the SVs in the terminal suggests that Cdk5 inhibition has increased the size of the available SV pool. Kim and Ryan (2010) concluded that an inhibition of Cdk5 via Roscovitine leads to an elevation of the recycling vesicle pool size by converting the SP vesicles into functional recycling vesicles.

Kim and Ryan (2013) have further claimed that the balance of Cdk5 with Calcineurin operates a release probability of SV pools, and it is mediated through $Ca_v 2.2$ voltage-gated calcium channels (N-type Ca^{2+} channel). Such studies and others outlined below suggest that Cdk5 has an important role in regulation of the SP and other vesicle pools, and also outline which proteins Cdk5 could potentially work on in this regulation (Kim and Ryan, 2013).

1.5 Cdk5 Phosphorylation targets

1.5.1 Dynamin I

Cdk5 is known to phosphorylate Dyn I at Ser 778 (Evans and Cousin, 2007) and in the absence of this, Ser-774 cannot be phosphorylated by GSK3 (Clayton *et al*, 2010) and both of these sites are targets of calcineurin (CN)-induced dephosphorylation. These sites have been found to be involved in clathrin-dependent endocytosis (Armbruster *et al*, 2013) and it was also suggested that they may be involved in the control of phospho-dependent bulk endocytosis of SVs (Clayton and Cousin, 2009). As Dyn I requires Cdk5 phosphorylation for its continued recycling activity, it is likely to be involved in SP recycling and re-releasing following release of this pool. Intriguingly, Dyn can also be involved in the regulation of the actin cytoskeleton (Gu *et al*, 2010).

1.5.2 Myosin 2

The role of non-muscle myosin 2 (NM-II) in exocytosis has been highlighted in various studies on non-neuronal cells (Neco *et al*, 2008; Bhat and Thorn, 2009; Doreian *et al*, 2009) and Ashton's group has shown that it has a role in regulating the FP of SVs in nerve terminals (Bhuva, 2015; Singh, 2017). It is also possible that NM-II may regulate the SP independent of its fusion mode. In studies focused exclusively on the RRP and RP, the myosin light chain kinase (MLCK) inhibitors were shown to perturb (Ryan, 1999) or augment (Srinivasan *et al*, 2008) the release while other works have shown that the role of MLCK is independent of actin cytoskeleton (Tokuoka and Goda, 2006). Actin microfilaments may be involved in the regulation of the SP. A study on *Drosophila* NMJ has found that the SP SVs require actin microfilament for their recruitment (Kuromi and Kidokoro, 2005). It is therefore, possible that one might be able to link the properties of NM-II as a motor protein for the SP and its requirement for actin microfilaments (e.g. Neco *et al*, 2004; Dorein *et al*, 2008; Haviv *et al*, 2008). Hence, it will be worth studying the phosphorylated state of non-muscle myosin under the condition investigating the regulation of the SP (Ludowyke *et al*, 2006; Beach *et al*, 2011; Sanborn *et al*, 2011).

1.5.3 Synapsin I

Syns are SV associated phosphoproteins that are proposed to have a key role in the regulation of neurotransmitter release and synapse formation. They are substrates of multiple kinases that phosphorylate the proteins at several distinct sites (Cesca *et al*, 2010). Syn was first discovered by Paul Greengard's group. The neuronal specific Protein I (later named Syn I) was found to be one of the main endogenous substrates for cAMP-dependent protein kinase (PKA) in synaptic fractions. Early evidences has demonstrated that Syn phosphorylation was induced following electric stimulation in rabbit cervical ganglia (Nestler and Greengard, 1982) and in the rat neurohypophysis (Tsou and Greengard, 1982). Later, Syn phosphorylation by CaMKII was studied intensively as such phosphorylation

induced a major conformational change in Syn (Benfenati *et al*, 1990) and this reduced its association with SVs (Schiebler *et al*, 1986) and with the actin cytoskeleton (Valtorta *et al*, 1992). The relevance of this to synaptic transmission was shown by the fact that microinjections of Syn phosphorylated at the CaMK II sites failed to stop the SV release, whilst dephospho-Syn inhibited release (Llinas *et al*, 1985, 1991). However, it is now clear that Syn function *in vivo* is regulated through multiple activity dependent phosphorylation pathways, and PKA, Cdk5, and CaMK II all have important roles in Syn regulation (Cesca *et al*, 2010; Shupliakov *et al*, 2011; Bykhovskala, 2011).

The Syn family consists of ten homologous proteins, Syn Ia-b, IIa-b, and IIIa-f, and an analysis of the amino acid sequence of Syn I and Syn II allowed the domain structure of the Syn family to be elucidated. Syn are composed of a highly homologous N-terminal region, and a more variable C-terminus. The N-terminal region can be split into three domains, called domain A, B, C, which except from domain B, are highly conserved across isoforms and species. In contrast, the C-terminal region of Syn is more divergent, and is composed of various spliced domains (domain D-I). Domain A is a short N-terminal region, that exist in all Syn isoforms. It contains the phosphorylation site (site 1) for PKA, CaMK I and IV. Domain B, shows relatively weak similarity between Syn isoforms, and it is suggested to be a linker region connecting domain A to domain C. In Syn I, domain B contains phosphophrylation sites 4 and 5 for MAP kinase/Erk. Domain C is a large region of about 300 amino acid which consists of both hydrophobic and highly charged sequences with the potential to assume α -helix and β -sheet conformations. It is considered to be important region for Syn interaction with the actin cytoskeleton and SV phospholipids, as well as contributing to Syn homo or heterodimerisation. The amino acid sequence diverges after domain C. However, all isoforms contain a proline-rich domain (domain D in Syn Ia and Ib; domain G in Syn IIa, domain G and H in Syn IIb, and domain J in Syn IIIa). Domain D in Syn Ia and Ib contains phosphorylation site 2 for CaMKII, site 3 for CaMKII

and PAK, and sites 6 and 7 for MAPK/Erk, Cdk1 and Cdk5 (Cesca *et al*, 2010) (see Fig 1.3).

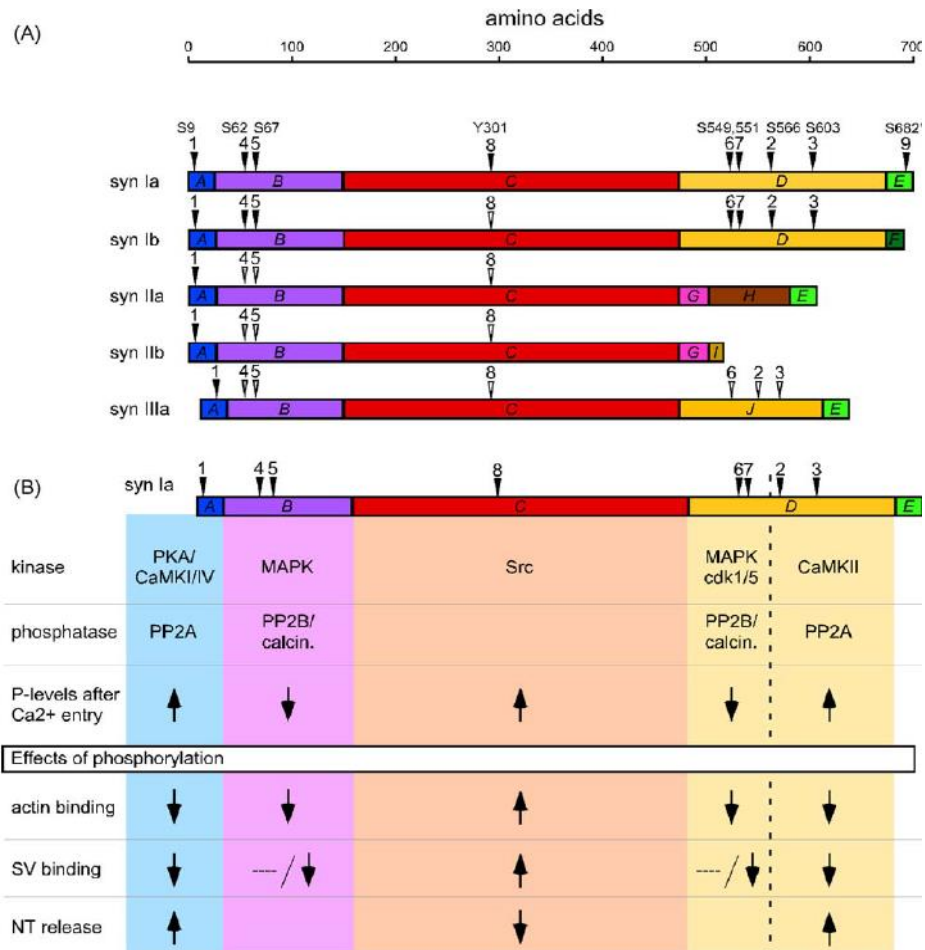


Figure 1.3. Phosphorylation sites in synapsins. (A) Phosphorylation sites in synapsins Ia-IIIa; (B) Summary of kinases and the phosphorylation sites in synapsin Ia, the diagram describes changes in phosphorylation levels in response to Ca²⁺ entry and the effect that site specific phosphorylation has upon synapsin function (Taken from Cesca *et al*, 2010).

The exact functions of Syn are not yet fully elucidated. The classical view suggests that vesicles are tethered to the cytoskeleton by Syn and cages these vesicles. Phosphorylation of Syn leads to these vesicles becoming uncaged and makes these vesicles available for release (Bykhovskala, 2011). An early study in squid giant synapses from Llinas and colleagues (1985) demonstrated that the presynaptic injection of dephosphorylated Syn I reduced the amplitude and rate of rise of postsynaptic potential (i.e. neurotransmitter release was decreased) whilst injection of either phosphorylated or heat inactivated

dephosphorylated Syn I had no effect. Injection of CaMKII was found to increase the post synaptic potentials by increasing release (Llinas *et al*, 1985, 1991). Later, the introduction of dephosphorylated Syn I, phosphorylated Syn I or activated CaMKII into rat brain synaptosomes produced a similar result *in vitro* (Nichols *et al*, 1992), outlining that Syn dephosphorylation acts as an organiser of the SV pool, keeping SVs together and connecting them to actin filaments, whereas phosphorylated Syn allows SV to become untethered so that they can fuse with the PM. In addition, presynaptic injection of a highly conserved peptide fragment of domain E into the squid giant synapse revealed a drastically reduced number of SVs located distal from the AZ and this increased the synaptic depression following relevant stimulation. Similar results were also observed when a peptide corresponding to domain C was injected. Importantly, both peptides were found to inhibit the Syn-actin interaction, indicating the importance of Syn I in maintaining the SV pools distal to the AZ through an interaction with actin (Hilficker *et al*, 1998, 2005).

Other characteristics of Syn have been highlighted in relatively recent research. Kim *et al* (2017) have observed alterations in SVs at presynaptic terminal on mice exposed to 835 MHz RF-EMF (Radiofrequency electromagnetic fields), and in such mice there is a marked decrease of expression of Syn I and II genes and their protein product (Kim *et al*, 2017). Furthermore, the phosphorylation of Syn I was found to be reduced upon Lead (Pb) exposure. Lead is a toxin that impairs the nervous system and it was found that it reduces presynaptic neurotransmission through the disarrangement of the distribution, and a decrease in the density, of presynaptic vesicles. These authors were able to reverse the effect of the Pb exposure using Roscovitine, suggesting that Pb disrupted the distribution of SVs and impaired the neurotransmitter release by changing the Cdk5 dependent phosphorylation levels of Syn I through Cdk5 (Ding *et al*, 2018).

Much research has linked Syn activity to regulation and maintenance of SVs located distal to AZ (Li *et al*, 1995b; Samigullin *et al*, 2004; Siksou *et al*, 2007; Akbergenova and Bykhovskaia, 2007; Fornasiero *et al*, 2012; Orenbuch *et al*, 2012). This suggests that Syn

is one of the major proteins that contribute to the SP regulation. Electron microscopy (EM) investigation of boutons from Syn deficient mice has demonstrated that Syn maintains vesicle clustering at the periphery of the bouton. Syn deficiency did not affect the mixing of the RP and SP but it did selectively reduced the size of the SP. Intriguingly, under intense stimulation, a significant amount of vesicles were found to be distributed at the central core of the bouton in the presence of Syn, but in the absence of Syn, the area occupied by vesicles appeared unchanged. Further, whilst strong stimulation led to an elevated basal release in Syn deficient terminals, this was not the case in Syn containing terminals indicating that Syn may direct vesicles to the SP (Akbergenova and Bykhovskaia, 2010). Verstegen *et al* (2014) demonstrated that Cdk5 phosphorylation of Syn I at Ser 549 (site 6) and Ser 551 (site 7) isolates recycling SVs to the SP via a mechanism involving the actin cytoskeleton. They claimed that the phosphorylation of Syn I with Cdk5 at Ser551 site enhances its interaction with F-actin. F-actin can dynamically regulate SV transmission and may be responsible for scaffolding and the cycling, turnover, and mobility of SVs (Cingolani and Goda, 2008). This cytoskeletal component does not regulate the RP size, although, an absence of F-actin was reported to perturb the spatial segregation of recycling SVs (Marra *et al*, 2012; Ratnayaka *et al*, 2012). Such information led Verstegen *et al* (2014) to conclude that increased phosphorylation of Syn I with Cdk5 leads to an elevation of SV interaction with F-actin, leading to the relocation of the recycling SVs to the SP, such that SV in the recycling pool are reduced (i.e. the RRP and the RP) (Verstegen *et al*, 2014).

Recent evidence has reported that Cdk5 phosphorylates Tomosyn I, a SNARE binding protein, and this can also regulate the SP. This protein appear to exert its function through an interaction with Syn I via Rab3A-GTP and this tomosyn function is independent of its SNARE binding properties (Cazares *et al*, 2016). Clearly such studies demonstrate that phosphorylation of Syn I plays an important role in organising the SV pools located distal from the AZ, and leads to the idea that changes in the phosphorylated state of Syn I (at

various phosphorylation sites) may potentially contribute to the regulation of the exocytosis of the SP.

1.5.4 α -Synuclein

The synuclein protein family consists of α -, β -, and γ -synuclein. Amongst all the synuclein proteins, interest in the α - form of the protein is high due to the fact that it has previously been found to contribute to Parkinson disease (PD) (Polymeropoulos *et al*, 1997; Clayton and George, 1999; Spinelli *et al*, 2014). An exact role of α -synuclein in the synapse has yet to be discovered. Previous studies investigating the protein's structure and localisation suggest that it does feature in various synaptic transmission processes including SV endocytosis, regulation of SV pool size, SV mobilisation and the trafficking between synapses (Gedalya *et al*, 2009; Cabin *et al*, 2002, Nemani *et al*, 2010; Scott and Roy, 2012; Vargas *et al*, 2014). The study by Vargas and colleagues (2014) used optical imaging, electron microscopy and slice electrophysiology to determine that synucleins are required for rapid and efficient clathrin dependent SV endocytosis, and by comparing the WT synapses to those from Dyn DKO synapses led to the suggestion that synuclein acts at an early step of SV endocytosis. Others have suggested that α -synuclein is organised into multimers and these cluster SVs and restrict their motility (Wang *et al*, 2014). Another study demonstrated that the α -synuclein decreases the trafficking of recycling pool vesicles between presynaptic boutons – such SVs constitute a pool known as the superpool – and that α -synuclein also has a role in maintaining the overall size of the recycling pool. Overexpression of α -synuclein led to a smaller recycling pool size and blocked the trafficking between the synaptic boutons. Whereas, removal of this protein resulted in larger recycling pools and enhanced trafficking between boutons (Scott and Roy, 2012). Nemani and colleagues (2010) had previously suggested that overexpression of α -synuclein reduced the size of the SV recycling pool and this significantly inhibited NT release. These authors demonstrated a decreased SV density at the AZ and defects in the

reclustering of SV after endocytosis by using ultrastructural analysis. Clearly, α -synuclein does participate in synaptic transmission and as it is involved in regulation of the size of the recycling pool it may also be potentially involved in the regulation of the SP. Although this thesis does not address the role of α -synuclein, it is felt that data contained in this thesis may lead on to some studies to investigate the role of this enigmatic protein. That is why it is mentioned here.

1.6 Fluoxetine

Recently, it has been found that the antidepressant drug, Fluoxetine can induce extra release from synapses (Jung *et al*, 2014). Fluoxetine is a selective serotonin reuptake inhibitor (SSRI) and it is one of the most widely prescribed treatment for depression. SSRIs are understood to operate through an inhibition of the uptake of exocytosed serotonin into the presynaptic terminal, and this leads to an increase of serotonin levels in the synaptic clefts of drug treated patients suffering from depression. Jung *et al* (2014) reported that a clinically relevant dosage of Fluoxetine, 1 μ M, had an effect on SV recycling and plasticity, and that the drug mobilises the SP of SVs so that they can be released. Higher drug concentrations attenuated evoked exocytosis. They showed that the observed increase of SVs exocytosis was due to an increase in the number of active vesicles after Fluoxetine incubation (Jung *et al*, 2014). This study is significant as it could reflect that the antidepressant effect of SSRIs might involve an expansion of the releasable SVs from nerve terminals.

Research in this thesis utilises synaptosomes prepared from rat cerebral cortex. Such preparation contain 80% glutamatergic terminals but only a very small % of serotonergic terminals. Therefore, it would be interesting to investigate whether Fluoxetine could produce equivalent effect to the one from Jung and colleagues' study utilising these cortical synaptosomes. This is some evidence from earlier study that Fluoxetine could affect the release of nerve terminals that do not involve serotonin. Bymaster *et al* (2003)

showed that Fluoxetine increases that extracellular levels of dopamine and norepinephrine in the hypothalamus, cortex and prefrontal cortex (Bymaster *et al*, 2003). Although, studies highlighted claimed that Fluoxetine has several additional effects besides inhibiting neuronal serotonin reuptake and this includes effects on glutamate release from nerve terminals and it was found that Fluoxetine inhibited 4-aminopyridine (4AP) evoked glutamate release from cerebral cortical synaptosomes primarily by suppression of P/Q type calcium channels (Wang *et al*, 2003).

1.7 SV cycling

SV cycling has two major stages; exocytosis and endocytosis. In nerve terminals, NTs are stored in SVs, and such NTs are release through exocytosis. Subsequently, empty SVs can be rapidly recycled by undergoing endocytosis to enable them to become ready for reuse (For detailed review, see Rizzoli, 2014). Much progress has been made in our knowledge about exocytosis, but details on certain specific mechanisms and endocytosis regulation are less well understood.

A study from Heuser and Reese in the early 1970s, contributed to the establishment of a concept of SV recycling using EM on frog NMJs. The study proposed that SV membranes are recycled by clathrin mediated endocytosis (CME) via cisternal structures located at AZs (Heuser and Reece, 1973). Intriguingly in the preparation using a distinct stimulation paradigm, Ceccarelli and colleagues suggested an alternative clathrin-independent fast mode of SV recycling called Kiss and Run (KR) that involves a transient FP opening (Ceccarelli *et al*, 1973). Later on it was shown that a sustained strong stimulation of nerve terminals could trigger activity dependent bulk endocytosis (ADBE) of extensive membrane patches containing membrane. This pathway may serve during very high frequency stimulation, as an emergency response, as it might not selectively recover SV proteins alone. For definite, this produces a large endosome and SVs have to bud off from this before entering the cytosol and being able to load up NT. Recently, data using high-

pressure freezing EM paired with optogenetic stimulation proposed that at invertebrate and mammalian synapses there was another distinctive mode of SV recycling, called ultrafast endocytosis (UE) existed (Fig 1.4) (Kononenko and Haucke, 2015; Soykan *et al*, 2016; Watanabe *et al*, 2017).

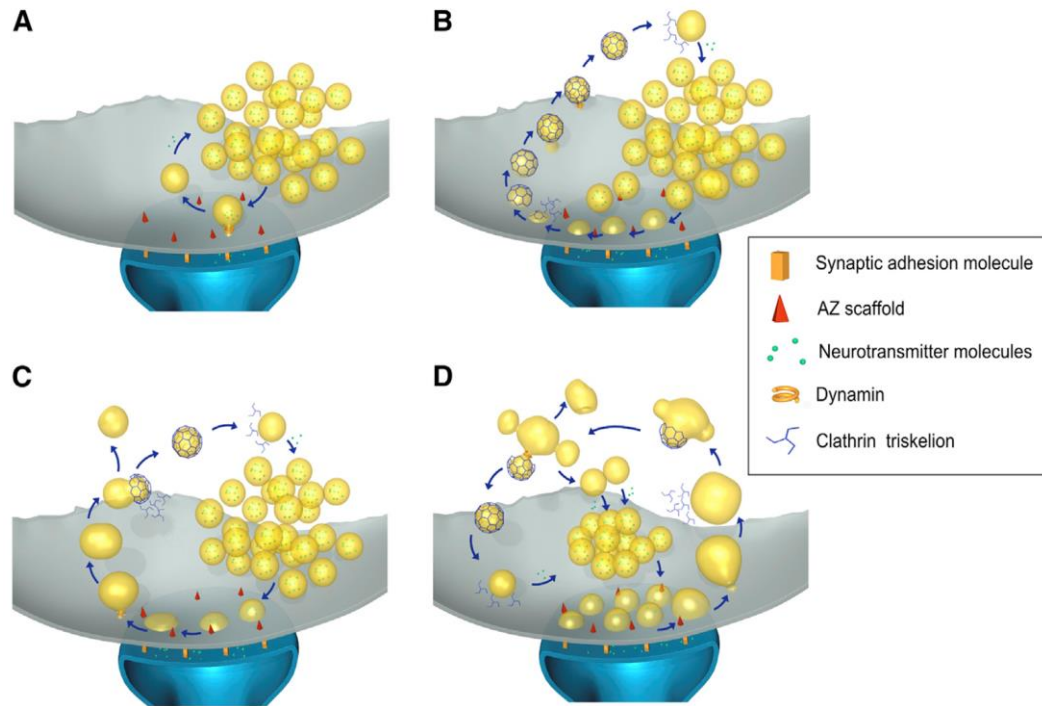


Figure 1.4. Overview of KR, CME, UE, ADBE. (A) Kiss and Run mode. Characterised with a transient opening of a fusion pore to discharge SV content followed by closure and detachment of the SV from the plasma membrane and directly reused through a fast mechanism. (B) CME. Classical model of endocytosis with open of a fusion pore followed by complete flattening of SV to the plasma membrane. Subsequently, SV components are retrieved directly from the cell surface via formation of a clathrin coated vesicle. (C) UE. Fast invagination of a larger area of the PM (2 to 4 times larger than the area that one SV would produce which then becomes an endosome and SVs pinch off of this via a clathrin dependent process. (D). Strong stimulation results in appearance of large bulk endocytic structures, which later resolved into SVs through clathrin dependent or clathrin independent mechanisms (ADBE) (From Kononenko and Haucke, 2015).

Each pathway of recycling operates through distinctive mechanism to retrieve SVs from the PM and each possesses its own advantages and disadvantages (He *et al*, 2006; Granseth *et al*, 2007; Watanabe *et al*, 2013, 2014). Which endocytic pathway is the most prevalently used is still a matter of fierce debate, although it is clear that this can be dependent on many factors such as stimulation intensity and duration. For instance, CME maybe the dominant SV endocytosis mode during low levels of stimulation, and at even milder neuronal activity, UE is proposed to be the most prevalently used pathway. This is because this has routinely only been measured after the equivalent of one AP and even then for one SV fusion, there appear to be 2-4 SV recycled. This clearly could not be maintained over a strong stimulation period otherwise the terminal would shrink. At elevated stimulation, these two mechanisms saturate and ADBE is found to get triggered and therefore, ADBE may be the predominant pathway during elevated neuronal activity (Granseth *et al*, 2006; Harata *et al*, 2006; Wu and Wu, 2007; Mellander *et al*, 2012; Nicholson-fish *et al*, 2015; Morton *et al*, 2005; Kokotos *et al*, 2018).

For these three distinctive pathways of endocytosis, CME, ADBE, and UE SV undergo classical exocytosis such that vesicles fully collapse into the PM prior to their endocytotic retrieval. In this exocytotic mode, vesicles are found to be completely flattened into the PM via FF (Rizzoli and Jahn, 2007). Following these types of exocytosis, endocytosis involves invagination of membrane containing vesicular component that may require Dyn-dependent vesicle fission. Whilst CME utilises clathrin at the PM invagination step, in UE, the Dyn-dependent fission produces an endosome and clathrin acts at the endosomal stage – at physiological temperature – to produce pinched off SVs (Watanabe *et al*, 2014). Whilst Dyn has been suggested to pinch off a large invagination to produce an endosome during ADBE, this is controversial since bulk endocytosis still occurs in Dyn deficient nerve terminals. Subsequent uncoating, trafficking, re-acidification and recharging with transmitter allows the vesicle to be ready for reuse (Brodin *et al*, 2000; Smith *et al*, 2008).

1.8 Kiss-and-Run

The other mode of release known as KR is characterised with a transient FP without complete loss of vesicle identity. Since the KR mechanism does not involve collapse of the vesicular membrane it possesses some advantage over FF in terms of speed of recycling. Studies estimate that in KR mode of fusion process, the vesicle recycles within 1s, which is faster compared to FF that takes ~20s, although, others have claimed that CDE can occur in <10s, but this is still slower than KR. Also, KR allows one to utilise less energy than full vesicles collapse and subsequent vesicle reformation. There is also rapid clearance of the vesicle membrane and proteins from the AZ release site if KR recycling occurs, which can facilitate vesicle replenishment of the release sites. Although, UE can allow some SV membrane to endocytosed in 30 ms, faster than KR, the actual recycled endosomal compartment needs SVs to pinch off from this and then take up NT and this process actually takes about 5s and so UE is still slower than KR in producing a SV that is ready to re-release (Zhang *et al*, 2007; Park *et al*, 2012; Alabi and Tsien, 2013; Watanabe *et al*, 2014).

SVs are proposed to use different modes of exocytosis depending on various factors such as intensity of stimulation. Evidence supporting this hypothesis was proposed from Elhamdani *et al* (2001) studying chromaffin granule exocytosis. The group used amperometric recording to monitor single exocytotic events in chromaffin cells and found that the intensity of stimulation determines the amount of catecholamine release through an individual FP. These authors reported that at low frequency stimulation, 0.25 Hz, the quantal size was more than two-fold smaller compared to under high frequency, 10 Hz (Elhamdani *et al*, 2001). Research from Fulop *et al* (2005) has obtained a similar result. This group revealed that the quantal size of amperometric spikes triggered by 0.5 Hz stimulation was more than two-fold smaller than the one induced by 15 Hz stimulation. Additionally, the size of amperometric spikes at 0.5 Hz was very similar to the value of the one from pre-spike current recorded at 15 Hz. This part of spike is often referred to as

'foot', and these currents represent the slow release of catecholamine through the FP. At this stage, FP can either close or expand into a larger pore. In the case of the FP closing, one may get an incomplete release of the vesicle as it may close before all the catecholamine has been released. Thus, at a lower frequency, the catecholamine is partially released through a relatively narrow FP that closes back after short period of time, whilst under higher frequency stimulation, the FP totally expands into the PM and so there is complete release of the vesicular contents (Fulop *et al*, 2005). In these chromaffin cells, the rapid closure of a non-expanded FP represents KR whilst the full release of an expanded FP is FF (Cardenas and Marengo, 2016).

Ceccarelli and colleagues (1973) showed morphological vesicle depletion and the elevated plasma membrane area under 10 Hz stimulation (i.e. FF), as reported by others (Heuser and Reese, 1973), but they did not get an equivalent result under a lower frequency of stimulation, 2 Hz where there was neither a substantial reduction in the amount of SVs nor evidence of any coated vesicles. Moreover, a 10 Hz stimulation for 20 minutes led to an increased number of dimples (representing exo-endocytosis events) near the AZ but the number and location of SVs were unchanged during the first minute of recovery when endocytosis would predominate. Additionally, under quick-freeze procedure, the image of dimples remained the same during 2, 5, and 10 ms after initial stimulation, and they were also found inside the AZ. Vesicles were often observed to form narrow pores while in contact with PM under conditions in which neurotransmission occurred. Based on these observations, Ceccarelli and colleagues proposed the mechanism of KR in which there was vesicular retrieval on the spot without the vesicle collapsing into the PM and losing its identity (Harata *et al*, 2006).

There is strong evidence for KR using preparations with fluorescently labelled SVs. SVs can be filled with FM dyes during recycling, and subsequent rounds of stimulation evokes these fluorescent dyes to exocytose. Direct measurement of this dyes to determine properties of exocytosis has been used for a substantial time period (FM dyes first used in

the 1990s). Work carried out by Richard Tsien and colleagues (Aravanis *et al*, 2003; Harata *et al*, 2006) and earlier by Stevens and colleagues (Stevens and Williams, 2000) suggested that whilst some SVs underwent exocytosis with release of FM dye, other SVs underwent exocytosis without the release of the dye. This was due to the fact that FM dye takes time to depart from the vesicle membrane after it is exposed to the extracellular buffer following exocytosis and if the initial FP formed closes quickly ($<0.5s$) the dye will not be released, although glutamate will be, and this represents KR. For FF all dye will be released. The use of bromophenol blue (BPB) also revealed that there was a significant proportion of FM dye that was retained in a BPB sensitive pool. BPB will quench FM dye fluorescence but it is membrane impermeable. However, BPB is a small molecule and so it can penetrate into the vesicles through fusion pores formed during exocytosis even though these pores maybe too short lived for FM dyes to depart and escape. However, under such circumstances the FM dye fluorescence will be quenched by the BPB. However, vesicles undergoing FF will lose all the dye in FM fluorescence and so this reduction in FM fluorescence during exocytosis will not be altered by BPB. The fact that significant proportion of FM dye could remain in a BPB sensitive pool allowed one to interpret that this pool of SVs must be undergoing KR (Rizzoli and Jahn, 2007).

The KR mode of exocytosis is regulated through various mechanisms, including the Ca^{2+} level and the presence or absence of various proteins (Dyn, myosin, or actin cytoskeleton). As previously mentioned, KR is the prevalent exocytosis mechanism used under low frequency stimulation whilst FF is the dominant mechanism for high frequency. This result would appear to suggest that a lower increase in $[Ca^{2+}]_i$ may induce KR whilst a higher level may induce FF. However, Ashton and colleagues (Bhuvana, 2015; Singh, 2017) have found that it is the RRP that undergoes KR and this is released under mild stimulation whilst the RP undergoes FF and this would only be released under high frequency stimulation. Furthermore, the RRP SVs docked at the AZ release sites will be nearest to the Ca^{2+} channels involved in release and so these SVs will see the highest local $[Ca^{2+}]_i$

whereas the RP SVs that come on line are exposed to a lower $[Ca^{2+}]_i$ as they get activated and move and fuse at the AZ after the RRP SVs. Importantly, it was shown that an increase of extracellular calcium concentrations shifted the preferred mode of exocytosis to the KR mechanism in calcium dependent manner (Ales *et al*, 1999). The level of Ca^{2+} has been linked to the regulation of KR via synaptotagmins. Synaptotagmin (Syt) are a family of membrane proteins that are well characterised as a Ca^{2+} sensors that initiate SNARE-dependent vesicle fusion during synaptic transmission (Xie *et al*, 2017). Amongst this large family of Syt, Ca^{2+} interaction with Syt 7 C2A domain could regulate the triggering of the fusion pore opening. Such pore opening through this process is unstable, so that the pore closure leads to KR fusion events (Segovia *et al*, 2010, Neuland *et al*, 2014).

Modification of Ca^{2+} level has also been implicated in the regulation of dynamin and actin meshwork (Cardenas and Marengo, 2016) which may play a role in regulating the fusion mode. Dyn is a large GTPase that has been established to control fission of invaginated pits that are produced during some forms of endocytosis. Dyn forms rings or collars around the necks of budding endocytic vesicles inducing GTP hydrolysis which result in membrane remodelling and eventual fission of the invaginated pit. However, the role of Dyn GTPase activity has also been linked to the regulation of FP expansion (Decamilli *et al*, 1995; Warnock and Schmid, 1996; Ramachandran, 2011; Anantharam *et al*, 2011). Samasilp *et al* (2012) showed that under elevated stimulation, Dyn I is dephosphorylated at Ser-774 site by CN and this leads to an association between Dyn I-syndapin binding, but that disruption of this interaction may limits FP (Samasilp *et al*, 2012). Recently, Wu *et al* (2019) reported that most Ca^{2+} induced exocytosis occurs through the KR mode; author referred to this as subquantal mode because in chromaffin granules not all catecholamine is release by KR mode. The study proposed that this releasing mode is promoted by Dyn I because in the absence of it, substantial increase of FF was identified (Wu *et al*, 2019).

Actin microfilaments, in conjunction with NM-II, have also been suggested to regulate KR. Doreian *et al* (2008) demonstrated that at low frequency stimulation, actin microfilaments were found to play an important role in stabilising the KR fusion event. Under increased stimulation, actin was disrupted and FF fusion became abundant. These authors tried to correlate the activity of NM-II with this cytoskeleton-dependent control of the fusion event since inhibition of NM-II or blockade of MLCK led to perturbation of FP dilation during increased stimulation frequencies which maintains the granule in KR mode of exocytosis (Doreian *et al*, 2008). These results were in chromaffin cells, which are distinct from nerve terminals. Ashton and colleagues (Bhuva, 2015; Singh, 2017) have actually found that NM-II can regulate the KR mode of the RRP of SVs in nerve terminals because this mode is switched to FF if the motor protein activity is blocked by Blebbistatin. The activator of NM-II does appear to involve protein kinase C (PKC) induced phosphorylation (Bhuva, 2015; Singh, 2017). Others have found that inhibition of NM-II with Blebbistatin led to a decreased mobility of the granule near to the AZ. A reduction in FP expansion speed and longer FP life times were identified when actin microfilaments were disassembled with cytochalasin D. This study in chromaffin cells demonstrated an increase spike half widths in amperometric recordings without change in quantal size after either NM-II or actin activities were silenced. These authors proposed that actin and NM-II facilitate release from individual chromaffin granules by accelerating dissociation of catecholamines from the intragranular matrix potentially via generation of mechanical forces which is distinct from regulating the exocytotic mode and such regulation would not occur in glutamatergic SVs in which glutamate is not bound to a matrix (Berberian *et al*, 2009).

Thus, there has been much research suggests that regulation of the KR mode of exocytosis involves the contribution of numerous proteins, including Dyn, NM-II, and actin, and these may be regulated by Ca^{2+} levels. Further, investigation into the precise properties of such proteins would be helpful in furthering the understanding of the mechanism mediating the release mode of the SVs.

1.9 AIMS

The research in this thesis involves studying both the different pools of SVs and also investigating further the properties of the distinct modes of exocytosis. This work will all be carried out using rat cerebrocortical synaptosomes from adult animals. Some of the research represents a total new area for research for the Ashton laboratory whereas others represents a continuation of research that has been going on in the lab for over 10 years.

The areas to be investigated in this thesis are as follows:

(i) Release of the silent pool (SP) of SVs. This pool is not normally released but previous work on hippocampal cultured cells utilising electrophysiological measurements suggested that roscovitine is able to induce the release of the SP of SVs. Thus, we will employ Roscovitine and determine whether we can indeed induce extra glutamate release from treated nerve terminals. Provided that we can study the SP we will perform further experiments to determine: (a) the calcium requirements for SP release; (b) the voltage dependent Calcium channel requirements for SP release; (c) the regulation of the SP release by Protein Kinase C; (d) the release of the SP following the stabilisation of actin microfilaments; (e) a correlation between roscovitine induce release of the SP with changes in the phosphorylation of Syn 1 at various Ser residues that are regulated by distinct protein kinases and phosphatases.

(ii) the use of Fluoxetine to study the silent pool of SVs. Recently, Jung et al (2014) suggested that this anti-depressant actually can induce the release of the SP of glutamatergic SVs. Thus, we will seek conditions to induce the SP of GLU containing SVs in synaptosomes following treatment with Fluoxetine. We will establish that any extra release is truly coming from the SP.

(iii) The role that actin cytoskeleton has on the release of distinct pools of SVs. The effect that actin disassembly (using Latrunculin) or actin microfilament stabilisation (using Jasplakinolide) has on the release of the RRP and the RP and also what effect this might

have on the modes of exocytosis can be determined. This will be studied by measuring GLU release evoked by either high potassium (HK5C) or Ionomycin (ION5C). Subsequently, SV exocytosis can be studied using FM2-10 dye release and any differences in the requirements for these 2 stimuli may reveal differences in the Dyn dependent KR mode (induced by ION5C) and the NM-II dependent KR mode (induced by HK5C). This work is required before one could investigate any role of this cytoskeleton on the release of the SP.

(iv) Determining whether Dyn is already present on a membrane compartment during synaptic vesicle exocytosis involving the Dyn dependent KR mode. This can be done using a drug MITMAB that prevents dynamin binding to membranes.

(v) Determining whether the Dyn dependent KR mode requires the activity of endogenous PKA whilst the NM-II dependent KR mode does not. This will be investigated by inhibiting PKAs with KT 5720.

(vi) Determining whether the Dyn dependent KR mode and the NM-II dependent KR mode can be regulated by distinct voltage dependent Calcium channels. This will be investigated by blocking P/Q, N and L-type channels with distinct toxins/drugs and investigating whether this regulates the distinct modes.

Chapter 2:

Methods and Materials

2.1 Materials

2.1.1 Buffering Reagents

- Physiological buffer (L0): 125 mM NaCl, 5 mM KCl, 1 mM MgCl₂, 20 mM Hepes and 10 mM glucose; pH 7.4. Note, where required, 5 mM Ca²⁺ was added to this (final concentration).
- Homogenisation sucrose buffer: 320 mM sucrose and 10 mM Hepes; pH 7.4
- Stock high potassium (HK0) buffer: 130 mM KCl, 20 mM Hepes, 1 mM MgCl₂ and 10 mM glucose; pH 7.4. Note, where required, 25 mM Ca²⁺ is added to this such that when diluted the final concentration of KCl is 30 mM and that of CaCl₂ is 5 mM.
- Bioenergetics buffer: 120 mM NaCl, 14 mM D-glucose, 3 mM KCl, 2 mM MgSO₄, 12 mM NaSO₄, 1.3 mM CaCl₂, 0.4 mM KH₂PO₄, 10 mM pyruvate, 60 μM bovine serum albumin (BSA), pH 7.4. This was employed as previous synaptosomal bioenergetics studies in the Seahorse flux analyser has utilised this buffer (Seahorse Bioscience, N.D).

2.1.2 Stimulation Solutions

The current study employed three 5 mM Ca²⁺ based stimuli, High potassium (30 mM K⁺; HK5C), Ionomycin (5 μM ionomycin; ION5C) and 4-aminopyridine (1 mM 4-aminopyridine; 4AP5C) to induce SV release. It has been established from previous studies by Ashton and colleagues that 5 mM Ca²⁺ with HK or ION containing buffers give maximal release of glutamate (GLU) from both the RRP and the RP, and equivalent amount of 4AP only gives maximal release of GLU exclusively from the RRP (see appendix 1). This latter stimulus, therefore allows investigation of RRP separately from the RP using the assays listed below (Bhuva, 2015; Singh, 2017; Rostron, 2019). Ca²⁺ free solutions; HK0 and 4AP0, were employed for HK5C and 4AP5C as a basal condition for

GLU assays (such Ca²⁺ free stimuli may induce some non-vesicular glutamate release), while L0 was used for the FM 2-10 dye assay as this only measure vesicular exocytosis which is totally Ca²⁺ dependent. The natural characteristic of ION where it can insert into terminal membranes and also internal membranes to cause Ca²⁺ release from intracellular stores disallowed the possibility of creating Ca²⁺ free solution contacting ION alone, therefore L0 was used instead. A. Ashton has established through comparison studies that L0 produces indistinguishable results from HK0 and 4AP0 for FM 2-10 dye, and therefore L0 was used as the control condition for these experiments, as the latter two have no impact upon vesicular release (as mentioned above).

2.1.3 Drugs employed and their final concentrations (all Dissolved in DMSO unless specified otherwise)

All optimum concentration of the following drugs have been established previously in A.Ashton's laboratory.

- Roscovitine (10 µM, 33 µM, 100 µM, 200 µM)
- Dynasore (80-160 µM)
- Blebbistatin (50 µM)
- Pitstop 2TM (15 µM)
- Phorbol 12-myristate 13-acetate (PMA) (40 nM, or 1 µM)
- Go6983 (1 µM)
- KT5720 (2 µM)
- Latrunculin (LAT) (15 µM)
- ω-Conotoxin GVIA (CONO) (1 µM)
- ω-Agatoxin TK (AGA) (50 nM)
- Nifedipine (NIF) (1 µM)
- Jasplakinolide (JASP) (2.5 µM)

- Cyclosporine A (Cys A) (1 μ M)
- Okadaic acid (OA) (0.8 μ M)
- Fluoxetine (1 μ M, 200 nM, 100 nM, 60 nM, 40 nM, 20 nM, 5 nM)
- KN-93 (10 μ M)

Drug utilised in bioenergetics measurements (stock and final)

- Oligomycin (32 μ M, 4 μ M Final)
- FCCP (18 μ M, 2 μ M Final)
- Rotenone (50 μ M, and 5 μ M, or 5 μ M and 0.5 μ M Final)
- Antimycin A (50 μ M, 5 μ M or 5 μ M and 0.5 μ M Final)

2.1.4 Other drugs employed

- 1 x sample buffer with DTT for NuPAGE gel system (Life Technologies)
- 1 x NuPAGE MES SDS Running buffer
- 3-5 μ l Unstained MagicMarkTM XP Western Protein Standard
- 3 ml SuperSignalTM West Dura Extended Duration Substrate
- 15 ml RestoreTM PLUS Western Blot Stripping Buffer
- 35 milli-Units (mUnits) of glutamate dehydrogenase type-II (GDH)
- 1 mM NADPH
- 100 μ M FM 2-10 dye
- 5 μ M Fura-2 AM

2.1.5 Measuring Instruments

- Tecan Genius Pro Infinite 200 multimode microplate reader.
- Seahorse Bioscience – Xfp extracellular flux analyser
- Motor driven, Teflon (pestle)-based homogeniser (Similar to a Potter-Elvehjem tissue homogeniser)

- Beckman-Coulter Avanti® J-25 series centrifuge, utilising the JA-17 rotor.
- PowerEase 500 power packs.
- Thermo Fisher – iBlot and iBlot 2.
- NuPAGE gel electrophoresis tanks and pre-cast gel system
- Bio-Rad ChemiDoc XRS+ imaging system with Image Lab software version 3.0.1.

2.1.6 Antibodies used for Western blotting

For western blot analysis, specific commercially available antibodies shown in figure 2.1 were employed to investigate the phosphorylation profile of Syn-I. All antibodies were sourced from Santa Cruz Biotechnology, Inc., USA.

Primary antibody raised against	Dilution	Secondary antibody	Dilution
<u>Pan synapsin I</u>	1:2000	<u>Anti-rabbit</u>	1:2000
<u>Phospho-Ser-9 Synapsin I</u>	1:2000	<u>Anti-rabbit</u>	1:2000
<u>Phospho-Ser-553 Synapsin I</u>	1:4000	<u>Anti-rabbit</u>	1:2000
<u>Phospho-Ser-603 Synapsin I</u>	1:1000	<u>Anti-rabbit</u>	1:2000

Figure 2.1: Antibodies employed for Western Blotting

2.2 Preparation of Synaptosomes

A Wister rat was killed by cervical dislocation and the cerebral cortex was removed. The dissected brain tissue was then homogenised in chilled homogenising buffer (320 mM sucrose, 10 mM Hepes, pH 7.4). The suspension was centrifuged at 1941 x g for 10 min at 4°C with Beckman 25 centrifuge. The pellet was discarded, and the supernatant centrifuged at 21,075 x g for 20 min at 4°C. The supernatant was discarded, and the pellet

was resuspended and homogenised in 40 ml chilled, gassed basal physiological buffer. Supernatant was then re-centrifuged at 21,075 x g for 20 min at 4°C. The supernatant was discarded, and pellet resuspended and homogenised in gassed L0 (varying volumes that depended upon the assay being employed). The resulting synaptosomes (P2) were kept on ice and gassed with oxygen until use. Note that synaptosomes were resuspended in physiological buffer that has been saturated with oxygen.

2.3 Glutamate Release Assay

This glutamate (GLU) release assay was developed by Nicholls *et al* (1987) and adapted by Sim *et al* (2006) for use on a fluorescence plate reader. A volume of 2 ml synaptosomes (from an 8 ml initial suspension) were centrifuged with L0 and resuspended in 1 ml of L0. The resulting suspension was then stimulated for 90 sec with HK5C (induce all the releasable vesicles to exocytose). Synaptosomes were then centrifuged, resuspended in L0, centrifuged and resuspended in L0, this ensured complete removal of the stimulus. The synaptosomes were then incubated at room temperature (RT) for 10 min to allow all the originally stimulated exocytosed SVs to recycle. Subsequently, the appropriate drug or equivalent amount of drug solvent (DMSO only in control tests) was added to the synaptosomes and these were incubated at 37°C for 5, 10, or 20 min depending on the particular drug being used. The samples were then washed, and resuspended in 1.6 ml of L0 containing the relevant concentration of drug being tested (control simply had the equivalent amount of DMSO added) in order to prevent the reversibility of the drug action.

A volume of 121 µl aliquots of the resulting sample was then added to each of 12 wells of a row of a Grenier 96 well microtitre plate (black with transparent bottom); 20 µl of L0 was also added to these wells. Subsequently, 10 µl NADP⁺ (20 mM stock NADP⁺, 1 mM final conc.) and 9 µl (36 mUnits final conc.) of glutamate dehydrogenase type-II (GDH) were then added to each well and synaptosomes were incubated at RT for 10 min. At this

stage, non-evoked extracellular glutamate is converted to α -ketoglutarate by GDH in the presence of NADP^+ which is itself converted to NADPH (see the equation below).



The NADPH is measured by its fluorescence; this enables all the non-evoked GLU to be reacted and a background fluorescence to be established. After the incubation, an appropriate stimulus without Ca^{2+} (e.g. HK0) was added to wells 6-12 and the corresponding Ca^{2+} containing stimulus (e.g. HK5C) was added to well 1-5. For ION, L0 was added to the basal sample (6-12) whilst L0 + 5 mM Ca^{2+} plus 5 μM ION was added to wells 1-5. For 4AP5C, 4AP0 was added to wells 6-12 whilst 1 mM 4AP plus 5mM Ca^{2+} was added to wells 1-5.

The plate was inserted into Tecan GENIOS pro infinite 200 plate reader (at excitation wavelength: 340 nm; emission wavelength: 465 nm; gain: 100; read mode: bottom) and measurements were made for 21 cycles for wells 1-9 (this represented just over 5 minutes at which times all the release GLU had reacted with GDH). After these measurements, 10 μl of L0 was added to wells 7-9 and to wells 10-12, 10 μl of 1 mM GLU (freshly prepared from 679 mM stock glutamate) was added. The plate was reinserted into the plate reader, and the effect of the addition of this stock GLU (10 nmol) was measured for 15 cycles using the same settings as above but just measuring wells 7-12. Subtracting the average background values (6-9) from the average stimulation values (1-5) provided a measure of the Ca^{2+} dependent GLU release. This was in arbitrary fluorescent units (AFU). The AFU measured following the inclusion of 10 nmol GLU enables one to convert the data from AFU to nmol of evoked GLU release. Also, since 10 nmol GLU was added after the measurement of each row of the microtitre plate, this value of fluorescence could be utilised to correct for the sensitivity of the assay in each row which allows a direct comparisons between rows containing different conditions within the same experiment and this can also be used between different trial of experiments to ensure all samples

measure are normalised to similar sensitivity. The corrected values for all relevant stimulated samples from all experiments were averaged and the SD determined as were the corresponding basal release mean determined plus its SD. The basal mean was subtracted from the release in the presence of the stimulus to produce the Calcium dependent release. The SD for the release induced by the stimulus was squared and was added to the square of the SD for the basal condition. The square root of this sum represented the SD of the Calcium dependent evoked release. The two conditions were compared using two-tailed Student's t-test, with a significance threshold of 0.05. This was following the averaging of at least 3 independent repeats of the experiment (see further comments below).

2.4 FM 2-10 Styryl Dye Release Assay

A volume of 1 ml synaptosomes was taken from an initial 8 ml final resuspension stored in ice, prepared as outlined above and pelleted, and re-suspended in 1 ml L0 at room temperature. 100 μ M of FM 2-10 dye (final) was added to this and incubated for 60s followed by stimulation with HK5C for 90 sec.

After the incubation, the stimulus was removed via centrifugation and the synaptosomes were resuspended in 1 ml L0 containing FM 2-10, and spun down again (to ensure stimulus removed), it was then resuspended in buffer containing 100 μ M FM2-10 dye and incubated for 10 min; this allowed all SVs labelled with FM dye to recycle. Subsequently, synaptosomes were treated with the desired amount of drug or equivalent amount of DMSO (control samples) and incubated at 37°C for 5-20 min. A 4 μ l of 250 mM advasep-7 (1 mM final) was then added to the mixture (at RT), this removes the FM 2-10 dye from the synaptosomal plasma membrane and reduces the background fluorescence. The samples were then washed twice and re-suspended in 1.5 ml of L0 along with the corresponding concentration of the drug or DMSO.

A volume of 160 μ l of aliquots were then added to the 8 wells of Greiner 96 well microtitre plate (black with opaque bottom). A Tecan GENIOS Pro infinite 200 plate reader was used

to determine fluorescence measurement with the following settings; excitation wavelength: 465 nm; emission wavelength: 555 nm; gain: 40; read mode: top; number of cycles: 461. Each well was measured individually (just over 2 min per well)

Just before measuring the fluorescence, the synaptosomes in the well were stimulated using the relevant stimulus (HK5C, ION5C, or 4AP5C) or were subjected to the equivalent amount of L0. For each row, 4 wells were stimulated and 4 just had basal buffer added (L0). These steps repeated for the eight rows of the plate for different treatment conditions. The precise treatment conditions were repeated again during the same experiment, but this time, the order of wells that had stimulus or basal buffer added was changed to ensure that there were at the end of the experiment 8 readings for basal and 8 for stimulus and that the time before the measurement of each well were on average equivalent. After the experiment, the basal data were subtracted from the average stimuli data (for the relevant treatment). Prior to this, all individual wells were corrected such that they had the equivalent starting value of FM 2-10 dye fluorescence. This normalisation allowed the one to directly compare each individual experiments. This value represented the true Ca^{2+} -dependent FM dye released, expressed in terms of decrease in fluorescence.

The actual starting fluorescence allowed one to see whether the drug treatment perturbed the total dye labelled SV content prior to stimulation (see appendix 3).

Significance values were calculated using a two-way student's t-test with a significance threshold of 0.05. This was following a minimum of 3 independent repeats of the experiment.

2.5 Fura-2 Assay

2.5.1 Background

The current study has used Fura-2-acetoxymethyl ester (Fura-2-AM) assay to measure the evoked change in the level of intracellular Ca^{2+} level ($[\text{Ca}^{2+}]_i$). Fura-2-AM is a Ca^{2+}

insensitive, cell permeable ester which when it is taken up by a cell, its AM is cleaved off by esterases. Following this procedure, the drug (free Fura-2) is unable to cross the plasma membrane but it is now Ca^{2+} sensitive, which binds to the Ca^{2+} within the cell. When it combines with Ca^{2+} Fura-2 produces an increase in fluorescence when excited at a wavelength of 340 nm and fluorescence measured at 535 nm. When it is in a Ca^{2+} free environment, Fura-2 produces a maximum fluorescence when excited at a wavelength of 380; the emission wavelength of Fura-2 is always 535. Hence the ratio between the collected 340:380 fluorescence values is proportional to the concentration of $[\text{Ca}^{2+}]_i$ (nM). This can be calculated via the Grynkiewicz equation (Grynkiewicz *et al.*, 1985):

$$[\text{Ca}^{2+}]_i(\text{nM}) = K_d \times B \times \frac{(R - R_{\min})}{(R_{\max} - R)}$$

K_d represent the constant of Ca^{2+} binding: 224 nM; B is the ratio of average fluorescence at 380 nm under Ca^{2+} free and Ca^{2+} bound condition; R stand of the ratio of 340/380; R_{\min} is 340/380 ratio in Ca^{2+} free environment; R_{\max} is 340/380 ratio in a Ca^{2+} saturated environment.

2.5.2 Procedure

Cerebrocortical synaptosomes were prepared by the above method and resuspended in 10 ml L0. Then 50 μg Fura-2-AM in 50 μl DMSO (1 mM stock; 5 μM final) was added and the synaptosomes were incubated for 30 min at 37°C. Subsequently, 3 ml L0 were added to this suspension and 12 x 1 ml fractions were taken, then spun down in an Eppendorf centrifuge, each fraction was then washed with 1 ml L0 at room temperature before being centrifuged again. These samples were resuspended 12 x 0.7 ml L0 (cold buffer) pooled and kept on ice and oxygenated. When required, a 1 ml aliquot of stimulus was added to 0.25 ml (130 mM K^+ , 25 mM Ca^{2+}) i.e. HK5C, and incubated for 90 sec. The samples were then spun down and resuspended in 1 ml L0 following another centrifugation (to reproduce the pre-stimulation used for GLU and FM dye release assays) and then resuspended in

0.88 ml L0 (final volume 1 ml as pellet has some volume) before being incubated for 10 minutes at room temperature. Then, either control solvent or drug was added and the resulting synaptosomes were incubated for 5-20 min at 37°C before being centrifuged. Subsequently, the sample was washed with 1 ml L0 buffer and recentrifuged before being resuspended in 1.6 ml L0 containing relevant drug or solvent. 12 x 0.12 ml aliquots were added to wells 1-12 of a black flat bottom plate and 40 µl L0 was also added to these wells. The plate was then inserted into the plate reader.

The plate reader was programmed with the following settings; measurement mode: top; excitation wavelength: 340 or 390 nm; emission wavelength: 535 nm; gain 30; well kinetics 40 (no injection) or 160 (injection); injection volume: 40 µl. Pump A contained: 130 mM K⁺ containing buffer, 25 mM Ca²⁺ or L0 plus 25 mM Ca²⁺, or 5 mM 4AP in L0 plus 25 mM Ca²⁺. Pump B contained L0. Fluorescence was measured from each well individually. The first well was read for 40 cycles at the excitation wavelength of 340 nm and emission wavelength 535 nm, which is equivalent to approximated 10s, providing an average, baseline-fluorescence value. Subsequently, 40 µl of either a particular stimuli or L0 was injected into the well and the well was measured for 160 cycles, which took ~40 sec, at the same excitation and emission wavelength. For the next well, a similar procedure is used, but this time the excitation is at 390 nm (this was the nearest filter available to 380 nm, but it had a bandwidth which includes 380 nm).

The benefit of using two excitation wavelengths is that it allows calculation of the 340/390 ratio metric value for these wells. For each row, six wells were injected with 40 µl of a stimuli (for ION, it could not be injected and thus it was added to the relevant well just prior to the injection of L0 containing 25 mM Ca²⁺ (final concentration of it was 5 µM)), and other six wells were injected with 40 µl of L0. The 340/390 ratio calculated for L0 treated wells were subtracted from the ratio from stimulated wells in order to determine the change in [Ca²⁺]_i evoked by the stimulation alone. Hence each row produces three 340/390 ratio sets for stimulation and control conditions of the drug treatment.

Following the measurements of all 12 wells in a row, aliquots of 2.25 mM Ca^{2+} and 0.3% Triton X-100 (final concentrations) were added to the six wells that had been injected with a stimuli (final volume: 240 μl). For the other six wells with L0, aliquots of 15 mM EGTA and 0.3% Triton X-100 (final concentration) were added. Subsequently, all 12 wells were measured for 40 cycles, first at the excitation wavelength 340 nm then at excitation wavelength 390 nm. Data collected through this procedure allowed one to calculate R_{max} and R_{min} from samples treated with 2.25 mM Ca^{2+} and 15 mM EGTA respectively. A spreadsheet was designed which used the Grynkiewicz equation (see equation above) to calculate the concentration of $[\text{Ca}^{2+}]_i$. Significance values were calculated using two-tailed student's t-test, with a significance threshold of 0.05, after the experiment had been performed at least 3 independent times.

2.6 Data analysis

The data shown herein are the average of several independent experiments (n). All basal values and stimulated values from all experiments were averaged. The average basal value was subtracted from average stimulated value with the statistical analysis performed using Microsoft Excel. The values were statistically analysed by comparing control and tested values using two-tailed student's t-test with $P < 0.05$ being considered as significant. The results were shown in graph as a percentage of maximum control. For a convenience in presentation, selective data points at an interval of 10 sec were shown, wherein the error bar indicates the standard error of mean (S.E.M). In chapter 3-6, 'n' value shown in the figures represents is the total number of independent replicates performed whilst in the legends of figure this same n values is shown together with the total number of independent experiments. Previously, A. Ashton had ascertained that the data exhibited a normal distribution with these types of experiments and that two-way ANOVA produced exactly the same P values as the student's t-test. Thus, we used the student's t-test in the experiments herein.

2.7 Western Blotting

2.7.1 Sample Preparation

Synaptosomes were prepared by above method, pre-stimulated with HK5C, incubated for 10 mins at RT and then treated with the relevant drugs or DMSO (control) for 5 min at 37°C. Following this treatment and the relevant washes, the appropriate stimulus (HK5C, ION5C, 4AP5C or L0) was applied for various time points (2, 15, 30, 120 sec) before the reaction was terminated by the applying LDS (lithium dodecyl sulfate) sample buffer containing reducing agent DTT (dithiothreitol). Samples were then heated for 10 min at 70°C. Subsequently, samples were stored at -20°C until required.

2.7.2 Bradford Assay

Protein concentration in each sample was determined using Bradford assay. Final concentration of the protein was adjusted to 1.5 mg/ml. Bradford assay measurements were read on a Tecan GENIOS Pro infinite 200 plate reader (absorbance wavelength: 595 nm). Note an equivalent sample to that used on stimulation for western blotting was used for the protein assay, but no LDS was added. Samples were solubilised in 1 M NaOH and then diluted to 0.25 M NaOH. All standards also dissolve in 0.25 M NaOH.

2.7.3 Electrophoresis and Transfer

The frozen stored samples were re-heated for 10 min at 70°C before carrying out electrophoresis on 4-12% NuPAGE™ gels in the NuPAGE™ gel system from Life Technologies using NuPAGE™ MES running buffer. Western blotting was then performed using iBlot™ or iBlot2 from Thermo Fisher, transferring the proteins to PVDF membrane. The membrane was subsequently blocked for 60 min with either 30 ml of blocking buffer (3% dried milk powder, 1% Tween-20 in tris buffered saline (TBS); pH 7.4) or 15 ml of Startingblock™ T20 blocking buffer. The blocking buffer was discarded and the blots were washed for 10s with 1% Tween-20 in TBS.

2.7.4 Probing and Chemiluminescence

After the transferring of the PVDF membrane, it was then probed for the study of specific phosphorylation sites on proteins by adding 10-15 ml buffer (dried milk powder, 1% Tween-20 in TBS; pH 7.4) containing specific primary antibody for 60-90 min at room temperature (see table above for dilution of antibody employed). Antibody solution was removed from the membrane and membrane was washed for 6 x 5 min with 25 ml wash buffer (0.5% Tween-20 in TBS; pH 7.4). Wash buffer was then discarded and a HRP conjugated secondary antibody, relevant to the primary antibody, was then added. This was added to 10-15 ml antibody buffer and incubated for another 60-90 min at room temperature.

After the incubation, antibody buffer was removed and washed using same procedure. Then, PVDF membrane were incubated with 3 ml SuperSignal™ West Dura Extended Duration Substrate chemiluminescence agent for 5 min and then its bands were visualised using BioRad ChemiDoc XRS+ with Image lab software. For re-probing of blots, they were stripped using 15 ml Restore™ PLUS Western Blot Stripping Buffer and blocked ready for antibody probing (Bhuva, 2015).

2.7.5 Quantification of bands

The combination of ChemiDoc XRS+ system with Image Lab software reads the chemiluminescence of protein bands on the membrane, where signal intensity is directly associated with the amount of protein or phospho-protein in the band of interest. However, the signal intensity is also closely related to duration of exposure, whereby a longer exposure time means higher chance of error to occur in band quantification because of over-exposure. Thus each blot was developed for many exposure times to ensure the linearity of the chemi-luminescence signal (see appendix 2).

Such semi-quantification analysis also employed internal controls whereby bands are quantified relative to each other and the relevant internal control. Bands of interest were quantified via the volume calculation tool from the Image Lab software where the user could draw a box around the bands of interest and the software calculates average signal intensity within the box (higher the intensity of the box means higher reading in arbitrary units). In addition, the software could also reduce the localised errors as it accounts for changes in background signal intensity between bands, reducing artefacts potentially been detected by uneven background signal. Once all the bands from the blot are quantified through this method, they were expressed as a percentage of the unstimulated control sample (in order to get the relative quantities of protein present in the given set of bands). Note usually the phospho-band was detected and quantified. Then the same blot was stripped and re-probed for the total content of that protein (pan antibody). Then the phospho-bands could be normalised to the total pan-content of the band.

2.8 Bioenergetic measurement with Seahorse XF machine

2.8.1 Background

The XF Cell Mito stress test measured the mitochondrial respiratory activity of synaptosomes under various conditions. Mitochondria are acknowledged as an essential energy supplier for the cell and it is responsible of producing the majority of energy in the form of ATP through numerous pathways (Johri and Beal, 2012). Hence such measurement could indicate whether any of the drugs employed in this study might perturb the bioenergetics of the terminals. This could indicate a non-specific action of such drugs. The protocol measured key parameters of mitochondria function via the direct measurement of oxygen consumption rate (OCR) from the synaptosomes. The machine used modulators of respiration which focused on the components of the electron transport chain (ETC) of the mitochondria; thus, revealing the key parameter of metabolic function (see diagram 2 and 3). The compounds (oligomycin, FCCP, and rotenone/anitimycin A)

were serially injected into the well and these revealed levels of ATP production, maximal respiration, and non-mitochondrial respiration. Proton leak (represents a remaining basal respiration not coupled to ATP production, hence showed the mitochondrial damage) and spare respiratory capacity (measure of the cell's ability to respond to increased energy demand) could then be calculated using these parameters then compared to basal respiration (Seahorse Bioscience, N.D)

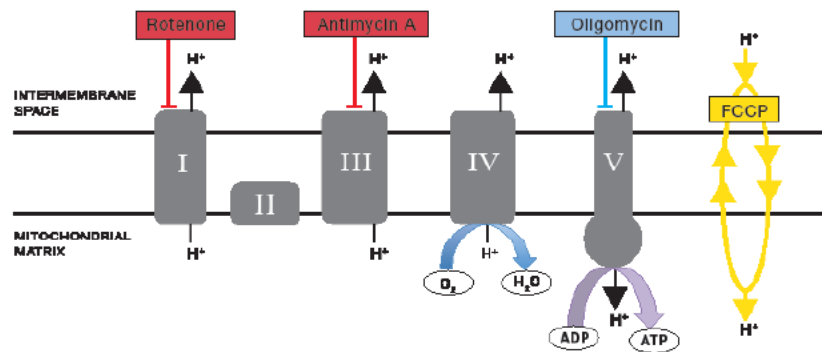


Figure 2.2. Diagram showing the key parameters of mitochondrial respiration measured by the instrument; Oxygen consumption rate (OCR) is a parameter to study mitochondrial function (Taken from Seahorse Bioscience, N.D).

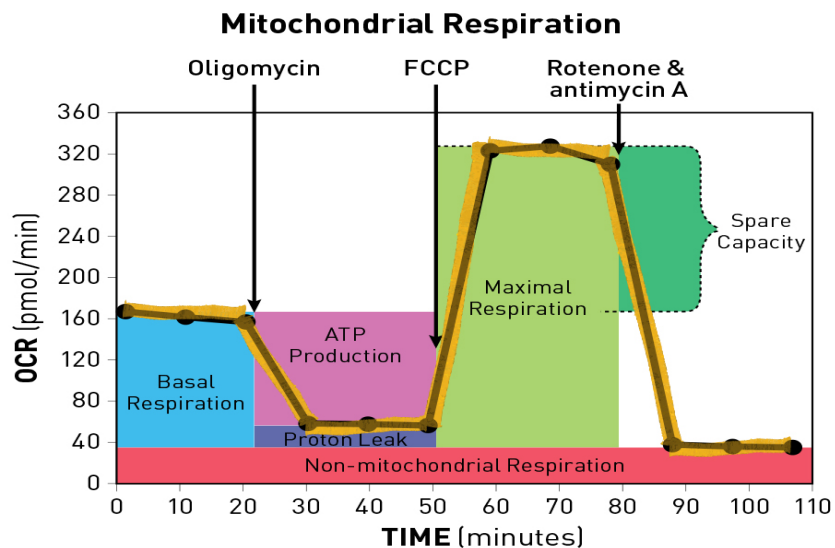


Figure 2.3. Diagram showing the complexes in electron transport chain (ETC) that each modulators targets (Taken from Seahorse Bioscience, N.D).

Oligomycin ($C_{45}H_{74}O_{11}$) disturbs ATP synthase and the injection of this drug leads to the decrease in OCR which represents the basal mitochondrial respiration associated with cellular ATP production. Carbonyl cyanide-4 (trifluoromethoxy) phenylhydrazone (FCCP) ($C_{10}H_5F_3N_4O$) is an uncoupling agent that collapses the proton gradient and disrupts the mitochondrial membrane potential. Consequently, electrons flow into the electron transport chain (ETC) and this leads to maximum oxygen consumption by the cell, such measurement could then be calculated to reveal spare respiratory capacity. The third injection included a combination of rotenone ($C_{23}H_{22}O_6$) (complex I inhibitor) and antimycin A ($C_{28}H_{40}N_2O_9$) (a complex III inhibitor). These stopped the mitochondrial respiration and allowed the determination of the non-mitochondrial respiration driven by processes outside the mitochondria (see Fig 2.3) (Seahorse Bioscience, N.D).

2.8.2 Method

A volume of 0.04 ml of the final synaptosomes suspension (from 8 ml total) was centrifuged and resuspended in 1.2 ml of the bioenergetics solution containing 4 mg/ml bovine serum albumin (60 μ M) (see sections 2.1.1 for buffer composition: note this was carefully titrated to pH 7.4 just prior to its use after 10 mM pyruvate had been added). 0.175 ml of this synaptosomal suspension was aliquoted into wells B-G of XF Miniplate which has been pre-treated with 1:1500 dilution of a 50% solution of polyethylenimine (plate coated overnight, and then solution removed and plate allowed to dry). The synaptosomes were then spun in an Eppendorf A-2 MTP swing out rotor for 20 min at 4°C at 2000 x g for synaptosomes adherence onto the well floors. The supernatant in the wells were removed from the immobilised synaptosomes and these were then treated with 37°C bioenergetics buffer containing the required concentration of selected drug dissolved in DMSO into wells A-D or buffer and DMSO only into wells E-H for control. This was incubated for 5-20 min at 37°C prior to two washes at RT, with the bioenergetics buffer. Note that wells A and H are a background control hence it just has buffer and DMSO added without synaptosomes.

A sensor cartridge was hydrated overnight at 37°C in calibration buffer (supplied by company but represents phosphate buffered saline). The relevant drugs for the mitochondrial stress test assay were dissolved in DMSO, apart from antimycin A which was in ethanol, and were added into the injector ports (32 µM oligomycin in port A, 18 µM FCCP in port B, 50 µM or 5 µM rotenone/antimycin A in port C) prior to the experiment. The sensor cartridge was added to XP extracellular flux analyser to calibrate and the loaded miniplate was added. The synaptosomes had to be fresh so only one experiment was run per synaptosomes preparation. The measurement were performed at either 37°C or RT (22-27°C) and the Seahorse XFp flux analyser was kept at 37°C with the inbuilt heater or the heater was not employed and with the aid of a cooling mobile air conditioning unit the temperatures was kept at RT. This was dependent on the actual RT which varied such that the actual measurement temperature varied between 22°C to 27°C.

The machine then measured 3 x 3 min measurement of basal oxygen consumption rate (OCR). Then oligomycin was automatically injected into each well and a further 3 x 3 min measurement performed. Subsequently, FCCP were injected and 3 x 3 min measurements taken. Lastly, rotenone/antimycin A was injected and another 3 x 3 min measurement made. The result enabled one to obtain average oxygen consumption rate (OCR) traces of the wells following the drug treatment (wells B-D) and control (wells E-F), minus the baseline (wells A and H). The data was saved in an Excel spreadsheet and the raw data for each well could then be analysed and such data was then combined with the repeated experiments and produced average values which then could be statistically analysed with two-tailed Student's t-test.

Chapter 3:

Roscovitine and the Silent Pool

3.1 SP SVs are released by HK5C or ION5C following pre-treatment with Roscovitine

The SP of SVs has been largely an enigma because it is not released under normal physiological conditions, and therefore it is difficult to explore its properties. Kim and Ryan (2010) in their research have used Roscovitine, a Cdk5 inhibitor, to induce extra release from hippocampal cultured cells, which they suggested is from the SP. The results from the following research has indicated that it is possible to investigate the properties of the SP by pre-treating synaptosomes with Roscovitine and then evoking release with various stimuli.

3.1.1 100 μ M Roscovitine induced maximum HK5C evoked GLU release

It was essential to establish whether a suitable concentration of Roscovitine could induce more GLU release than just that due to exocytosis of the RRP and RP (see appendix 1 Fig A1). A dose-response curve for Roscovitine action on HK5C evoked GLU release was established. Synaptosomes were pre-treated with 10 μ M, 33 μ M, 100 μ M, and 200 μ M Roscovitine and the GLU release was evoked using HK5C. The results demonstrate that Roscovitine increased the amount of HK5C evoked GLU release in a dose dependent manner with 100 μ M inducing the maximum release (Fig 3.1). As HK5C maximally released the RRP and the RP (see appendix 1 Fig A1), it can be deduced that the extra release must be from the SP. Increasing the concentration of Roscovitine from 100 μ M to 200 μ M failed to produce any further release relative to that induced by HK5C in the presence of a 100 μ M (Fig 3.2).

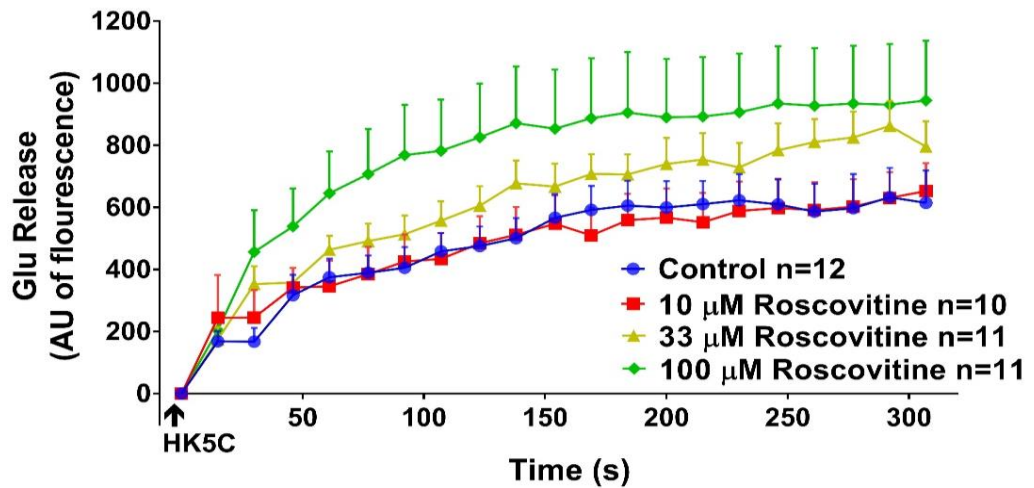


Figure 3.1. Increasing Roscovitine concentration induced greater HK5C evoked GLU release relative to non-drug treated control. Data are mean \pm SEM, N=3 independent experiments; P < 0.05 for 100 μ M i.e. 100 μ M Roscovitine can evoke a significant increase in release of GLU compared to control.

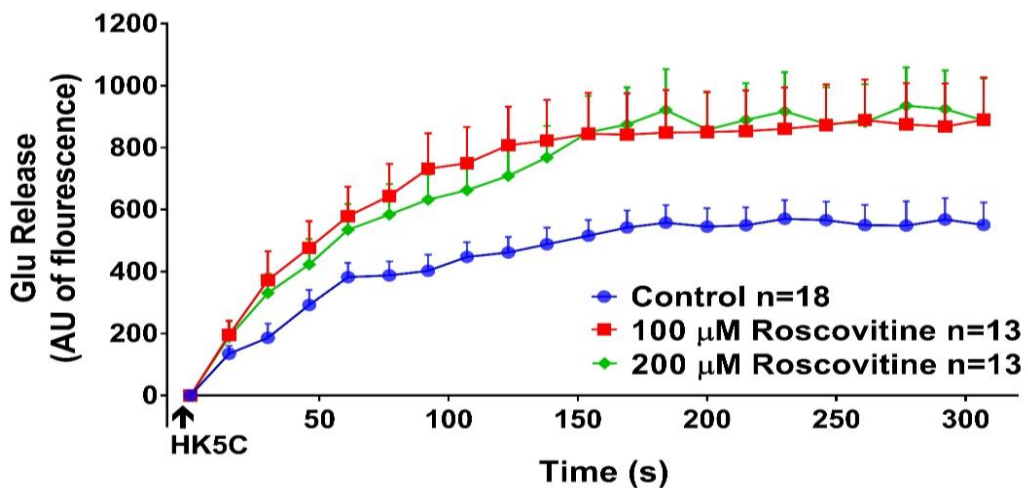


Figure 3.2. 200 μ M Roscovitine does not evoke significantly higher GLU release compared to 100 μ M Roscovitine. HK5C evoked GLU release following treatment with 100 μ M and 200 μ M Roscovitine. Data are mean \pm SEM, N=3 independent experiments; P < 0.05 for both 100 and 200 μ M drug.

3.1.2 ION5C also releases the SP following 100 μ M Roscovitine treatment

Ionomycin (ION) has a different mechanism than HK action but it can induce the maximal release of the RRP and RP in the presence of 5 mM Ca^{2+} (see appendix 1 Fig A1). This ionophore bypasses the requirement for activated Ca^{2+} channels, as it transports Ca^{2+} across the PM, thereby increase the $[\text{Ca}^{2+}]_i$ level throughout the cell. It was important to establish that the SP could be released using ION5C and Roscovitine. Indeed, there was a significant increase in the ION5C evoked GLU release when terminals were treated with 100 μ M Roscovitine (Fig 3.3).

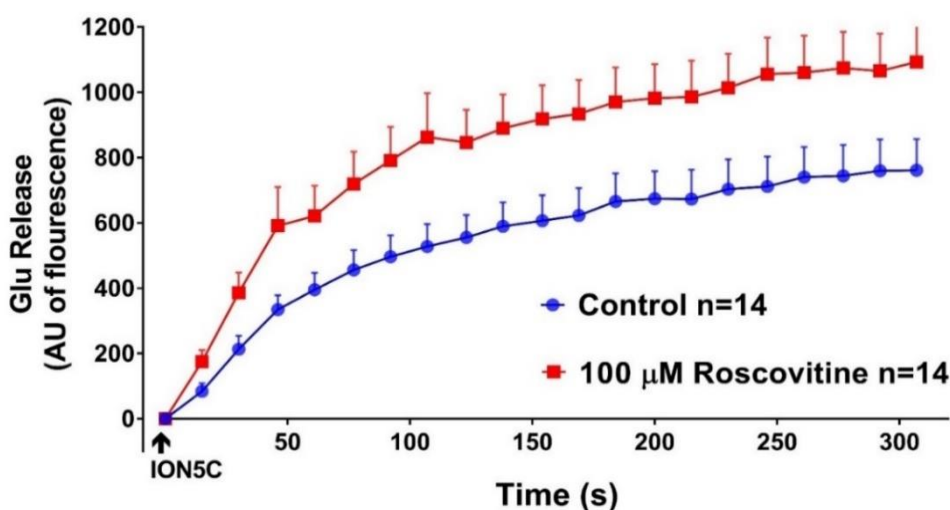


Figure 3.3. 100 μ M Roscovitine is able to produce significantly higher ION5C evoked GLU release compared to non-drug treated control. ION5C evoked GLU release following 100 μ M Roscovitine pre-treatment. Data are mean \pm SEM, N=3 independent experiments; P <0.05.

3.1.3 Inhibition of Cdk5 with Roscovitine does not perturb the HK5C and ION5C-induced changes in $[Ca^{2+}]_i$ in synaptosomes

As Ca^{2+} levels play a pivotal role in regulating the release of the neurotransmitter, it was important to establish whether the SP release induced by HK5C and ION5C in Roscovitine treated terminals was due to any changes in evoked $[Ca^{2+}]_i$. The change in $[Ca^{2+}]_i$ induced by HK5C was measured using the Fura-2 assay for both 100 μ M Roscovitine and in non-drug treated terminals. However, Roscovitine did not affect the HK5C-evoked change in $[Ca^{2+}]_i$ (Fig 3.4).

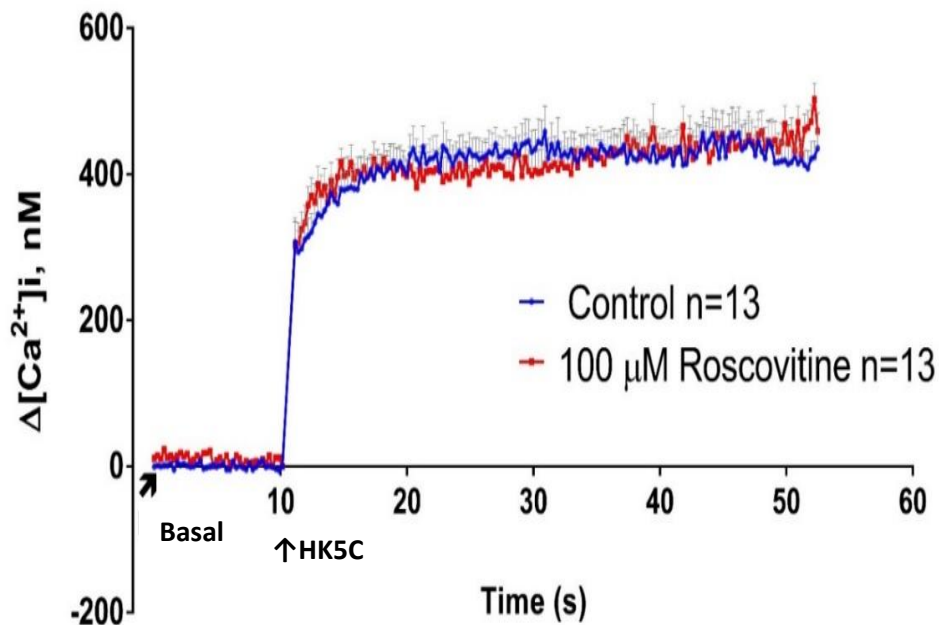


Figure 3.4. 100 μ M Roscovitine treatment did not change HK5C evoked $\Delta[Ca^{2+}]_i$ compared to control. $\Delta[Ca^{2+}]_i$ induced by HK5C in control and 100 μ M Roscovitine treated terminals. Data are mean \pm SEM, N=3 independent experiments; $P>0.05$ for test compared to control (i.e. no significant differences).

Similarly, there were no significant differences in $\Delta[Ca^{2+}]_i$ identified between control and 100 μ M Roscovitine treated conditions when ION5C was employed (Fig 3.5).

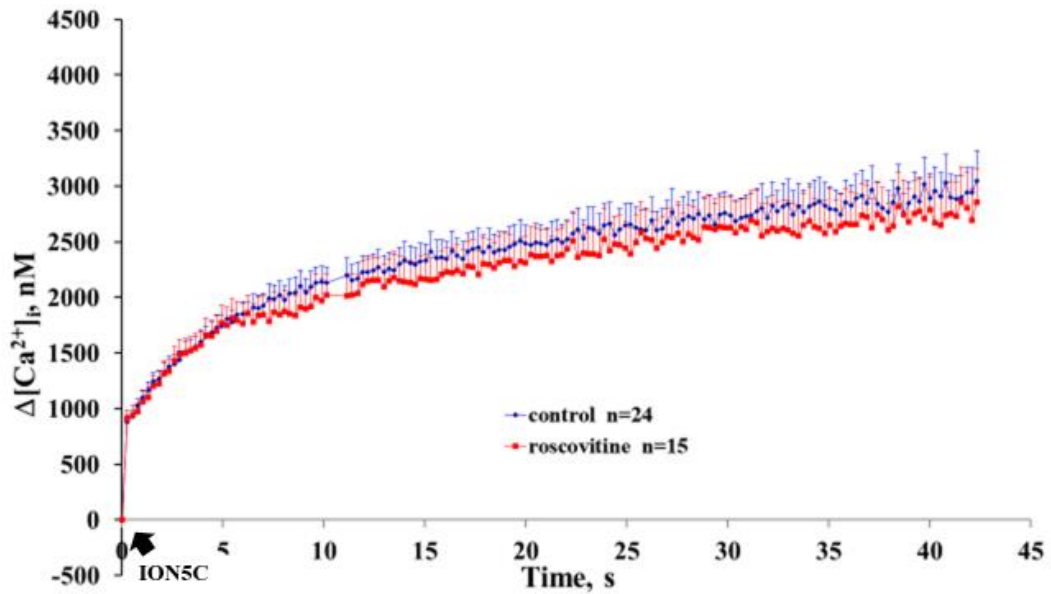


Figure 3.5. ION5C evoked $\Delta[Ca^{2+}]_i$ was unaffected by Roscovitine treatment compared to control. $\Delta [Ca^{2+}]_i$ induced by ION5C in control and 100 μ M Roscovitine treated terminals. Data are mean \pm SEM, N=7 independent experiments; $P>0.05$ for test compared to control (i.e. no significant differences).

3.2 Roscovitine did not induce recycling and re-release of the RRP and the RP

Research from Ashton's group has shown that neither HK5C nor ION5C can induce more than one round of release of the RRP and the RP, such that there is no recycling, reloading and re-release of these vesicle pools in the presence of these stimuli (see Appendix 1 Fig A3). However, there was still a potential that Roscovitine – by blocking Cdk5 activity – could actually enable the recycling, reloading, and re-release which mean the release observed could possibly be from recycling of the vesicle from the RRP and the RP rather than release from the SP. As such, this study checked this by blocking all forms of Dyn dependent endocytosis including bulk endocytosis and clathrin mediated endocytosis by inhibiting the GTPase of Dyn with 160 μ M Dynasore (i.e. Macia *et al*, 2006). Comparing

HK5C evoked release in control and 100 μ M Roscovitine treated terminals (Fig 3.6a) vs HK5C evoked release in control and 160 μ M Dynasore plus 100 μ M Roscovitine synaptosomes (Fig 3.6b) clearly demonstrated that SVs recycling via a Dyn dependent process did not contribute to the extra GLU release. Similarly, inhibition of clathrin-dependent endocytosis with 15 μ M Pitstop2TM (Dutta *et al*, 2012) failed to perturb the extra release evoked by HK5C in Roscovitine treated terminal (Fig 3.6c). The concentration of 80-160 μ M dynasore has been shown by others to inhibit dynamin dependent endocytosis (e.g. Macia *et al*, 2006). Likewise, 15 μ M Pitstop 2TM has been shown to inhibit clathrin dependent endocytosis. Further, A.Ashton (unpublished results) has shown that pre-treatment of synaptosomes with either of these drugs – at these concentrations – prior to HK5C pre-stimulation, inhibits the recycling of those SVs that recycle by a clathrin and or dynamin dependent pathway; these represent those SVs that undergo FF during the pre-stimulation phase. These earlier results clearly indicate that the concentration of the drugs employed and the incubation condition used do allow such drugs to act on their target in synaptosomes

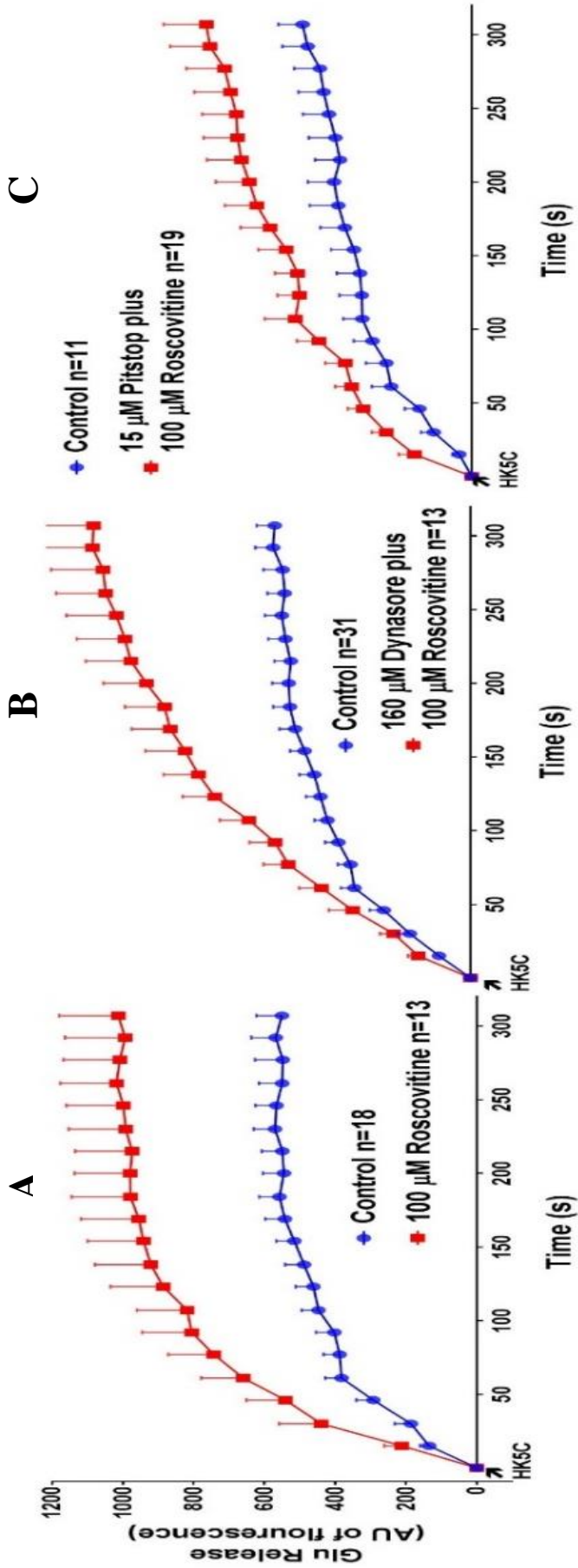


Figure 3.6. Extra release of GLU in Roscovitine treated terminals were not a result of recycling, reloading, and re-release of RRP and RP. HK5C evoked release in control and in terminals treated with A) 100 μ M roscovitine; B) 160 μ M Dynasore plus 100 μ M Roscovitine. C) 15 μ M Pitstop2TM plus 100 μ M Roscovitine. The number of independent experiments for A, B was 4 and for C was 3. Data are mean \pm SEM; P < 0.05 when comparing control to drug treated synaptosomes.

3.3 Roscovitine induces the HK5C evoked release of the SP of SVs independently of NM-II activity

A previous study has shown that non-muscle myosin II (NM-II) activity can regulate the kiss-and-run (KR) mode of the RRP SVs evoked by HK5C (Bhuva, 2015; appendix 1 Fig A8, A9) and others have suggested a role for this motor protein regulating the release of various SV pools including the SP. Therefore, this study used the inhibitor Blebbistatin (50 μ M) (Kovacs *et al*, 2004; Shu *et al*, 2005) to block the enzyme activity of NM-II and looked to see whether this had any impact on Roscovitine's action on the SP released by HK5C. Note that this concentration was shown to inhibit NM-II previously (e.g. Kovacs *et al*, 2004) and it was shown to exhibit an effect on the mode of RRP SV exocytosis evoked by HK5C (Bhuva, 2015; Singh 2017). The result show that Blebbistatin did not prevent the SP from being released from Roscovitine treated terminals (Fig 3.7)

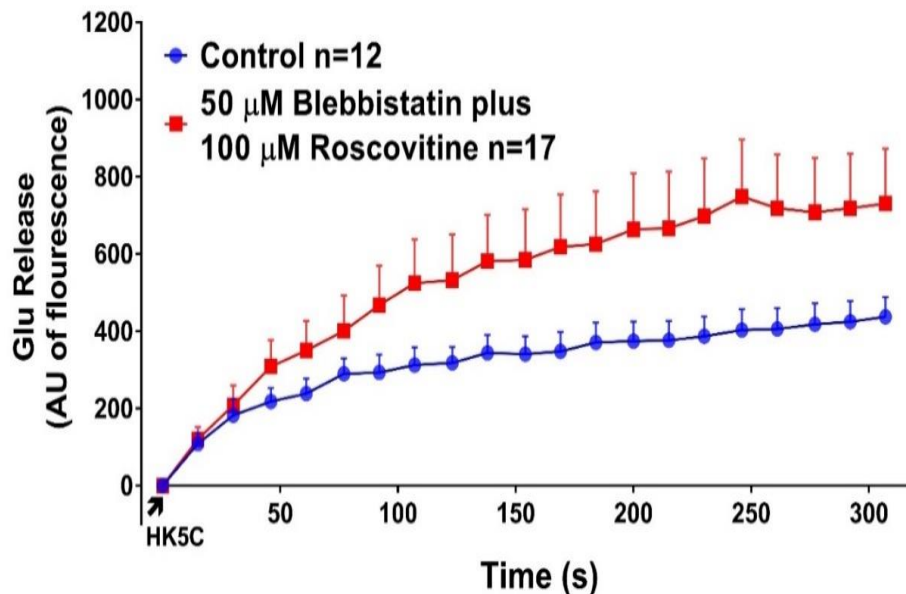


Figure 3.7. Extra release of GLU in Roscovitine treated terminals are independent of NM-II activity. HK5C evoked GLU release with 50 μ M Blebbistatin plus 100 μ M Roscovitine. Data are mean \pm SEM, N=3 independent experiments; P <0.05 between control and drug treated samples.

3.4. Calcium dependency of Roscovitine induced SP release

Entry of external calcium ions into the cytosol of the nerve terminal via Ca^{2+} channels has been acknowledged as a major step in neurotransmitter release. An arrival of action potential to a nerve terminal leads to opening of Ca^{2+} channels, which promote highly localised, transient rise in intracellular Ca^{2+} level at the active zone. Subsequently, Ca^{2+} stimulates synaptic vesicle exocytosis, release of the neurotransmitters contained within such vesicles and this initiates synaptic transmission. This mechanism was elucidated in the classical study on neuromuscular junction (NMJ) by Katz and Miledi (1967) (Sudhof, 2012). Katz and Miledi (1968) later tested whether a residue of the active calcium entering the cell during the nerve impulse could be responsible for short term facilitation. This was tested through varying the external calcium level so that in the first of two nerve impulse $[\text{Ca}^{2+}]_e$ is much lower than that for the subsequent impulse. They found that facilitation was more substantial in the latter condition; this was in accordance with the calcium hypothesis (Katz and Miledi, 1968). Calcium was also proposed to have two distinct role in vesicle recruitment; its role in accelerating SV docking and the buildup of a release machinery, and the other enhancing the coupling between releasable vesicles and the Ca^{2+} channels (Neher and Sakaba, 2008). In addition, Luo *et al* (2015) has also reported that SV exocytosis in NMJ is mainly triggered by calcium ion entering through the nearest calcium channel to the SV that is open, highlighting not only calcium entry as an essential feature of initiating the neurotransmission, but also an importance of the role calcium channels have in the course of exocytosis.

The presynaptic active zone contains various types of voltage dependent calcium channels (VDCC), including N-type, P/Q-type and L-type. The role and specificity of such calcium channels on various processes occurring in active zones has been an issue of debate for a long time (Catterall *et al*, 2013). Previously for the release of the SP, evidence has been provided for some Ca^{2+} channel specificity. For instance, an electrophysiological study - using specific calcium channel blockers for each subtype - has demonstrated that Cdk5

inhibition with Roscovitine led to enhanced Ca^{2+} influx through the P/Q-type VDCCs (Tomizawa *et al*, 2002). Intriguingly, research showed that the intracellular loop connecting domains II and III ($\text{L}_{\text{II-III}}$) between amino acid residues 724 and 981 of the rat brain α_{1A} subunit of P/Q-type Ca^{2+} channels was phosphorylated by Cdk5, but that such phosphorylation perturbed the interaction of $\text{L}_{\text{II-III}}$ with SNAP-25 and synaptotagmin I. However, this information led to the suggestion that Cdk5 prevents neurotransmitter release through the phosphorylation of P/Q-type VDCC and downregulation of the channel activity (Tomizawa *et al*, 2002). Clearly this does not fit in with our results, but Kim and Ryan (2013) reported that the SP exocytosis triggered with Roscovitine (i.e. increased release) is predominately operated through N-type calcium channel. They showed this by pharmacologically blocking each channel types with specific toxins and then stimulating the SP release with Roscovitine in hippocampal neurons. This study indicated that in the condition when P/Q type was blocked with AGA, further release was identified when Roscovitine was treated together with AGA, whilst when N-type channel was blocked using CONO, no further release was observed, which suggest that it is N-type calcium channel that operates the SP release (Kim and Ryan, 2013). Herein, we re-examined the Ca^{2+} and Ca^{2+} channel requirement for release of the SP.

3.4.1 Higher $[\text{Ca}^{2+}]_e$ did not support the SP release

Whether higher $[\text{Ca}^{2+}]_e$ combined with HK and 100 μM Roscovitine pre-treatment may give a further increase in the release of the SP was investigated. As previously shown (e.g. appendix 1 Fig A), relative to HK5C, HK10C (Fig. 3.8a) or HK20C (Fig. 3.8b) failed to produce any further release in control terminals. Furthermore, in 100 μM Roscovitine pre-treated terminals HK10C (Fig 3.9a) or HK20C (Fig 3.9b) did not produce any release from the SP, therefore, it would appear that the higher $[\text{Ca}^{2+}]_e$ did not support exocytosis of the SP in rat cerebrocortical synaptosomes.

For further understanding of the result, the intracellular Ca^{2+} level was measured with Fura-2 assay. Employing HK10C (Fig 3.10) or HK20C (Fig 3.11), the $\Delta[\text{Ca}^{2+}]_i$ level was reduced in Roscovitine treated terminal compared to that for non-drug treated and this implies that the higher $[\text{Ca}^{2+}]_e$ level may perturb the SP release by actually reducing the evoked change in intracellular Ca^{2+} levels in such Roscovitine treated synaptosomes.

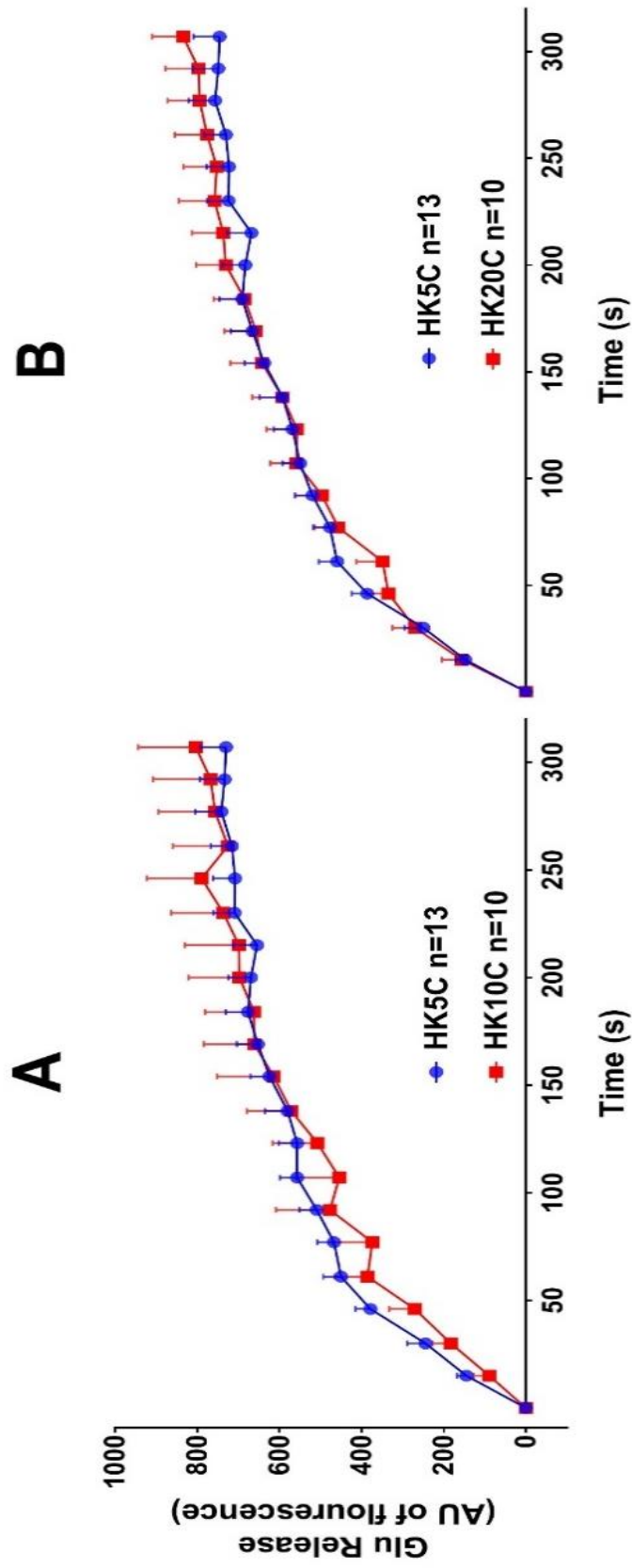


Figure 3.8. HK10C and HK20C do not evoke significantly higher GLU release compared to HK5C. GLU release evoked by HK5C and a) HK10C or b)

HK20C in non-drug treated control synaptosomes. Data are mean \pm SEM, N=3 independent experiments; P>0.05.

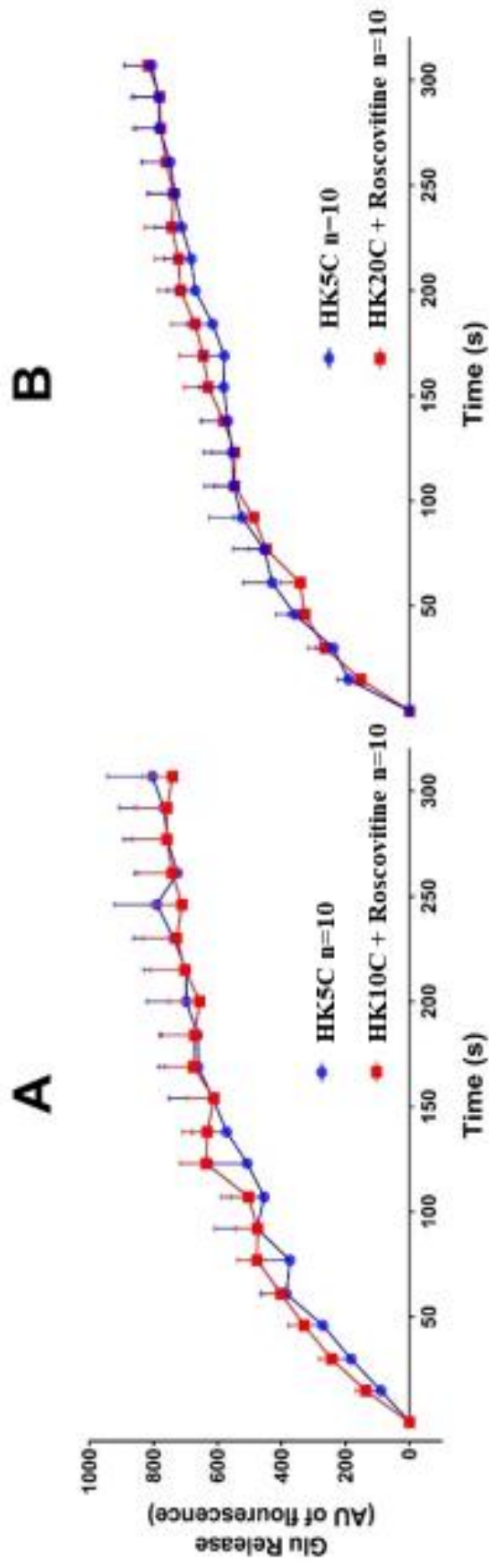


Figure 3.9. HK10C and HK20C with Roscovitine do not evoke significantly higher GLU release compared to HK5C in control terminals. GLU release evoked by HK5C in control terminals and a) HK10C or b) HK20C in 100 μ M Roscovitine treated synaptosomes. Data are mean \pm SEM, N=3 independent experiments; P>0.05.

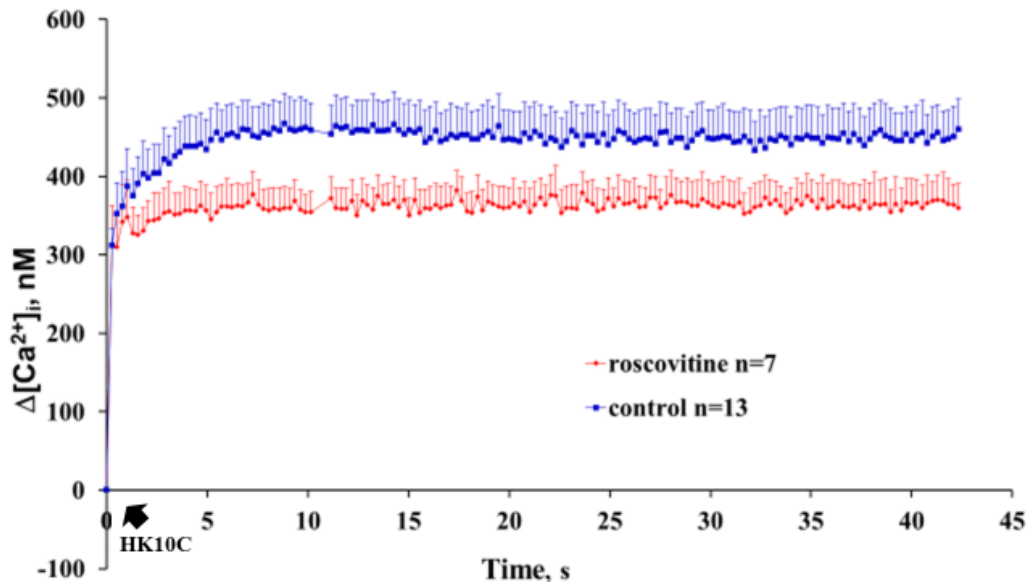


Figure 3.10. HK10C evoked $\Delta[Ca^{2+}]_i$ in Roscovitine treated terminals were significantly lower than non-drug treated terminals. Change in $[Ca^{2+}]_i$ induce by HK10C in control and 100 μM Roscovitine treated synaptosomes. Data are mean \pm SEM, N=3 independent experiments; P<0.05.

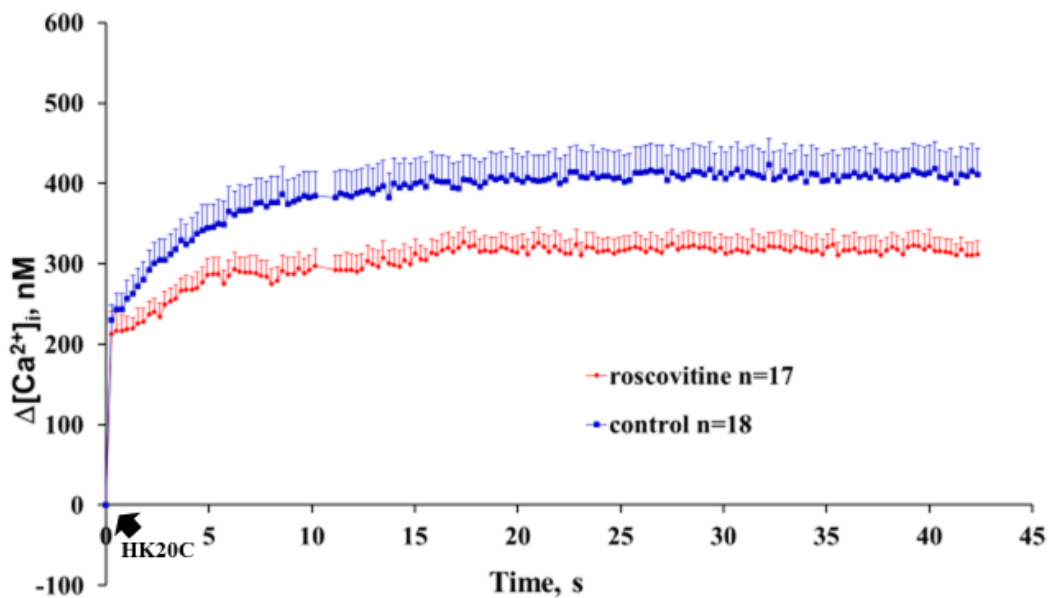


Figure 3.11. HK20C evoked $\Delta[Ca^{2+}]_i$ in Roscovitine treated terminals were significantly lower than non-drug treated terminals Change in $\Delta[Ca^{2+}]_i$ induced by HK20C in control and 100 μM Roscovitine treated terminals. Data are mean \pm SEM, N=3 independent experiments; P<0.05.

3.4.2 Regulation of PKC activity can inhibit the SP release evoked in Roscovitine-treated synaptosomes

The previous result from 3.4.1 has revealed that the higher extracellular calcium levels (i.e. HK10C or HK20C) do not support the SP exocytosis in the Roscovitine treated synaptosomes and in fact such conditions reduced the intracellular calcium level, This suggests a critical role for the precise $[Ca^{2+}]_i$ level for SP exocytosis. This may involve Ca^{2+} dependent regulation of certain enzymes. Therefore, we looked to see if changes in PKC activation could regulate the SP. 1 μ M Phorbol 12-myristate 13-acetate (PMA) (Virmani *et al*, 2005) was employed to activate most PKCs within the terminal and the effect this had on the SP in Roscovitine-treated terminals was investigated. PMA pre-treatment failed to perturb normal amount of the SP in HK5C stimulated Roscovitine treated terminals (Fig 3.12). Thus, activation of PKCs does not interfere with the action of Roscovitine in inducing the SP release evoked by HK5C. However, HK5C alone activates some specific PKC, which complicates the conclusion derived from using PMA. ION5C, unlike HK5C, appears not to activate certain PKCs at the active zone (Ashton, unpublished observation) so we also tested this stimulus. PMA pre-treatment failed to induce any further increase in the release evoked by ION5C (Fig 3.13a). However, such pre-treatment prevented the ION5C evoked release of the SP in terminals that were also treated with Roscovitine (Fig 3.13b). Therefore, under certain circumstances the activation of PKCs can inhibit the release of the SP induced when Cdk5 is inhibited.

Fura-2 measurements were performed under the same conditions outlined above and the results demonstrated that HK5C evoked $\Delta[Ca^{2+}]_i$ was similar in Roscovitine or Roscovitine plus PMA treated terminals (Fig 3.14) whilst higher $\Delta[Ca^{2+}]_i$ was observed in Roscovitine plus PMA relative to Roscovitine alone when ION5C was employed (Fig 3.15). As it was found that PMA treatment blocked ION5C evoked SP in Roscovitine treated terminals, it would appear that this failure to induce the SP is due to an increase of

the intracellular Ca^{2+} level elicited by stimulation with ION5C. It should be noted that in these experiments ION5C induced a larger $\Delta[\text{Ca}^{2+}]_i$ than HK5C which may explain the results. Furthermore, the difference between HK5C and ION5C may reflect the difference in activation of certain PKCs.

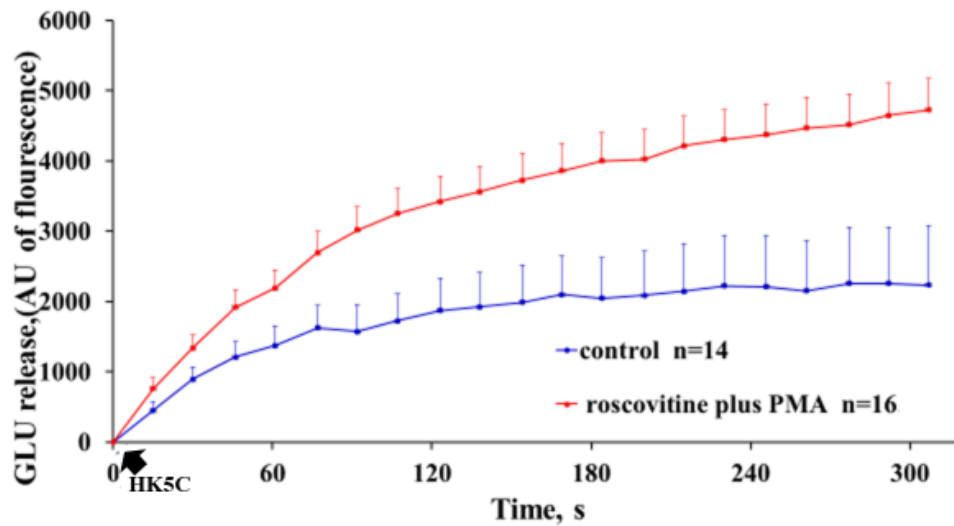


Figure 3.12. Supramaximal activation of PKC with 1 μM PMA pre-treatment failed to perturb normal amount of the SP in HK5C stimulated Roscovitine treated terminals. HK5C evoked GLU release in non-drug treated control and 1 μM PMA plus 100 μM Roscovitine treated synaptosomes. Data are mean \pm SEM, N=3 independent experiments; P <0.05 between control and drug treated samples.

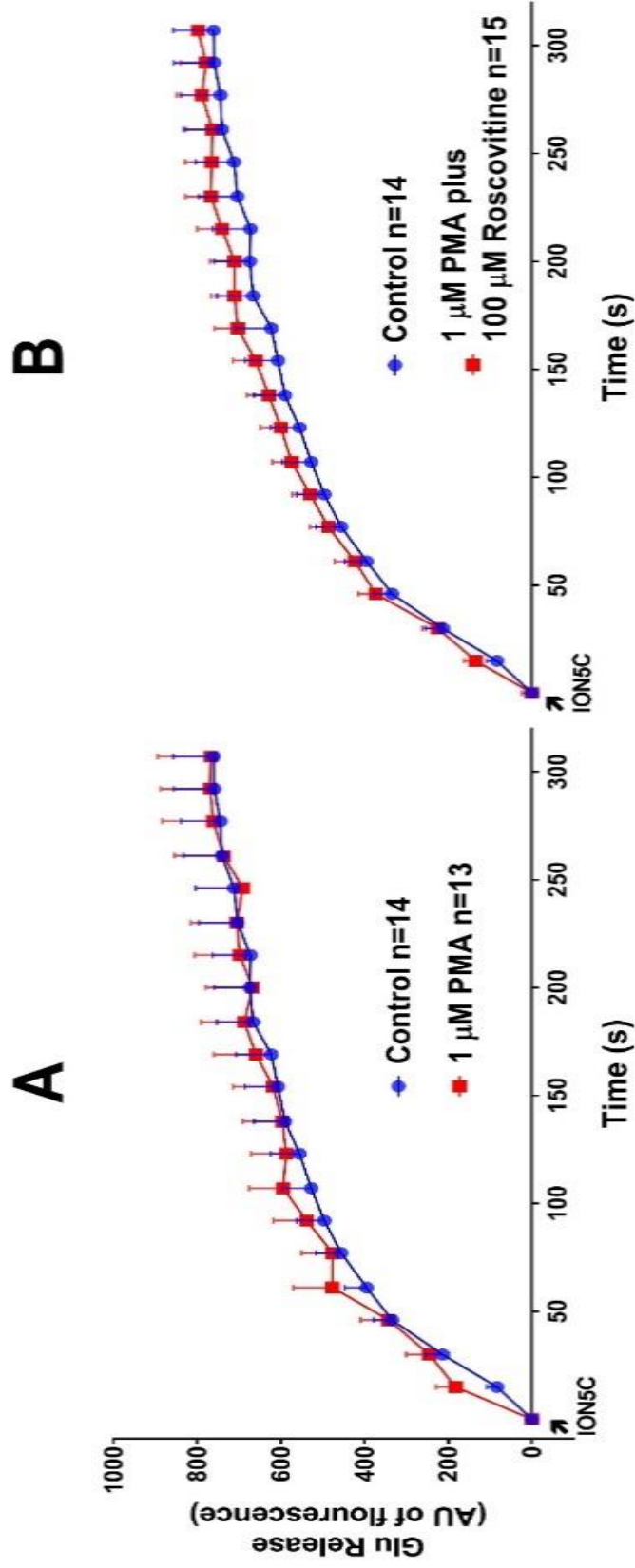


Figure 3.13. Supramaximal activation of PKC with 1 μ M PMA perturbed ION5C evoked release of the SP in Roscovitine treated terminals. ION5C

evoked GLU release in control and a) 1 μ M PMA treated terminal and b) 1 μ M PMA plus 100 μ M Roscovitine treated terminal. Data are mean \pm

SEM, N=4 independent experiments. Note that there was no significant difference ($P>0.05$) in GLU release between drug-treated and control terminals.

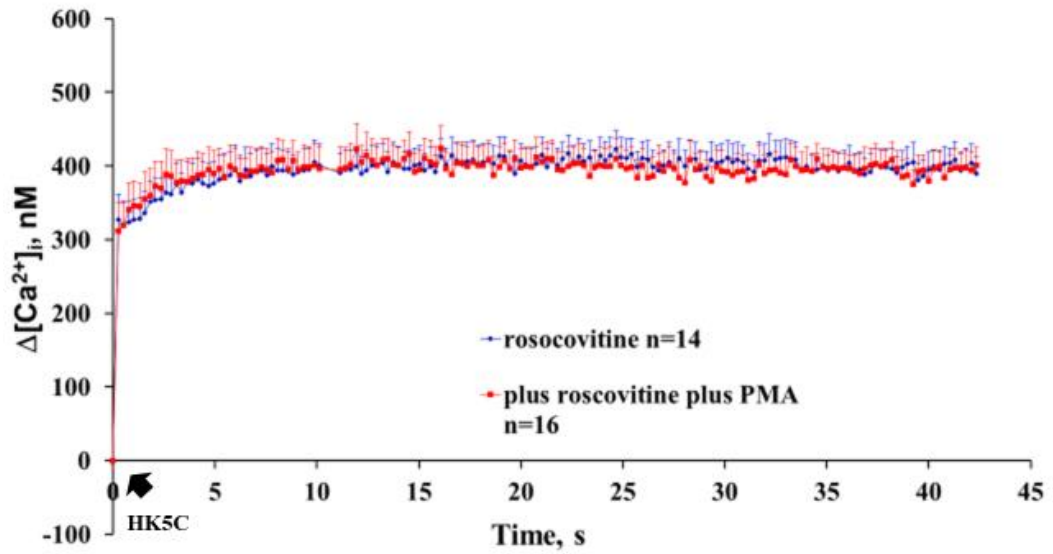


Figure 3.14. HK5C evoked $\Delta[Ca^{2+}]_i$ was similar in Roscovitine treated terminals and Roscovitine plus PMA treated terminals. HK5C evoked $\Delta[Ca^{2+}]_i$ comparing Roscovitine alone and 1 μ M PMA plus 100 μ M Roscovitine. This results are an average from 3 independent experiments and there is no significant difference ($P>0.05$) between these conditions.

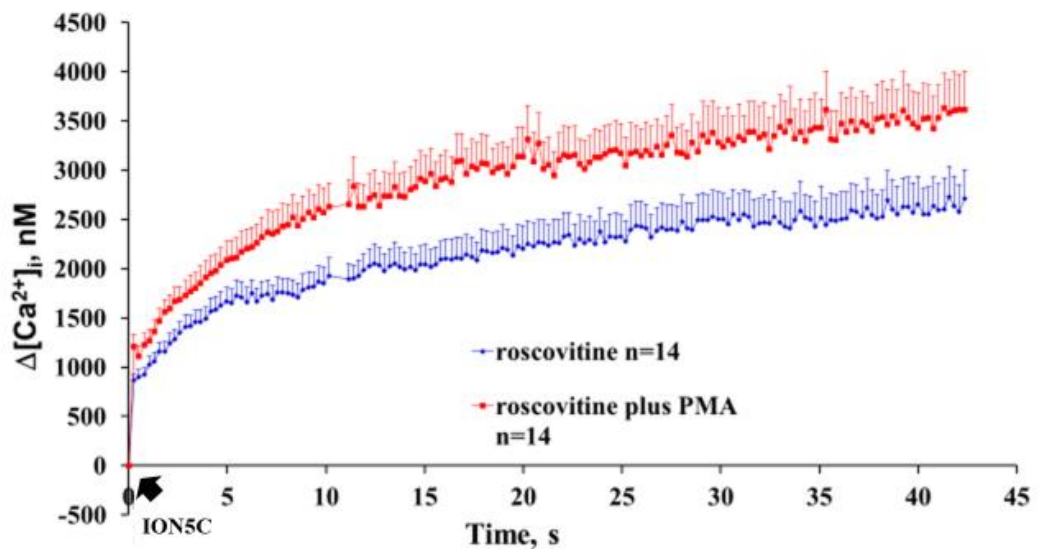


Figure 3.15. Roscovitine plus PMA shown higher $\Delta[Ca^{2+}]_i$ relative to Roscovitine alone when ION5C was employed. ION5C evoked $\Delta[Ca^{2+}]_i$ in Roscovitine plus 1 μ M PMA and 100 μ M Roscovitine treated terminals. These traces are an average from 3 independent experiments and there is a significant difference between the 2 conditions ($P<0.05$).

Intriguingly as HK5C is able to activate certain PKCs at the AZ, there was actually the possibility that the release of the SP in Roscovitine treated terminals was not maximal with HK5C because some of this pool was being blocked by the activated PKCs. To test this, we pre-treated the terminals with 1 μM of the PKC inhibitor Go6983 (this is known to inhibit conventional, novel and atypical PKCs (Gschwendet *et al*, 1996) and A.Ashton (unpublished) has shown that this blocks PMA evoked effects in both release assays and phosphorylation assays in synaptosomes) with or without 100 μM Roscovitine and then stimulated the terminals with HK5C. Terminals in which PKCs are inhibited with Go6983 had a similar amount of release evoked by HK5C as control (Fig 3.16a). Moreover, inhibition of PKCs with Go6983 did not perturb the HK5C evoked release of the SP in Roscovitine treated terminal (Fig 3.16b). Thus, the activation of certain active zone PKCs with HK5C did not perturb the release of the SP in Roscovitine treated terminals. A possible explanation for the earlier finding that very high $[\text{Ca}^{2+}]_e$ plus HK (HK10C or HK20C) actually blocks the SP is that this level of $[\text{Ca}^{2+}]_e$ was able to stimulate PKCs further and this may fit in with the data in ION5C experiments with PMA and Roscovitine.

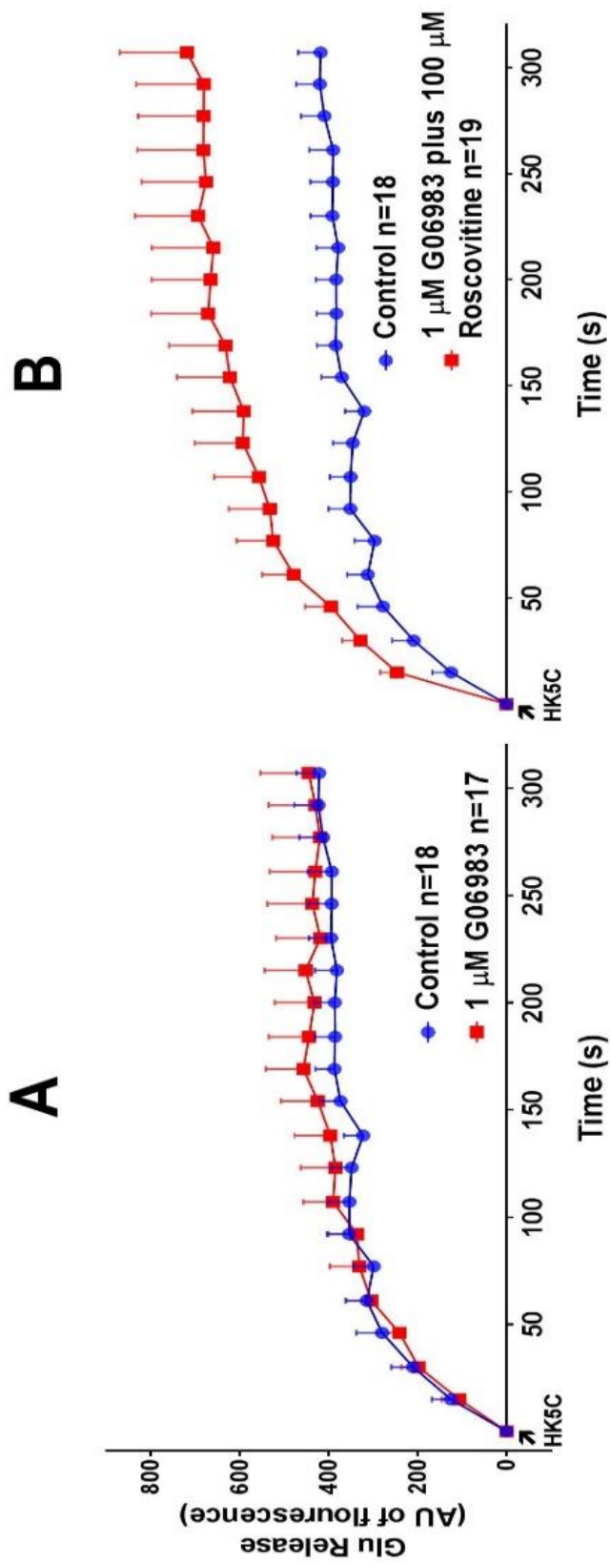


Figure 3.16. PKC inhibition with Go6983 did not perturb HK5C evoked SP release in Roscovitine treated terminals. HK5C evoked GLU release in control and a) 1 μ M Go6983 b) 1 μ M Go6983 + 100 μ M Roscovitine treated terminal. Data are mean \pm SEM, N=5 independent experiments. Note that in a, $P > 0.05$ (i.e. no significant differences) whereas in b, $P < 0.05$ for test comparing control and drug treatment.

3.4.3 Inhibition of Ca²⁺ entry through N-, P/Q-, L-type Ca²⁺ channels does not perturb the HK5C evoked release of the RRP and the RP but it does inhibit the release of the SP in Roscovitine treated terminals.

Previously, Ashton's group has shown that N-type Ca²⁺ channel blockade with 1 μM ω-conotoxin GVIA (CONO) fails to inhibit the release of the RRP and the RP SVs evoked by HK5C and this study repeated the findings (Fig 3.17a): this is despite the fact that this toxin does reduce the HK5C evoked change in [Ca²⁺]_i (Fig 3.18). However, addition of CONO did inhibit the HK5C evoked release of the SP in Roscovitine treated terminals (Fig 3.17b). The toxin's action in reducing HK5C evoked changes in [Ca²⁺]_i was still apparent in the Roscovitine treated terminals (Fig 3.19). This result suggests that the SP does require a certain level of change in [Ca²⁺]_i for it to be induced and this does not occur in CONO treated terminals.

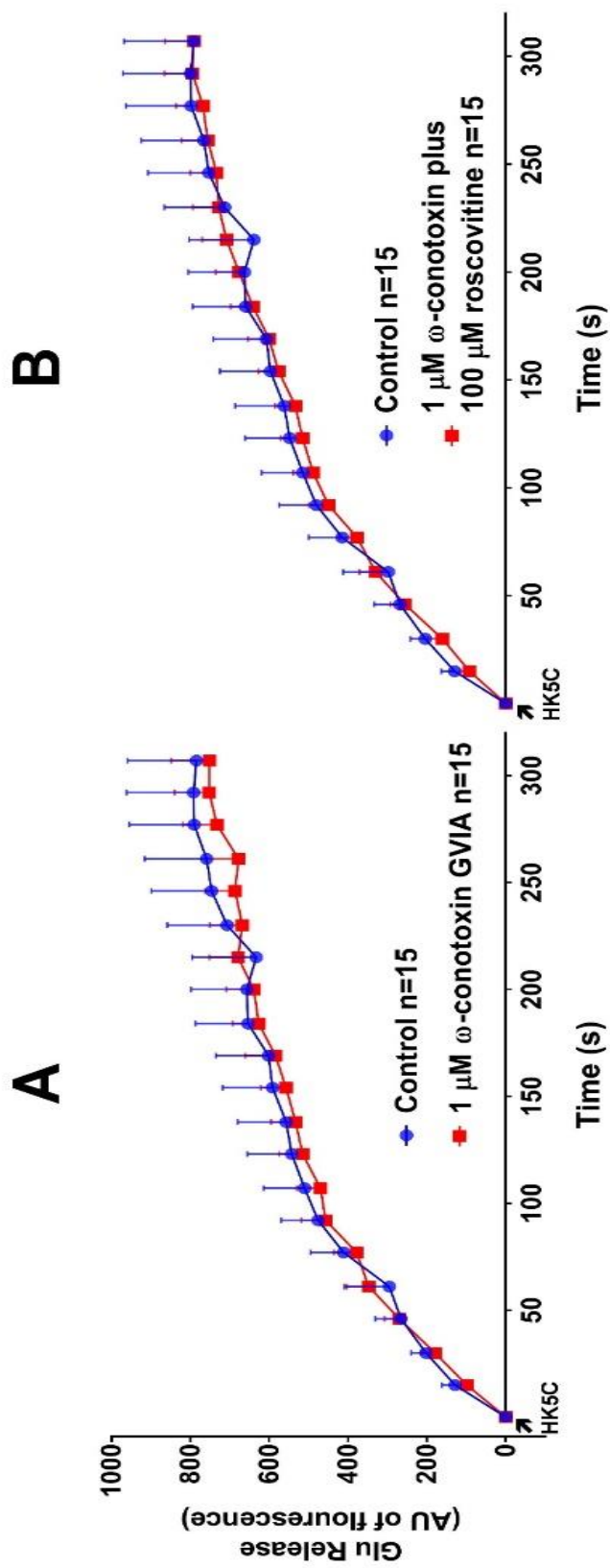


Figure 3.17. HK5C evoked SP release is perturbed in Roscovitine treated terminal when N-type Ca^{2+} channel is inhibited with CONO. HK5C evoked GLU release in control and a) 1 μM CONO b) 1 μM CONO plus 100 μM Roscovitine treated terminals. Data are mean \pm SEM, N= 4 independent experiments; P>0.05, and there were no significant difference between control and the drug treated conditions.

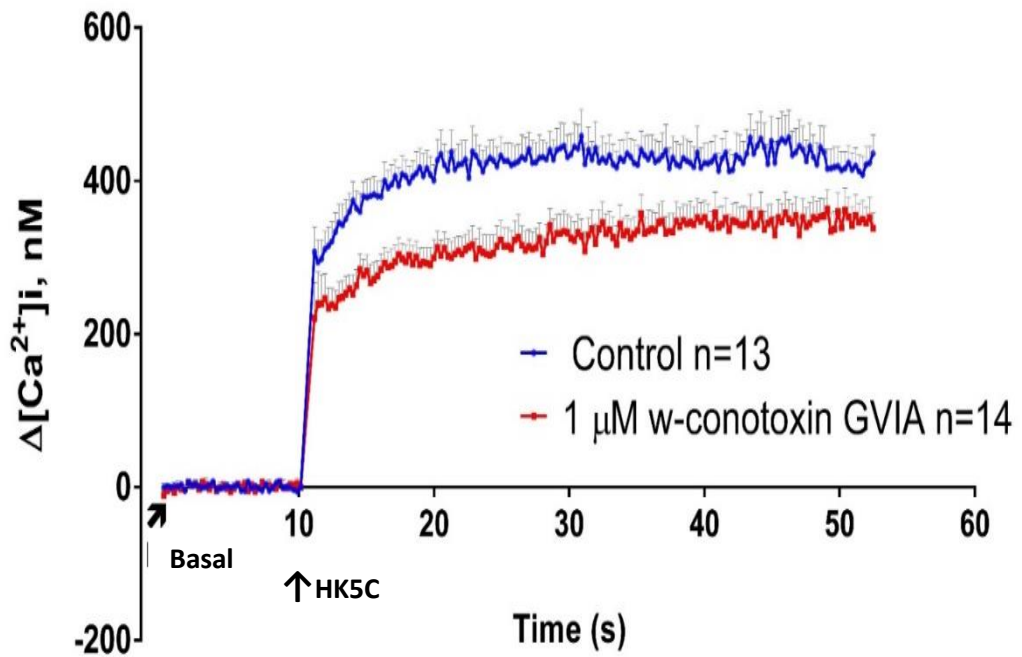


Figure 3.18. Inhibiting N-type Ca^{2+} channel reduce HK5C evoked $\Delta[\text{Ca}^{2+}]_i$. HK5C evoked $\Delta[\text{Ca}^{2+}]_i$ in control and 1 μM CONO treated synaptosomes. The number of independent experiments was N=3. Note that there was significant decrease in $\Delta[\text{Ca}^{2+}]_i$ with 1 μM CONO treatment ($P < 0.05$).

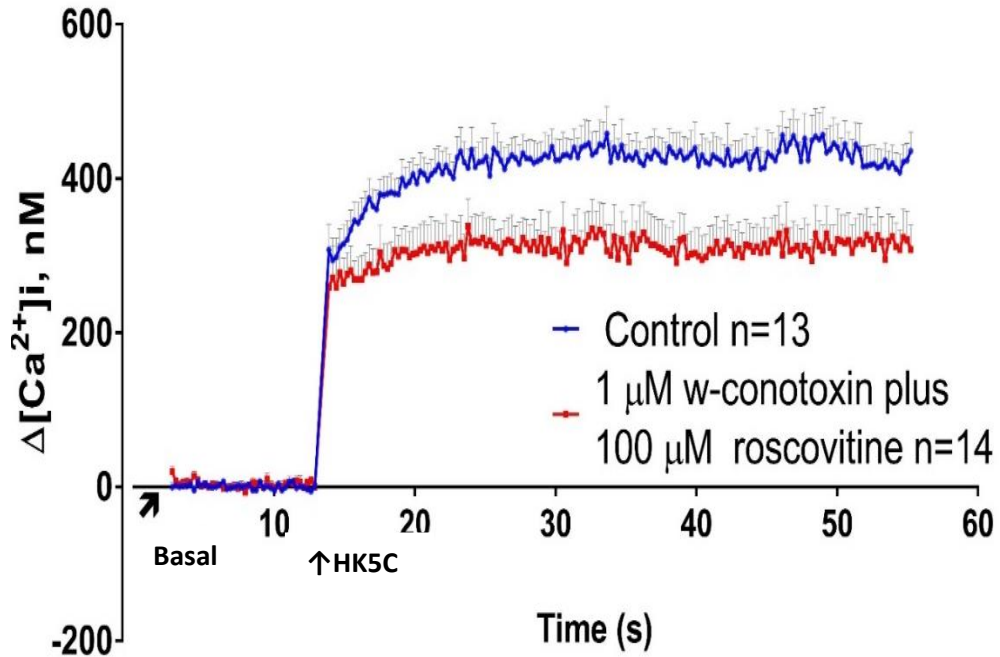


Figure 3.19. CONO plus Roscovitine treatment reduced the HK5C evoked $\Delta[Ca^{2+}]_i$ compared to control. HK5C evoked $\Delta[Ca^{2+}]_i$ in control and 1 μ M CONO plus 100 μ M Roscovitine treated terminals. This trace is an average from 3 independent experiments. There was a significant decrease in $[Ca^{2+}]_e$ with 1 μ M CONO plus 100 μ M Roscovitine compared to control ($P > 0.05$).

50 nM ω -Agatoxin TK (AGA) was used to block P/Q-type Ca^{2+} channels in synaptosomes. HK5C evoked GLU release in AGA plus Roscovitine treated terminals was not significantly different compared to release from control non-drug treated terminals (Fig 3.20 a) and also it was significantly lower compared to Roscovitine alone (Fig 3.20 b) indicating that this toxin does prevent the SP from being released. Furthermore, it was apparent in the Fura-2 assay that AGA plus Roscovitine treatment has significantly reduced HK5C induced $\Delta[Ca^{2+}]_i$ in comparison with either control (Fig 3.21 a) or Roscovitine treated terminals (Fig 3.21 b) (Note this latter experiment was performed twice so statistical analysis could not be conducted).

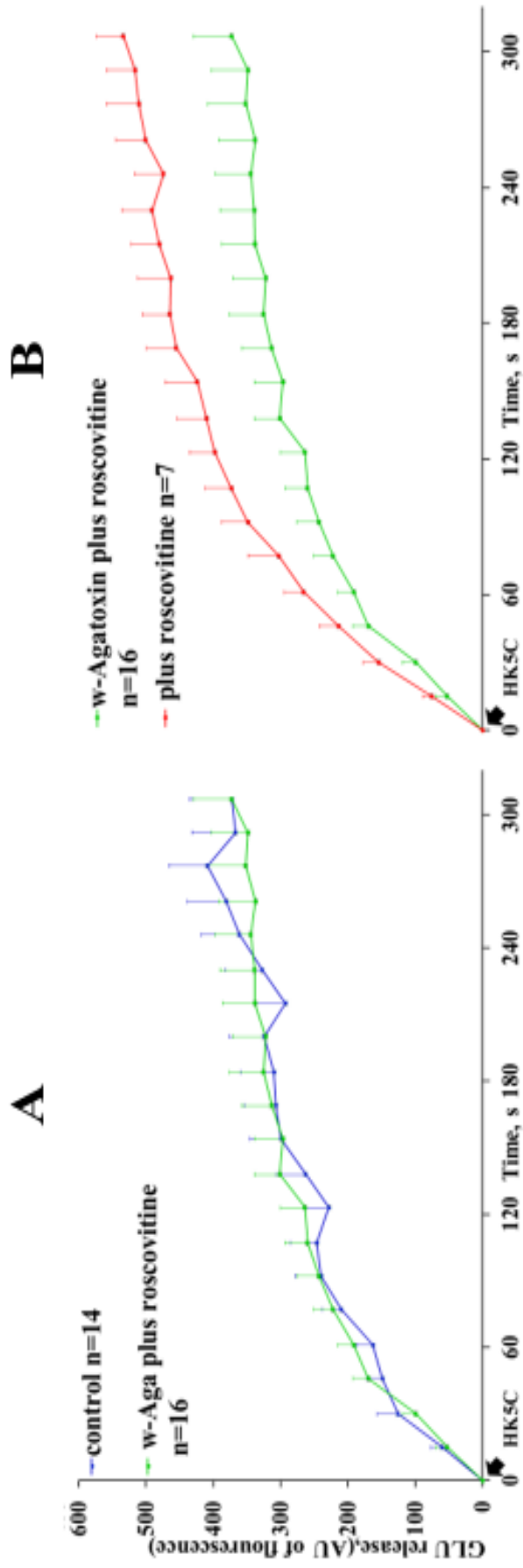


Figure 3.20. HK5C evoked SP release is perturbed in Roscovitine treated terminal when P/Q-type Ca^{2+} channel is inhibited with AGA. HK5C evoked GLU release comparing a) control with 50 nM AGA plus 100 μ M Roscovitine b) 50 μ M AGA plus 100 μ M Roscovitine with 100 μ M Roscovitine. Data are mean \pm SEM, N=5 independent experiments for a; N=2 independent experiments for b; there is significant difference between the 2 conditions in b ($P < 0.05$).

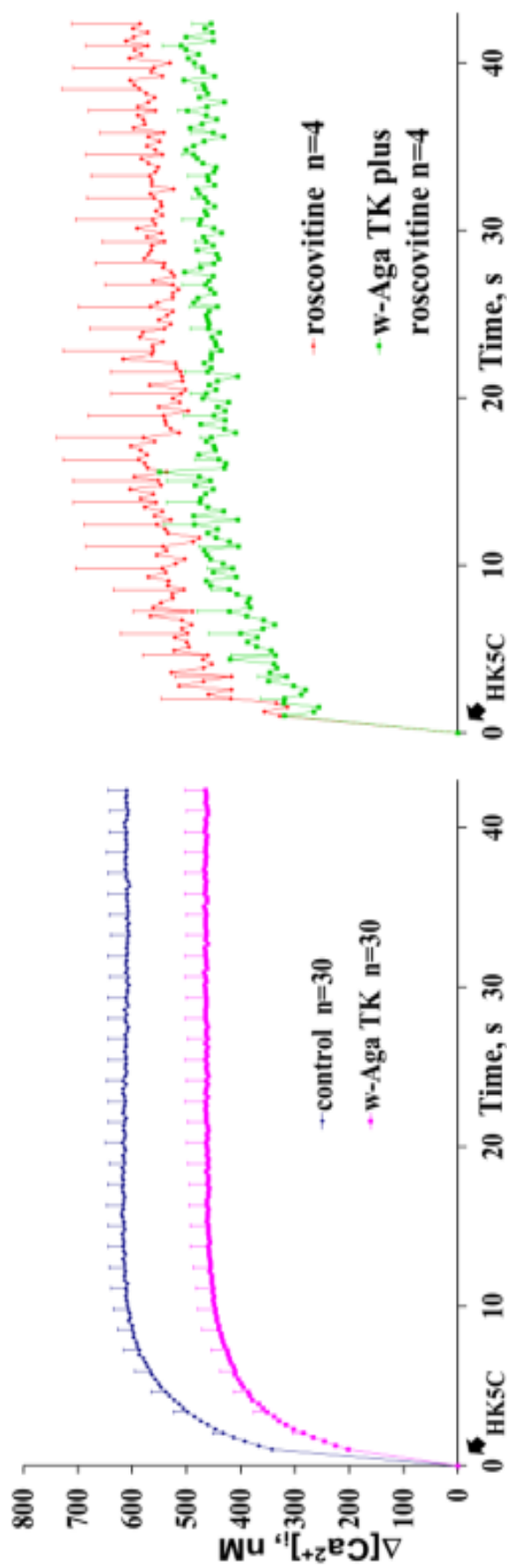


Figure 3.21. P/O type Ca^{2+} inhibition with AGA the HK5C evoked $\Delta[Ca^{2+}]_i$ compared to control in Roscovitine treated terminals. HK5C evoked changes in $\Delta[Ca^{2+}]_i$ comparing a) control and 50 nM AGA b) 100 μ M Roscovitine with 50 nM AGA plus 100 μ M AGA plus 100 μ M Roscovitine; $P < 0.05$. The number of independent experiments was N=6 for a; N=2 for b.

L-type Calcium channel blockade with Nifedipine (NIF) produced results that were similar to the other Ca^{2+} channel blockers. Its presence substantially attenuated the HK5C evoked release compared to Roscovitine alone (Fig 3.22 b) and its presence produce a similar amount of HK5C evoked release in Roscovitine treated terminals as found in the non-drug treated controls (Fig 3.22 a). Clearly, SP release is perturbed by the treatment with NIF. Fura-2 assay has demonstrated that NIF treatment of Roscovitine treated terminals leads to significant decrease in the HK5C evoked $\Delta[\text{Ca}^{2+}]_i$ compared to Roscovitine treated terminals (Fig 3.23 b) and to non-drug treated control synaptosomes (Fig 3.23 a). Note that the choice of concentrations of calcium channel blockers to use was taken from the literature including papers that studied synaptosomes (Thomas *et al*, 1994; Meder *et al*, 1997). It is clear that these blockers do exert an action as they were shown to reduce the HK5C evoked change in $[\text{Ca}^{2+}]_i$ and Asthon and colleagues (unpublished) have shown that the combination of all three drugs can greatly perturb the HK5C evoked change and each drug can work more extensively if a lower $[\text{Ca}^{2+}]_e$ is employed (0.3 mM).

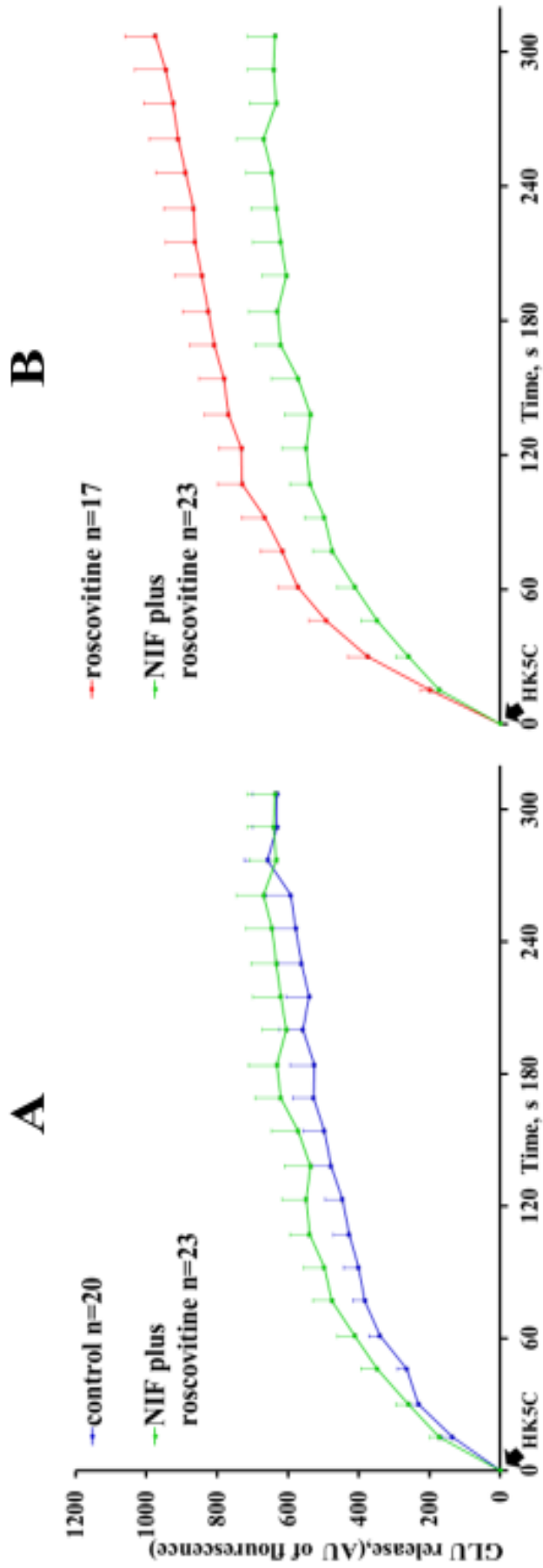


Figure 3.22. HK5C evoked SP release is perturbed in Roscovitine treated terminal when L-type Ca^{2+} channel is inhibited with NIF. HK5C evoked GLU release comparing a) control with 1 μ M NIF plus 100 μ M Roscovitine b) 1 μ M NIF plus 100 μ M Roscovitine with 100 μ M Roscovitine. Data are mean \pm SEM, N=5 independent experiments; $P > 0.05$ control and drug treated samples for a whilst $P < 0.05$ between two conditions for b.

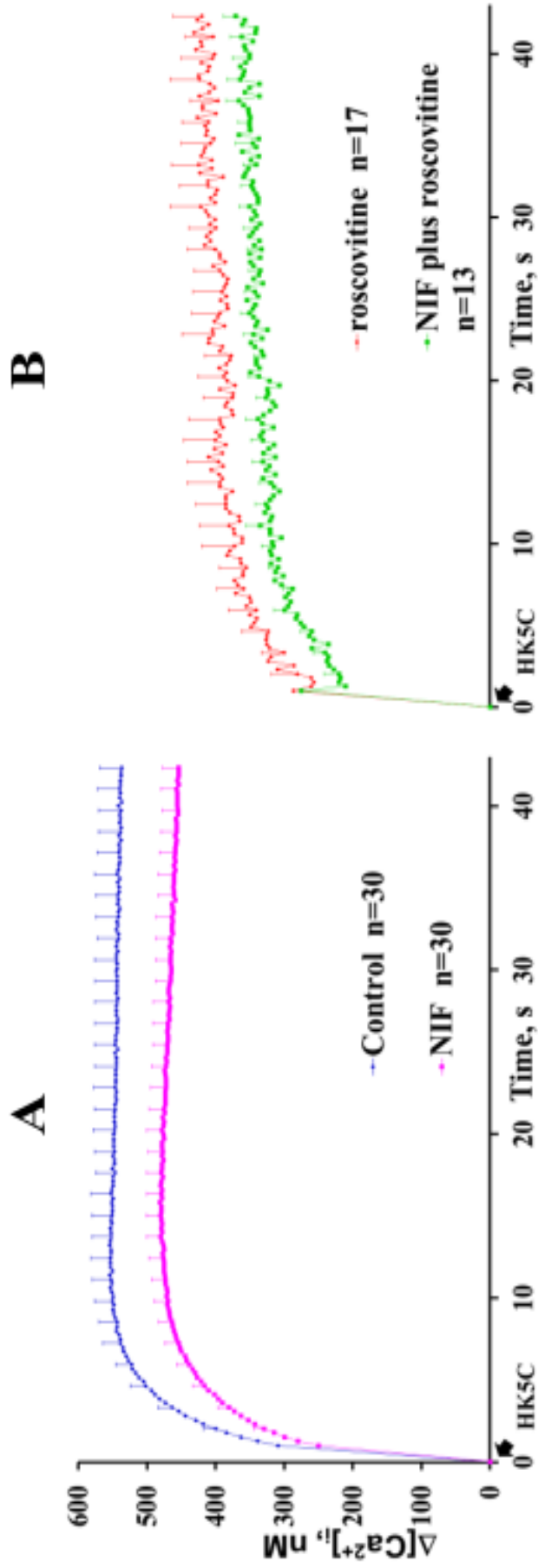


Figure 3.23. L-type Ca^{2+} inhibition with NIF the HK5C evoked $\Delta[Ca^{2+}]_i$ compared to control in Roscovitine treated terminals. HK5C evoked changes in $\Delta[Ca^{2+}]_i$; comparing a) control and 1 μ M NIF b) Roscovitine with 1 μ M NIF plus Roscovitine. The number of independent experiments was N=5 for a) and N=6 for b). Note that there was significant decrease in $\Delta[Ca^{2+}]_i$ with NIF treatment in both a and b ($P < 0.05$).

3.5 The role of actin microfilament in the SP exocytosis

Several lines of evidence have suggested that Actin dynamics play a major role in presynaptic functions and is implicated in various stages of the synaptic vesicle cycle, including vesicle clustering, neurotransmitter exocytosis, and endocytosis (Pollard, 2014). Morales *et al* (2000) have used Latrunculin (LAT), a toxin promoting actin depolymerisation by sequestering actin monomers, to monitor the role of actin on fusion of a single SV, represented with spontaneous mEPSCs. They have treated the preparation with LAT and found it rapidly increased the frequency of mEPSC by 5-fold. They have also treated the sample with Jasplamide, which promotes the stabilisation of actin filaments, and found this blocks the LAT induced increase in mEPSC frequency, indicating that the LAT triggered increase was derived from regulation of actin dynamics instead of a non-specific effect of the drug. This research suggested that LAT did not induce this effect by increasing the actual size of the RRP (Morales *et al*, 2000). Cole *et al* (2000) suggested that actin filaments facilitate a transmitter release rather than delaying it. They have tested this by treating nerve-muscle preparations from garter snake with LAT and measured the FM 1-43 release and found that LAT treatment reduced the evoked destaining (due to FM dye release) which suggests that transmitter release is partially blocked by the drug treatment (Cole *et al*, 2000).

Actin microfilaments are known to interact with several other proteins, such as Syn I and α -synuclein, to play pivotal role in presynaptic functions (Lee *et al*, 2018). Bloom *et al* (2003) used immunogold electron microscopy to investigate the subcellular localisation of actin and Syn and found that in synapses at rest, Syn was localised near to the vesicle cluster that was located distal from the AZ, but that during synaptic activity, Syn migrated to the pool of vesicles near to the AZ. Furthermore, actin and Syn were seen to colocalise in a dynamic filamentous cytomatrix at the endocytic zone. These results highlight that actin and Syn co-operate during their participation in synaptic activity (Bloom *et al*, 2003). In the study from Bellani *et al* (2010), it was indicated that actin is a possible target for α -

synuclein (α -syn) function. The precise role of α -syn in synaptic function is not yet fully understood but few studies have suggested that it is important in regulation of SV mobility. In this study, α -syn binds to actin and, through regulation of actin dynamic, α -syn participates in the tuning of the vesicle release process, and consequently modulate synaptic function and plasticity (Bellani *et al*, 2010). Clearly, from such research it is evident that actin contributes to neurotransmission, and therefore, an investigation to ascertain whether the actin microfilaments are also involved in the release or regulation of the SP is warranted.

3.5.1 The SP cannot be studied following disassembly of actin microfilaments as the RP is perturbed

An investigation into how actin microfilaments could affect the properties of the SP appears an important point to study and we aimed to explore this by employing LAT to disassemble the actin microfilaments. However, before studying the release of the SP, it was necessary to first ascertain the effect that disassembly of actin microfilaments may have on the release of the RRP and RP (Chapter 6 outlines these results). Whilst for 4AP5C evoked release of GLU from the RRP of synaptosomes (Fig 6.1c) there were no difference between non-drug treated control and terminals treated with 15 μ M LAT (10 min at 37°C), for HK5C or ION5C stimulation - where both RRP and the RP are exocytosed - the release appears to be reduced by LAT compared to control (Fig 6.1a and b). This indicated that whilst the RRP is not blocked, the RP release has been blocked by disassembly of actin. This means that our results would be complicated if we determined the effect of Roscovitine after the disassembly of actin by LAT. The SP may not release at all because the RP is not released because SP release only occurs after all of the RP is released. Thus this result would not actually indicate any actin filament requirement for the SP.

3.5.2 RRP, RP, and SP SVs release normally when actin microfilament is stabilised

As disassembly of actin microfilaments by LAT was shown to perturb the RP exocytosis (concluded as RRP induced by 4AP5C is not perturbed), we investigated whether actin stabilisation would affect the release of either the RRP or the RP. 2.5 μ M Jasplakinolide (JASP) (a drug that promotes the stabilisation of the actin) was applied to the synaptosome and GLU release was subsequently measured. These experiments revealed that JASP treatment failed to effect HK5C evoked GLU release as this was the same as in drug-free control (Fig 6.11). This indicates that, in contrast to disassembly of the actin, the RRP and the RP are released normally when actin is stabilised.

From our results on the RRP and RP, the properties of SP was investigated when actin is stabilised (see chapter 6). Synaptosomes were pre-treated with Roscovitine and JASP, and GLU release was subsequently evoked by HK5C. A significant increase in HK5C evoked GLU release was found in JASP plus Roscovitine treated terminals compared to control (Fig 3.24) and this release was similar to that with Roscovitine is treated alone (Fig 3.25). This indicates that the stabilisation of actin microfilaments does not have significant detrimental effect upon the evoked release of the SP SVs in Roscovitine treated terminals. Note that it is known that 2.5 μ M JASP is exerting its effect on actin microfilament because pretreatment of synaptosomes with this drug prevents 15 μ M LAT from perturbing the release of the RP (see chapter 6).

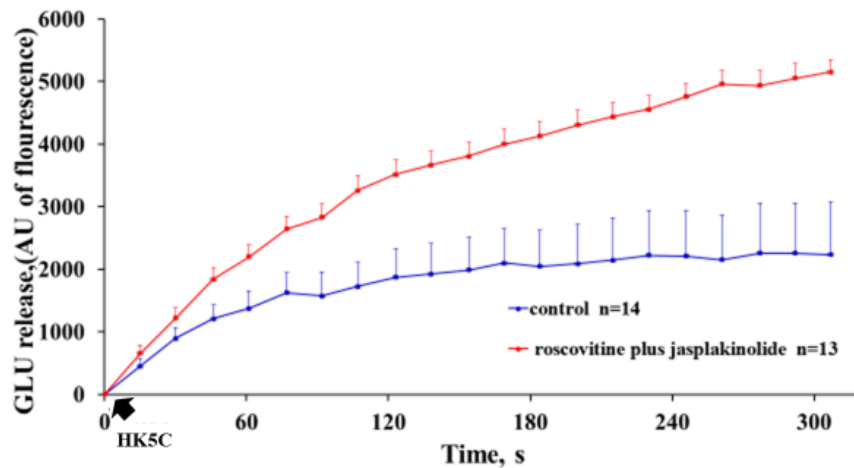


Figure 3.24. HK5C evoked SP release in Roscovitine treated terminals are unaffected by Actin stabilisation. HK5C evoked GLU release from terminals treated with or without 100 μ M Roscovitine plus 2.5 μ M JASP. Data are mean \pm SEM, N=13-14 from 4 independent experiments; There is a significant difference between control and Roscovitine plus JASP treated samples ($P < 0.05$).

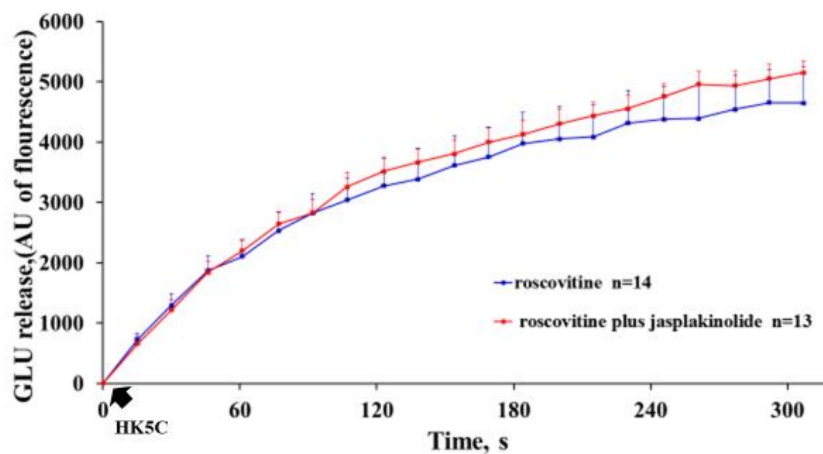


Figure 3.25. Actin stabilisation had no effect on HK5C evoked SP release in Roscovitine treated terminals. HK5C evoked GLU release from 100 μ M Roscovitine or 100 μ M Roscovitine plus 2.5 μ M JASP treated synaptosomes. Data are mean \pm SEM, N=13-14 from 4 independent experiments; Note that there were no significant difference between the 2 conditions ($P > 0.05$).

3.6 Antagonism between Cdk5 and PP2B

It was highlighted by Kim and Ryan (2013) that the balance between Cdk5 and Calcineurin (CN, PP2B) can regulate neurotransmission. The study reported that a removal of CN activity significantly reduces AP-driven calcium influx and exocytosis, whereas inhibition of Cdk5 activity leads to a large potentiation of calcium influx and exocytosis (Kim and Ryan, 2013). We investigated these interaction between Cdk5 and CN in synaptosomes using Roscovitine to inhibit Cdk5 and cyclosporine A (Cys A) to inhibit CN.

3.6.1 Inhibition of CN and Cdk5 with Cys A and Roscovitine did not affect the RRP and the RP release but inhibited the SP exocytosis.

Synaptosomes were treated with 1 μ M Cys A and Roscovitine together and results were compared with non-drug treated control and Roscovitine treated terminals. Previous work has shown that 1 μ M Cys A does not inhibit the release of the RRP or RP evoked by HK5C (appendix 1 Fig 10a). Cys A plus Roscovitine treated synaptosomes released the same amount of HK5C evoked GLU as the non-drug treated control (Fig 3.26b), indicating that the RRP and RP SVs undergoing exocytosis following this dual treatment but intriguingly the SP SVs were prevented from undergoing exocytosis. When release was compared to that in Roscovitine treated terminals, clearly the SP release has been suppressed following the treatment with Cys A (Fig 3.26a). These results suggest that there is clear antagonism existing between CN and Cdk5 and that such enzymes may contribute towards the SP exocytosis under varying conditions.

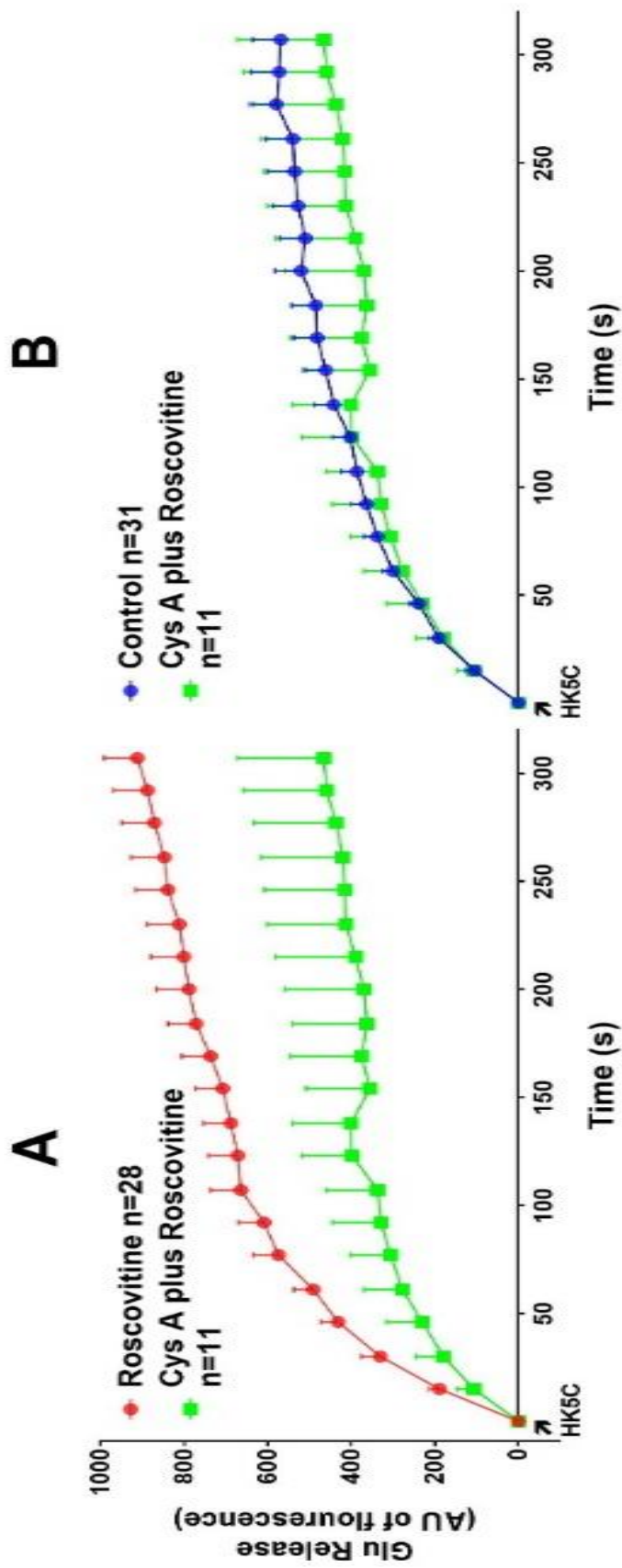


Figure 3.26. Inhibition of CN with Cys A prevented HK5C evoked SP release in Roscovitine treated terminals. HK5C evoked GLU release in terminals treated with a) 100 μ M Roscovitine compared to 1 μ M Cys A plus 100 μ M Roscovitine treated b) no drug (control) terminals vs 1 μ M Cys A plus 100 μ M Roscovitine. Data are mean \pm SEM, N= 3-8 independent experiments; There was significant difference between the 2 conditions in panel (a) ($P<0.05$) but there were no significant difference between 2 conditions in panel b ($P>0.05$).

3.6.2 The SP exocytosis is disturbed following Cys A plus Roscovitine treatment because of reduction in the HK5C evoked $\Delta[\text{Ca}^{2+}]_i$.

Previous observation from A.Ashton has discovered that Cys A treatment elevates the HK5C evoked $\Delta[\text{Ca}^{2+}]_i$ levels compared to the control (see Fig 3.27b). Intriguingly, treatment with Roscovitine plus Cys A has led to substantial reduction in $\Delta[\text{Ca}^{2+}]_i$ level evoked by HK5C compared to that achieved by HK5C stimulated in Roscovitine treated synaptosomes (Fig 3.27a). Thus, inhibition of Cdk5 antagonises the normal effect of blocking CN so that rather than getting an increased $\Delta[\text{Ca}^{2+}]_i$ following HK5C stimulus compared to the control, there is a reduction. Such results again demonstrate that evoked calcium entry strongly regulates the release of the SP.

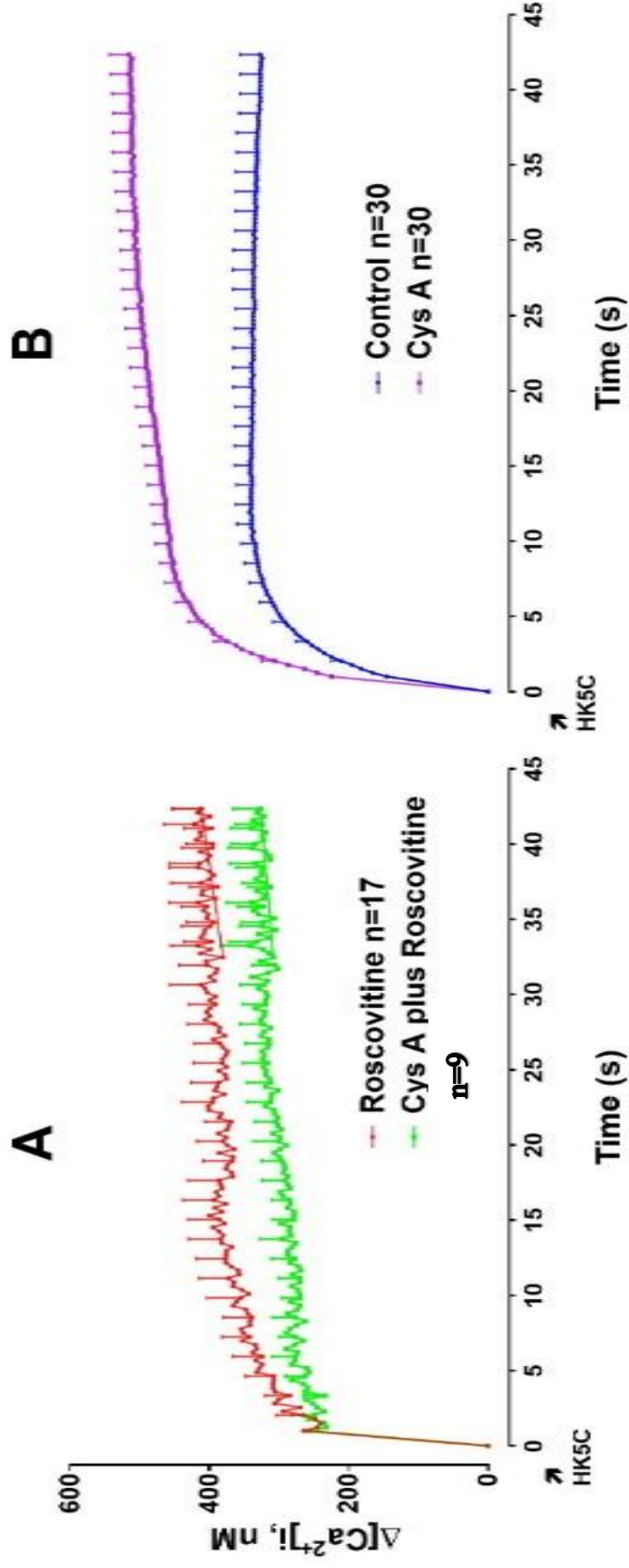


Figure 3.27. Dual treatment of Cys A and Roscovitine reduced HK5C evoked $\Delta[Ca^{2+}]_i$ and this may explain why Roscovitine plus Cys A treatment fails to allow the exocytosis of the SP. HK5C evoked $\Delta[Ca^{2+}]_i$ in terminal treated with a) 100 μ M Roscovitine plus 1 μ M Cys A compared to 100 μ M Roscovitine treatment alone b) drug free control compared to 1 μ M Cys A treatment. Data are mean \pm SEM, N=3 independent experiments for (a) and 6 for (b); $P < 0.05$ for both a and b.

3.7 Measurement of the bioenergetics of synaptosomes following various drug treatments

It was important to determine that the effect of the drugs employed, herein, were specifically acting on the pathway/substrate that were being tested and that they were not affecting the SV exocytosis non-specifically by perturbing the bioenergetics of the synaptosomes. Fortunately, it was possible to measure certain bioenergetics parameters by utilising the Seahorse XFp flux analyser and the mitochondria stress test assay. It should be noted that whilst the terminals were treated with the drugs for the same time as for the release assays, the synaptosomes were then actually incubated for an extended period (100 min) in order to carry out the stress test assay. Thus, this could mean that over this greater period (much longer than used for the other tests) some detrimental effects of the drugs could possibly be determined. Furthermore, whilst the initial incubation with the drugs were done at 37 °C, all the release assays employed herein were then performed at room temperature. However, some of the initial bioenergetics measurement (highlighted in figure legends and text) were performed at 37 °C because this was the lowest temperature that originally could be employed with the Seahorse XFp flux analyser. Thus, not only were the synaptosomes incubated for an extended period but they were incubated at a higher temperature. Fortunately, the Seahorse Company recently made a manifold that allowed the machine to incubate at lower temperatures and following the purchase of this, it was then possible to do the assays at room temperature. It was discovered that one difference in carrying out these assays at the two temperatures is that at 37°C, 0.5 µM rotenone and 0.5 µM antimycin A was able to fully work and enable the values for proton leakage and non-mitochondrial respiration to be determined, but at RT these drugs (in the time scale) did not fully work. However, this study herein determined that by using 10 times more of each of these drugs (5 µM of each) then these were able to block all mitochondrial respiration. For some of the drugs tested in the Seahorse XFp analyser at room temperature – PMA, Dynasore – these higher rotenone/antimycin A concentrations

were not employed and so one was unable to determine the proton leakage and the non-mitochondrial respiration.

The data are shown as Oxygen consumption vs time for the different conditions. These data could then be used to determine the following parameters: basal respiration; ATP production; spare capacity; maximal respiration; proton leakage; non-mitochondrial respiration. These values were determined by using the three individual time points for the different conditions (in some cases one time point might have been erroneous and this was removed) for each experiment, and combining these for the repeated experiments so that one obtained an average and a SEM for each condition in the assay.

3.7.1 100 μ M Roscovitine

The treatment with 100 μ M Roscovitine failed to perturb the bioenergetics of synaptosomes even using the extended 37°C conditions (Fig 3.28). This is made more obvious when the different parameters are plotted in Fig 3.29 A-F.

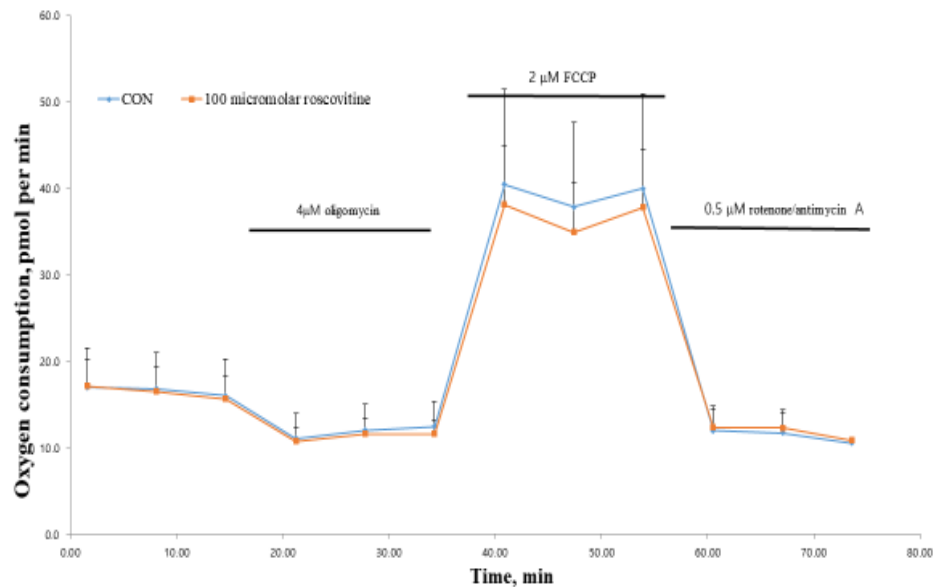


Figure 3.28. Synaptosomal bioenergetics were unaffected by 100 μ M Roscovitine treatment using the extended 37°C conditions. The experiment was repeated 3 times and the data represents the average of 8 individual synaptosome samples. Data points represent the mean and the error bars represent the SD; $P > 0.05$ which means that there is no significant difference between drug treated and non-treated synaptosomes.

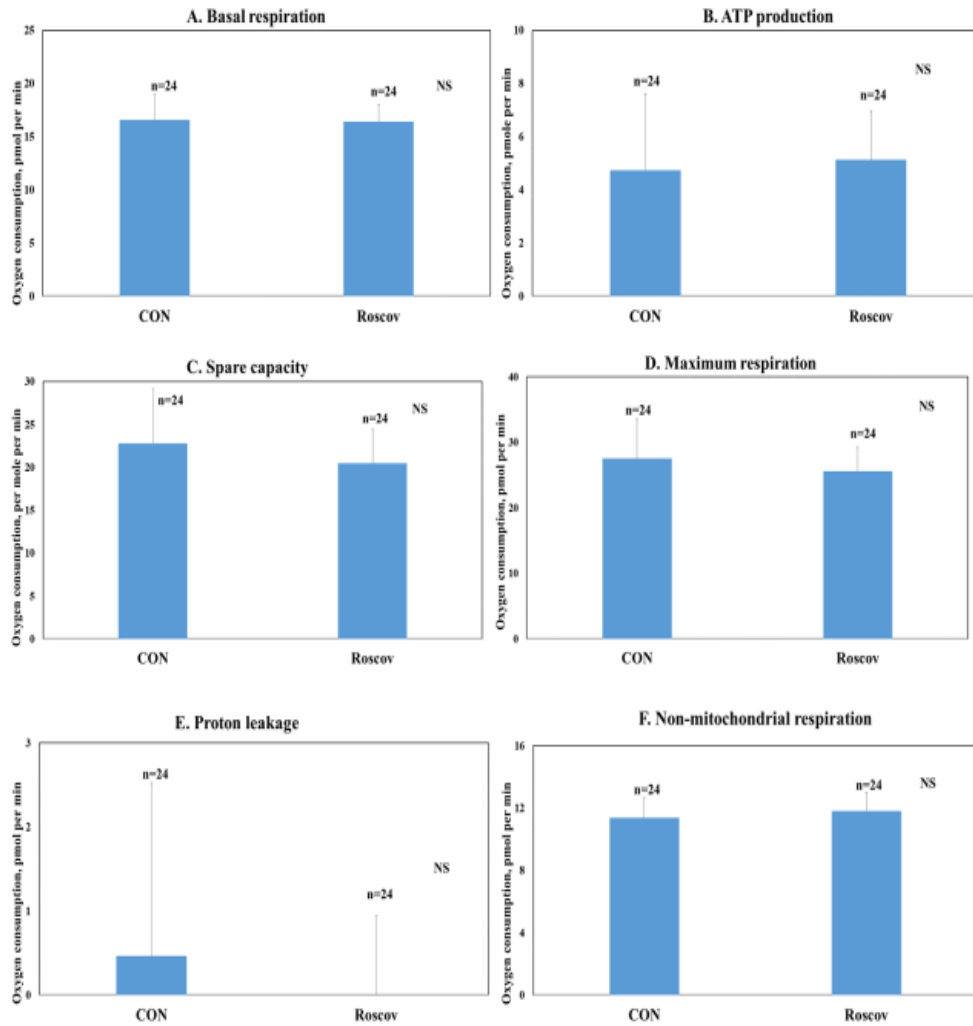


Figure. 3.29. 100 μ M Roscovitine treatment did not perturb any bioenergetics parameter measured as it looks similar to those for the controls. Bar charts showing the effect of 100 μ M Roscovitine compared to non-drug treated control on (A) basal respiration, (B) ATP production, (C) spare capacity, (D) maximal respiration, (E) proton leakage and (F) non-mitochondrial respiration. The data was calculated from the average of the three time points for each condition in the assay and these were averaged for the 3 repeat independent experiments shown in Fig 3.27. The histograms represent the mean and the error bar shows the SEM; $P > 0.05$.

It should be noted that 200 μ M Roscovitine, that had also been employed in release assays was also tested. However this concentration also did not perturb the bioenergetics integrity of the synaptosomes. Thus, Roscovitine action is not due to some non-specific perturbation of the respiratory capacity of the synaptosomes.

3.7.2 Dynasore

As Roscovitine did not perturb the synaptosomes, the effect of some of the individual drugs that was employed in conjunction with Roscovitine were also tested to ensure that these did not perturb the bioenergetics integrity of the nerve terminals.

An amount of 160 μM Dynasore pre-treatment of synaptosomes had negligible effect on the bioenergetics of the terminals employing assay at 27°C (Fig 3.30). Although, there appears to be a slight difference in these curves the only parameter that showed any significant difference was in the basal respiration and this was minimal (Fig 3.31 A-D). Note that this study only used 0.5 μM rotenone/ 0.5 μM antimycin A and it was not possible to measure proton leakage and non-mitochondrial respiration.

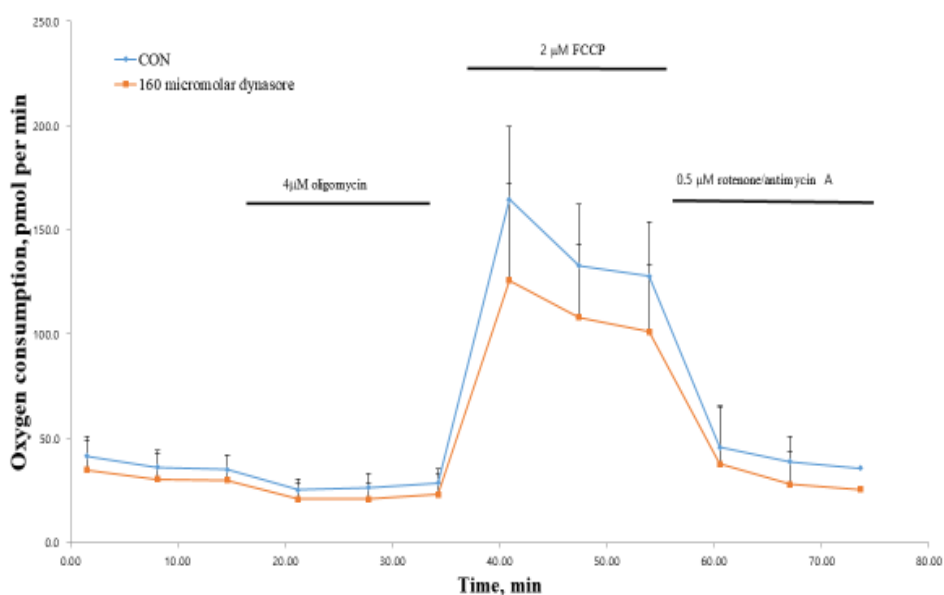


Figure 3.30. Synaptosomal bioenergetics were unaffected by 160 μM Dynasore treatment.

Data are mean \pm SD, n=6 from 3 independent experiments. Note that there was no significant difference ($P > 0.05$) in the data comparing control with test.

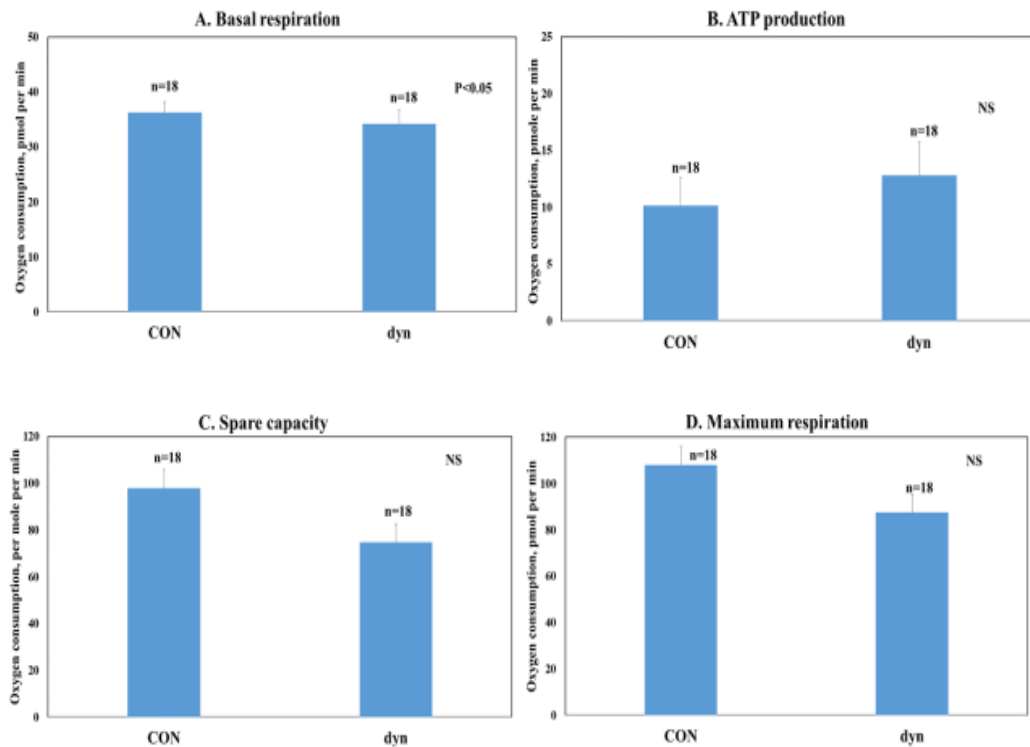


Figure 3.31. 160 μ M Dynasore treatment did not perturb majority of the bioenergetics parameter measured as it looks similar to those for the controls. Bar charts showing effect of 160 μ M Dynasore on (A) basal respiration, (B) ATP production, (C) spare capacity, and (D) maximal respiration. The data was calculated from the average of the three time points for each condition and included data from 3 independent experiments shown in Fig 3.30 (n=18). The histograms represent the mean and the error bar shows the SEM. Note that there was no significant difference ($P > 0.05$) in the data comparing control with test apart from basal respiration and this was a minimal difference.

The use of 80 μ M Dynasore produced no effect on any parameter. However, if the assay was done with the extended time course at 37°C, it was evident that Dynasore did seem to perturb certain parameters (data not shown). This result might actually be important for the use of Dynasore to study Dyn action. This study only used Dynasore acutely and it is tested only after about 20 mins post-initial incubation at RT. At this time, the Dynasore does not appear to have much detrimental effect on the bioenergetics. However, clearly

after the prolonged 37°C incubation Dynasore starts affecting the bioenergetic integrity of the terminals. This interesting finding could explain some recent findings (Park et al, 2013) which claimed that Dynasore had an off target effect that meant that it could not be used to study Dyn. However, they treated fibroblasts for many hours (24 hours or more) with Dynasore and this may very well disturb the cells bioenergetics which would then produce some extra effects. In fact, this may still reflect a specific action of Dynasore on a Dyn but rather than Dyn I, this could be that the drug can also block the mitochondrial specific Drp I (Dyn-related protein 1). Such a perturbation could very well disturb mitochondrial function. However, in the present studies by only using an acute treatment with Dynasore and not a chronic treatment it would appear that the experiment is specifically targeting on Dyn 1. Although, Dynasore also works on Dyn 2, the Asthon group (unpublished observation) has shown that inhibiting Dyn 2 specifically (using a low dose of a drug called Dyngo-4aTM (50 nM)) does not have any effect on SV exocytosis or GLU release.

3.7.3 Blebbistatin

Acute treatment with 50 μM Blebbistatin failed to perturb the bioenergetics of synaptosomes (Fig 3.32, Fig 3.33 A-F) even with the extended 37°C assay employed with the Seahorse XFp flux analyser.

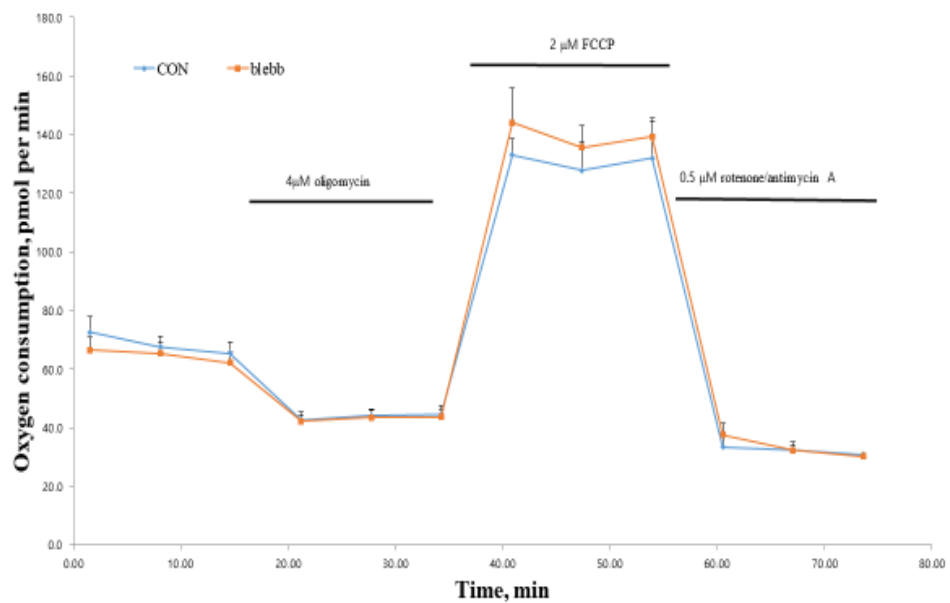


Figure 3.32. Synaptosomal bioenergetics were unaffected by 50 μM Blebbistatin treatment.

The experiment was done three times and the mean values represent an average of 6 independent measurements and error bars represent the SD. Note that there was no significant difference ($P > 0.05$) in the data comparing control with test.

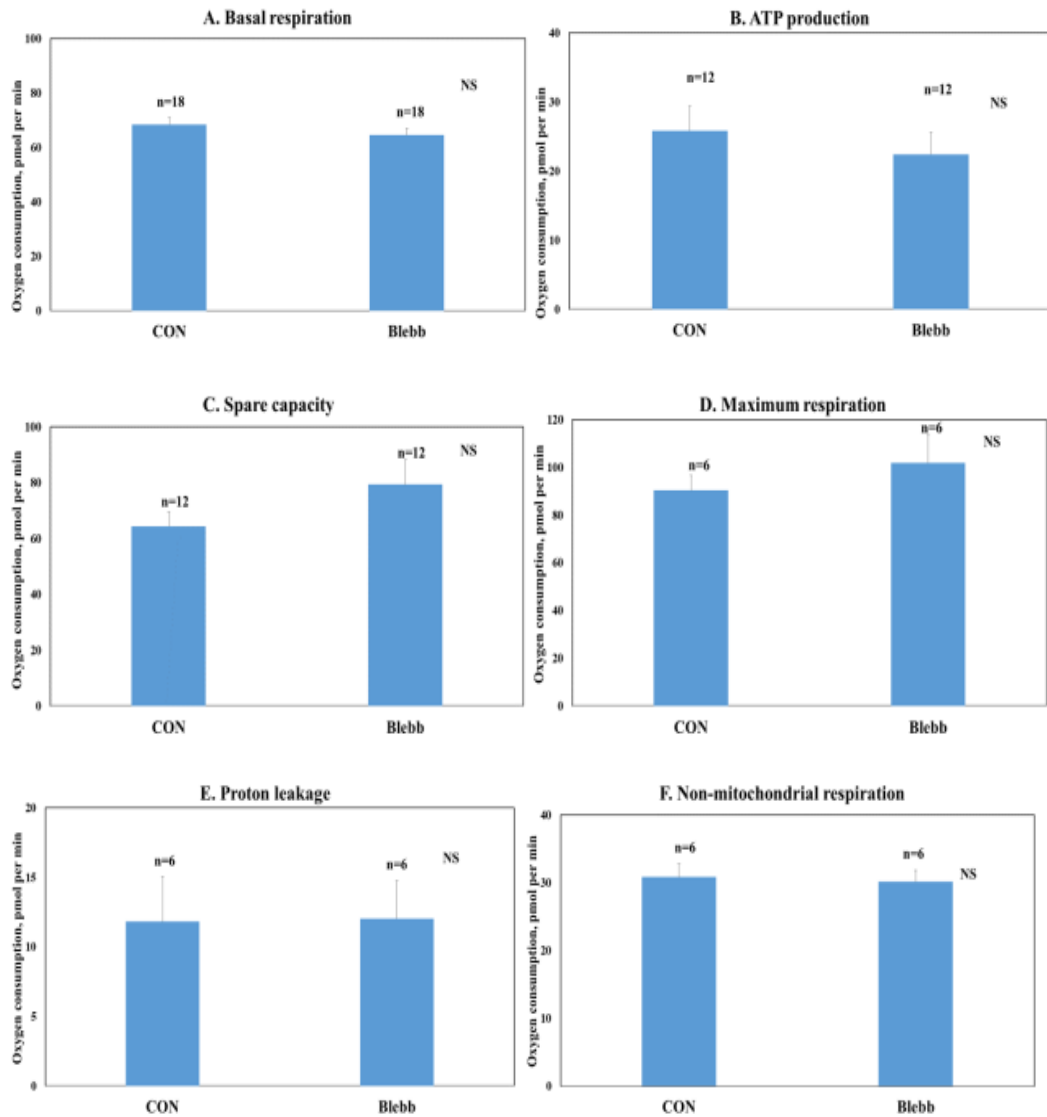


Figure 3.33. 50 μM Blebbistatin treatment did not perturb any bioenergetics parameter measured as it looks similar to those for the controls. The effect of 50 μM Blebbistatin on (A) basal respiration, (B) ATP production, (C) spare capacity, (D) maximal respiration (E) proton leakage, and (F) non-mitochondrial respirations. The data was calculated from the average of the three time points for each treatment shown in Fig 3.32. Depending on the number of values that were removed due to error the different parameters have different numbers of values employed in their analysis (as shown in the figures). The histograms represent the mean and the error bar shows the SEM. Note that there was no significant difference ($P > 0.05$) in the data comparing control with test.

3.7.4 PMA

Although, we tested PMA with Roscovitine, it was necessary to initially test PMA alone. Acute treatment with 1 μM PMA failed to perturb the bioenergetics of synaptosomes (Fig 3.34, Fig 3.35 A-D) with the extended 27°C assay employed with the Seahorse XFp flux analyser.

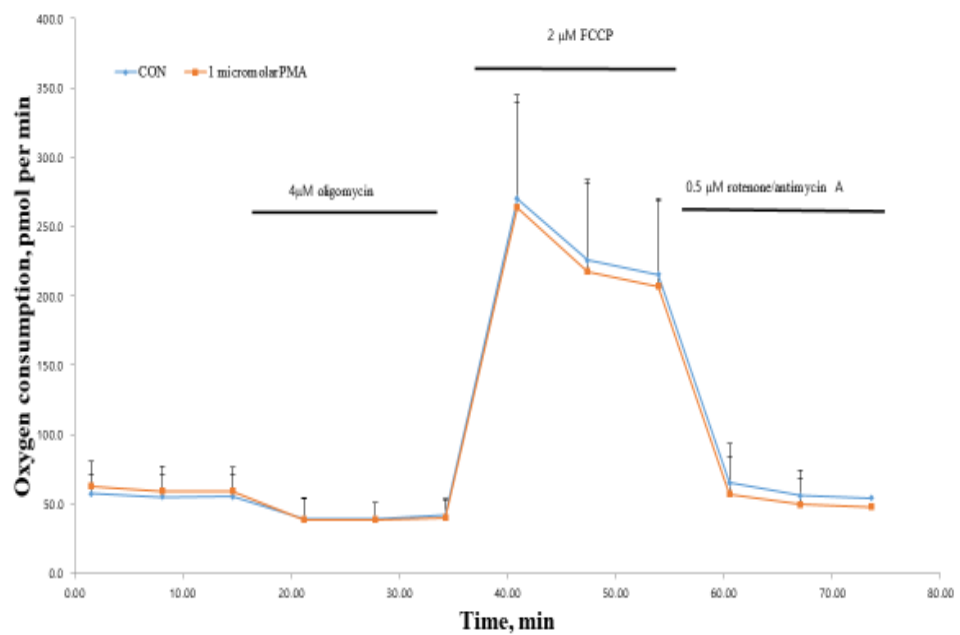


Figure 3.34. The effect of 1 μM PMA on the bioenergetics of synaptosomes using the Seahorse XFp analyser at 27°C. The experiment was done three times and the mean values represent an average of 9 independent measurements and error bars represent the SD; $P > 0.05$.

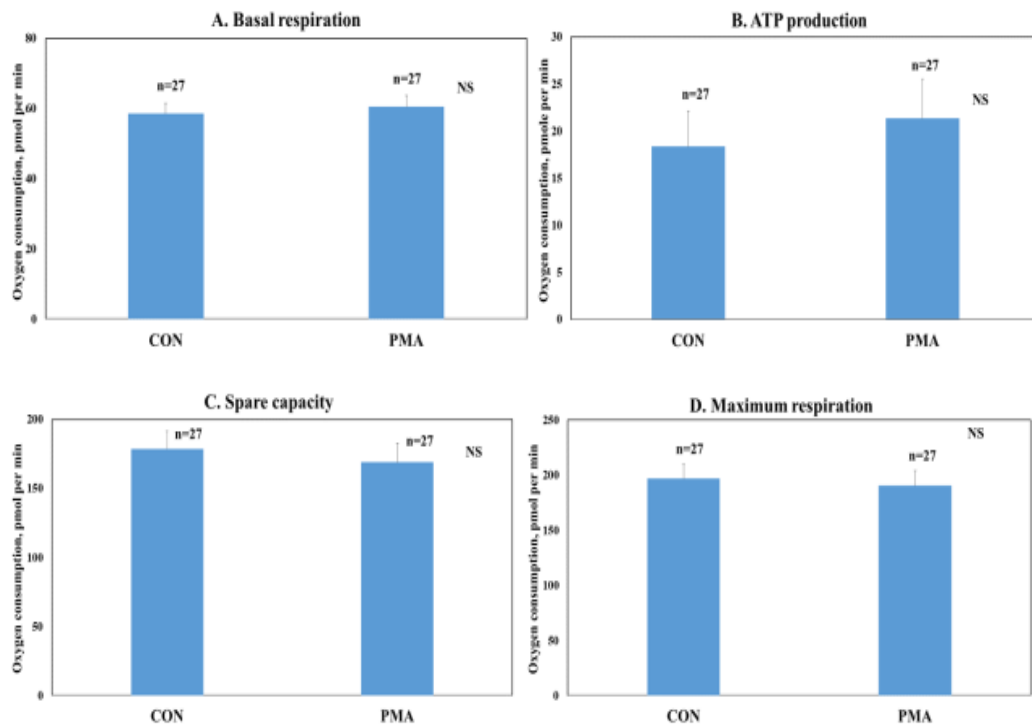


Fig 3.35. The effect of 1 μ M PMA on (A) basal respiration, (B) ATP production, (C) spare capacity, and (D) maximal respiration. The data was calculated from the average of the three time points for each treatment and average data from the 3 independent experiments shown in Fig 3.34. The histograms represent the mean and the error bar shows the SEM.

3.7.5 PMA with Roscovitine

Acute treatment with 1 μM PMA plus 100 μM Roscovitine failed to perturb the bioenergetics of synaptosomes (Fig 3.36, Fig 3.37 A-F) with the Seahorse XFp flux analyser.

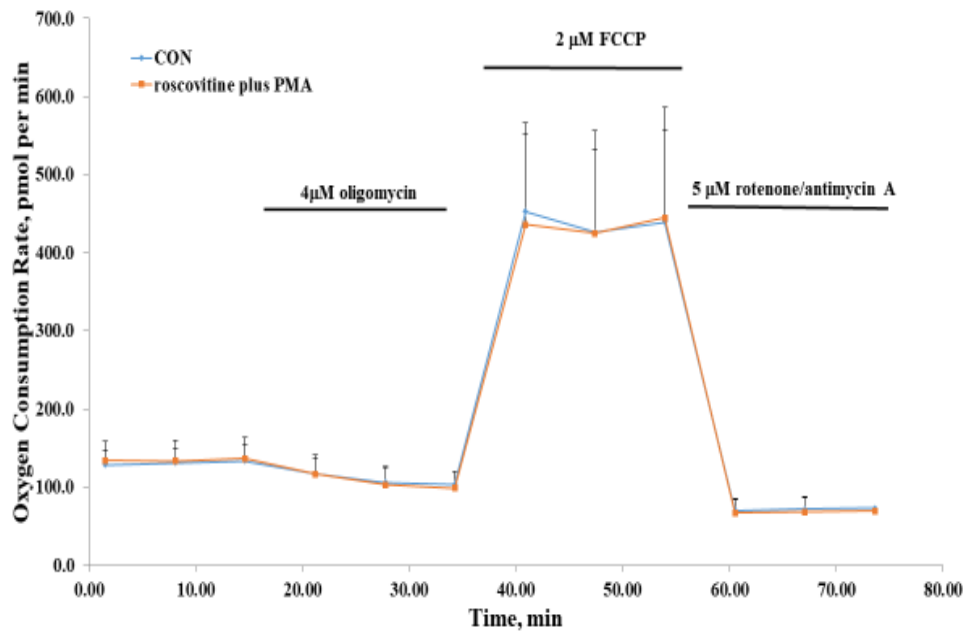


Figure 3.36. The effect of 1 μM PMA plus 100 μM Roscovitine on the bioenergetics of synaptosomes using the Seahorse XFp analyser at 27°C. The experiment was done three times and the mean values represent an average of 9 independent measurements and error bars represent the SD. There is no significant difference between drug treated and control for any components of the mito stress test assay ($P>0.05$).

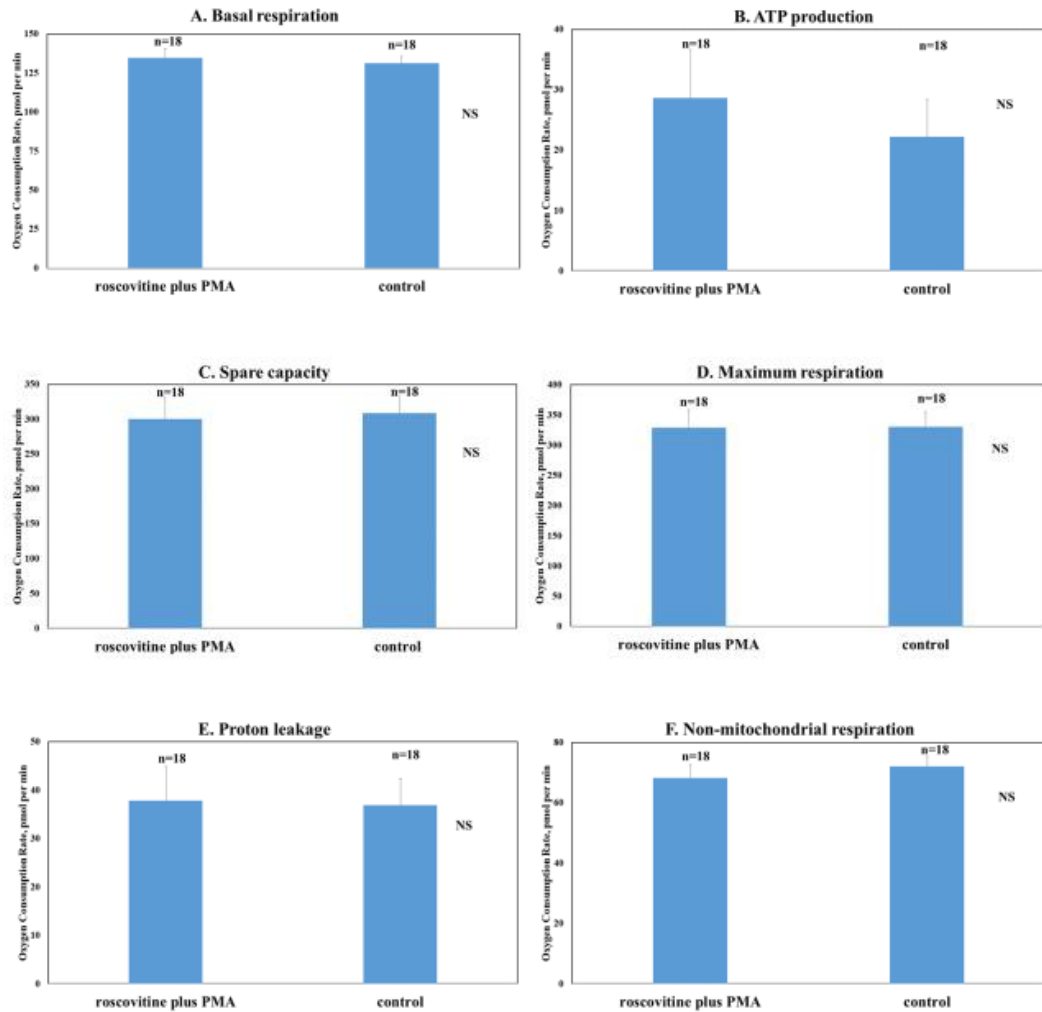


Figure 3.37. The effect of 1 μ M PMA plus Roscovitine on (A) basal respiration, (B) ATP production, (C) spare capacity, (D) maximal respiration, (E) Proton leakage, and (F) Non-mitochondrial respiration. The data was calculated from the average of the three time points for each treatment and averaged the 3 independent experiments shown in Fig 3.36 (n=18 as some values were incorrect and removed). The histograms represent the mean and the error bar shows the SEM.

3.7.6 Go6983

Although, we tested Go6983 plus Roscovitine, there was a need to check Go6983 alone first. Acute treatment with 1 μM Go6983 failed to perturb the bioenergetics of synaptosomes (Fig 3.38, Fig 3.39 A-F) even with the extended 37°C assay employed with the Seahorse XFp flux analyser.

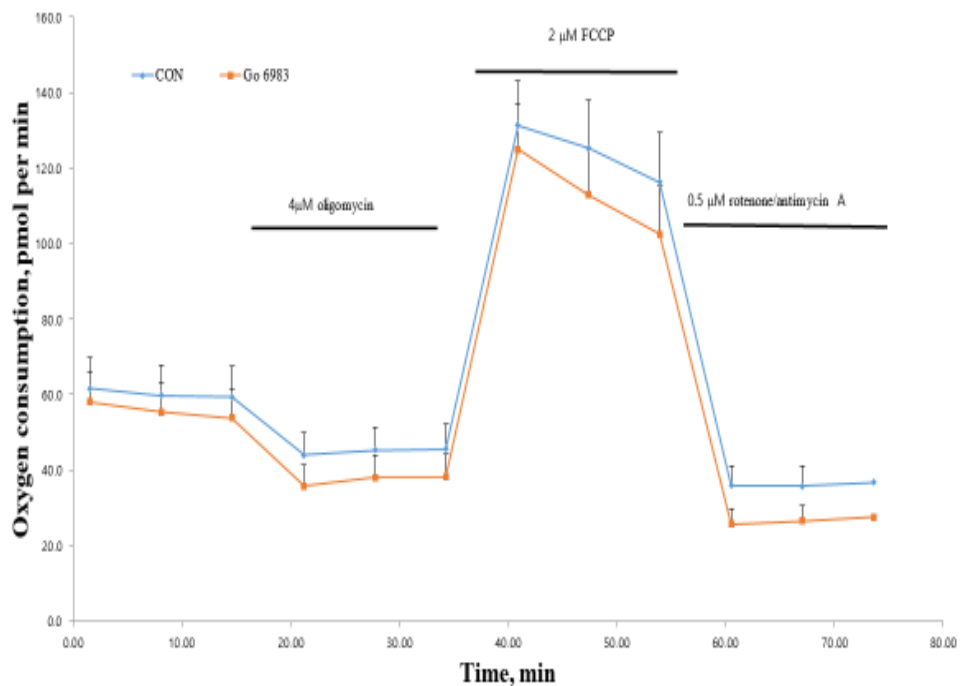


Figure 3.38. The effect of 1 μM Go 6983 on the bioenergetics of synaptosomes using the Seahorse XFp analyser at 37°C conditions. The experiment was done three times and the mean values represent an average of 9 independent measurements and error bars represent the SD. Note that there was no significant difference ($P > 0.05$) in the data comparing control with test.

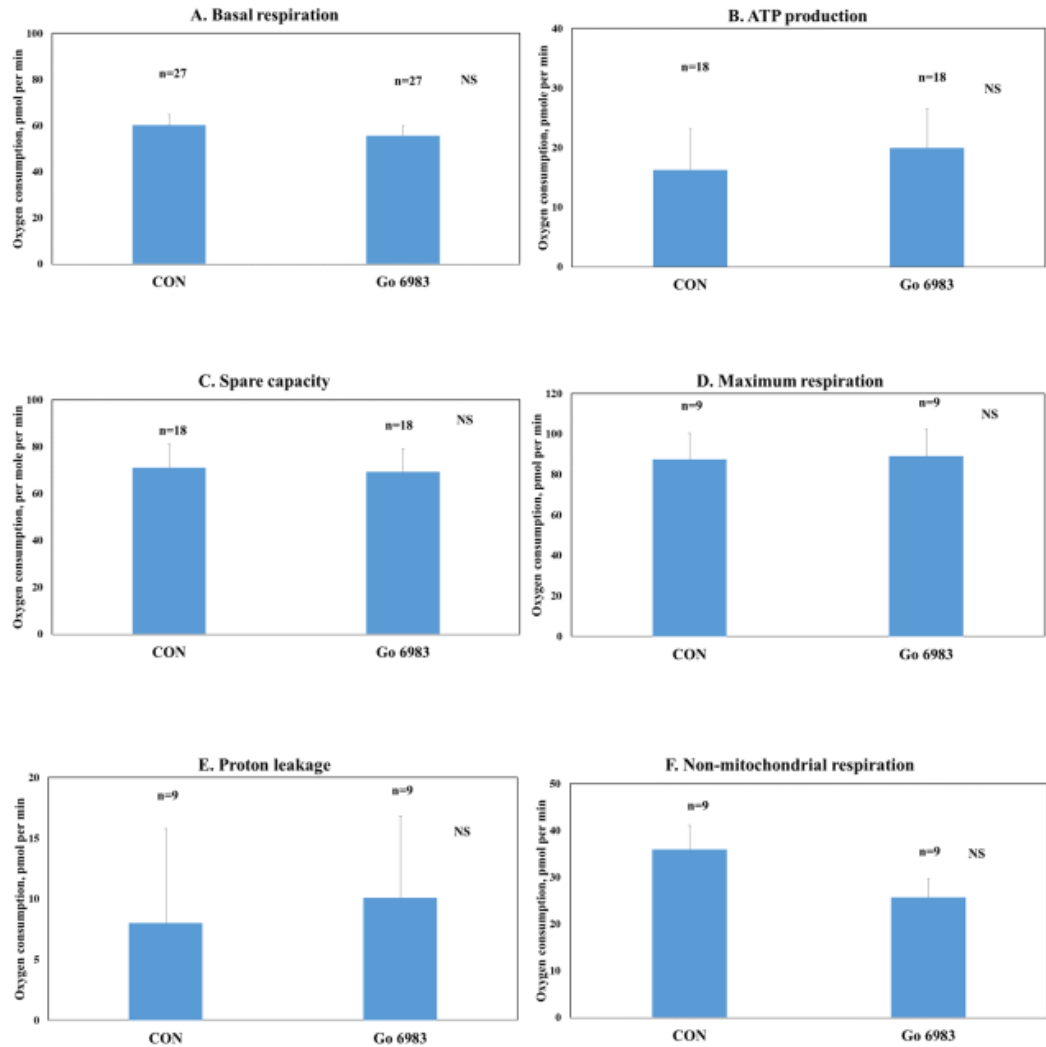


Figure 3.39. The effect of 1 μM Go 6987 on (A) basal respiration, (B) ATP production, (C) spare capacity, (D) maximal respiration, (E) proton leakage and (F) non-mitochondrial respiration. The data was calculated from the average of the three time points for each treatment shown in Fig 3.38 and average for the 3 independent experiments. However, for some measurement, certain values were wrong and so were removed. The histograms represent the mean and the error bar shows the SEM. Note that there was no significant difference ($P > 0.05$) in the data comparing control with test.

3.7.7 Go6983 with Roscovitine

Acute treatment with 1 μM Go6983 plus 100 μM Roscovitine failed to perturb the bioenergetics of synaptosomes (Fig 3.40, Fig 3.41 A-F) even with the extended 37°C assay employed with the Seahorse XFp flux analyser.

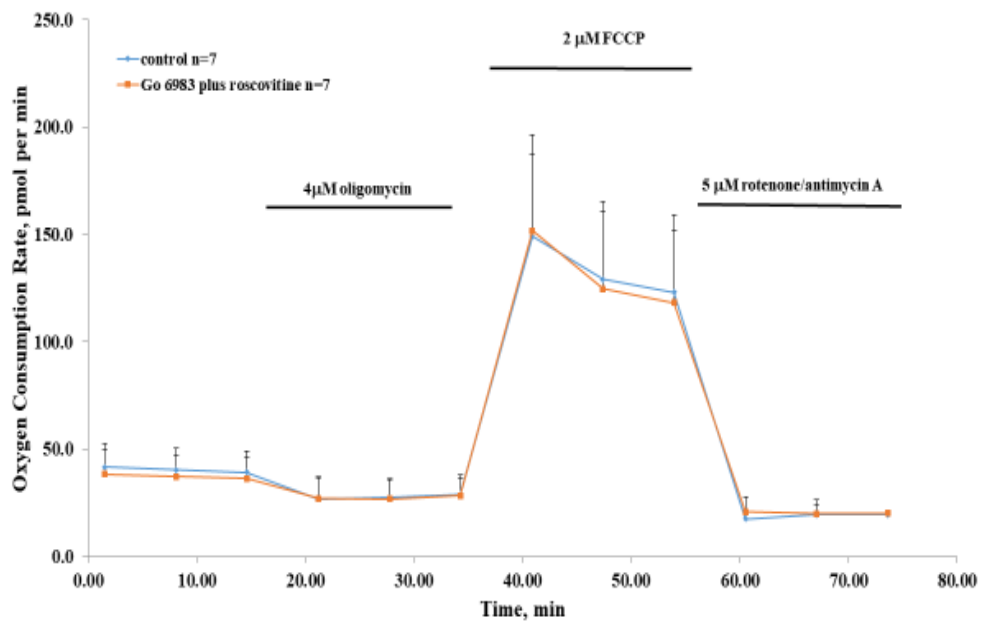


Figure 3.40. The effect of 1 μM Go 6983 plus 100 μM Roscovitine on the bioenergetics of synaptosomes using the Seahorse XFp analyser at 37°C. The experiment was done three times and the mean values represent an average of 7 independent measurements and error bars represent the SD. Note that there was no significant difference ($P > 0.05$) in the data comparing control with test.

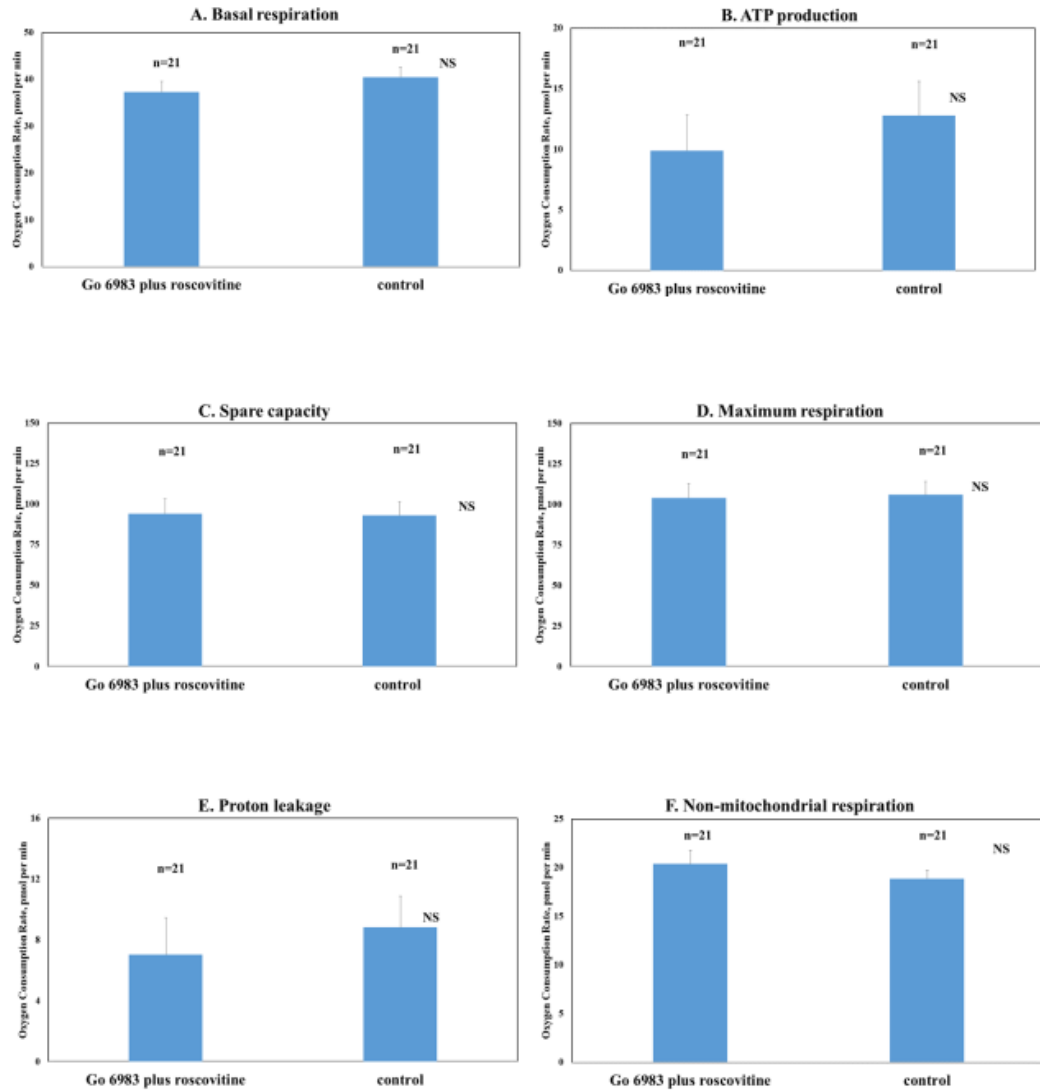


Figure 3.41. The effect of 1 μ M Go6983 plus 100 μ M Roscovitine on (A) basal respiration, (B) ATP production, (C) spare capacity, (D) maximal respiration, (E) Proton leakage, and (F) Non-mitochondrial respiration in synaptosomes. The histograms represent the mean and the error bar shows the SEM. Note that there was no significant difference ($P > 0.05$) in the data comparing control with test.

3.7.8 JASP plus Roscovitine

Treatment with 2.5 μM JASP alone had no effect on the bioenergetics (see Fig 6.28 and 6.29) and furthermore, treatment with 2.5 μM JASP plus 100 μM Roscovitine failed to perturb the bioenergetics of synaptosomes when assay performed at 24°C (Fig 3.42, Fig 3.43 A-F).

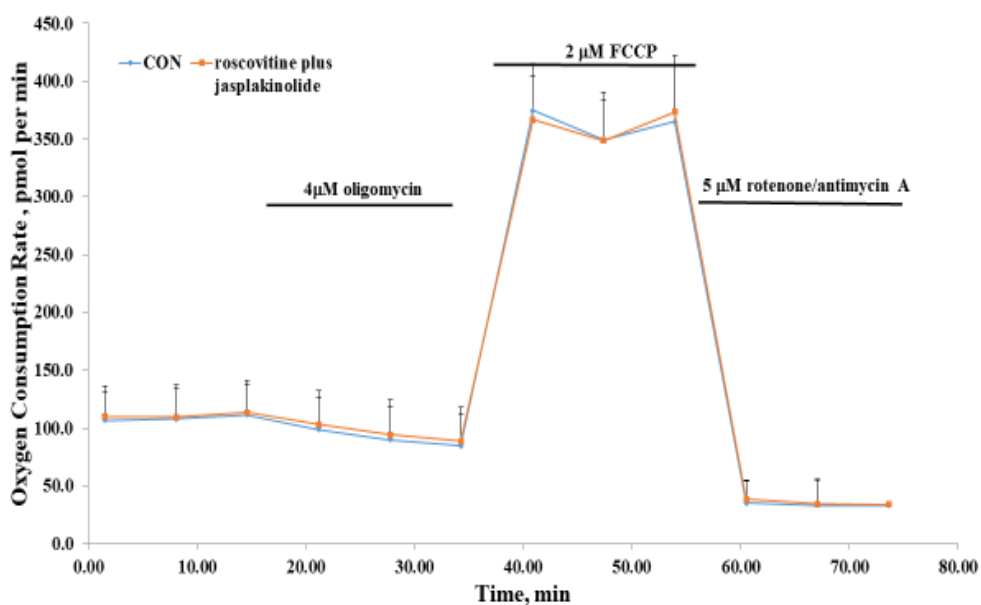


Figure 3.42. The effect of 2.5 μM JASP plus 100 μM Roscovitine on the bioenergetics of synaptosomes. The experiment was done 3 times and the mean values represent an average of 8 independent measurements and error bars represent the SD. Note that there was no significant difference ($P > 0.05$) in the data comparing control with test.

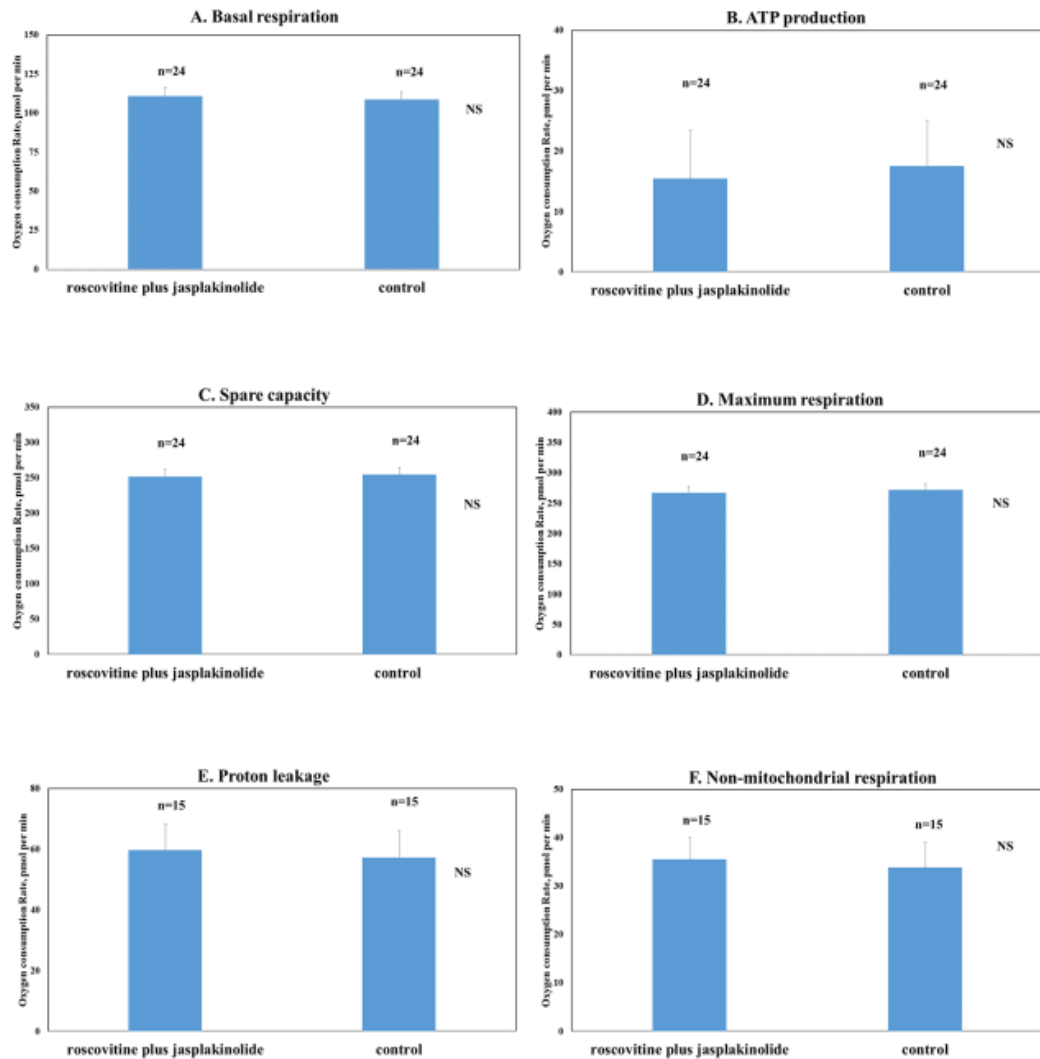


Figure. 3.43. The effect of 2.5 μ M JASP plus 100 μ M Roscovitine on (A) basal respiration, (B) ATP production, (C) spare capacity, (D) maximal respiration, (E) proton leakage and (F) non-mitochondrial respiration. The histobars represent the mean and the error bar shows the SEM. Note that there was no significant difference ($P > 0.05$) in the data comparing control with test.

3.7.9 Cys A plus Roscovitine

Treatment with 1 μM Cys A plus 100 μM Roscovitine failed to perturb the bioenergetics of synaptosomes when assay performed at 24°C (Fig 3.44, Fig 3.45 A-F).

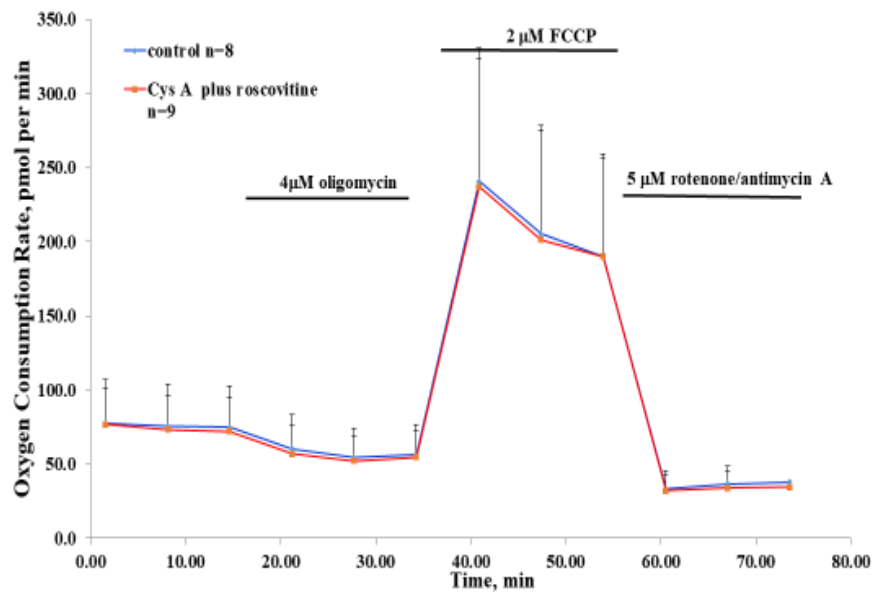


Figure 3.44. The effect of 1 μM Cys A and 100 μM Roscovitine on the bioenergetics of synaptosomes. The experiment was done 3 times and the mean values represent an average of 9 independent measurements and error bars represent the SD. Note that there was no significant difference ($P > 0.05$) in the data comparing control with test.

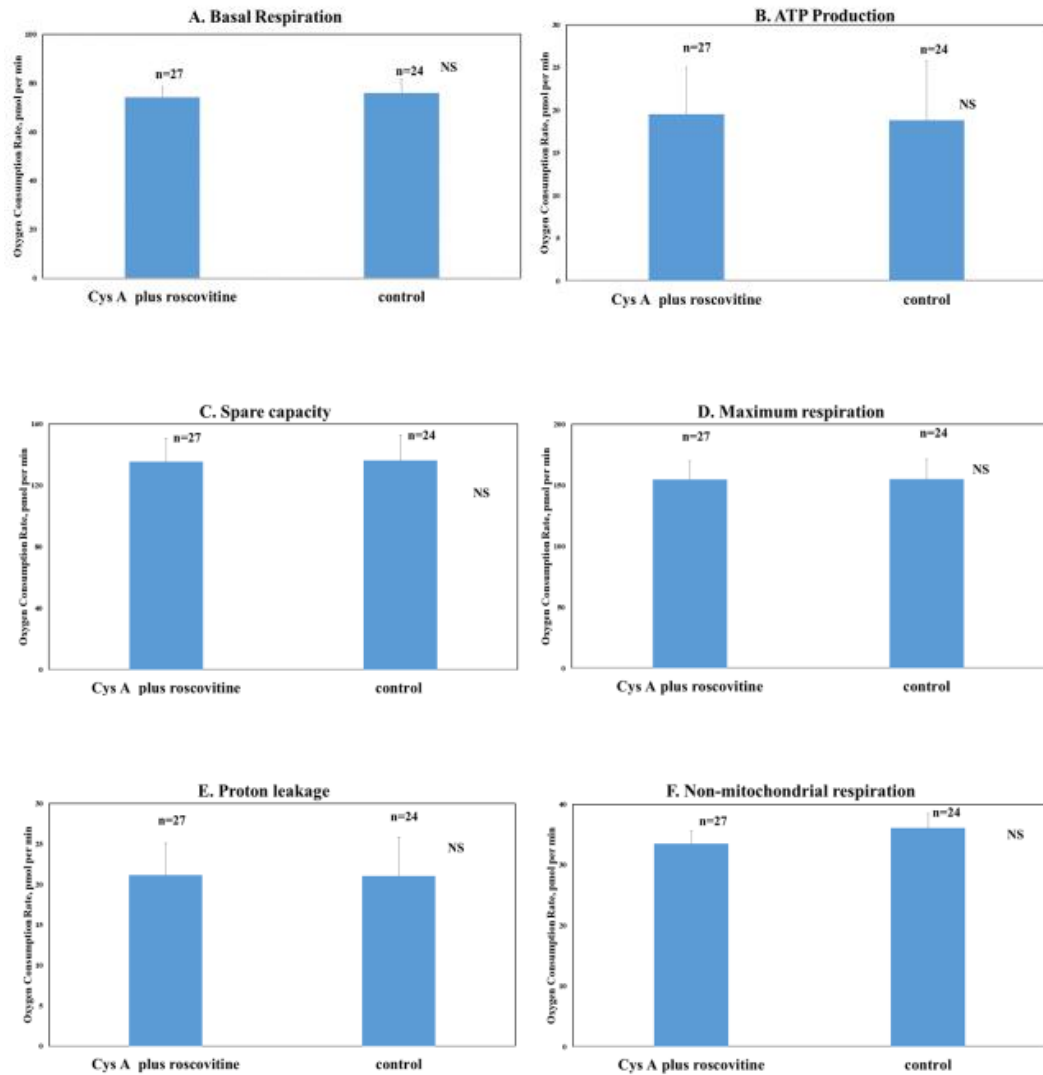


Figure 3.45. The effect of 1 μ M Cys A plus 100 μ M Roscovitine on (A) basal respiration, (B) ATP production, (C) spare capacity, (D) maximal respiration, (E) proton leakage and (F) non-mitochondrial respiration. The histograms represent the mean and the error bar shows the SEM. Note that there was no significant difference ($P > 0.05$) in the data comparing control with test.

3.8 Phosphorylation profiles of various sites in Syn I following Roscovitine treatment

Earlier we have showed that 100 μ M Roscovitine treatment of synaptosomes allows HK5C and ION5C to evoke SP release. Roscovitine is a Cdk5 inhibitor, thus the HK5C or ION5C evoked SP release following application of this drug is proposed to be due to an attenuation of Cdk5 activity. However, a detailed understanding of how Cdk5 inhibition leads to the evoked SP release is not fully known. One of the methods used to investigate this is to study phosphorylated profiles of particular proteins that are speculated to be involved in the SP regulation. One such protein is Synapsin I (Syn I) and its phosphorylation can be studied using western blotting following the evoked release of the SP after Roscovitine treatment.

3.8.1 Results

To determine the effect of Cdk5 inhibition on the phosphorylated state of different sites on Syn I, synaptosomes were treated with Roscovitine (to block Cdk5) or 10 μ M KN-93 (to block CaMKII) (i.e. Sumi *et al*, 1991) (shown previously to induce specific action on synaptosomes (Bhuva, 2015; Singh, 2017)) in the first trial and Roscovitine or 2 μ M KT5720 (to block PKA) (i.e. Murray, 2008) (shown previously to induce specific action on synaptosomes (Rostron, 2019)) in the second trial. Following such drug treatment, synaptosomes were subsequently stimulated with various stimuli (4AP5C, HK5C, and ION5C) for different time points (2s, 15s, 30 s and 120 sec) before being solubilised in NuPAGE sample buffer and subsequently used for western blotting. Note, in first trial, lane 1-4 of the blots contained samples with non-drug treated control, lane 5-8 samples treated with KN-93, and lane 9-12 samples treated with Roscovitine, whilst in second trial, 1-4 contained samples with non-drug treated control, 5-8 contained samples treated with Roscovitine, and 9-12 contained samples pre-treated with KT5720. Since, major interest

in this study is the stimulation evoked SP release in the presence of Roscovitine, only non-drug applied control vs Roscovitine conditions were subjected to analysis.

Phosphorylation in all Western blots were determined by chemi-luminescence that detected phospho-specific sites on Syn I with densitometric analysis as mentioned in Chapter 2, and the range (for the blots that were tested at least twice) to measure the average changes in phosphorylation compared to the respective L0 condition, based on the number of experiments conducted. It is important to remember that 4AP5C stimulation evokes release of the RRP only even in the presence of Roscovitine, whilst HK5C and ION5C with Roscovitine treatment have been shown to release the RRP, the RP and the SP. The mechanism of ION5C evoking the release is distinct from HK5C as this ionophore by-passes Ca^{2+} channels and increase the Ca^{2+} level throughout the terminal whereas HK5C depolarises terminals and allow Ca^{2+} entry via the opening of voltage dependent Ca^{2+} channels.

Previous studies have demonstrated that the phosphorylation of specific sites on Syn I are due to the action of distinct kinases. Ser-9 site is known to be phosphorylated by cAMP dependent kinases (PKA) (Yamagata and Neirn, 2015), Ser-553 by cyclic dependent kinases (Cdk) 1/5 (Cesca *et al*, 2010; Verstegen *et al*, 2014), and Ser-603 site by CaMK II (Sakurada *et al*, 2002).

3.8.2 Phosphorylation of Syn I Ser-553 *in vivo*

Syn I-Ser-553 site is phosphorylated by Cdk5, a kinase that is inhibited by Roscovitine treatment (Verstegen *et al*, 2014). Careful observation of the phospho-Ser-553 probed blots revealed that at 15 sec, there is a reduction in phosphorylation in Roscovitine treated conditions (lane 5-8) compared to non-drug treated controls (lane 1-4) (Fig 3.46 A-B).

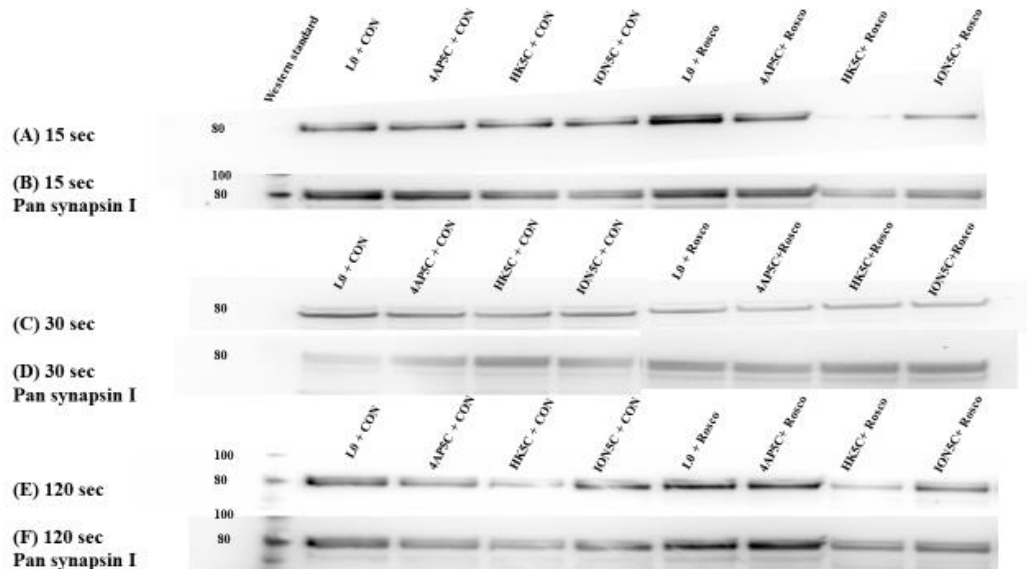


Figure 3.46. The effect of 100 μ M Roscovitine treatment upon the phosphorylation Syn I on the Ser-553. A) 15 sec stimulation B) Reprobing of this blot for 15 sec with Pan-Syn I C) 30 sec stimulation D) Reprobing of this blot for 30 sec with Pan-Syn I E) 120 sec stimulation F) Reprobing of this blot for 120 sec with Pan-Syn I. This is a representative blot (All blots N=2)

Following a 30 sec stimulation, Roscovitine treated nerve terminal are appear to contain less phosphorylated Ser-553 Syn I compared to no drug treated sample (Fig 3.46 C). This was also evident after 120 sec stimulation, where a reduction in the specific phosphorylation site in the presence of Roscovitine treatment appears to be definite (Fig 3.46 E). Note that in 30 sec (Fig 3.46 D) and 120 sec stimulated samples (Fig 3.46 F) re-probed with pan Syn I demonstrates that total protein was greater in the Roscovitine treated conditions for some reason but this suggests that the reduction in phosphorylation could potentially be more significant following the application of Roscovitine.

The results are not clear cut looking at the blots but one can normalise the Ser-553 phosphorylation relative to the Pan-Syn I signal and then one compares all result to the basal condition. This will reveal only stimulus evoked change in the phosphorylated serine and will take in to account the change in total protein. Bar charts in Figure 3.47 A-C are showing semi-quantitative analysis of phospho-Ser-553 probed blots presented in Figure 3.46. At early time points representing combined values of 2 sec and 15 sec,

phosphorylation following Roscovitine treatment was found to be reduced for 4AP5C stimulation, and for HK5C compared to non-drug treated samples. Such a decrease in Ser-553 phosphorylation of Syn I following Roscovitine treatment compared to non-drug treated control appear to be enhanced at 30 sec and 120 sec as both time points show visibly lower phosphorylation in Roscovitine treated conditions compared to drug free control in all stimuli employed. Clearly, the phosphorylation of phospho-Ser-553 site on Syn I is reduced in the presence of Roscovitine compared to its absence and the following result may suggest that the well characterised action of this drug on Cdk5 activity is shown to be connected to inhibition of phosphorylation of Ser-553 on Syn I. This is a preliminary set of experiments and needs to be repeated more times in order to determine statistical significance (Fig 3.47 A-C).

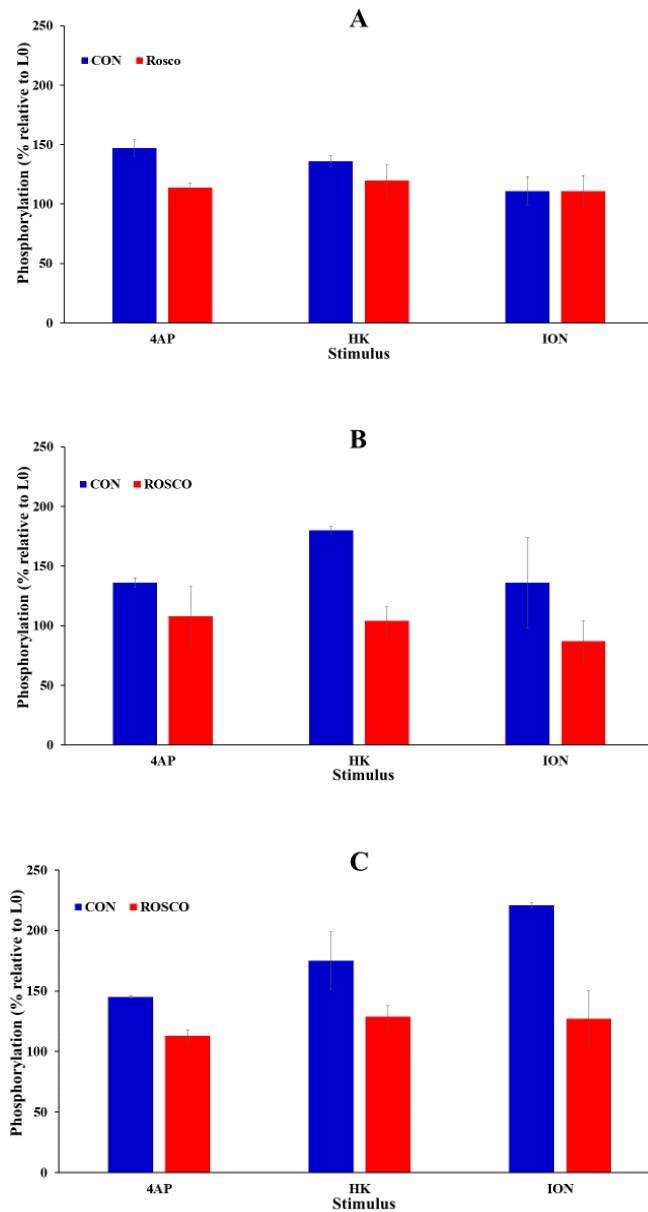


Figure 3.47. The effect of 100 μ M Roscovitine upon Syn I Ser-553 phosphorylation following various stimulation for a) early time points (2 sec+15 sec) b) 30 sec c) 120 sec; N=4 A; N=2 in B and C. All results are normalised to the L0 control value. a) shows a reduction of phosphorylation following Roscovitine treatment under 4AP5C stimulation relative to non-drug treated control, and HK5C with Roscovitine also shows some reduction compared to condition without Roscovitine treatment but these values were not significantly different. These differences become greater for longer stimulation periods and at b) 30 sec and c) 120 sec there appears to be clear differences between Roscovitine treated and non-treated conditions.

3.8.3 Phosphorylation of Syn I Ser-9 in synaptosomes

Roscovitine has been established to inhibit Cdk5 activity, although, it is possible that the drug induced increase of releasable SVs from the SV pools may also involve the phosphorylation of Syn I by other kinases, such as PKA or CaMK II. Therefore we have investigated phosphorylation profiles of Syn I at the sites other than Cdk5 site in stimulated terminals following Roscovitine treatment. PKA phosphorylates Syn I at Ser-9 site and with the careful observation of the blot probed with Phospho-Syn I Ser-9, the Roscovitine samples appear to contain more phosphorylated Ser-9 than the non-drug treated samples following a 2 sec stimulation (Fig 3.48 A), However, this may have actually been due to relatively more total protein contents in Roscovitine treated samples as the corresponding pan-Syn I blot appear darker (Fig 3.48 B). This finding cannot be explained since all samples were adjusted to the same protein concentration.

At 15 sec stimulation, HK5C + Roscovitine and ION5C + Roscovitine conditions appear to be less phosphorylated compared to basal and 4AP5C stimulation with Roscovitine, and to their corresponding drug free control conditions (Fig 3.48 C). However, re-probing blots for pan-Syn-I revealed that the level of Syn-I protein contained in these two lanes were much less compared to other samples (Fig 3.48 D). Thus only by normalising the data to the pan-Syn I content can one make any interpretation.

At 30 sec stimulation, there is little detectable increase of phosphorylation in Ser-9 identified in the samples treated with Roscovitine relative to drug free control (Fig 3.49 A-B). Following 120 sec stimulation there may be some Roscovitine induced increase in phosphorylation of Ser-9 for 4AP5C and ION5C stimulation compared to drug free samples. HK5C appear to induce lower Ser-9 phosphorylation in the Roscovitine treated samples, however this can be explained because pan-Syn-I blot indicates a lower amount of protein in this sample (Fig 3.49 C-D).

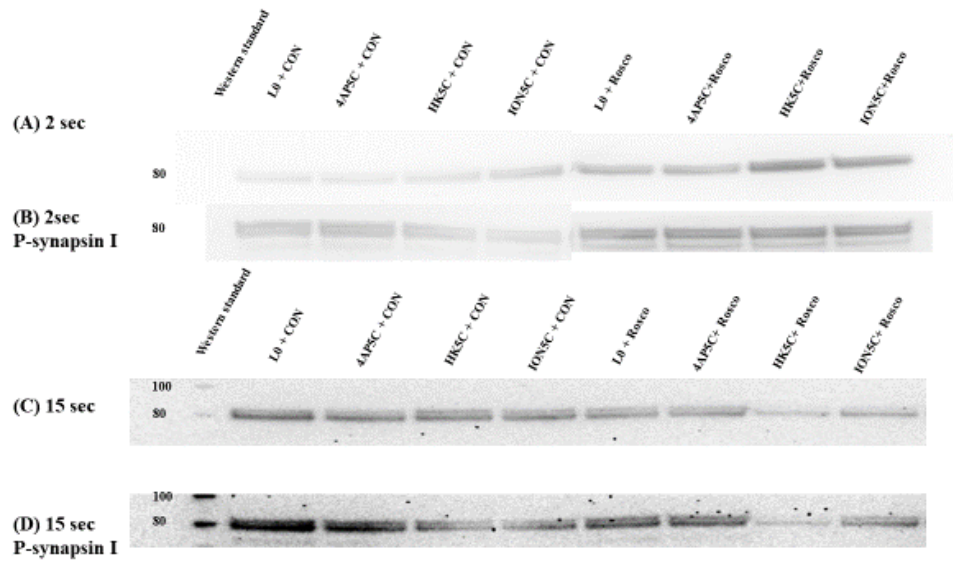


Figure 3.48. The effect of 100 μ M Roscovitine treatment upon the phosphorylation of Ser-9 in Syn I. A) 2 sec stimulation B) Pan-Syn I blot reprobred for the 2 sec stimulation C) 15 sec stimulation D) Pan-Syn I blot reprobred for the 15 sec stimulation. This is a representative blot (All blots are N=2).

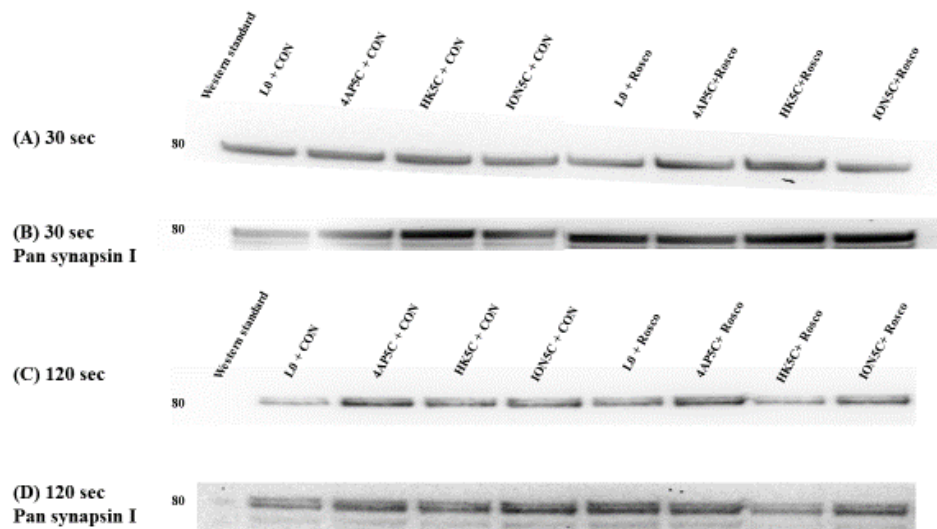


Figure 3.49. The effect of Roscovitine treatment upon phosphorylation of Ser-9 for Syn I. A) 30 sec stimulation B) Pan-Syn I blot reprobred for the 30 sec stimulation C) 120 sec stimulation D) Pan-Syn I blot reprobred for the 120 sec stimulation condition. This is a representative blot (A is N=2; B is N=1).

Semi-quantitative analysis is presented as a bar charts in figure 3.50. There appears to be a stimulus dependent increase in phosphorylation of Ser-9 with the different stimuli releasing a maximum effect at different times. ION5C induces maximum early whilst 4AP5C takes longer. At early time points, there appeared to be higher phosphorylation for the Roscovitine treated terminals compared to non-drug treated controls for 4AP5C and HK5C (Fig 3.50 A). At 30 sec (Fig 3.50 B), it may be that the difference between 4AP5C plus Roscovitine and HK5C plus Roscovitine conditions and non-drug treated control may still be larger and this is apparent still with same stimuli employed for 120 sec stimulation (Fig 3.50 C). However, it would appear that Roscovitine has no real effect on ION5C evoked changes in phospho-Ser-9 of Syn I. Again, this experiment has to be repeated multiple times in order to obtain data that can be statistically tested.

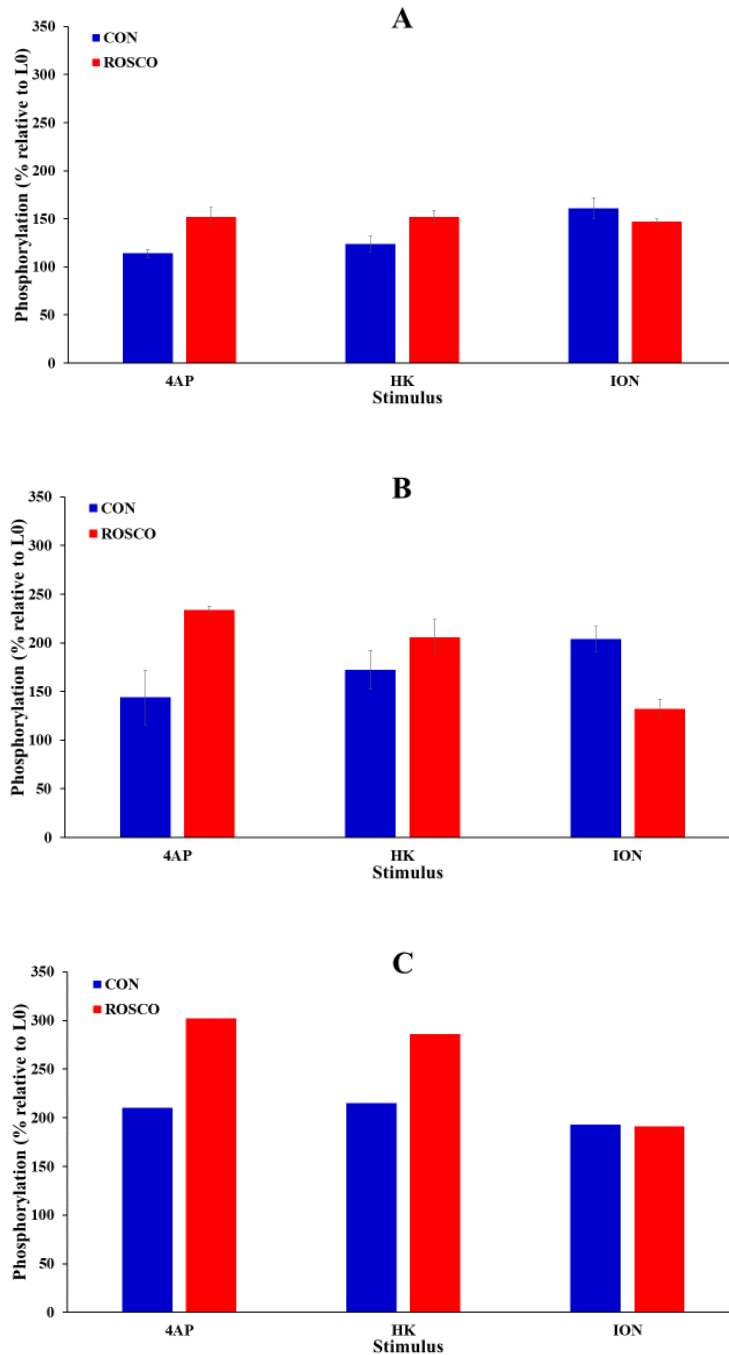


Figure 3.50. The effect of 100 μ M Roscovitine treatment upon Syn I Ser-9 phosphorylation following various stimulation for a) early time points (2 sec+15 sec) b) 30 sec c) 120 sec; N=4 for A and N=2 for B and C. All results are normalised to the L0 control value. a) The combined early time points show that phosphorylation was higher in the presence of Roscovitine relative to control for 4AP5C and HK5C stimulation. Such increase is time dependent as b) 30 sec with 4AP5C and HK5C in the presence of Roscovitine was higher compared to non-drug treated control and the values reach maximum at c) 120 sec

3.8.4. Phosphorylation of Syn I Ser-603 in nerve terminals

The SP release can be stimulated following Roscovitine treatment and this may involve the activity of not only Cdk5 but other kinases that can phosphorylate Syn I, including CaMKII. CaMKII phosphorylates Syn I at Ser-603 site, and we can study the phosphorylation of this site following Roscovitine treatment. Roscovitine treatment appears to increase the phosphorylation of Syn I- Ser-603 site relative to non-drug treated control at (Fig 3.51 A), but as there is a difference in the pan-Syn I content (Fig 3.51 B), this probably can account for the difference (See Fig 3.51 A).

At 15 sec, Roscovitine treatment has reduced the HK5C and ION5C evoked phosphorylation compared to non-drug treated control (Fig 3.51 C), however again this was due to the difference in the pan-Syn-I blot densities, such that total Syn-I protein contents in HK5C plus Roscovitine and ION5C plus Roscovitine found to be visibly lower compared to non-drug treated control samples with same stimulations applied (Fig 3.51 D),

However, 30 sec HK5C stimulation in Roscovitine treated samples does induce more phosphorylation of Ser-603 of Syn I than in the drug-free control (Fig 3.52 A-B). Such increase was also evident at 120 sec stimulation in Roscovitine treated samples compared to control samples, especially if you take into account the pan-Syn-I blot (Fig 3.52 C-D).

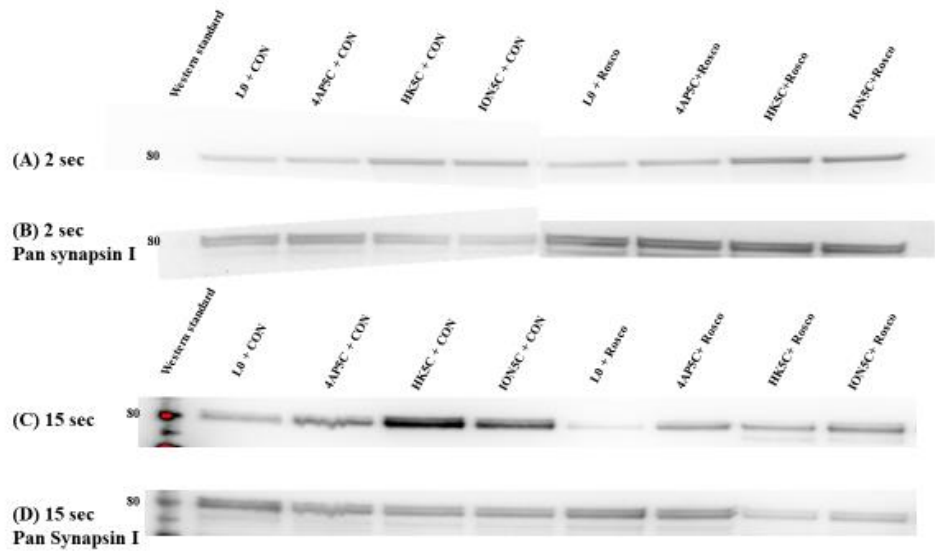


Figure 3.51. The effect of 100 μ M Roscovitine treatment upon phosphorylation of Ser 603 of Syn I. A) 2 sec stimulation B) Pan-Syn I blot reprobed for the 2 sec stimulation C) 15 sec stimulation D) Pan-Syn I blot reprobed for the 15 sec stimulation. This is a representative blot (A and B are N=2; C and D are N=1)

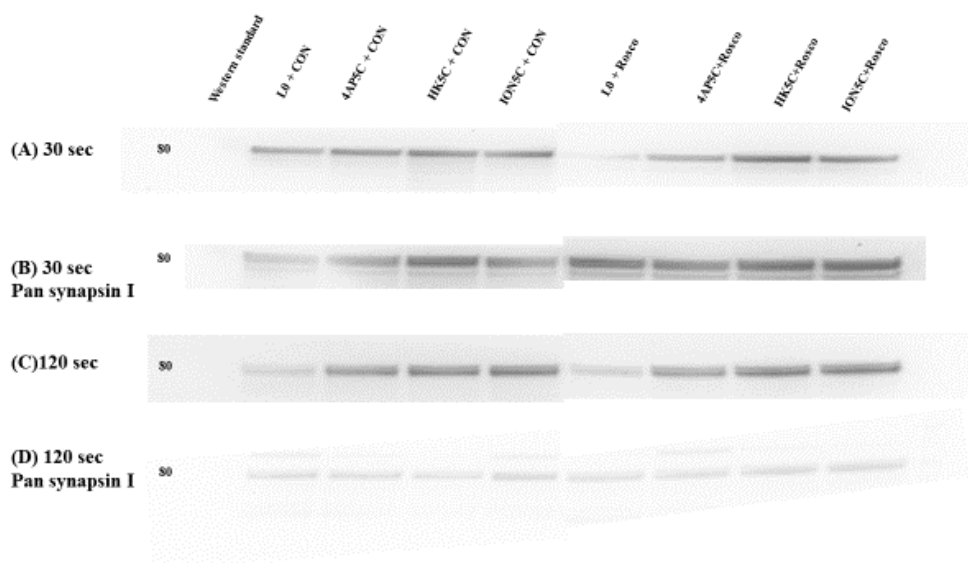


Figure 3.52. The effect of 100 μ M Roscovitine treatment upon the phosphorylation of Ser-603 in Syn I. A) 30 sec stimulation B) Pan-Syn I blot reprobed for the 30 sec stimulation C) 120 sec D) Pan-Syn I blot reprobed for the 120 sec stimulation. This is a representative blot (All blots N=2)

Bar charts presented in figure 3.53 show the semi-quantitative analysis performed on the blots representative ones which are shown in figure 3.51 and 3.52. There appears to be some time dependent increase in phosphorylation of Ser-603 of Syn I in control terminals stimulation with 4AP5C and ION5C, although maximum for HK5C is achieved early on. According to these charts, at early time points (2 sec+15 sec), HK5C evoked and ION5C evoked phosphorylation in the presence of Roscovitine maybe slightly higher compared to drug free control condition and these stimuli produced phosphorylation that was higher compared to 4AP5C evoked phosphorylation in the presence of Roscovitine (Fig 3.53A). At 30 sec, 4AP5C plus Roscovitine and ION5C plus Roscovitine were similar to non-drug treated control with same stimuli employed. Although, HK5C evoked phosphorylation in the presence of Roscovitine was increased compared to when Roscovitine was absent (Fig 3.53 B). At 120 sec (Fig 3.53 C), there were clear increases in Roscovitine treated conditions throughout all stimuli employed, and these were visibly higher than the non-drug treated control conditions. All the data collected so far does seem to suggest that CaMK II is activated upon stimulation as Ca^{2+} enters the terminal activates CaMK II (represented by HK5C and ION5C showing higher phosphorylation than 4AP5C in the presence of Roscovitine) which then phosphorylates Syn I on Ser-603 site. It would appear that there is a gradual increase in the phosphorylation of Ser603 with time and 120 sec has the maximum.

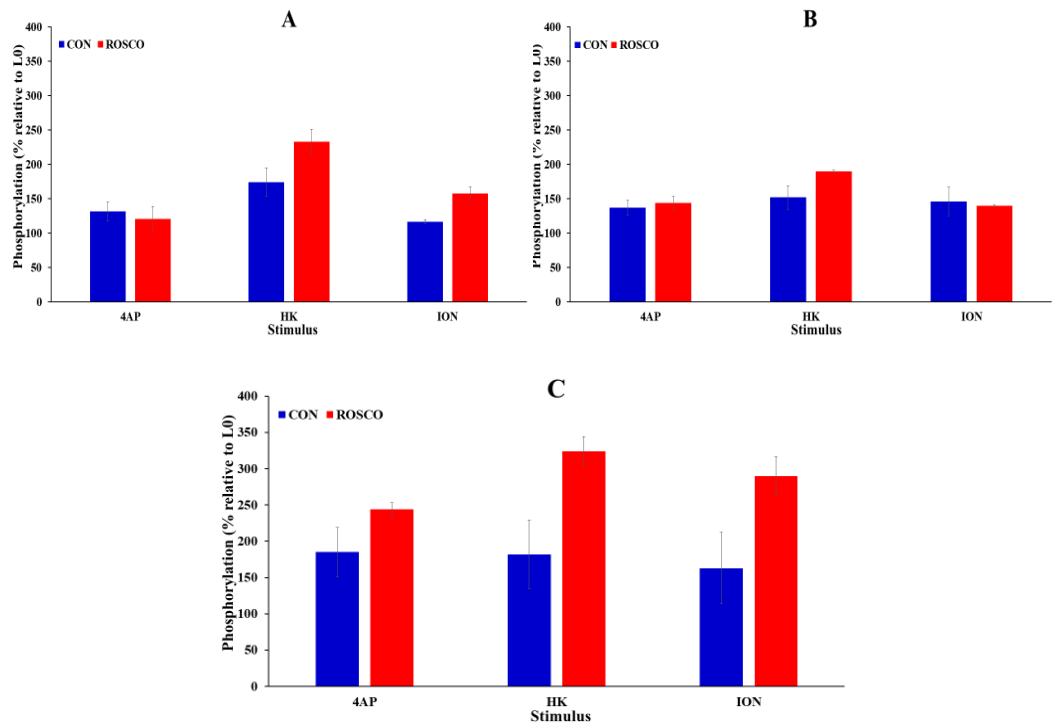


Figure 3.53. The effect of Roscovitine upon the phosphorylation of Syn I Ser-603 following various stimulation for a) Early stimulation time points (2 + 15 sec) b) 30 sec stimulation c) 120 sec stimulation; A is N=3; B and C are N=2. A) Phosphorylation induced by HK5C or ION5C in Roscovitine treated terminal was relatively higher than non-drug treated controls at combined early time points. Note both these cause higher $\Delta[Ca^{2+}]_i$ entry than 4AP5C and at 2s stimulation, 4AP5C shows little increase of phospho-Ser 603 with or without Roscovitine pre-treatment. B) HK5C stimulation in Roscovitine treated synaptosomes evoked greater phosphorylation than drug free control at 30 sec stimulation whilst Roscovitine had negligible effect on changes in phosphorylation of Ser 603 induced by 4AP5C or ION5C. C) There was substantial increase in phospho-Ser 603 of Syn I in Roscovitine treated samples for all stimuli employed relative to non-drug treated control after 120 sec stimulation.

#	Figure #	Assay (s)	Stimulus	Drugs employed (conc.)	Key findings
1	3.1-3.2	GLU	HK5C	Roscovitine (10 μ M, 33 μ M, 100 μ M, 200 μ M)	Roscovitine treatment allowed HK5C to evoke further GLU release compared to control which is assumed to be from the SP. 100 μ M Roscovitine treatment provided maximum SP release from the synaptosomes.
2	3.3	GLU	ION5C	Roscovitine (100 μ M)	100 μ M Roscovitine also allowed ION5C to evoke the SP release
3	3.4-3.5	Fura-2	HK5C, ION5C	Roscovitine (100 μ M)	No change in $\Delta[Ca^{2+}]_i$ identified for HK5C and ION5C stimulated terminals in the presence of 100 μ M Roscovitine
4	3.6-3.7	GLU	HK5C	Roscovitine (100 μ M), Dynasore (160 μ M), Pitstop2 TM (15 μ M), Blebbistatin (50 μ M)	Extra GLU release observed in Roscovitine treated terminals are not a result of the RRP and RP recycling, and it does not involve Myosin II
5	3.8-3.11	GLU, Fura-2	HK5C, HK10C, HK20C	Roscovitine (100 μ M)	Higher $[Ca^{2+}]_e$ perturbed extra release in Roscovitine treated terminal and it was due to the reduction in $\Delta[Ca^{2+}]_i$
6	3.9-3.16	GLU, Fura-2	HK5C, ION5C	Roscovitine (100 μ M), PMA (1 μ M), Go6983 (1 μ M)	PMA only perturbed ION5C, not HK5C, evoked SP release in Roscovitine treated terminal and this might be due to reduced $\Delta[Ca^{2+}]_i$ level.
7	3.17-3.23	GLU, Fura-2	HK5C	Roscovitine (100 μ M), CONO (1 μ M), AGA (50 nM), NIF (1 μ M)	Ca^{2+} channel blockade perturbed HK5C evoked SP release in Roscovitine treated terminal. Although, there was no specificity in Ca^{2+} channel type identified.
8	3.24-3.25	GLU	HK5C	Roscovitine (100 μ M), JASP (2.5 μ M)	Roscovitine allowed HK5C to evoke an extra release when actin is stabilised
9	3.26-3.27	GLU, Fura-2	HK5C	Roscovitine (100 μ M), Cys A (1 μ M)	Inhibition of PP2B and Cdk5 inhibited the SP exocytosis and this might be due to reduced $\Delta[Ca^{2+}]_i$
10	3.28-3.45	Bioenergetics		All drugs employed in this chapter	No significant changes in bioenergetics of synaptosomes identified
11	3.46-3.55	Western blotting	4AP5CH K5C, ION5C	Roscovitine (100 μ M)	Although it is still a preliminary result, Ser-553 (Cdk5 site) phosphorylation appears to be decreased in Roscovitine treated terminals whilst Ser-9 (PKA site) and Ser 603 (CaMKII site) phosphorylation appears to be increased.

Figure 3.54. Summary of the findings in chapter 3.

3.9 Discussion

3.9.1 Roscovitine effect on the SP release

The silent pool (SP) has been an enigma mainly due to the fact that it is not released under the normal physiological conditions which makes it difficult to study. Roscovitine, a Cdk5 inhibitor, can be employed to allow further evoked release after the RRP and the RP have been fully exocytosed and this represents the SP (Kim and Ryan, 2010; Kim and Ryan, 2013). Herein this study has used Roscovitine under different conditions and attempted to elucidate properties of the SP. Note that Kim and Ryan (2010) measured release by the electrophysiological recording of the postsynaptic response to GLU release from hippocampal cultured cells. We have reproduced their findings in cortical synaptosomes measuring directly the release of the GLU.

The current study first showed that Roscovitine dose dependently induced extra release from the nerve terminal with the maximum effect being induced by 100 μM while 200 μM was unable to induce any further release. It has previously been established that HK and ION with 5 mM $[\text{Ca}^{2+}]_e$ maximally release GLU from synaptosomes (see appendix A. 1.1.1) which is considered to be representing the total release of the RRP and RP. However, Roscovitine treatment allowed HK5C to evoke significantly higher GLU release compared to non-drug treated control, which indicates that SV pools other than the RRP and RP is releasing. Therefore, this extra release was assumed to be from the SP. This study further tested ION5C as well and found it could also release the SP in the presence of Roscovitine. ION5C is an ionophore that bypasses any Ca^{2+} channel requirement, and this useful information suggests that the level of Ca^{2+} influx through channels might not play a pivotal role in the release of the SP (See below). Please note that Ashton and colleagues have shown that the RRP and RP have distinct biochemical properties that can help identify them (see Bhuvu, 2015; Singh, 2017; Rostron, 2019) and it was hoped that difference between these and the SP could be determined.

The study further investigated the actual intracellular Ca^{2+} levels evoked in Roscovitine treated terminal by employing a Fura-2 assay. However whilst 100 μM Roscovitine induces the SP to release, it does not affect HK5C evoked changes in $[\text{Ca}^{2+}]_i$.

Even though this study obtained extra GLU release with Roscovitine and employing ION5C or HK5C as the stimulus, it was still debatable whether this release was actually from the SP as there was still a chance that the inhibition of Cdk5 might actually promote the recycling of the RRP and the RP and their re-release during the stimulus period. This could mean that the study was observing a recycling of these two pools rather than release of the SP. However, this was found not to be the case since even after the inhibition of recycling through perturbation of Dyn and clathrin, the SP release was observed.

This study also tested if additional extracellular Ca^{2+} could induce further HK5C evoked release in the presence of Roscovitine. However, this was not the case as HK10C and HK20C in Roscovitine pre-treated terminal failed to release the SP. Thus higher extracellular Ca^{2+} levels do not support the release of the SP. Further investigation revealed that for both HK10C and HK20C, the evoked $\Delta[\text{Ca}^{2+}]_i$ was found to be reduced compared to HK5C in the Roscovitine treated terminals. This is interesting because although higher extracellular calcium concentrations were present, the result indicates that the quantity of calcium going into the terminal (as measured by $\Delta[\text{Ca}^{2+}]_i$) was reduced which indicates that there is a certain concentration of calcium required to induce the SP release.

An intriguing result of this study was that supra-maximally induced PKC could actually block the SP release evoked by ION5C in Roscovitine treated terminals. 1 μM PMA - that supra-maximally induce PKC activation - was used and it was found that the SP release was perturbed for ION5C evoked GLU release in Roscovitine treated synaptosomes. It is noteworthy that, although previous investigations on SP release are relatively lacking, there are few studies demonstrated a link between PKC activation with regulation of the RRP and RP. Stevens and Sullivan (1998) showed that PMA activation of PKC elevates

the rate of the RRP refilling. Another study has reported that Platelet activating factor (PAF) increased the size of the RRP and the exocytosis rate of the RP through elevation of calcium within the terminal and PKC activation (Hammond *et al*, 2016). However, it is difficult to make a direct comparison due to the fact that the models employed were different, and the stimulation protocol varied between these two studies and the study outlined here.

A similar experiment was also conducted using the PKC inhibitor, Go6983, instead of PMA but the SP was still released by HK5C in Roscovitine treated synaptosomes. This, in combination with the previous result where additional amounts of Ca^{2+} have perturbed the SP release, represents novel result whose precise mechanism awaits to be elucidated. The results using HK10C and HK20C under Roscovitine pre-treatment also were further investigated by employing Go6983. It was demonstrated that in the presence of Go6983, HK10C and HK20C was still unable to evoke the SP release in Roscovitine treated terminals whereas with HK5C, Go6983 did not prevent SP release in synaptosomes treated with Roscovitine. As in the Roscovitine treated terminal, HK10C and HK20C failed to support the SP release but Go6983 did not perturb the SP release, it would appear that the changes in $[Ca^{2+}]_e$ does not act to perturb the SP by activating PKCs because otherwise Go6983 by blocking activation of such PKC should have allowed HK10C and HK20C to release the SP.

Previously, Ashton's group have found that N-type Ca^{2+} channel blockade with 1 μ M CONO fails to inhibit the HK5C evoked release of the RRP and the RP. In the repeat experiment performed herein it is re-shown that it does not perturb the RRP and the RP release, but it does stop the release of the SP when both Roscovitine and CONO are employed. This clearly demonstrated that the SP requires a certain amount of Ca^{2+} influx through the channel for it to be released but in this study, because the N-type Ca^{2+} channel has been blocked by CONO, the SP was not able to be exposed to sufficient Ca^{2+} and, thereby the SP release has been perturbed. Equivalent experiments were done for P/Q- and

L-type calcium channels. For P/Q-type channel, AGA was used whilst for L-type channel NIF was employed. In both conditions the result was similar to what was revealed in N-type Ca^{2+} channel blockade experiment where the RRP and the RP were released as normally whilst the SP release was not supported. These data demonstrate that the presence of calcium channels is essential for normal SP release, however, this is not operated through particular type of channel.

Actin stabilisation with JASP was found not to reduce the release of the RRP and RP (see chapter 6). Further, JASP pre-treatment did not prevent HK5C evoked SP in Roscovitine treated terminals. Thus, stabilisation of actin microfilaments does not appear to inhibit the release of the RRP, RP, or SP.

It is clear from all the data obtained measuring the bioenergetics of synaptosomes that none of the drugs tested in the current research perturbed the energy producing capacity of the nerve terminals. Since there are no detrimental effects identified, it is concluded that the changes each drug may induce on synaptosomal exocytosis are not due to non-specific effects. This is an important point since perturbation of ATP levels will change the amount of Ca^{2+} - dependent exocytosis, $[\text{Ca}^{2+}]_i$ and any evoked changes $[\text{Ca}^{2+}]_i$ levels and it may possibly induce Ca^{2+} independent non-vesicular GLU release (Sobieski *et al*, 2017).

3.9.2 Phosphorylation of Syn I following Roscovitine treatment

We have presented the preliminary data of phosphorylation profiles of various sites in Phospho-Syn-I, including Ser-553 (Cdk 5 site), Ser-9 (PKA site), and Ser-603 (CaMKII site), in response to Roscovitine pre-treatment. As this drug allows HK5C and ION5C to evoke the SP of SVs from the nerve terminal, such phosphorylation results allow one to investigate a changes of Syn I phosphorylation when the SP is undergoing exocytosis. This should aid in elucidation of the mechanism of Roscovitine allowing evoked release of the SP.

Syn-I-Ser-553 site is known to be phosphorylated by Cdk5. Semi-quantitative analysis demonstrated that Cdk5 inhibition with Roscovitine has led to time-dependent decrease in phosphorylation at Ser-553 site compared to non-drug treated control. Benfenati's group has demonstrated that the phosphorylation of Syn I with Cdk5 at Ser-551 (homologous site with Ser 553) site promoted its interaction with actin microfilament and they suggested that this leads to an elevation of SV interaction with F-actin, moves recycling SVs to the SP, and leads to reduction in releasable SVs in the recycling pool (Verstegen *et al*, 2014). In this study, Roscovitine treatment also led to the reduction in the phosphorylation of Syn I at Ser-553 site and this seems to have allowed the SP SVs being able to exocytose. Therefore, these results may suggest that inhibition of Cdk5 by Roscovitine led to a reduction in Cdk5 phosphorylation of Syn I, which allows the previously immobilised SVs now available for exocytosis, such that these previously immobilised SP SVs can now release their content. It is noteworthy that this result is from preliminary study and require a further investigation.

However, we investigated whether there were other Syn I phosphorylation sites that could play a role in the release of the SP. A semi-quantitative analysis on blots probing for the phosphorylation of Ser-9 – a PKA site - demonstrated that such phosphorylation was found to be elevated following Roscovitine treatment relative to non-drug treated control for 4AP5C and HK5C but not ION5C. Although these are still preliminary results, it is possible to suggest that these two former stimuli, by activating Ca²⁺ channels at the AZ, can activate PKA in some way (perhaps via calmodulin dependent adenylate cyclase). Indeed, PKA phosphorylation on Syn I has been highlighted in several studies to promote exocytosis by regulating the dissociation of the protein from the SV membrane and enhance the recycling of the SVs (Hosaka *et al*, 1999; Bonanomi *et al*, 2005). Indeed, a mutation of Ser-9 so this site could not be phosphorylated, resulted in an absence of this enhancement of release (Flumara *et al*, 2004). Menegon *et al* (2006) also reported that phosphorylation of Syn I by PKA promotes dissociation of Syn I from SVs, and facilitates

the rate of SV exocytosis under sustained stimulation. These authors suggested PKA mediated SV exocytosis is primarily caused by calmodulin (CaM)-dependent activation of cAMP pathways activated by increased $[Ca^{2+}]_i$; rather than the direct activation of CaM kinases by Ca^{2+} . Therefore, there clearly can be crosstalk between cAMP- and CaM-dependent cascades which can regulate Syn via its PKA site to modulate SV exocytosis (Menegon *et al*, 2006).

Syn I is also a substrate of CaMKII at the Ser-603 site. Previous studies have indicated that some of Syn I effects were abolished by CaMKII mediated phosphorylation. Syn I reversibly anchors the SVs to the actin cytoskeleton of the nerve terminal, promoting polymerisation and bundling of actin filaments and forming ternary complex, but CaMKII phosphorylation of Syn I abolishes the formation of this network (Llinas *et al*, 1985, 1991; Petrucci and Morrow, 1987; Valtorta *et al*, 1991; Ceccaldi *et al*, 1995; Wang *et al*, 2008). Herein, stimulus evoked increase in the phosphorylation of Ser-603 which is increased by Roscovitine and these changes are most distinct after 120 sec of stimulation. Interestingly, the CaMKII site appears to show the best Ca^{2+} dependent stimulation evoked phosphorylation increase. At 2s 4AP5C induced less of an increase in phospho-Ser-603 than either HK5C or ION5C and although there appears to be greater amounts of this phosphorylation, after 120 sec stimulus, 4AP5C is still less than HK5C or ION5C at inducing Syn I Ser-603 phosphorylation. This fits in with the known greater induced increase in $[Ca^{2+}]_i$ with the latter two stimuli. Overall, it is possible that a further increase in phosphorylation of the Ser-603 site in Syn I may be associated with Roscovitine treatment and so this may also be related to the support for evoked release of the SP. Although, it is not clear whether decrease in Cdk5 expression and increase in CaMKII phosphorylation at Syn I are correlative. Again, these are preliminary data and further research is required.

It is important to remember that 4AP5C is incapable of inducing the release of the SP in Roscovitine treated terminals so it is likely that any changes seen with 4AP5C may not be

related to release of the SP. For the phosphorylation of Ser-553, 4AP induces slightly less than HK5C which is slightly less than ION5C. However, Roscovitine reduces this phosphorylation to a level not too dissimilar for all these stimuli. Thus, perhaps it is the larger decrease of phosphorylation induced by HK5C or ION5C in Roscovitine treated terminals which can free the SP SVs and allow them to be released. However, 4AP5C may allow such SP SVs to be released from their attachments but there is insufficient increase in $[Ca^{2+}]_i$ to actually cause these to exocytose.

Intriguingly, by 120 sec all 3 stimuli have increased 2-fold the phosphorylation of Ser-9 on Syn I but, whereas Roscovitine can increase this to 3-fold for both 4AP5C and HK5C, there is no change for ION5C. As mentioned earlier, this could be related to the activation of voltage dependent Ca^{2+} channels by 4AP5C and HK5C (ION5C does not act via such channels) and subsequent activation of calmodulin dependent adenylate cyclase, increase in cAMP locally and specific activation of PKA. However, as HK5C and ION5C induced SP release in Roscovitine treated terminals, then this phosphorylation site may not contribute to the SP release, similar are what can be made for the phosphorylation of Ser-603. HK5C and ION5C induced a larger increase in phosphorylation at this site in Roscovitine treated terminals. Thus the larger increase may be important for SP SVs to undergo exocytosis.

3.10 Future research

This study requires further research on several areas in order to elucidate various properties of the SP. Future experiments include investigating the reversibility of Roscovitine, any PKA involvement in Roscovitine induced SP exocytosis, and additional repeat of western blot experiment for Syn I.

3.10.1 Reversibility of Roscovitine

In this thesis, we have been able to induce the SP of SVs following Roscovitine treatment but we have not studied the exocytosis of the SP utilising FM dyes. In order to conduct FM 2-10 Styryl dye release assay on the SP, all SV from the nerve terminal have to be pre-released, labelled with the dye and then such SVs must then recycle into the terminal. Subsequently, evoked release is induced and fluorescence changes as measured (See chapter 2.4 of method section). However, this experiment is probably only viable if Roscovitine effect can be reversed after the pre-treatment and pre-stimulation. This is because Cdk5 inhibition may perturb the recycling of the labelled SVs or the subsequent mode of exocytosis. However, as the reversibility of Roscovitine is not yet been established, the mode of the SP exocytosis is unable to be investigated. This would be interesting data because it would reveal the mode of the exocytosis that SP SV undergo which would then partially reveal some of the proteins that are involved in SP regulation and may indicate further distinct properties of the SP compared to the other two pools.

3.10.2 PKA Dependency of SP release

It has been found that PKC activity was able to regulate the SP release. Another essential kinase is PKA which is known to contribute heavily to the regulation of neurotransmission (see some results in chapter 5). PKA is present at nerve terminals, and it is known to phosphorylate serine and threonine residues. It can be activated by increasing cAMP levels (Seino and Shibasaki, 2005; Park *et al*, 2014). It is capable of regulating exocytosis of SVs via the regulation of the phosphorylated state of various protein, including Syn I (Fiumara *et al*, 2004; Menegon *et al*, 2006) and as Syn I may regulate the SP release (see phosphorylation results) (Orenbuch *et al*, 2012; Verstegen *et al*, 2014), PKA is a potential regulator of the SP exocytosis.

3.10.3 Repeat western blot experiment with same drug treatments

Due to the lack of time available for further experiments, the current study is reporting results from two independent experiments. A minimum of three independent experiments are required to produce statistically significant results, and so we are unable to prove the significance of the changes reported. Additional experiments with an equivalent drug treatment will need to be conducted and the resulting values need to be combined with those herein to clarify the results. It is for this reason that these results are not included as a separate chapter. However, it was felt that it was important to demonstrate the strategy being employed to determine the molecular mechanism of Roscovitine.

3.11 Conclusion

This chapter has shown Roscovitine, a Cdk5 inhibitor, can allow the SP to be released following HK5C or ION5C stimulation and utilising this fact an investigation has been performed on how the properties of SP changes dependent on various other drug treatments. However, higher $[Ca^{2+}]_e$ with the HK stimulus (HK10C or HK20C) blocked the SP release from Roscovitine-treated terminals but a reduction in evoked $\Delta[Ca^{2+}]_i$ data in Roscovitine treated terminals also blocked the release of the SP. This demonstrates that the SP requires a specific level of $[Ca^{2+}]_i$ for it to be released.

Activation of PKC, but not inhibition, was found to perturb the ION5C evoked SP release in Roscovitine-treated terminals. Likewise, the N-type Ca^{2+} channel blocker CONO prevented the HK5C-evoked SP release in Roscovitine-treated synaptosomes. However, similar results were also found when P/Q-type channels were blocked with AGA or when L-type channels were blocked with NIF. Thus, all these channels may have an important role in the SP regulation. Actin stabilisation with JASP did not perturb release of the SP, indicating that stabilisation of microfilaments does not prevent release of any pool.

It is, therefore, concluded that the SP of GLU containing SVs was induced to release GLU following treatment with Roscovitine, but such release was controlled by levels of $[Ca^{2+}]_i$, by entry of Ca^{2+} through three types of Ca^{2+} channels and by PKC activation.

Additionally, the preliminary data of western blotting experiments has shown that Cdk5 inhibition with Roscovitine might have led to decrease in phosphorylation at Ser-553 site (Cdk5 site) whilst increase of phosphorylation was observed at Ser-9 (PKA site) and Ser-603 (CaMK II site). Accordingly, it would appear that Roscovitine supported release of the SP may involve phospho-Syn I activity which include inhibition of the Cdk5 phosphorylation site and enhancement of the PKA and CaMK II phosphorylation sites. Although, it is not clear whether these two phenomena of positive and negative effect of Roscovitine on phosphorylated profiles of Syn-I are correlative. Additionally, it is also noteworthy that PKA phosphorylation was discovered by several researches to contribute to the dispersion of Syn I from SVs whilst CaMKII phosphorylation was implicated in the dissociation of actin microfilament and Syn I, thus inhibition of Cdk5 action with Roscovitine might have promoted phosphorylation at both ends of the actin-synapsin-synaptic vesicles network leading to increasing availability of SVs to exocytose. Clearly, these experiment are worthy to be repeated several more times as it could potentially lead to a key findings.

Chapter 4:

Fluoxetine and the Silent Pool

4.1 Introduction

Chapter 3 demonstrated that Roscovitine – through Cdk5 inhibition – enabled HK5C or ION5C to evoke the SP of SVs to release. Considering the complexities of release of SVs from all the pools, it is likely that other pathways besides the Cdk5 pathway may evoke the release of the SP. Herein, Fluoxetine has been investigated to see whether it could trigger the extra release from the SP in synaptosomes.

Fluoxetine was designed as a selective serotonin reuptake inhibitor (SSRI) and it is one of the most prevalently prescribed drugs for the treatment of depression (Prozac). The exact pathology of depression is yet to be fully elucidated, but the disruption in the serotonergic pathway has been widely acknowledged as a potential candidate. This is because the SSRI drugs, including Fluoxetine, that were assumed to target on the serotonergic pathway were found to relieve some of the major symptoms of depression (Rahn *et al*, 2015; Hamilton *et al*, 2016; Clevenger *et al*, 2018). SSRIs operate through blocking the uptake of serotonin following its release, and this consequently increases the level of the monoamine in the brain in drug treated patients (Dale *et al*, 2015). However, the association between synaptic transmission and the pathology of depression requires further investigation. Recently, studies have suggested that ketamine, an NMDA antagonist, produces rapid antidepressant responses in patients who were resistant to typical antidepressant treatments. Ketamine rapidly stimulates synaptogenesis and reverses the synaptic deficits caused by chronic stress, and such a result suggests that there are associations between synaptic transmission and the pathology of major depressive disorder (MDD), this led to the synaptogenic hypothesis of depression (Duman and Aghajanian, 2012).

If it is the case that manipulation of synaptic transmission has a contribution on depression phenotype, it could also imply that a regulation of the exocytosis of the pools including the SP may potentially be associated with the development of depression. Jung *et al* (2014) studied the action of 1 μ M of Fluoxetine on exocytosis from hippocampal cultured cell.

This treatment led to an increase in the size of the recycling pool of SVs by apparently allowing some SP SVs to contribute to release. This finding is significant because it has suggested that the pharmacological mechanism of this antidepressant could potentially involve an elevation of the SV release of non-monoamine transmitters, and importantly, such release involves mobilisation and release of the SP. In this chapter, the aim was to test whether Fluoxetine could release the SP of GLU containing SVs in the synaptosomal model used herein. It is noteworthy that the experimental model used in this study is cerebral cortical terminals, and these are 80% glutamatergic.

4.2 Establish optimum condition for Fluoxetine to allow HK5C evoked SP release.

4.2.1 5 min incubation with various doses of Fluoxetine

In Chapter 3, Roscovitine induced extra release from the SP was investigated and maximum SP release was established by treating synaptosomes for 5 min at 37°C with various concentrations of the drug (10 µM, 33 µM, 100 µM, 200 µM). In this chapter, the study aimed to elucidate whether Fluoxetine could release - same as Roscovitine – the SP and what conditions were needed to allow maximum SP release.

Synaptosomes were pre-treated with different concentrations (1 µM, 200 nM, 100 nM, 50 nM) of Fluoxetine for 5 min incubation time and the GLU release evoked by HK5C was measured. For 1 µM Fluoxetine treatment, the HK5C evoked release appeared to be reduced compared to non-drug treated control and, therefore this concentration has not only failed to induce the SP of SVs to exocytose, but may have also perturbed some release from the RRP and RP (Fig 4.1).

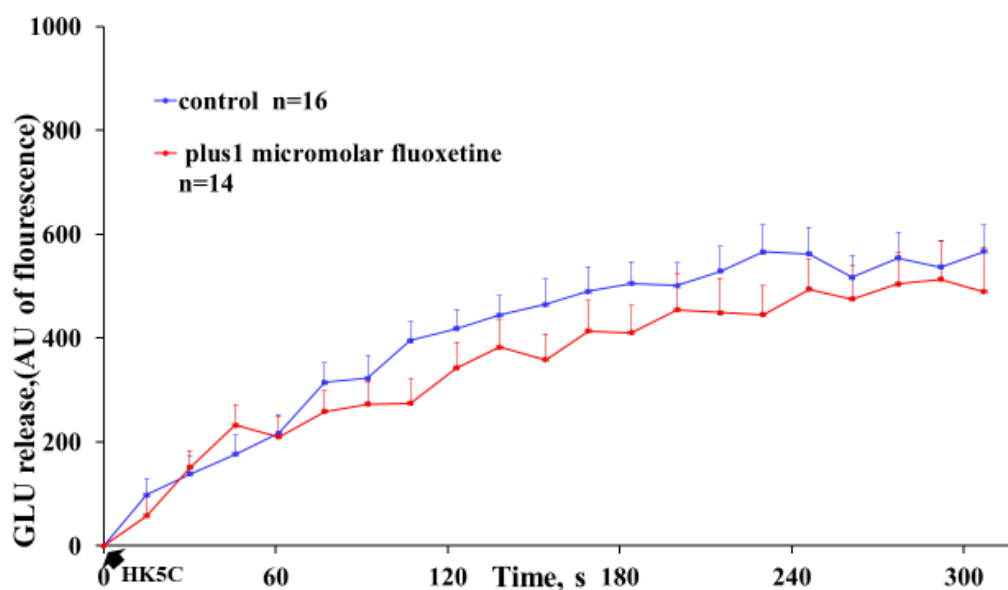


Figure 4.1. 1 μ M Fluoxetine treatment for 5 min in 37°C failed to allow HK5C evoked SP release. HK5C evoked GLU release in terminals treated with 1 μ M Fluoxetine compared to non-drug treated controls. Data are mean \pm SEM, N=5 independent experiments; Although the drug may actually reduce the release, this was not statistically significant ($P > 0.05$).

As 1 μ M Fluoxetine did not allow HK5C evoked release of the SP, the concentration of the drug was lowered to 200 nM and the HK5C evoked GLU release measured. However, this failed to allow extra release and the release was quite similar to control condition (Fig 4.2). Note in some of these preliminary studies only one experiment was performed for each drug concentration. It was argued that any concentration that induced the SP would be obvious and that much more repeats could then be performed on such concentration.

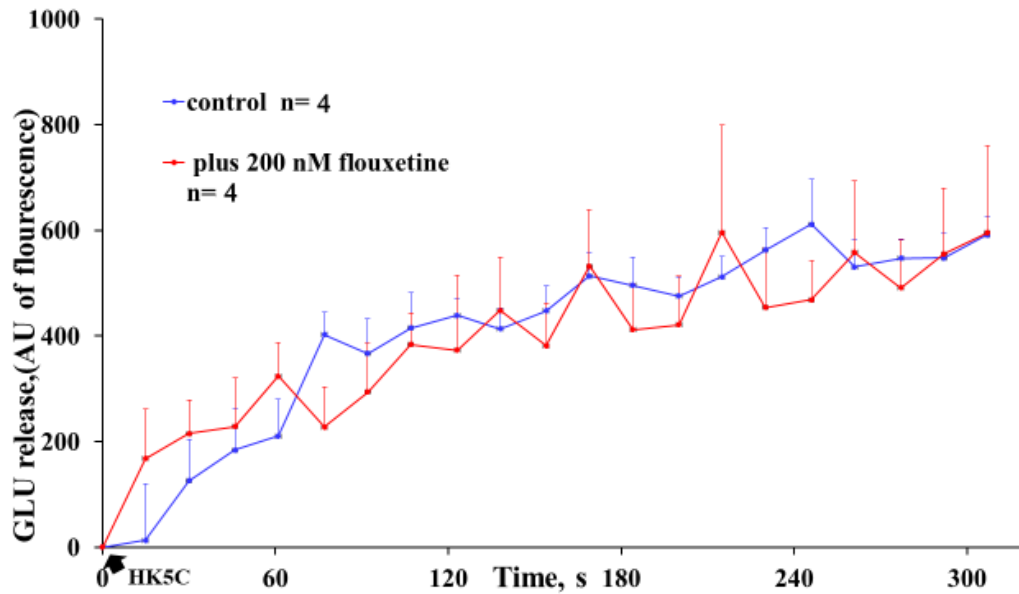


Figure 4.2. 200 nM Fluoxetine treatment for 5 min in 37°C failed to allow HK5C evoked SP release. HK5C evoked GLU release in terminals treated with 200 nM Fluoxetine compared to non-drug treated terminals. Data are mean \pm SEM, Note as there was no obvious difference we did not repeat this experiment.

100 nM (Fig 4.3) and 50 nM (Fig 4.4) Fluoxetine were also tested in preliminary experiments, but both conditions produced similar amount of HK5C evoked release of the RRP and RP compared to non-drug treated condition and no SP release was apparent. Thus, in these preliminary experiments, 5 min treatment with Fluoxetine failed to trigger any extra release from synaptosomes.

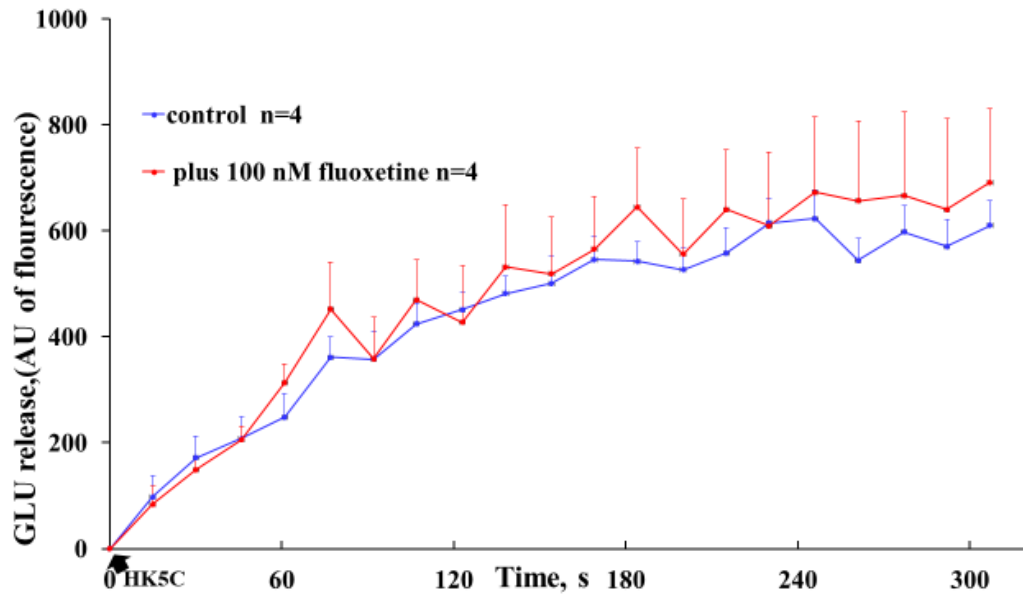


Figure 4.3. 100 nM Fluoxetine treatment for 5 min in 37°C failed to allow HK5C evoked SP release. HK5C evoked GLU release in 100 nM Fluoxetine pre-treated terminals compared to non-drug treated terminals. Data are mean \pm SEM, N=1 independent experiment.

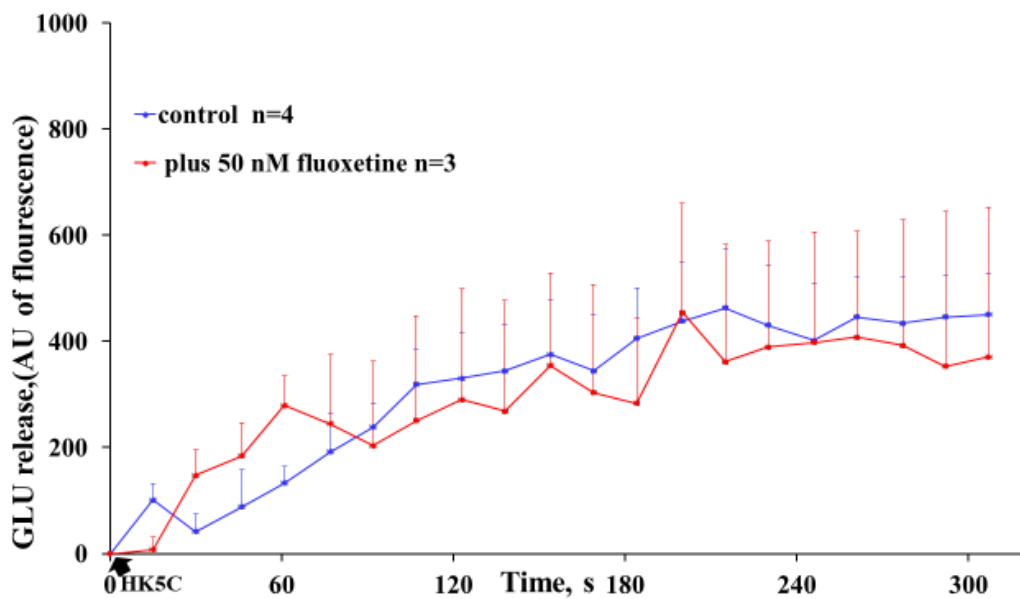


Figure 4.4. 50 nM Fluoxetine treatment for 5 min in 37°C failed to allow HK5C evoked SP release. HK5C evoked GLU release in terminals treated with or without 50 nM Fluoxetine. Data are mean \pm SEM, N=1 independent experiment.

4.2.2 20 min incubation with various doses of Fluoxetine

In the previous sets of experiment, the samples were treated with Fluoxetine for 5 min but with all concentrations employed HK5C failed to evoke any significant release of the SP. Thus, this drug may take longer to exhibit its action and we noted that Jung *et al* (2014) incubated for 20 min with the drug instead of 5 min. Thus, the Fluoxetine incubation time was extended from 5 min to 20 min.

Again samples were pre-treated with range of Fluoxetine concentrations (1 μM , 200 nM, 60 nM, 40 nM, 20 nM, 5 nM) for 20 min and subsequently the release evoked by HK5C was measured using the GLU assay.

There was no significant increase in the release identified at majority of the concentrations, instead, at 1 μM , the control was higher compared to drug-treated condition (Fig 4.5).

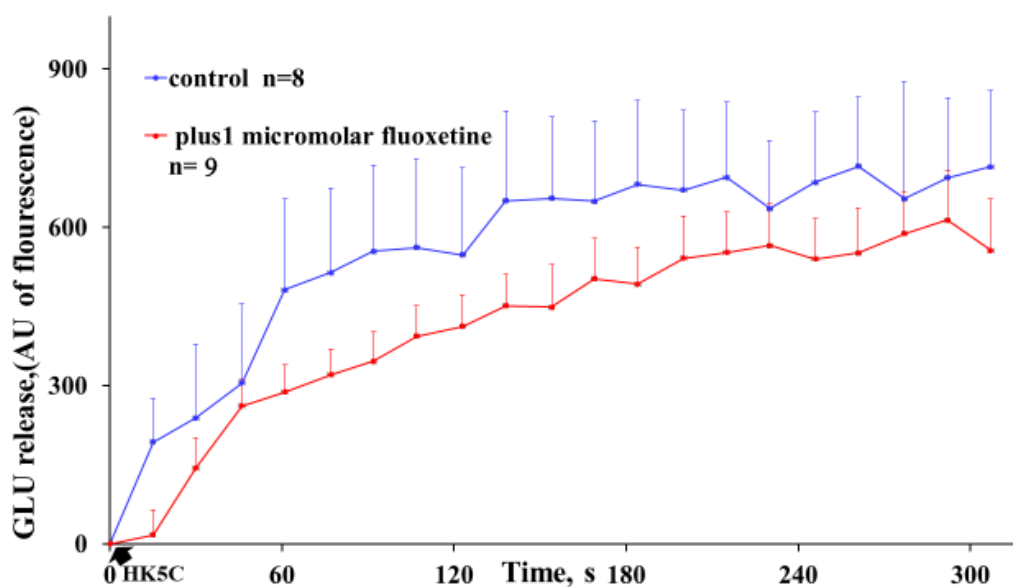


Figure 4.5. 1 μM Fluoxetine treatment for 20 min in 37°C reduced the HK5C evoked GLU release HK5C evoked GLU release following an extended 20 min incubation at 37°C with 1 μM Fluoxetine compared to non-drug treated control. Data are mean \pm SEM, N=3 independent experiments; P<0.05.

Performing a single experiment for 200 nM (Fig 4.6) and 100 nM (Fig 4.7), still suggested that in the control conditions HK5C evoked more release than drug-treatment conditions although the difference appeared to be smaller compared to 1 μ M Fluoxetine (Fig 4.5). Clearly, it would appear that 1 μ M, 200 nM, and 100 nM is perturbing some HK5C evoked release from the recycling pool and definitely not allowing any SP release.

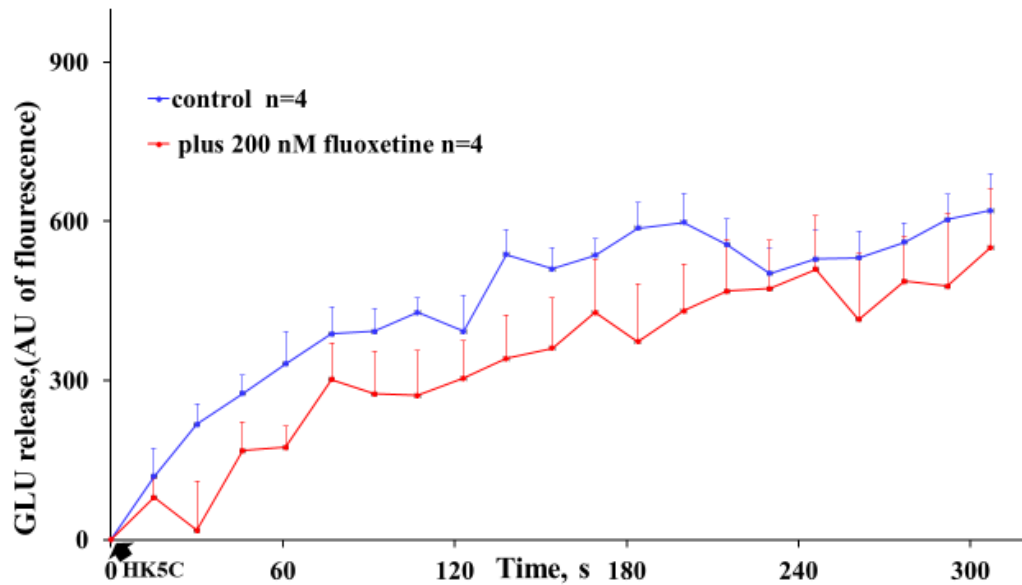


Figure 4.6. 200 nM Fluoxetine treatment for 20 min in 37°C perturb some HK5C evoked release from the recycling pool and not allowing any SP release. HK5C evoked GLU release following a 200 nM Fluoxetine incubation for 20 min at 37°C. Data are mean \pm SEM, N=1 independent experiment.

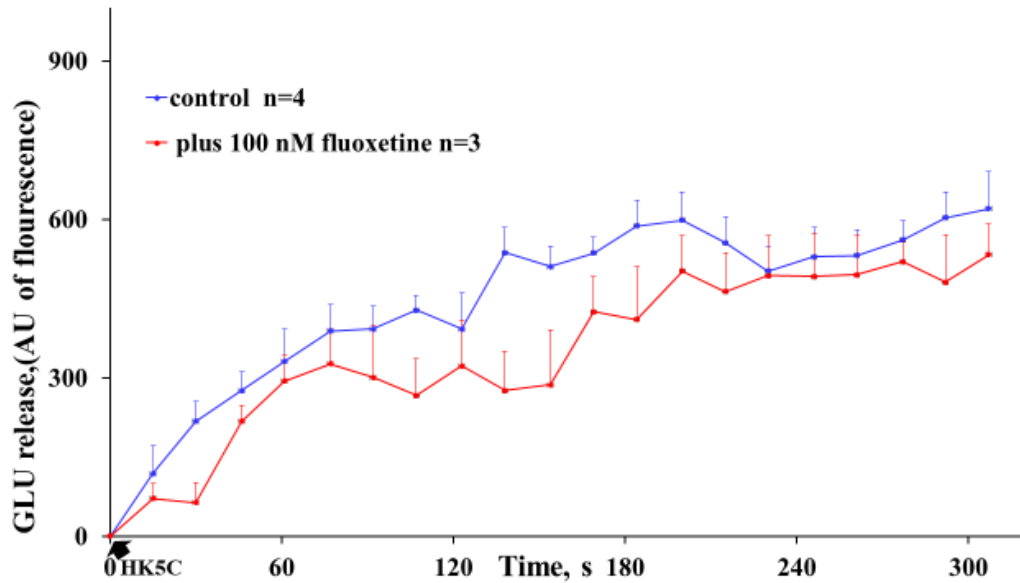


Figure 4.7. 100 nM Fluoxetine treatment for 20 min in 37°C perturb some HK5C evoked release from the recycling pool and not allowing any SP release. HK5C evoked GLU release following 100 nM Fluoxetine pre-treatment for 20 min at 37°C. Data are mean \pm SEM, N=1 independent experiment.

A lower concentration of Fluoxetine, 60 nM, did not perturb the HK5C evoked release since it was similar to that for non-drug treated control (Fig 4.8) so RRP and RP SVs were not being prevented from release but neither was the SP being allowed. As this was near to the concentration of 40 nM (see below) which did cause extra release we repeated this experiments 3 times to makes sure that the result was consistent.

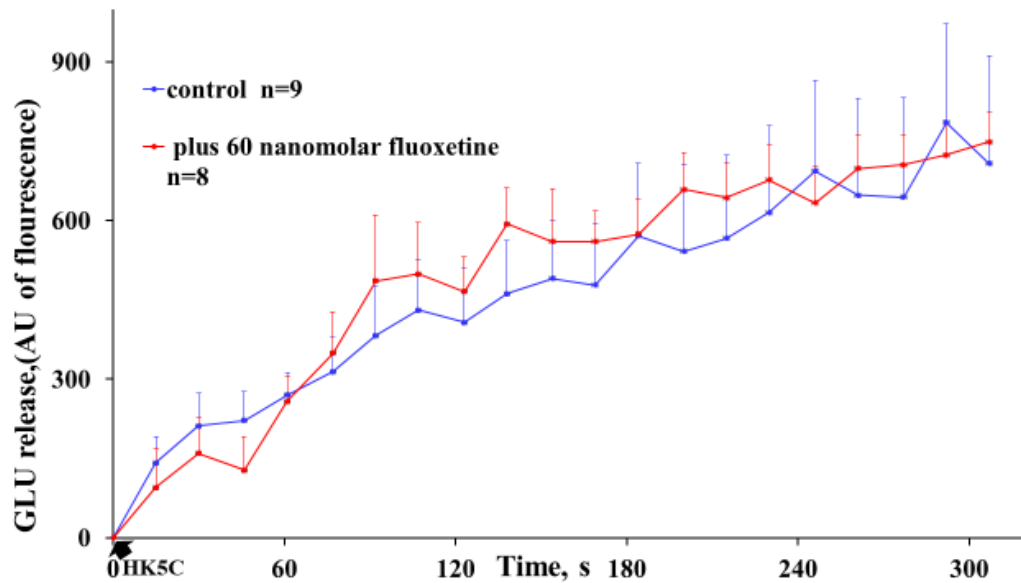


Figure 4.8. 60 nM Fluoxetine did not perturb the HK5C evoked RRP and RP release but neither was the SP being allowed. HK5C evoked GLU release in terminals treated 60 nM Fluoxetine pre-treatment with extended incubation for 20 min at 37°C compared to non-drug treated control. Data are mean \pm SEM, N=3 independent experiments; P >0.05.

With 40 nM Fluoxetine, the HK5C evoked release was found to be significantly higher than the control (Fig 4.9). This was also the case for 20 nM (Fig 4.10), although, the release appeared to be slightly lower compared to 40 nM (Fig 4.11) (did not show a difference statistically but chose to use 40 nM Fluoxetine from data in Fig 4.9). However, at 5 nM, Fluoxetine treatment did not induce any more HK5C evoked release compare to the non-drug treated condition (Fig 4.12). We have repeated this to ensure that truly 5 nM was not effective, 20-40 nM were, but by 60 nM, one could not get an extra release.

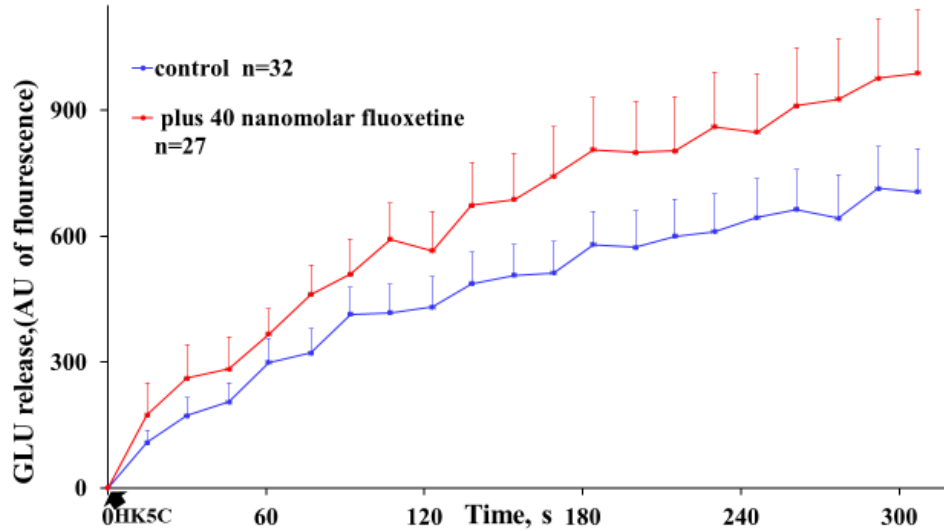


Figure 4.9. 40 nM Fluoxetine treatment for 20 min at 37 oC show significantly higher HK5C evoked release compared to the control. HK5C evoked GLU release following an incubation with 40 nM Fluoxetine for 20 min at 37°C compared to non-drug treated control. Data are mean \pm SEM, N=11 independent experiments. Note drug treated condition was significantly higher than control (P<0.05).

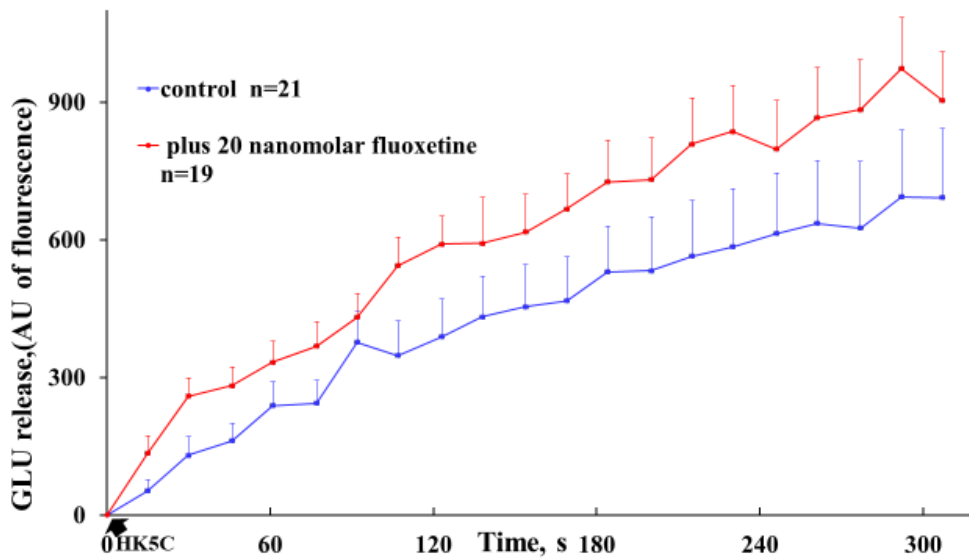


Figure 4.10. 20 nM Fluoxetine treatment for 20 min at 37 oC show significantly higher HK5C evoked release compared to the control HK5C evoked GLU release following 20 nM Fluoxetine incubation of 20 min at 37°C. Data are mean \pm SEM, N=7 independent experiments. Note drug treated condition was significantly higher than control (P<0.05).

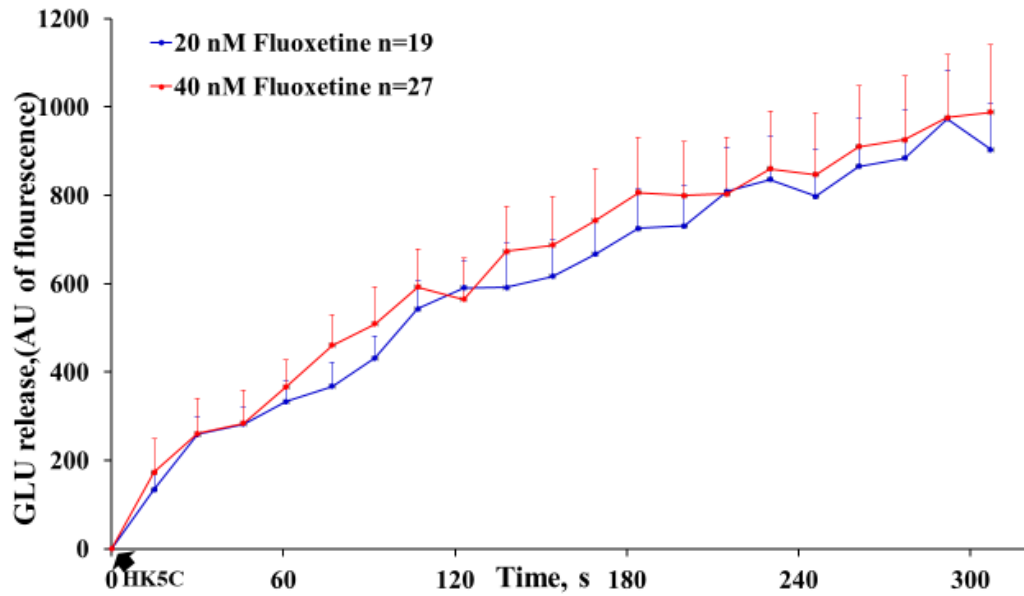


Figure 4.11. 40 nM Fluoxetine treated terminal show slightly higher HK5C evoked release compared to 20 nM Fluoxetine terminal, HK5C evoked GLU release following 20 nM Fluoxetine and 40 nM Fluoxetine incubation for 20 min at 37°C. Data are mean \pm SEM, N=7-11 independent experiments; P >0.05.

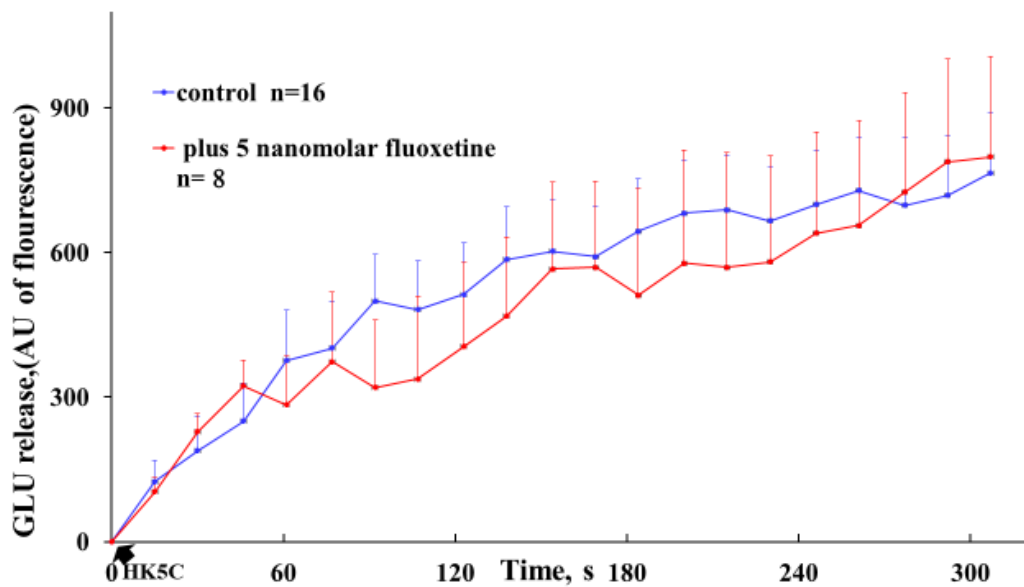


Figure 4.12. 5 nM Fluoxetine did not perturb the HK5C evoked RRP and RP release but neither was the SP being allowed HK5C evoked GLU release with 5 nM Fluoxetine pre-treatment following incubation for 20 min at 37°C. Data are mean \pm SEM, N=4 independent experiments; P >0.05

It is evident from the results that Fluoxetine has a biphasic effect on HK5C evoked release with 100 nM or more inhibiting some of the release whilst 40 nM induces greater additional release due to evoking the SP. Therefore, the 40 nM Fluoxetine was employed in later studies. These results demonstrate that one has to determine precisely the Fluoxetine concentration in the synaptosomal model to allow one to study the SP, it should be noted that in hippocampal culture cells 1 μ M was required whilst herein we only needed 40 nM. However, Jung *et al* (2014) also found a biphasic action of Fluoxetine on that 8 μ M was also shown to inhibit evoked release (Jung *et al*, 2014).

The effect of 40 nM Fluoxetine with extended incubation time (20 min) was compared to 5 min treatment of 100 μ M Roscovitine on HK5C evoked release (Fig 4.12). The two drugs were found to induce an equivalent amount of release. Considering 100 μ M Roscovitine has been previously found to induce the maximum SP release in the previous chapter (See Ch 3), the result clearly showcased that 40 nM Fluoxetine with 20 min incubation time has successfully evoked the SP exocytosis.

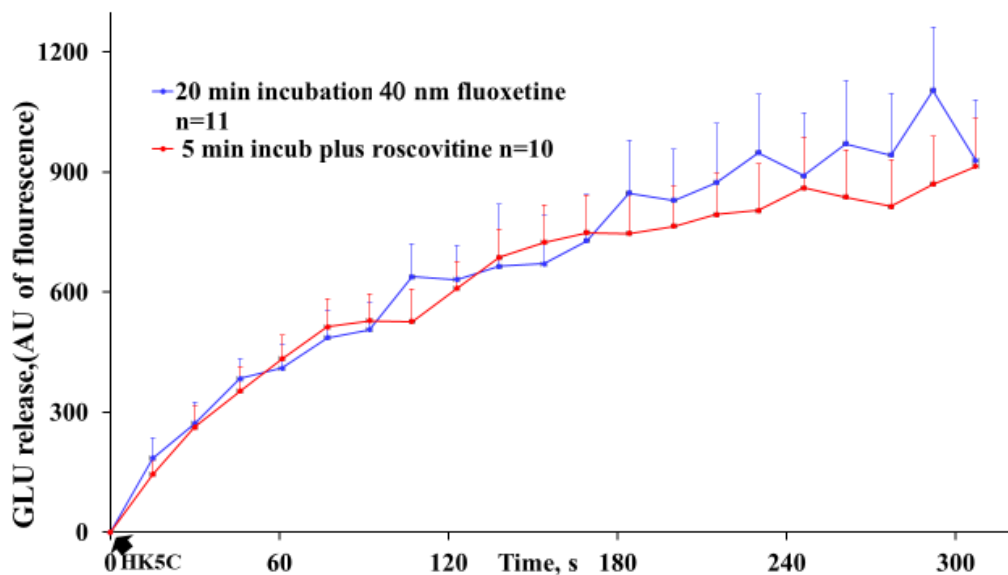


Figure 4.13. 40 nM Fluoxetine with 20 min incubation time show similar release to 100 nM Roscovitine with 5 min incubation. HK5C evoked GLU release following 5 min pretreated terminals with 100 μ M Roscovitine or 40 nM Fluoxetine treatment for 20 min at 37°C. Data are mean \pm SEM, N=3 independent experiments; P >0.05.

4.2.3 Dual treatment of Fluoxetine with Roscovitine produced equivalent amount of SP release

We have established that 20 min incubation with 40 nM Fluoxetine allows HK5C to trigger SP exocytosis to an apparent maximum amount. However, we investigated whether HK5C could evoke even more release from the SP. In these experiments, synaptosomes were incubated for 20 min at 37°C with no-drug (control), Roscovitine (for last 5 min of the 20 min incubation or Fluoxetine for 20 min with Roscovitine added for the last 5 min). By including synaptosomes with both 40 nM Fluoxetine and 100 µM Roscovitine, Roscovitine on its own allowed HK5C to evoke SP release as previously identified (Fig 4.14a) and when it was dual treated with Fluoxetine, there was still extra release evoked by HK5C compared to control (Fig 4.14b). Importantly, the amount of this extra release was equivalent to that induced by HK5C with only Roscovitine was treated (Fig 4.14c). Thus there was no further extra release evoked by HK5C following the double drug treatment. This could mean that 40 nM Fluoxetine treatment induces the maximum release of the SP release or it could imply that Roscovitine and Fluoxetine share a similar pathway that both work on the SP but such a pathway is maximally stimulated by either drug alone.

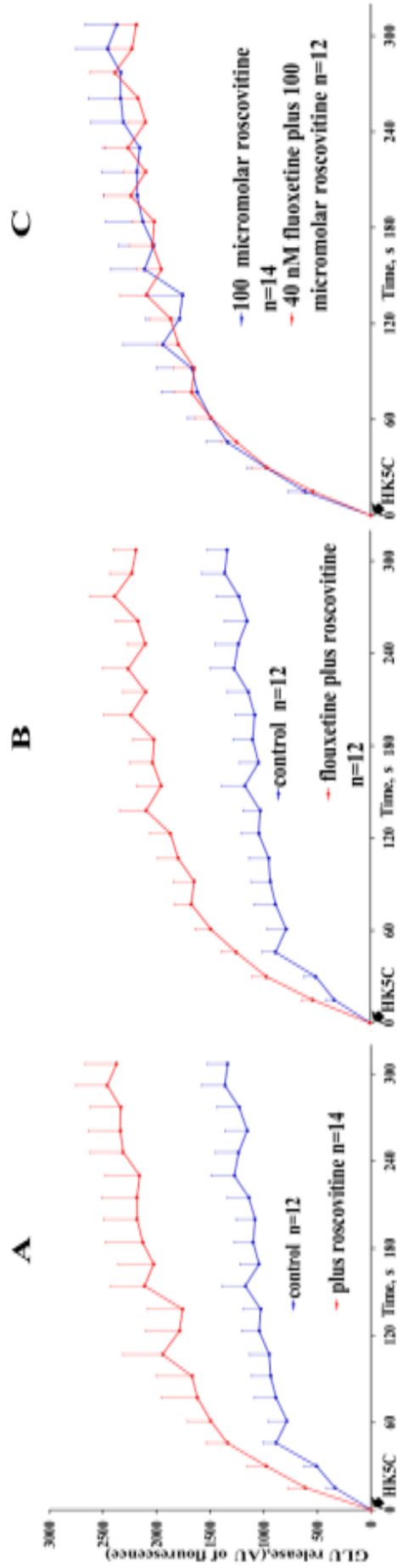


Figure 4.14. Dual treatment of Fluoxetine with Roscovitine produced equivalent amount of SP release. HK5C evoked GLU release in control and in terminals treated with a) 100 μ M roscovitine; b) 40 nM Fluoxetine plus 100 μ M Roscovitine c) 100 μ M Roscovitine or 100 μ M Roscovitine plus 40 nM Fluoxetine. The number of independent experiments for a, b and c was 4. Data are mean \pm SEM; $P < 0.05$ for a and b; $P > 0.05$ for c.

4.3 The effect of Fluoxetine on HK5C evoked $\Delta[\text{Ca}^{2+}]_i$

Previously in this chapter, 20 min of incubation with 40 nM and 20 nM Fluoxetine was found to enable HK5C to induce the SP release. However, it was also identified that 1 μM Fluoxetine treatment led to a reduction in HK5C evoked release by not only not allowing the SP release but also inhibited some release from the recycling pool consisting of the RRP and the RP. An investigation was, therefore, performed to see whether such effects were due to changes in evoked $\Delta[\text{Ca}^{2+}]_i$ using the Fura-2 assay. The sample was pre-treated with 1 μM Fluoxetine and HK5C evoked $\Delta[\text{Ca}^{2+}]_i$ was measured. 1 μM Fluoxetine treatment appeared to reduce the HK5C evoked $\Delta[\text{Ca}^{2+}]_i$ compared to the control (Fig 4.15). Therefore, it would be appeared that 1 μM Fluoxetine is reducing the release through blocking the entry of calcium into the nerve terminal following application of HK5C (see discussion).

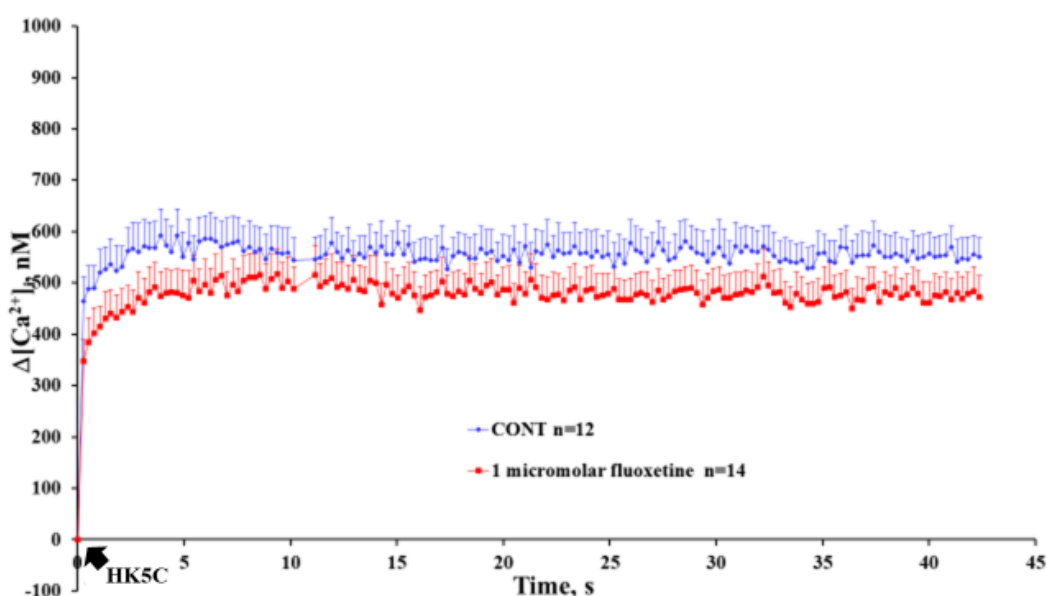


Figure 4.15. 1 μM Fluoxetine treatment reduced the HK5C evoked $\Delta[\text{Ca}^{2+}]_i$. The change in $[\text{Ca}^{2+}]_i$ induce by HK5C comparing control and 1 μM Fluoxetine. Data are mean \pm SEM, N=3 independent experiments; more experiments would be needed to prove this statistically.

4.4 Fluoxetine did not induce recycling and re-release of the RRP and RP

Research from Ashton's group has indicated that neither HK5C nor ION5C can induce more than one round of release of the RRP and RP, this mean that there are no recycling, reloading, and re-release of the SVs from their pool in the presence of these stimuli. Nevertheless, there was still a possibility that Fluoxetine, through unknown pathway, could enable the recycling, reloading, and re-release (see similar arguments for Roscovitine action in chapter 3). This is important because it could mean that the release we have observed may be derived from the recycled RRP and RP instead of the SP. In order to ascertain this is not the case, we pharmacologically disabled recycling machineries; 160 μM Dynasore for Dyn-dependent pathway and 15 μM Pitstop2TM for clathrin-dependent pathway. Comparing non-drug treated control condition vs Fluoxetine plus Dynasore (Fig 4.16 a) clearly revealed that 40 nM Fluoxetine was still allowing HK5C evoked release of SP when Dyn-dependent recycling pathways have been blocked. Pitstop2TM treated synaptosomes also still allow 40 nM Fluoxetine to support HK5C evoked SP release (Fig 4.16 b). Overall this confirms that the extra HK5C evoked release identified with 40 nM Fluoxetine treatment is actually from the SP.

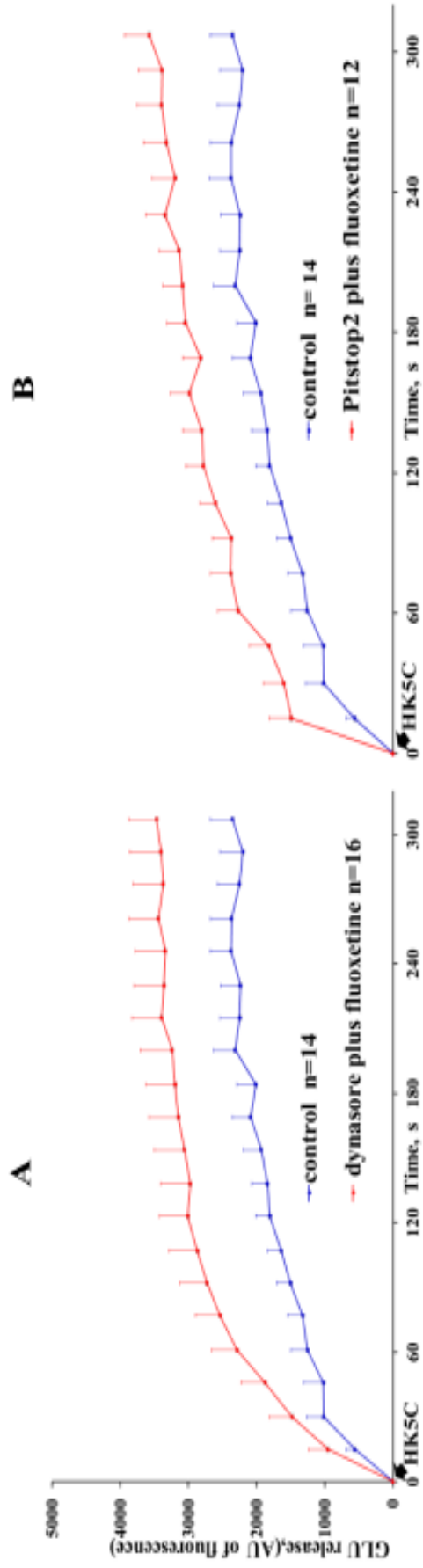


Figure 4.16. Extra HK5C evoked release identified with 40 nM Fluoxetine treatment is not a result of recycling, reloading, and re-release of recycling pool.

HK5C evoked GLU release in control and in terminals treated with A) 160 μ M Dynasore plus 40 nM Fluoxetine B) 15 μ M Pitstop plus 40 nM Fluoxetine.

The number of independent experiments for A was 5 and for B was 4. Data are mean \pm SEM; $P < 0.05$ when comparing control to drug treated

4.5 ION5C evoked SP release

4.5.1 40 nM Fluoxetine supports ION5C evoked SP release

The results so far employing Fluoxetine involved studying HK5C evoked release of the SP. Another type of stimulus that we often employ in our study to trigger exocytosis of SVs is ION. In contrast to HK5C, ION is an ionophore which bypasses calcium channels and increased the Ca^{2+} level throughout the nerve terminal, therefore it works through a different pathway from HK5C. Thus, it was important to ascertain that Fluoxetine can also release the SP employing ION5C stimulation. ION5C evoked exocytosis following 40 nM Fluoxetine treatment (20 min at 37°C) was also able to induce the release of the SP (Fig 4.17).

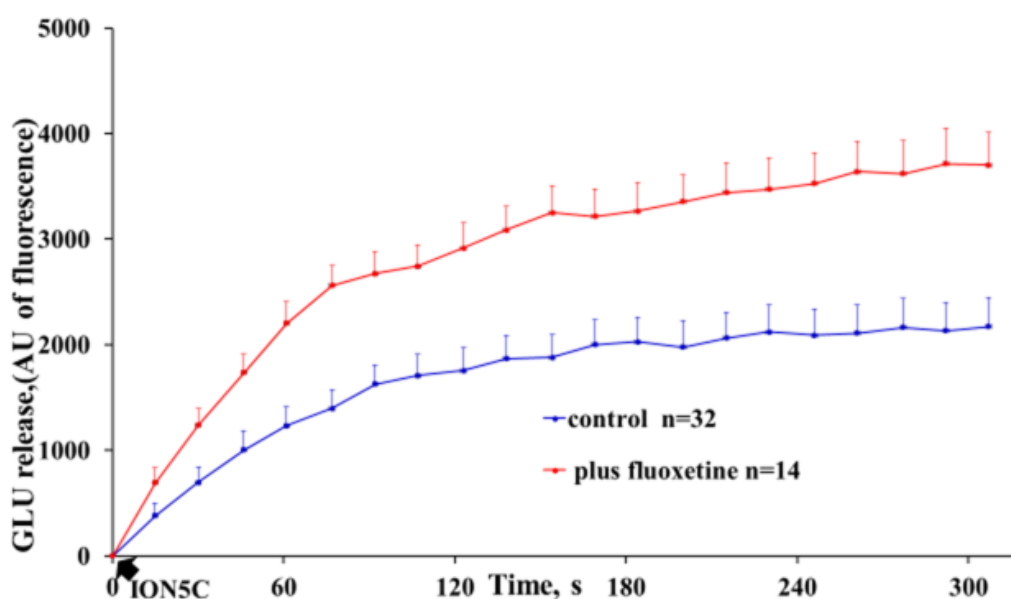


Figure 4.17. 40 nM Fluoxetine supports ION5C evoked SP release. ION5C evoked GLU release in 40 nM Fluoxetine pre-treated terminals compared to non-drug treated control. Data are mean \pm SEM, N=6 for control and N=4 for Fluoxetine independent experiments. Note Fluoxetine treated condition induces significantly higher ION5C evoked release than control ($P>0.05$).

4.5.2 Fluoxetine did not induce recycling and re-release of the RRP and RP under ION5C stimulation

As for HK5C evoked extra release following 40 nM Fluoxetine treatment, we also tested that Fluoxetine's effect on ION5C evoked release was not due to recycling, reloading, and re-release of the RRP and RP by pharmacologically blocking SV recycling with Dynasore and Pitstop2TM. ION5C evoked release in control vs 160 μ M Dynasore plus 40 nM Fluoxetine (Fig 4.18a) or in control vs 15 μ M Pitstop2TM plus 40 nM Fluoxetine (Fig 4.19a) were measured. It was evident from the results that under both the Dynasore treated conditions and Pitstop2TM treated conditions, Fluoxetine was still able to support the release of the SP evoked by ION5C stimulation. Clearly, this extra release is not due to recycled RRP and RP SVs. These results are more apparent when Fluoxetine treated condition was compared to either Fluoxetine plus Dynasore (Fig 4.18b) or Fluoxetine plus Pitstop2TM (Fig 4.19b) as in both conditions, the release were virtually unchanged.

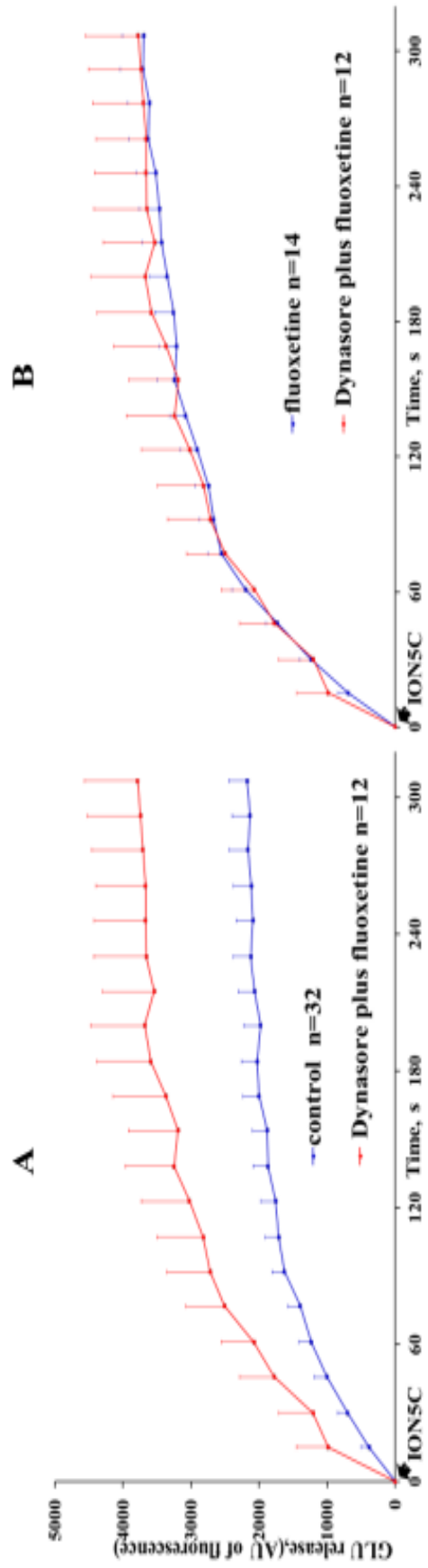


Figure 4.18. Extra ION5C evoked release identified with 40 nM Fluoxetine treatment is not a result of dynamin dependent recycling, reloading, and release of recycling pool. ION5C evoked GLU release comparing a) control and in terminals treated with 160 μ M Dynasore plus 40 nM Fluoxetine b) 40 nM Fluoxetine with 40 nM Fluoxetine plus 160 μ M Dynasore. The number of independent experiments for was 6 for control and 3 for the drug treatment. Data are mean \pm SEM; $P < 0.05$ when comparing control to drug treated synaptosomes.

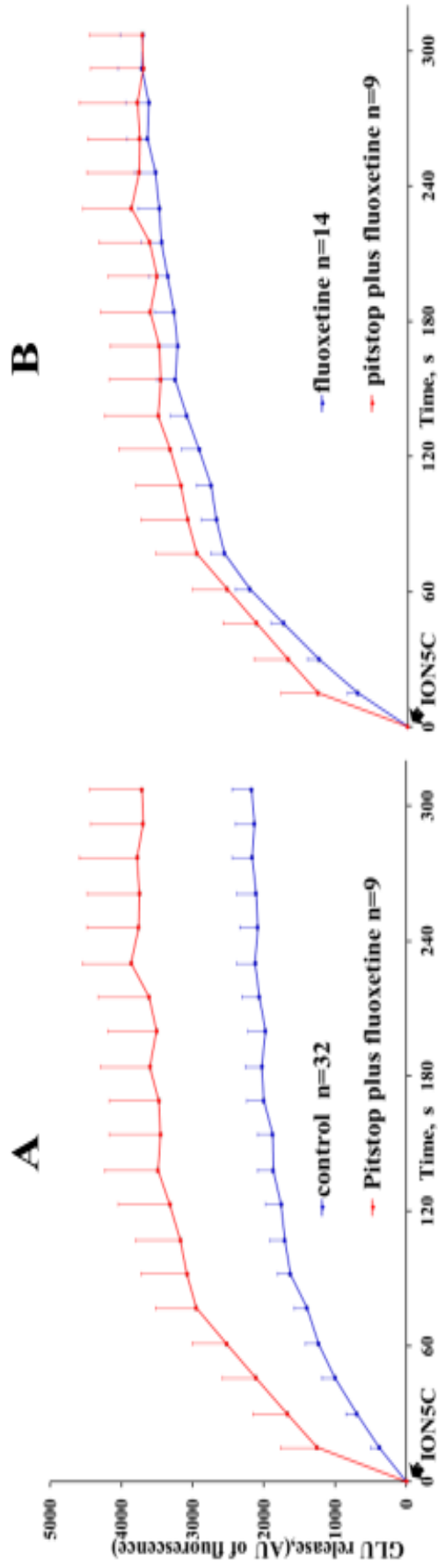


Figure 4.19. Extra ION5C evoked release identified with 40 nM Fluoxetine treatment is not a result of clathrin dependent recycling, reloading, and re-release of recycling pool. ION5C evoked GLU release comparing a) control and in terminals treated with 15 μ M Pitstop2TM plus 40 nM Fluoxetine b) 40 nM Fluoxetine and 15 μ M Pitstop2TM plus 40 nM Fluoxetine. The number of independent experiments for control was 6 and for drug treated was 3. Data are mean \pm SEM; $P < 0.05$ when comparing control to drug treated synaptosomes.

4.6 Bioenergetics results

4.6.1 5 min incubation with Fluoxetine concentrations

Bioenergetics of the 1 μ M Fluoxetine treated samples were measured with Seahorse XFp flux analyser. The purpose of this experiment was to clarify the drug does not have an off-target effect which perturbs the bioenergetics of nerve terminals. Specifically, Fluoxetine induced effect on the release is not derived from disruption in bioenergetics of the synaptosomes. In fact, as 1 μ M Fluoxetine was found to block some of the release from the RRP and RP, there is a chance that this effect may be derived from disturbance of bioenergetics in the terminals whereby there is less energy to support SV exocytosis.

The sample was pre-treated with 1 μ M Fluoxetine for 5 min at 37°C and then its oxygen consumption rate was measured during serial injections of oligomycin, FCCP, and rotenone/antimycin. This procedure has allowed various parameters to be measured; basal respiration, ATP production, spare capacity, maximum respiration, proton leakage, and non-mitochondrial respiration. Note this method was already outlined in more detail in Chapter 3. However, the acute treatment with 1 μ M Fluoxetine for 5 min has failed to significantly disturb any of the bioenergetics parameters (Fig 4.20, Fig 4.21 A-E).

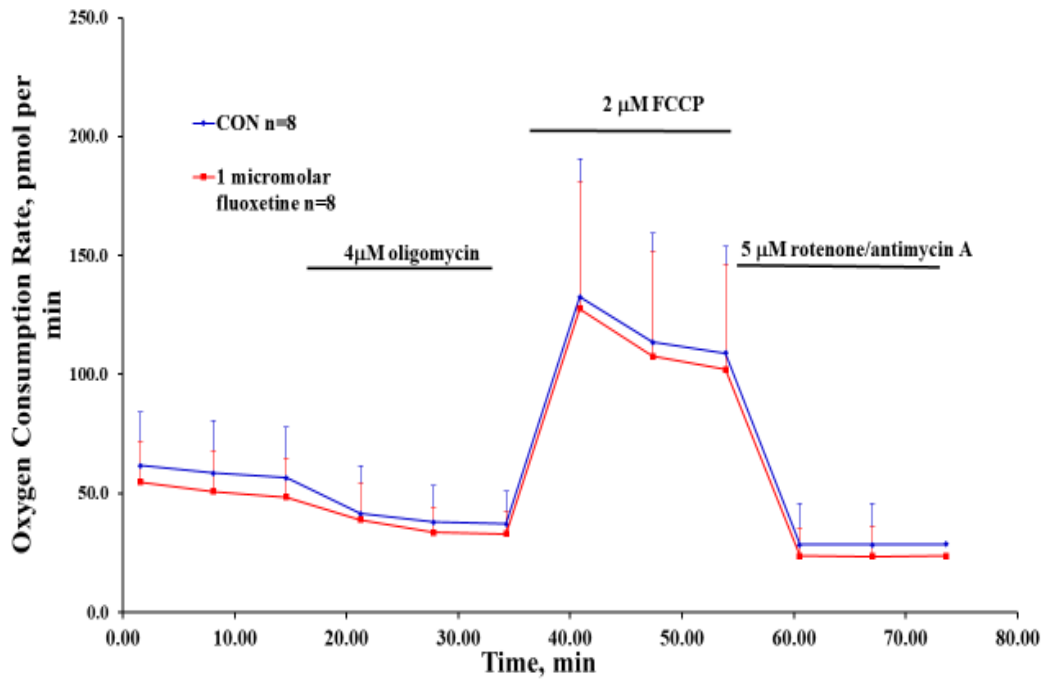


Figure 4.20. The reduction identified in HK5C evoked GLU release of nerve terminal treated with 1 μM Fluoxetine for 5 min was not a result of disturbance in bioenergetics. The effect of 1 μM Fluoxetine treatment on the bioenergetics of synaptosomes compared to non-drug treated control. The experiment was done three times and the mean values represent an average of 8 independent measurements and error bars represent the SD; P>0.05.

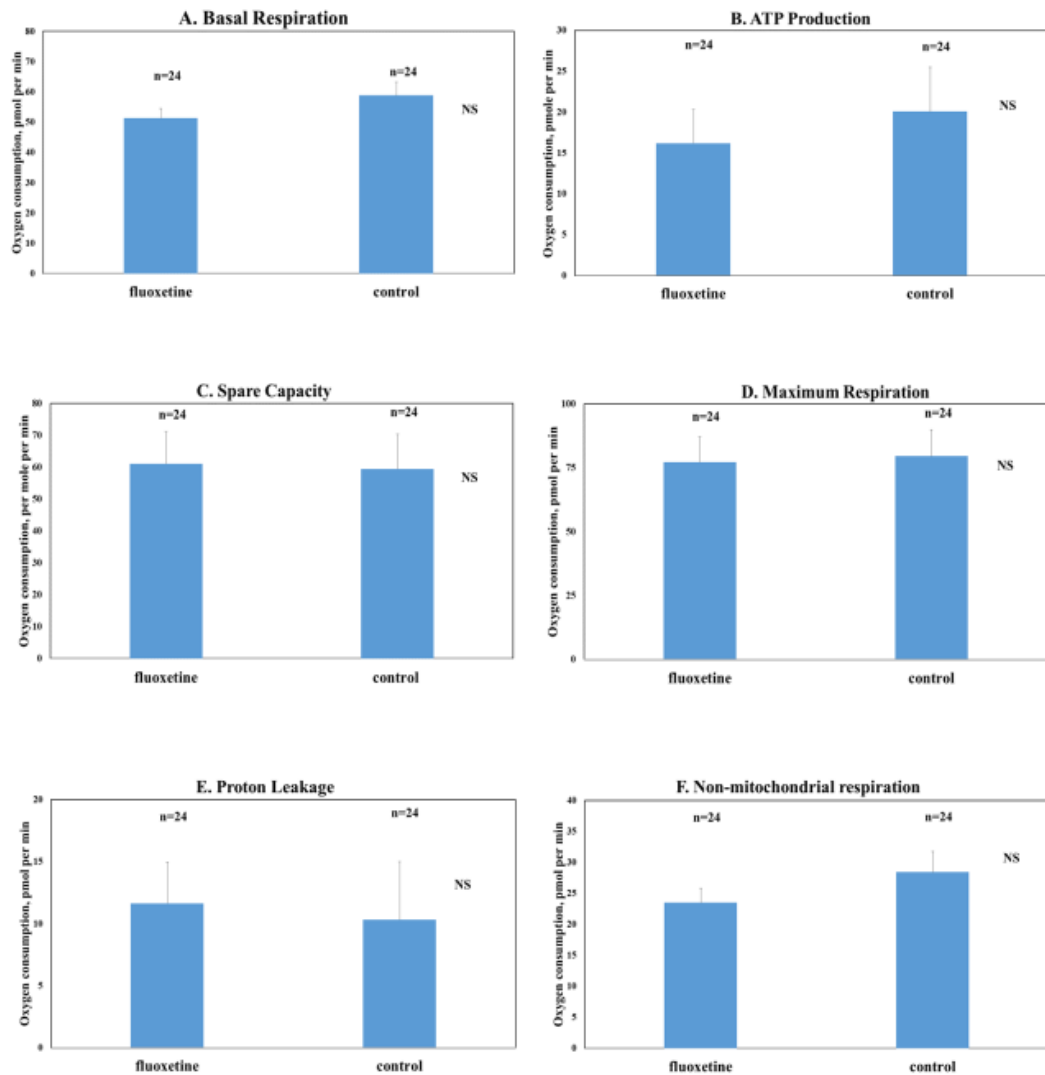


Figure 4.21. The reduction identified in HK5C evoked GLU release of nerve terminal treated with 1 μ M Fluoxetine for 5 min was not a result of disturbance in mitochondrial functions. The effect of 5 min 1 μ M Fluoxetine incubation at 37°C on various parameters measured on synaptosomes; (A) basal respiration, (B) ATP production, (C) spare capacity, (D) maximal respiration, (E) Proton leakage, and (F) Non-mitochondrial respiration. The histograms represent the mean and the error bar shows the SEM. There is no significant difference (NS) between control and Fluoxetine treatment.

4.6.2 The effect of 20 min Fluoxetine incubation on synaptosomal bioenergetics

Synaptosomes were initially pre-treated with range of Fluoxetine concentrations for 5 min but have failed to evoke any SP exocytosis (see ch 4.2.1). Therefore, the incubation time with the drug has extended to 20 minutes. Consequently, a 20 min pre-treatment of the drug also had to be tested to see whether it has an impact on bioenergetics of the sample. The acute treatment of the sample with 1 μM Fluoxetine for 20 min, which did inhibit some of the release of the RRP and RP, failed to produce any significant difference on any of the bioenergetic parameters (Fig 4.22, Fig 4.23 A-E). We argue that as 1 μM Fluoxetine failed to perturb the bioenergetics parameters, then clearly a lower concentration (40 nM) would not as this drug concentration is even less likely to have secondary effect.

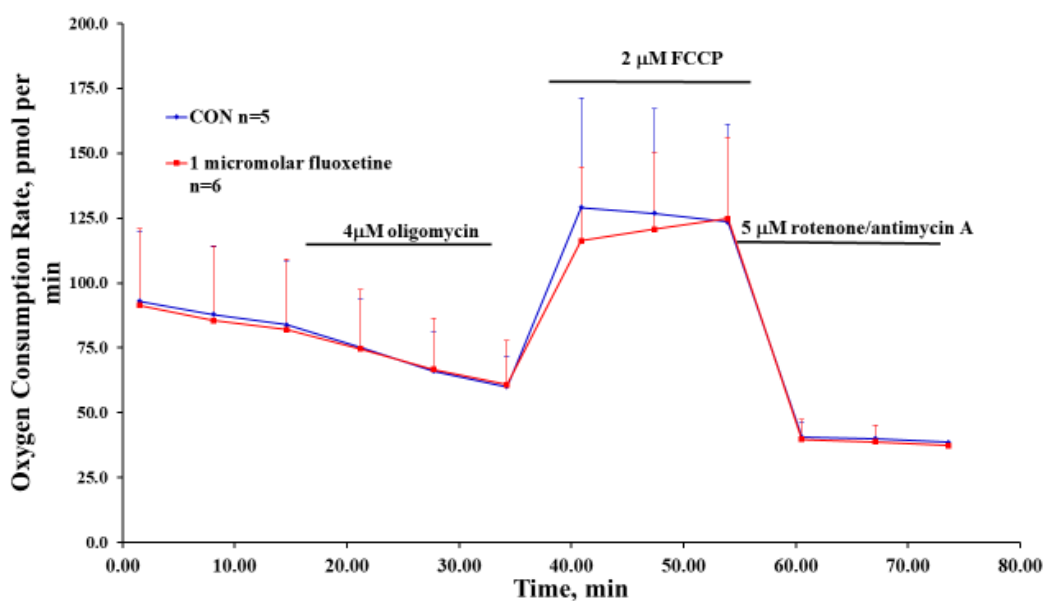


Figure 4.22. The reduction identified in HK5C evoked GLU release of nerve terminal treated with 1 μM Fluoxetine for 20 min was not a result of disturbance in bioenergetics. The effect of extended incubation of 1 μM Fluoxetine (20 min at 37°C) on the bioenergetics of synaptosomes. The experiment was done two times and the mean values represent an average of 6 independent measurements and error bars represent the SD; $P>0.05$.

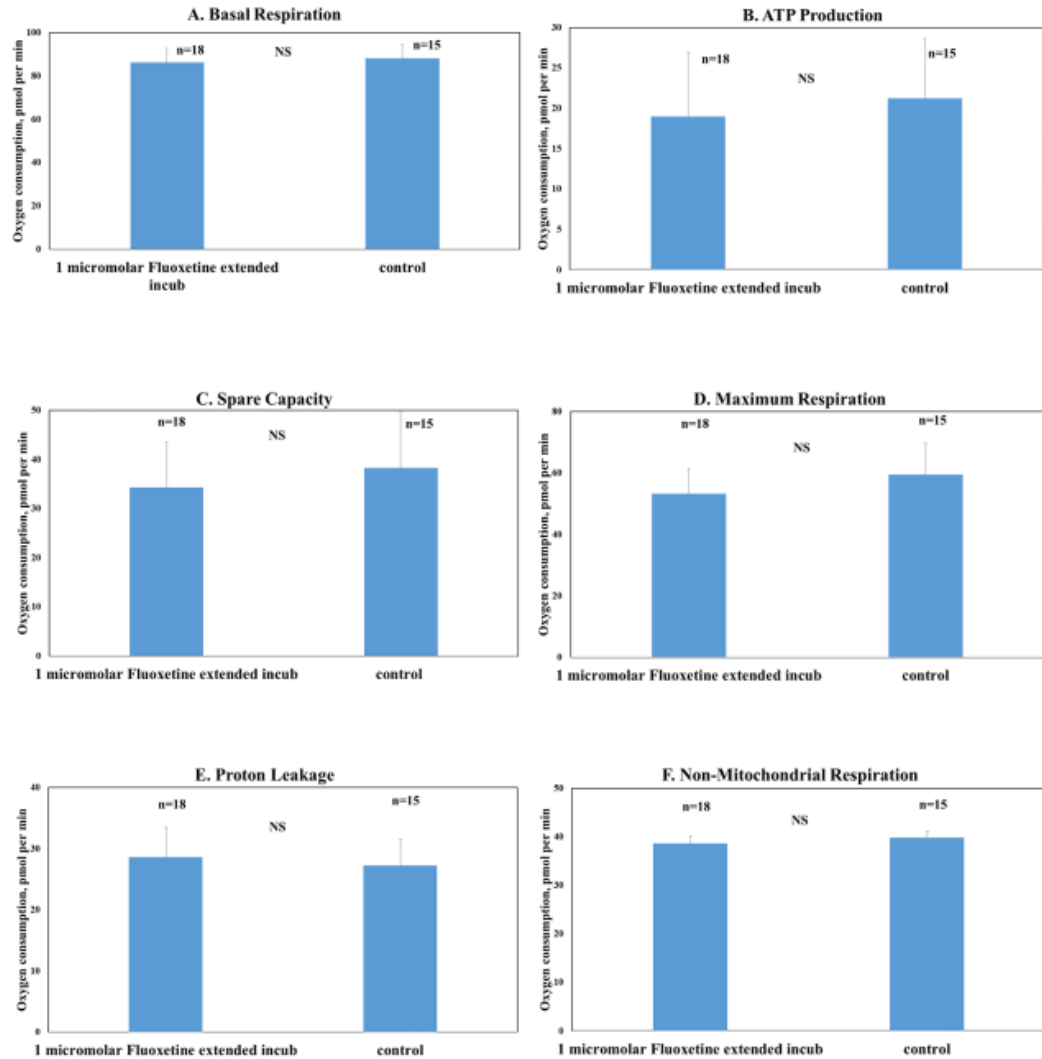


Figure 4.23. The reduction identified in HK5C evoked GLU release of nerve terminal treated with 1 μ M Fluoxetine for 20 min was not a result of disturbance in mitochondrial functions. The effect of 20 min 1 μ M Fluoxetine pre-incubation time on synaptosomes bioenergetics parameters; (A) basal respiration, (B) ATP production, (C) spare capacity, (D) maximal respiration, (E) Proton leakage, and (F) Non-mitochondrial respiration. The histograms represent the mean and the error bar shows the SEM. Note although only 2 independent synaptosomes preparations were used, the sample in individual wells were treated as independent. Using this one can show that there was no significant difference ($P > 0.05$) between control and drug treated terminals.

#	Figure #	Assays	Stimulus	Drugs employed (conc.)	Key findings
1	4.1-4.4	GLU	HK5C	Fluoxetine (1 μ M, 200 nM, 100 nM, 50 nM)	5 min incubation of synaptosomes in 37°C with Fluoxetine failed to allow HK5C to evoke SP release. Instead, 1 μ M appears to perturb some RRP and RP release.
2	4.5-4.13	GLU	HK5C	Fluoxetine (1 μ M, 200 nM, 100 nM, 60 nM, 40 nM, 20 nM, 5 nM)	20 min incubation with 1 μ M, 200 nM, 100 nM, appears to reduce the HK5C evoked GLU release compared to control. However, 40 nM and 20 nM Fluoxetine allowed an extra release with 40 nM providing the maximal release.
3	4.14	GLU	HK5C	Fluoxetine (40 nM), Roscovitine (100 μ M)	Treatment of the terminal with Roscovitine combined with Fluoxetine allowed HK5C to evoke an extra release. Importantly, Roscovitine alone and Roscovitine plus Fluoxetine conditions showed a similar amount of GLU release, shows that Fluoxetine is allowing maximum evoked SP release, and it also suggest that Fluoxetine and Roscovitine might operate in similar pathway to allow an extra SVs to be available.
4	4.15	Fura-2	HK5C	Fluoxetine (1 μ M)	20 min treatment of synaptosomes with 1 μ M Fluoxetine was found to perturb some release from the RRP and RP potentially due to reduction in $[Ca^{2+}]_i$ following Fluoxetine treatment.
5	4.16	GLU	HK5C	Fluoxetine (40 μ M), Dynasore (160 μ M), Pitstop 2 TM (15 μ M)	An extra HK5C evoked release observed in 40 nM Fluoxetine treated terminal is not a result of recycling of the RRP and RP.
6	4.17	GLU	ION5C	Fluoxetine (40 nM)	40 nM Fluoxetine with 20 min incubation also allows ION5C to evoke an extra release.
7	4.18-4.19	GLU	ION5C	Fluoxetine (40 nM), Dynasore (160 μ M), Pitstop 2 TM (15 μ M)	An extra ION5C evoked release following 40 nM Fluoxetine treatment is not a result of recycling of the RRP and RP.
8	4.20-4.23	Bio		Fluoxetine (1 μ M)	1 μ M Fluoxetine treatment for both 5 min and 20 min incubation in 37°C failed to perturb any of the bioenergetics parameters. This may suggest that some perturbations of the RRP and RP release observed in both incubation times are not due to the disturbance of bioenergetics of synaptosomes.

Figure 4.24. Summary of the findings in chapter 4.

4.7 Discussion

Selective serotonin reuptake inhibitors (SSRIs) are the most prevalently used antidepressants. They are suggested to work through blocking the uptake of exocytosed serotonin into the presynaptic terminal, which consequently increase the serotonin levels in the brain of the patient with depression. Fluoxetine is an SSRI and it has been found from the study of Jung *et al* (2014) that under the therapeutic dosage (1 μM), it is capable of mobilising the GLU containing SVs from the SP in hippocampal cultured cell. In the research model used herein (i.e synaptosomes for cerebral cortical cell), 80% of terminals utilised GLU as their neurotransmitter and we, therefore, investigated whether Fluoxetine could also evoke the release of the SP in this model.

4.7.1 GLU Assay

Synaptosomes were pre-treated with various concentrations of Fluoxetine for 5 min at 37°C and HK5C evoked GLU release was subsequently measured. Whilst 1 μM Fluoxetine, may reduce the release compared to the control condition, overall, none of the Fluoxetine concentrations employed were able to successfully allow HK5C to evoke the SP to exocytose. Therefore, the Fluoxetine incubation time was extended to 20 min and the synaptosomes were, again, pre-treated with different concentrations of Fluoxetine and its HK5C evoked GLU release was subsequently induced and measured. 1 μM Fluoxetine treatment for 20 min at 37°C significantly reduced HK5C evoked release compared to the control, indicating that this concentration of the drug reduced normal release rather than increasing it. Both 200 nM and 100 nM Fluoxetine also reduced the exocytosis of GLU containing SVs although the reduction was not as great as with 1 μM . With 60 nM Fluoxetine there was neither an inhibition or stimulation effect on HK5C evoked release so this release was to an equivalent level with the control, representing the normal release of the RRP and the RP. However, remarkably at 40 nM Fluoxetine, a significantly increase in HK5C evoked SV release was found. The amount of release was clearly above the non-

drug treated condition and, therefore, such treatment appears to have induced a release of SVs derived from a pool distinct from the RRP and the RP; this release can be assumed to be from the SP. The SP was also evoked by HK5C following 20 nM Fluoxetine treatment, but the level of extra release seems to be slightly lower compared to 40 nM. A 5 nM drug treatment release appeared to be equivalent to the control so there was no extra release; this concentration of drug probably had no effect on any pathway. This would suggest that 60 nM Fluoxetine may have both inhibiting action and a stimulatory action that cancel each other out. Overall, maximum release of the SP was observed by 40 nM Fluoxetine incubation for 20 min incubation prior to stimulation.

Even though a 20 min 40 nM Fluoxetine treatment at 37°C appeared to allow the SP to be release, there was still a potential that the drug, by an unknown mechanism, may have promoted recycling, reloading, and re-releasing of the RRP and RP pool. This possibility was investigated through pharmacologically inhibiting the recycling, with Dynasore and Pitstop2TM. The results clearly demonstrated that the extra release observed was from the SP of SVs as both conditions prevented recycling pathways of the RRP and the RP but Fluoxetine was still able to allow HK5C to induce extra release.

Having established that 40 nM Fluoxetine incubation for 20 min at 37°C appeared to make available the SP following stimulation, it was found that this treatment also allowed ION5C to evoke the SP and this was also not a result of recycling, reloading, and releasing as the stimulus was still able to induce an extra release under Dynasore and Pitstop2TM treatment. As these stimuli work by distinct means future experiments must help to ascertain the commonalities of their action on the SP.

4.7.2 FURA-2 Assay

It was apparent that the HK5C evoked $\Delta[\text{Ca}^{2+}]_i$ has been reduced following the treatment with 1 μM Fluoxetine compared to non-drug treated condition. Thus, it would be appear that 1 μM Fluoxetine is reducing the level of calcium entering the nerve terminal and this

may consequently lead to a reduction, this could also possibly explain the reduced release in terminals treated with 100 nM and 200 nM ($\Delta[\text{Ca}^{2+}]_i$ was not measured for this). Indeed, our observation could explain why Fluoxetine was dose-dependently reduced the level of release in the study by Jung *et al* (2014). This study used range of concentrations (0.9, 4.5, 9, 18 μM) of Fluoxetine and found out that the drug above the therapeutic dose (1 μM) were dose-dependently inhibiting the neurotransmission (Jung *et al*, 2014) (see earlier comments about differences in the dose required between synaptosomes and hippocampal cultured cells). Intriguingly, in some other cases Fluoxetine has been found to increase the Ca^{2+} entry. For instance, Charles *et al* (2017) reported that Fluoxetine induces an elevation in the cytosolic Ca^{2+} concentration and eventually results in necrosis of the cancer cell. They have claimed that this showcases the potential of Fluoxetine to be used in the cancer therapy (Charles *et al*, 2017). However, the study used 100 μM Fluoxetine which is much higher than used herein or used by Jung *et al* (2014). Nevertheless, results from other studies and the data obtained in current study demonstrate that Fluoxetine may require changes in $[\text{Ca}^{2+}]_i$ levels under certain circumstance and this could be investigated further in the future.

4.7.3 Bioenergetics

It is clear from the bioenergetic results that neither 5 min incubation nor a 20 min incubation with 1 μM Fluoxetine, disturbed the bioenergetics of the nerve terminals. These results confirm that the observed Fluoxetine induced effect on synaptic neurotransmission are not due to disturbance of synaptosomal bioenergetics. Furthermore, it also ensures that reduction in release of the recycling pool (RRP or RP) induced through 1 μM Fluoxetine treatment is not a consequence of the off-target effect of the drug on energetic integrity of the terminals.

4.8 Future Studies

4.8.1 Mechanism of Fluoxetine induced SP release

This chapter has successfully established that 20 min incubation with 40 nM Fluoxetine is capable of allowing the SP to be released from synaptosomes following stimulation. There are several future studies that are required, including elucidating the exact mechanism of Fluoxetine that allows the evoked triggering of the SP release. SSRI drugs are believed to work through blocking serotonin uptake into terminals, thereby, increasing the monoamine level in the synaptic cleft. However, the result from current study could suggest that the antidepressant effect of Fluoxetine may also involve glutamatergic neurotransmission, and furthermore, that SP exocytosis may contribute such antidepressant activity. The exact cause of depression is yet not fully understood but a widely accepted view is a lack of serotonin levels within the brain since the SSRI drugs, such as Fluoxetine, have managed to improve the symptoms of the patients. However, in this current study, Fluoxetine can allow extra exocytosis of GLU containing SVs from glutamatergic nerve terminals. Thus, it is possible that part of the antidepressant effect of drug may be derived from increasing the number of NT vesicles that can be stimulated to release and these effects would not be restricted to serotonergic terminals.

Indeed, it has been reported theoretically that the antidepressant effect of Fluoxetine may not be restricted to causing serotonin uptake inhibition. For instance, Bymaster *et al* (2002) has demonstrated that Fluoxetine induced an elevation in the extracellular level of dopamine and on norepinephrine in the hypothalamus, cortex and prefrontal cortex (Bymaster *et al*, 2002). Previously it was reported that Fluoxetine inhibited 4AP evoked GLU release from the cerebral cortical synaptosomes mainly through attenuation of P/Q type calcium channels (Wang *et al*, 2003). This result differs from herein as we use higher $[Ca^{2+}]_e$ and stimuli that release both the RRP and the RP. Fluoxetine was also found to be able to regulate neuroplasticity even under the condition where 5HT transporters were

absent (Levy *et al*, 2019). Clearly, further investigations on the precise mechanism of Fluoxetine allowing evoked SP exocytosis in synaptosomes may help elucidate the complete pharmacology of Fluoxetine and this may help in the further understanding the pathology of the depression. Such advances may help accelerate the development on future treatment options for a patients suffering from depression. As to whether serotonergic pathways have contributed to the extra GLU release that can be induced need to be studied, one could investigate whether other SSRIs could support release on SP or investigate whether activation of presynaptic serotonin receptor could do this. Currently, this seems unlikely as compared to glutamatergic terminals there are very few serotonergic terminals to release enough serotonin to act on all glutamatergic terminals and this assumes that these all contain presynaptic serotonin receptors.

4.8.2 Ca²⁺ dependency of Fluoxetine induced SP release

This chapter has shown that 1 μ M Fluoxetine treatment (in both 5 and 20 min incubation) failed to support HK5C evoked SP release but it perturbed some release from the other recycling pools. Such treatment reduced the HK5C evoked $\Delta[\text{Ca}^{2+}]_i$. Thus, it is likely that 1 μ M Fluoxetine treatment prevents some of the SVs from the recycling pools (RRP and RP) from releasing due to the attenuation of calcium entry into the nerve terminal. In chapter 3 the Roscovitine action to support the evoked SP release, it has been shown that SP exocytosis involved the regulation of calcium entry. Further, treatment of the samples with PMA, a PKC activator, perturbed the Roscovitine induced ION5C evoked SP release, as did increasing the extracellular calcium level ($[\text{Ca}^{2+}]_e$) by using HK10C and HK20C. Thus, future experiments should include studying Fluoxetine with PKC regulating drugs, including PMA (PKC activator) and Go6983 (PKC inhibitor), and also employing higher $[\text{Ca}^{2+}]_e$.

In the Roscovitine chapter, we have shown that inhibition of three distinct types of calcium channel blocks the Roscovitine action on HK5C evoked SP release but there was no

specificity observed as specific inhibition of each types of channel with toxins showed a similar result in that there was perturbation of the SP release. For Fluoxetine, some studies have implicated P/Q type calcium channels is in its action (Wang *et al*, 2003) whilst others have shown that Fluoxetine inhibits both L-type and N-type calcium channels (Deak et al, 2000). On the other hand, it has been reported that major depression disorders involve L-type calcium channel (Bhat *et al*, 2012) and others suggest that SSRI modulate synaptic plasticity through inhibition of L-type calcium channel and that this action was actually independent of 5-HT transporters (Norman *et al*, 2018; Alboghobeish *et al*, 2019). Therefore, it will be interesting to investigate whether Fluoxetine action on regulating the availability of the SP might involve the presence of various calcium channels, and importantly, if such action occurred through specific Ca²⁺ channels.

4.8.3 Reversibility of Fluoxetine

The use of FM 2-10 dye to study SP exocytosis has not been performed herein. This is because in order to load up the SP SVs with dye, one would have to pre-treat the terminals with either Fluoxetine or Roscovitine so that the SP is released and so could be labelled with the Fluorescence dye and following recycling, one would have labelled such SP SVs. However, Fluoxetine or Roscovitine would be needed to allow HK5C or ION5C to evoke the release of FM dye from the exocytosing SP of SVs. This may be complicated if such drugs can effect parts of the SV recycling cycle such that one may not be able to label SP SVs by this method. Possibly if drug actions are reversible then one could allow SP to be labelled and recycled and then re-load the drug; one could use one drug for pre-stimulation and the other drug for stimulation.

The mode of the Fluoxetine triggered SP exocytosis has yet to be established. Two modes of release, KR and FF, operate through distinctive machineries, and thus exploration into the mode of SP release may also help with elucidating the exact properties of exocytosis from such vesicles. It is noteworthy that Ashton's group has previously observed that

under non-drug treated conditions, stimulation with 4AP5C released only the RRP of SVs, with roughly half being via a KR mechanism and half being through FF during controls (see appendix Fig A5). ION5C and HK5C on the other hand, releases RRP exclusively by KR, and the RP exclusively by FF (see appendix 1). Further, Tsien's group has reported that the mode of the release is dependent on position of the SVs with long-dwelling vesicles more likely to undergo the KR mode of the release (Park *et al*, 2012). Therefore, in the future study, one may be able to utilise FM 2-10 release assay and Fluoxetine to discover the mode of SP exocytosis.

4.8.4 Phosphorylation

The preliminary phosphorylation experiments on specific phosphorylation sites on Syn I has tried to correlate specific sites with release of the SP (see chapter 3). Clearly, an analogous study should be performed in which the SP is able to be released following 40 nM Fluoxetine treatment.

4.9 Conclusion

In conclusion, a 20 min incubation at 37°C with 40 nM Fluoxetine provided the best condition for future studies for both HK5C and ION5C evoked SP release. 1 µM Fluoxetine treatment resulted in a decrease of the release. This may be due to this reducing the HK5C evoked $\Delta[\text{Ca}^{2+}]_i$.

Chapter 5:

Mode of Release: Role of Dynamin, PKA, Calcium Channels

5.1 Introduction

There are finite numbers of SV in the nerve terminal, thus after exocytosis, vesicles must be recycled and prepared for the subsequent round of release. Therefore, vesicle recycling is vital to refill the pre-synaptic SV pools, sustaining transmitter release during continuous stimulation, and maintaining presynaptic morphological and structural integrity. In response to the dynamics of vesicle reutilisation, it has been argued that exocytosis can occur by at least two different mechanisms; full-collapse fusion (FF), and Kiss-and-run (KR) fusion. In FF, the FP quickly dilates/expands, which leads to complete flattening of the vesicle into the planar surface of the target membrane and which may lead to the lipid and protein contents of the vesicle mixing with that of the PM. In KR, the vesicle releases its neurotransmitters through a narrow fusion pore, whilst maintaining its morphological shape (Alabi and Tsien, 2013) and subsequently the pore recloses and vesicle regains its integrity.

These two fusion modes are distinctive to each other, especially in the way transmitter is exocytosed and the details of subsequent retrieval and reuse. Heuser and Reese have established a role for FF and clathrin-mediated endocytosis (CME) in vesicle cycling. In small terminals of CNS neurons, FF leaves vesicle components on the plasma membrane for ~15 sec on average before the membrane and protein are retrieved by CME at perisynaptic zone (Heuser and Reese, 1973, 1989).

The biggest distinction of KR from FF is a rapid endocytic kinetics and the small size of the fusion pore formed during exocytosis. The recycling process after FF requires proteins such as clathrin and Dyn. Clathrin is a triskelion shaped scaffold protein, which through collaboration with adaptor proteins, invaginates the membrane containing vesicular components into clathrin-coated pits. These coated pits present on the PM for short duration, 1-2 sec, forming a narrow neck made out of lipids and/or proteins. This neck subsequently has to be detached from the membrane and the following role is performed

by Dyn (Rizzoli and Jahn, 2007). Dyn is a 100-KDa lipid-binding GTPase. It helps to pinch off the coated pit from the PM by oligomerising around the neck of clathrin pits in spirals. Dyn is a mechanoenzyme and during guanosine triphosphate (GTP) hydrolysis, its structural conformation changes, and this produces tension on the vesicle neck, consequently, destabilise the structure and this eventually leads to scission of the neck and consequently release of the coated vesicles (Hinshaw and Schmid, 1995; Sweitzer and Hinshaw, 1998; Hinshaw, 2000; Anantharam *et al*, 2011). If the coated vesicles has been formed from the SV content then as this vesicles moves away from the PM, clathrin and other scaffold proteins dissociate and the vesicle re-acidifies so it can subsequently refilled with NT. Clearly, Dyn has an important role in exocytosis and the regulation of the FP. However, it has been suggested that under specific stimulation conditions the regulation of the FP during KR can also be regulated through Dyn (Graham *et al*, 2002).

Along with Dyn, several other proteins are suggested to play a role in the regulation of the exocytotic mode including NM-II (Chan *et al*, 2010; Papadopulos, 2017). Myosin is a motor protein that has been reported to be involved in controlling the availability of secretory granules. In the chromaffin cells, Myosin V and several members of NM-II gene family are expressed. Myosin V is known to be involved in the mobilisation of chromaffin granules from interior space of the cell to the periphery site, and following the arrival of a stimulus, it dissociates from the granules. NM-II motor function can be regulated by the phosphorylation of the regulatory light chain subunits. With the Ca^{2+} entry, MLCK is activated and this kinase phosphorylate NM-II to regulate its motor function, this is therefore a calcium dependent function (Chan *et al*, 2010). In the study on chromaffin cells from Neco *et al* (2002), Myosin was found to actively transport chromaffin granules into the sub-plasmalemmal area in the early stage of the exocytosis. It was established in this study that NM-II is pre-dominantly abundant in the cell periphery and, it was therefore, concluded that such a subtype may be contribute to the early events of exocytosis (Neco *et al*, 2002). In a subsequent study, this group further reported that NM-II may also be

involved in a later phase of exocytosis by regulating the kinetics of exocytotic pore expansion (Neco *et al*, 2004). Later, they suggested that NM-II works as a molecular motor on the FP expansion whose dilation is hindered when phosphorylation sites on NM-II are perturbed (Neco *et al*, 2008).

Doreian *et al* (2008) have claimed that under low stimulation conditions, actin regulates the KR mode of release, and that following an increase in stimulation, the actin cortex gets disrupted and this leads to a switch of the mode to FF. Importantly, they discovered that NM-II activation is involved in the cytoskeleton-dependent regulation of the fusion mode as perturbation of NM-II led to continuous KR mode even under elevated stimulation (Doreian *et al*, 2008). Pharmacological disruption of the F-actin- NM-II network with Blebbistatin (inhibits NM-II ATPase activity) and JASP (stabilises actin microfilaments) has led to a slower single vesicle fusion kinetics and increased the distance between vesicles and the fusion site. This suggest that such interaction may have a key role in localisation of the SVs at AZ in nerve terminals and also may regulate the speed of the fusion events occurring (Vilanueva *et al*, 2012).

We have discussed these proteins in some detail because the experiments in this chapter investigate the contribution of some of these molecules in the regulation of the mode of exocytosis.

5.2 The effect of the Dyn inhibitor MITMAB on the mode of release

Dyn is known to regulate the KR mode of SV exocytosis. Dynasore is a drug used to block GTPase activity of Dyn and pharmacologically inhibits its action. It has been previously found that Dynasore treatment has led to the switch of mode from KR to FF for the RRP of SVs under certain stimulation conditions (Bhuva, 2015, Singh, 2017; see appendix 1 Fig A7). This clearly tells us that Dyn does indeed have a role in one type of KR release. However, it is unknown whether Dyns that are already present on membranes regulate the KR mode of exocytosis or whether Dyn has to translocate to the membrane during

exocytosis and only then regulate the exocytotic mode. This can be tested by using the drug MITMAB. MITMAB prevents Dyn translocating from the cytosol to membranes, i.e. it stops Dyn binding to membrane (i.e. Quan *et al*, 2007; Linares-Clemente *et al*, 2015). This drug prevents Dyn binding to phospholipids in membranes because it perturbs the pleckstrin homology (PH) domain present in Dyn. The use of MITMAB should reveal whether Dyn has to be translocated to membranes to regulate the mode or whether Dyn already on membrane can do this.

5.2.1 MITMAB does not change the HK5C, ION5C, 4AP5C evoked GLU release

Synaptosomes were pre-treated with 30 μ M MITMAB (5 min at 37°C) and subsequently GLU release evoked by three different stimuli (4AP5C, HK5C, ION5C) was measured. It is apparent from the results obtained that MITMAB treatment did not affect the release induced by 4AP5C (Fig 5.1a), HK5C (Fig 5.1b) or ION5C (Fig 5.1c). Note that 4AP5C only evokes release from RRP whilst HK5C and ION5C can trigger the release from both the RRP and RP, thus, these results prove that MITMAB does not change the amount of release from either the RRP or RP.

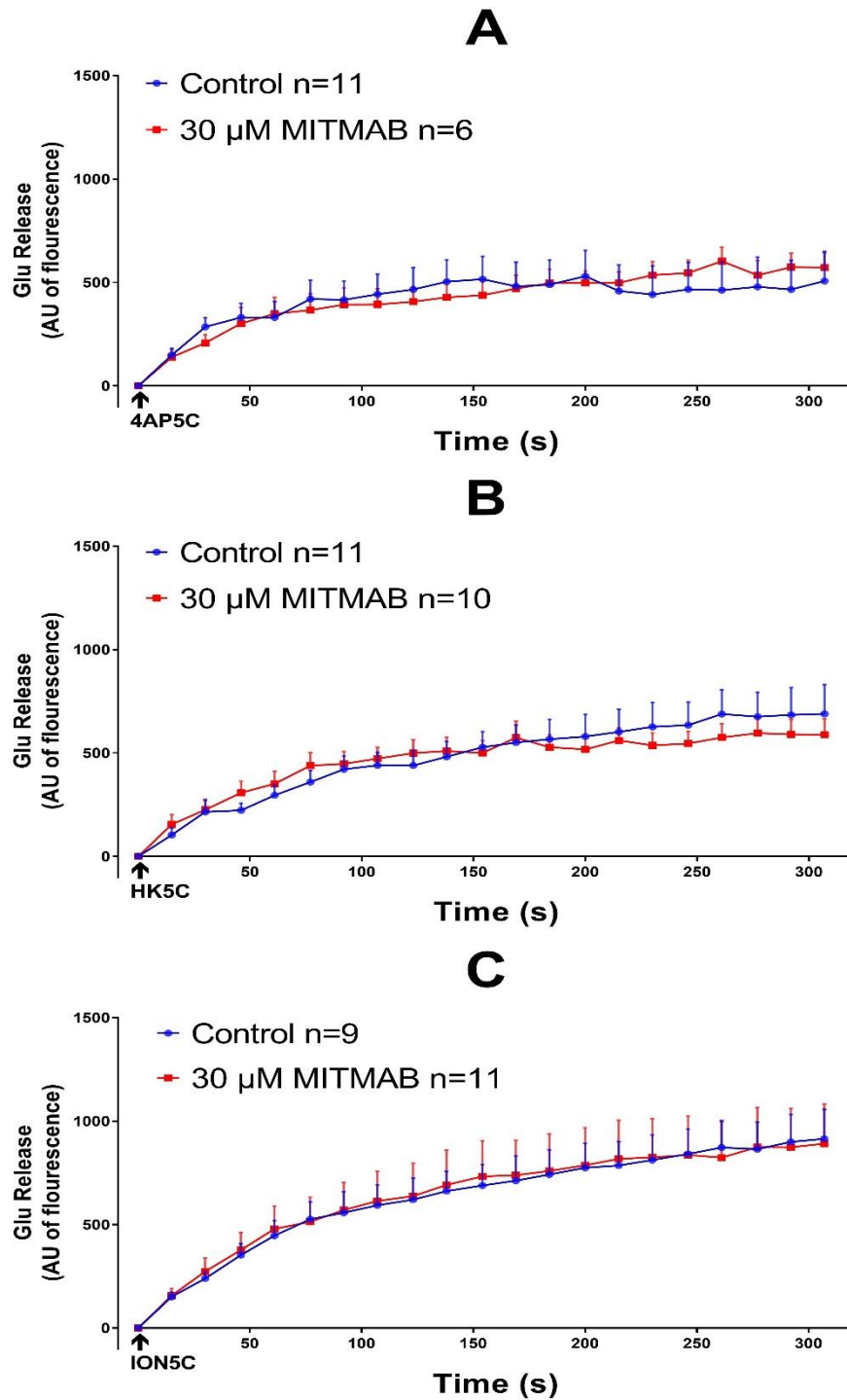


Figure 5.1. MITMAB does not change the amount of release from either the RRP or RP. Evoked GLU release induced by a) 4AP5C b) HK5C c) ION5C in control and 30 μ M MITMAB treated terminals. Data are mean \pm SEM, N=3 independent experiments. Note that there were no significant difference ($P>0.05$) in release amounts between drug treated and non-drug treated terminals for any of the stimuli employed.

5.2.2 MITMAB does not interfere with Dyn dependent KR pathway

MITMAB has been found not to affect the GLU release induced by the three stimuli employed. Therefore, we tested if it has any impact on the mode of the release by using the FM dye release assay. Synaptosomes were loaded with FM 2-10 dye, treated with MITMAB and FM dye release was evoked by HK5C and ION5C. Clearly, MITMAB does not affect the amount of FM dye release evoked by either HK5C (Fig 5.2a) or ION5C (Fig 5.2b) and, therefore, there is no mode switching to FF as there is no extra dye release. This implies that inhibition of Dyn translocation to membranes by MITMAB did not affect the Dyn dependent KR pathway normally activated by ION5C (appendix 1 Fig A5), which means that Dyn already present on membrane must regulate the KR mechanism. As HK5C works on the NM-II dependent KR pathway (appendix 1 Fig A5, A8, A9) one might have expected MITMAB not to have an affect but it was an important control experiment to perform.

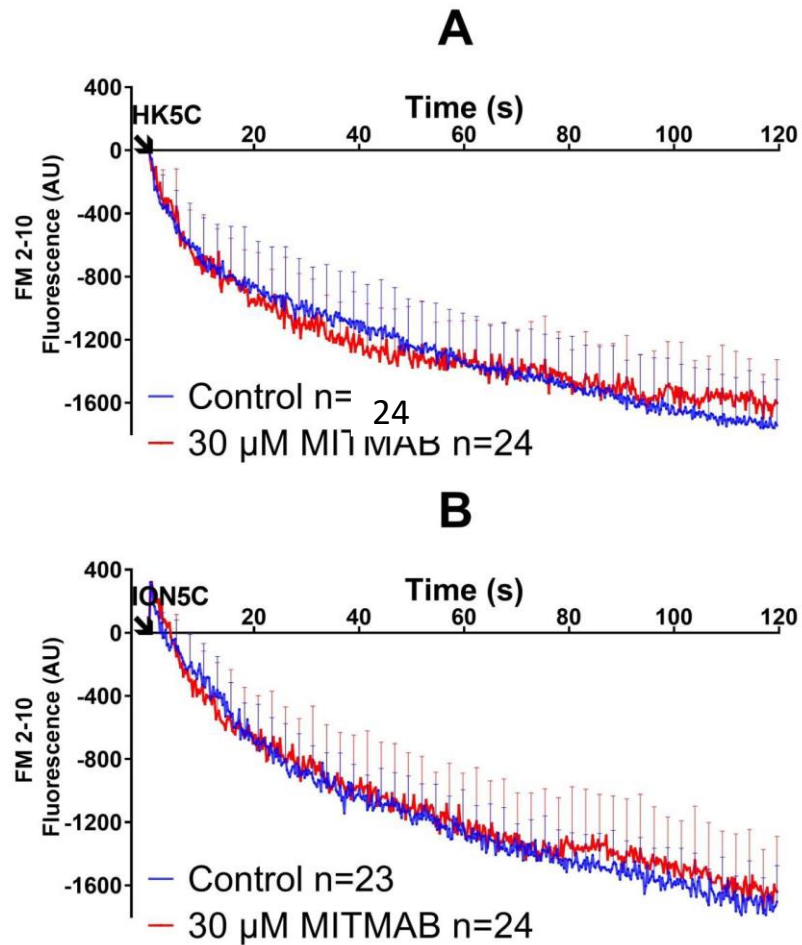


Figure 5.2. No mode switching to FF has been found following MITMAB treatment in either stimuli employed. FM 2-10 dye release evoked by a) HK5C b) ION5C in the presence or absence of 30 μ M MITMAB. Data are mean \pm SEM, N=4 independent experiments. Note that there were no significant difference ($P>0.05$) between control and MITMAB treated condition for both HK5C and ION5C evoked release.

5.2.3 MITMAB does not perturb calcium entry evoked by HK5C or ION5C

Changes in intracellular calcium level ($[Ca^{2+}]_i$) were measured to make sure calcium entry induced by the stimuli has not been changed by the drug treatment. Synaptosomes were pre-treated with MITMAB and stimulated with HK5C (Fig 5.3) and ION5C (Fig 5.4) evoked $\Delta[Ca^{2+}]_i$ measured. Clearly, calcium entry induced by either stimuli was not

affected by the drug treatment, as the $\Delta[\text{Ca}^{2+}]_i$ was similar in control and drug treated terminals. From such results we can conclude that MITMAB does not stop the Dyn dependent KR release, and does not interfere with the Dyn mediated KR mode.

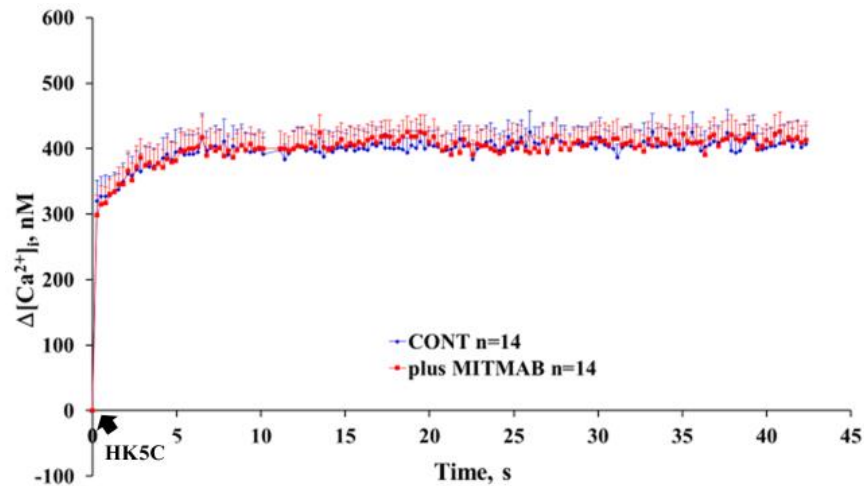


Figure 5.3. HK5C evoked $\Delta[\text{Ca}^{2+}]_i$ was not changed with MITMAB treatment. $\Delta[\text{Ca}^{2+}]_i$ induce by HK5C in control and 30 μM MITMAB treated terminals. Data are mean \pm SEM, N=3 independent experiments; There is no significant difference ($P>0.05$) for the data points for the 2 conditions.

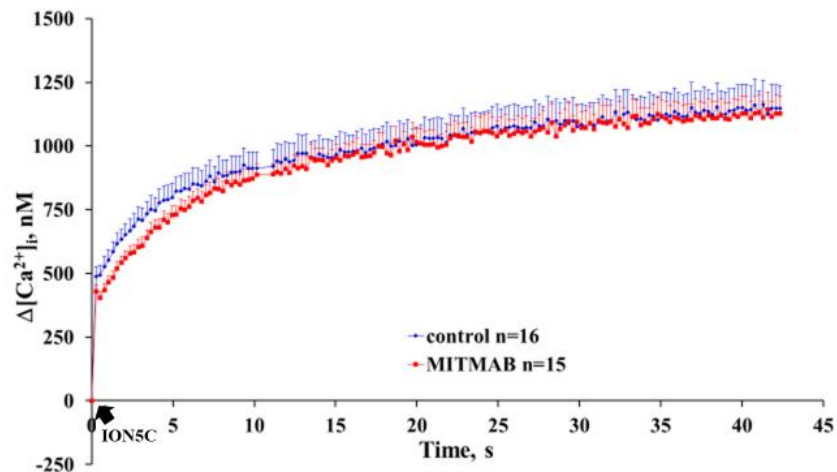


Figure 5.4. ION5C evoked $\Delta[\text{Ca}^{2+}]_i$ was not changed with MITMAB treatment. $\Delta[\text{Ca}^{2+}]_i$ induced by ION5C in control and 30 μM MITMAB treated terminals. Data are mean \pm SEM, N=3 independent experiments; There is no significant difference ($P>0.05$) between drug-free and drug-treated terminals.

5.3 Inhibition of endogenous PKA perturbs the Dyn dependent KR mechanism for the RRP SVs but not the NM-II dependent KR pathway

Dyn I has a key role in regulation of a KR mode of exocytosis. However, an exact mechanism of this regulation is not understood. SV endocytosis can be regulated by a set of proteins that collectively are termed dephosphins. The dephosphins are phosphorylated in nerve terminals, whilst they are dephosphorylated during endocytosis, and their subsequent rephosphorylation after endocytosis is vital for regulation of SV recycling and thus synaptic transmission. Dyn I is one of these dephosphins and during endocytosis, it is dephosphorylated by calcineurin and subsequently gets re-phosphorylated at certain serine residues (Robinson, 1991; Robinson *et al*, 1994; Simillie and Cousin, 2005; Graham *et al*, 2007). Thus, it is important to investigate the role of phosphorylation of Dyn in regards to the contribution of this protein to the KR mode of release.

Originally, PKC was shown to be a major kinase phosphorylating Dyn (Robinson, 1991, 1992, Powell *et al*, 2000) and Ashton's group has recently highlighted some evidence for PKC dependent Dyn I phosphorylation regulating the mode of release, although, such data also indicated other kinases maybe involved (Bhuva, 2015; Singh, 2017). Protein kinase A (PKA) could be one such kinase that could regulate the Dyn activity. PKA is activated following rise of cytosolic cyclic-AMP (cAMP) levels, it is present in nerve terminals, and it phosphorylates serine and threonine residues of target proteins. Thus, it could potentially regulate the mode of exocytosis by the phosphorylation of Dyn I at specific sites (Nguyen and Woo, 2003; Seino and Shibasaki, 2005; Park *et al*, 2014). Herein, we investigated the PKA dependency of the KR mode.

5.3.1 PKA inhibition with KT5720 does not affect GLU release evoked by 4AP5C, HK5C or ION5C.

Before studying the mode of exocytosis, one needed to establish whether PKA inhibition could affect the GLU release itself. Synaptosomes were treated with the PKA inhibitor, KT5720 (Murray, 2008), and GLU released with various stimuli (4AP5C, HK5C, and ION5C) was subsequently measured. 2 μ M KT5720 failed to modify the amount of GLU release evoked by 4AP5C (Fig 5.5a), HK5C (Fig 5.5b) or ION5C (Fig 5.5c).

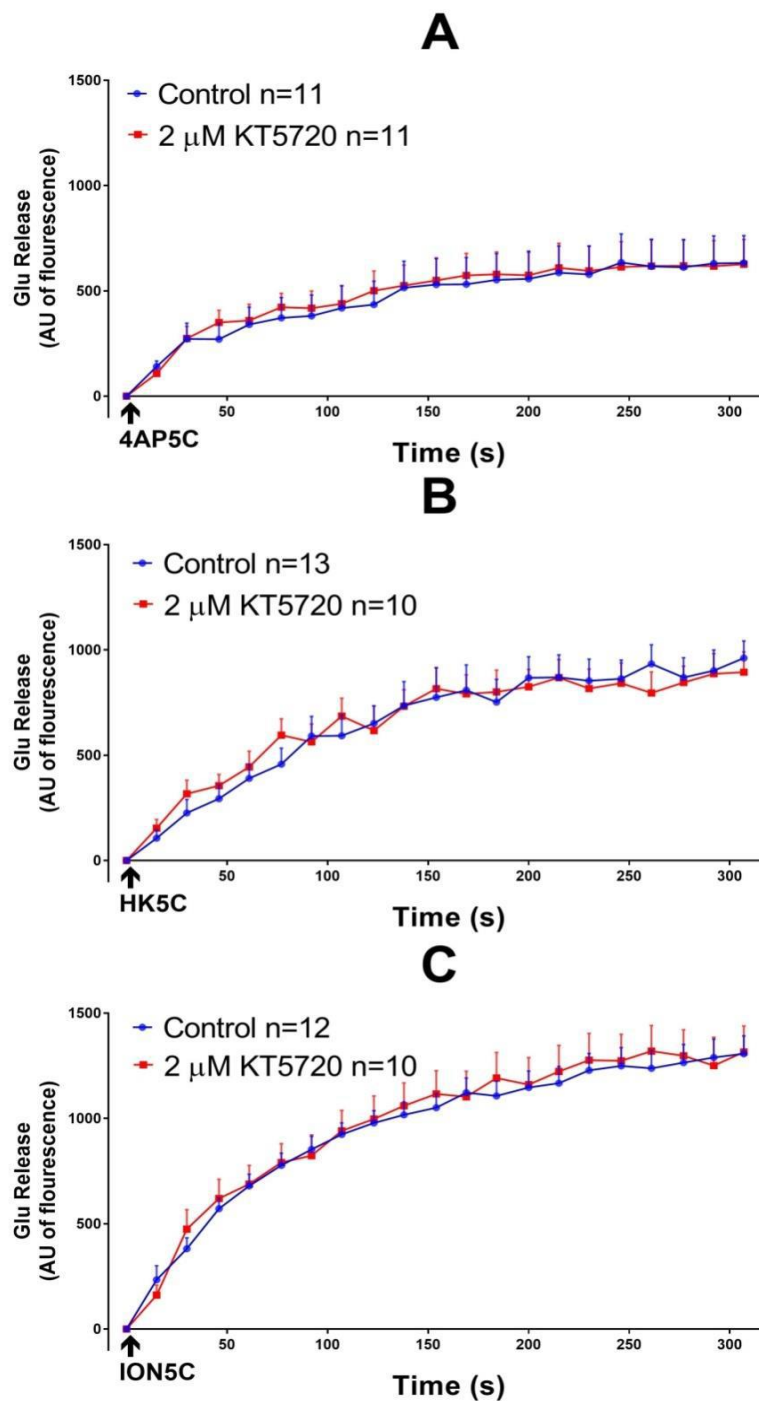


Figure 5.5. PKA inhibition does not affect GLU release evoked by either stimuli employed. GLU release evoked by a) 4AP5C b) HK5C c) ION5C in control and 2 μ M KT5720 treated terminals. Data are mean \pm SEM, N=3 independent experiments. However, there was no significant difference ($P>0.05$) between the control and drug treated terminals for any stimuli employed.

5.3.2 KT5720 treatment switches 4AP5C and ION5C induced release to FF but HK5C induced mode of the release remains unchanged

FM dye release experiments were performed for all three stimuli following PKA inhibition with KT5720. Intriguingly, for 4AP5C (Fig 5.6a) and ION5C (Fig 5.6b) there is an increase in FM dye release and this indicates that the RRP SVs have been fully switched to a FF mode. However, for HK5C (Fig 5.6c) stimulation, there was no extra release and the FM dye release was similar to the non-drug treated control, indicating that the drug treatment has not switched the RRP mode. From previous work, it is known that 4AP5C and ION5C evoke KR release through a Dyn-dependent pathway, whilst HK5C acts through a NM-II dependent pathway (Bhuva, 2015; Singh, 2017; see appendix 1). Therefore, these results might suggest that PKA inhibition with KT5720 switches the Dyn dependent KR mode to FF but it does not affect the NM-II dependent KR mode.

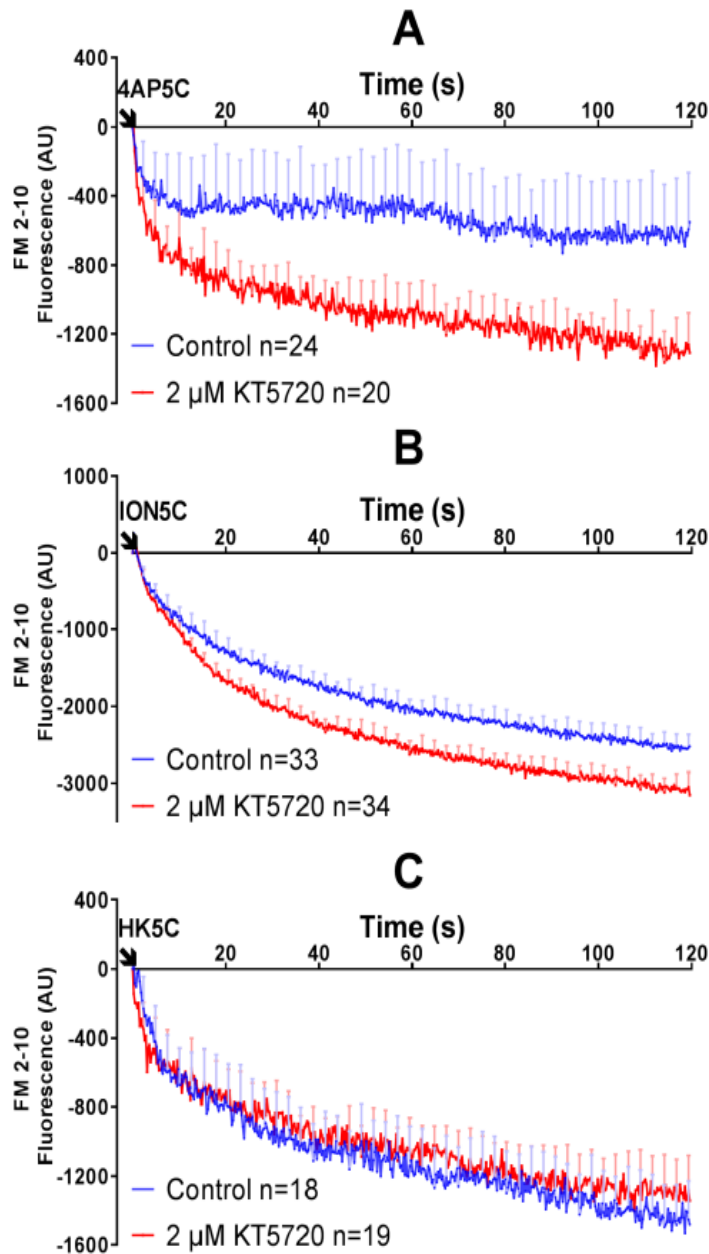


Figure 5.6. PKA inhibition switches 4AP5C and ION5C induced release to FF but HK5C induced mode of release was unchanged. FM dye release evoked by a) 4AP5C b) ION5C c) HK5C in the presence or absence of 2 μ M KT5720. Data are mean \pm SEM, N=4 (a, c) and 5 (b) independent experiments. There was a significant difference ($P < 0.05$) between control and KT5720 treated conditions for 4AP5C and ION5C evoked release but there was no significant difference ($P > 0.05$) for HK5C evoked release (Note that significance measured for representative time points throughout time course i.e. every 10 sec).

In fact, similar results were previously obtained after synaptosomes were treated with Dynasore, which inhibits the GTPase activity of Dyn. In this case, the Dyn dependent KR was switched to a FF mode (such results are shown in Fig 5.7 so one can compare to Fig 5.5 and Fig 5.6). Whilst, Dynasore treatment did not affect the GLU release for all stimuli (Fig 5.7 a-c), it was apparent that 4AP5C (Fig 5.7 d) and ION5C (Fig 5.7 e) evoked FM dye amount increased due to a release were switch to FF of the RRP whilst HK5C (Fig 5.7 f) evoked dye release remain unchanged. Results from KT5720 experiments, in combination with these Dynasore results, demonstrate that the PKA inhibition perturbs the distinct KR mode depending on which stimulus has been employed. One can hypothesise that the inhibition of endogenous PKA leads to a switch of the Dyn dependent KR to FF, but this has no effect on the NM-II dependent KR mode induced by HK5C.

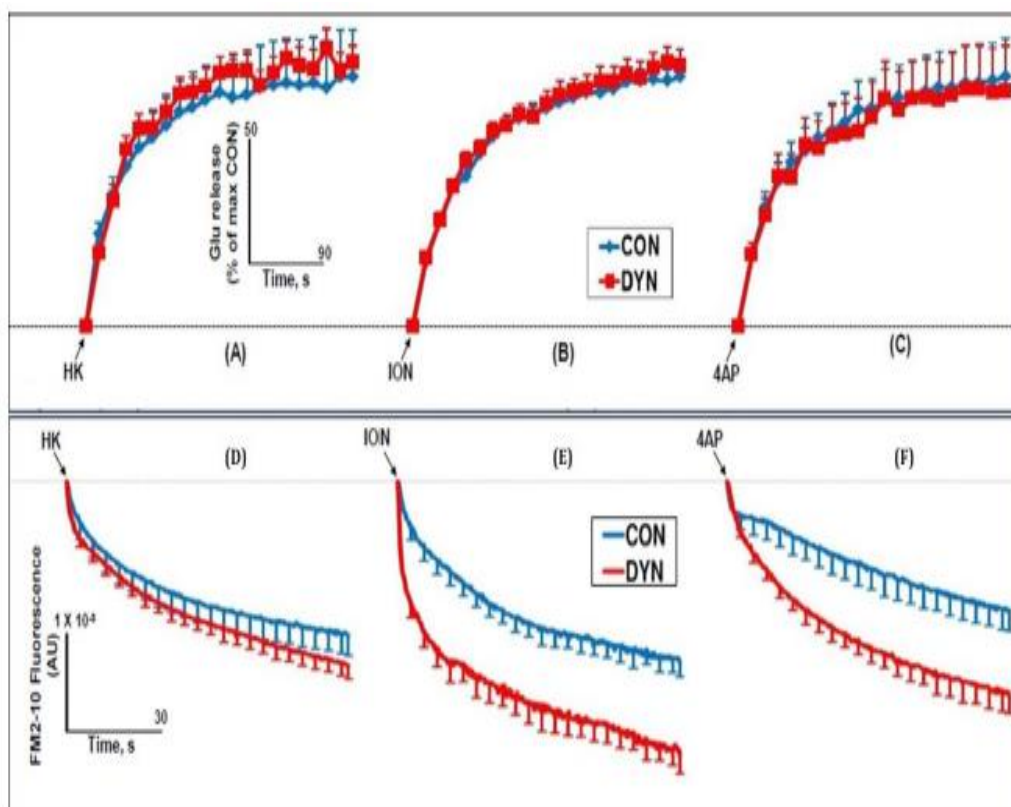


Figure 5.7. GLU and FM dye results when Dyn is inhibited produce similar result to when PKA is inhibited. GLU release evoked by a) HK5C b) ION5C c) 4AP5C and FM dye release evoked by d) HK5C e) ION5C f) 4AP5C evoked FM dye release in the control or 160 μ M Dynasore treated terminals. Data are mean \pm SEM of numerous experiments. Note for GLU release there was no significant difference ($P > 0.05$) between control and Dynasore treated conditions on for any stimulus. For FM-dye assay, HK5C evoked release was unchanged but ION5C and 4AP5C evoked release were significantly changed compared to controls. Note this figure was supplied by A.Ashton and was included so one can compare to the previous 2 figures. It is actually the same figure as A7 that in appendix 1. However, it was included here for easier comparison.

5.4 Conditions under which HK5C evokes Dyn dependent KR of the RRP depends upon active endogenous PKA

The hypothesis is that the inhibition of endogenous PKA leads to a switch of the Dyn dependent KR to FF, thus, HK5C action on NM-II KR is not perturbed. This can be further verified if HK5C is switched so that it acts on the Dyn dependent pathway instead of the NM-II dependent pathway. Fortunately, we can switch the action of HK5C as it was previously observed that PKC inhibition with Go6983 changed the pathway HK5C work through to induce a release, such that HK5C is now working through Dyn dependent pathway instead of NM-II dependent pathway (Bhuva, 2015; Singh, 2017; see appendix 1 Fig A 11 and A12).

5.4.1 KT5720 had no effect on HK5C evoked GLU release in Go6983 treated synaptosomes

Synaptosomes were pre-treated with Go6983 and KT5720 and subsequently HK5C evoked GLU release was measured. The GLU release was not perturbed under this dual drug treatment as the levels of release were virtually the same as for the non-drug treated condition (Fig 5.8).

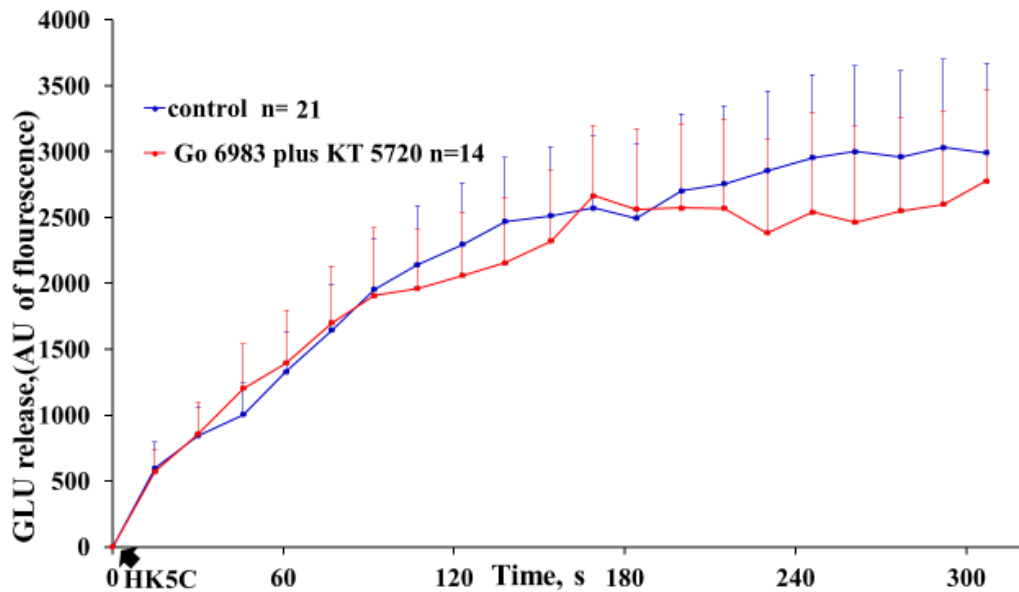


Figure 5.8. KT5720 had no effect on HK5C evoked GLU release in Go6983 treated synaptosomes. HK5C evoked GLU release from control and 1 μ M Go6983 plus 2 μ M KT5720 treated terminals. Data are mean \pm SEM, N=4 independent experiments; P <0.05 is used as a sign of significant difference. However, there was no significant difference of release between control and Go6983 plus KT5720 treated terminals.

5.4.2 HK5C evoked FM dye release switch to FF in terminals co-treated with Go 6983 and KT5720

It was previously hypothesised that HK5C evoked KR release is unchanged because PKA inhibition only affects Dyn dependent pathway. Go6983 treatment causes HK5C stimulation to stop operating through NM-II dependent pathway and switch to Dyn dependent pathway for the KR of the RRP. Indeed, it was found that pre-treatment with Go6983 and KT5720 has led to an increase in HK5C evoked FM dye release demonstrating a change of the RRP SVs releasing mode from KR to FF (Fig 5.9). Such results confirm the suggestion that PKA only affects the Dyn dependent KR pathway since HK5C working through the Dyn dependent pathway is also switched to FF just like for

ION5C and 4AP5C; this also indicates that FM results were not limited to a particular action of a specific stimulus.

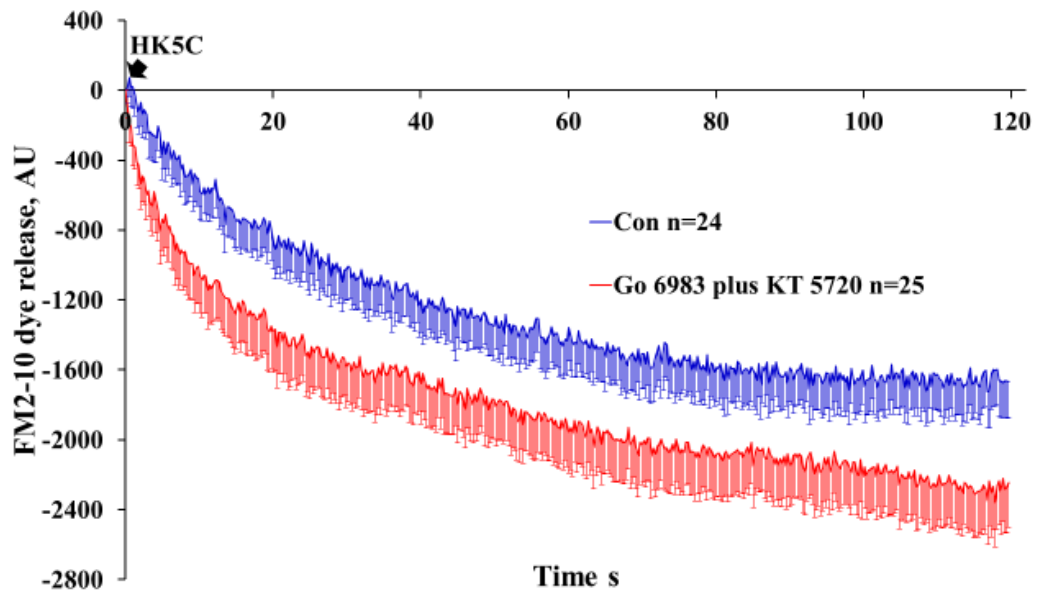


Figure 5.9. Dual treatment of synaptosomes with Go6983 and KT5720 switches HK5C evoked FM dye release to FF. HK5C evoked FM dye release in the presence of 1 μ M Go6983 plus 2 μ M KT5720 compared to non-drug treated control. Data are mean \pm SEM, N=4 independent experiments; Note that there were significant difference of release between control and double drug treated conditions ($P<0.05$).

5.5 The effect of Calcium channel blockers on NM-II and Dyn dependent regulation of RRP SV mode

Specific calcium channel dependencies of the release mode is an important area to address. A.Ashton's group has previously observed that at least one KR mode of exocytosis is dependent on L-type calcium channel. Various voltage dependent calcium channels were blocked by pre-incubating synaptosomes; 1 μ M NIF blocked L-type channels; 1 μ M CONO blocked N-type channels; 50 nM AGA blocked P/Q-type channels. In these preliminary observations it was found that HK5C evoked $[Ca^{2+}]_i$ decreased after blocking

all of these types of calcium channel (AGA, CONO, NIF) (Fig 5.10 a-c). However, no calcium channel inhibitors have actually perturbed HK5C evoked GLU release (Fig 5.10 d-f); this indicates that despite a reduction in HK5C evoked $\Delta[Ca^{2+}]_i$ there was still sufficient Ca^{2+} entering to enable the RRP and RP SVs to exocytose. However, for HK5C evoked FM 2-10 dye release there was only extra FM dye release – because the KR mode of the RRP has switched to FF - for L-type calcium channel blockade (Fig 5.10 i), whilst P/Q-type (Fig 5.10 g) and N-type (Fig. 5.10 h) channel inhibition did not perturb the KR mode evoked by HK5C. Overall, it was initially concluded that the KR of the RRP is predominantly regulated through L-type calcium channels. However, it has now been realised that this result actually applies to the NM-II dependent KR pathway as it utilises HK5C which works through this pathway. ION5C acts through the Dyn dependent pathway, but as ION5C is an ionophore that bypasses the calcium channel requirement, one could not utilise this stimulus to investigate the Dyn dependent pathway. However, it is possible to investigate Dyn dependent pathway using HK5C under conditions in which it works via this pathway by inhibiting PKC (see above). PKC inhibition with Go6983 changes the HK5C evoked KR from the NM-II dependent KR pathway to the Dyn dependent KR pathway.

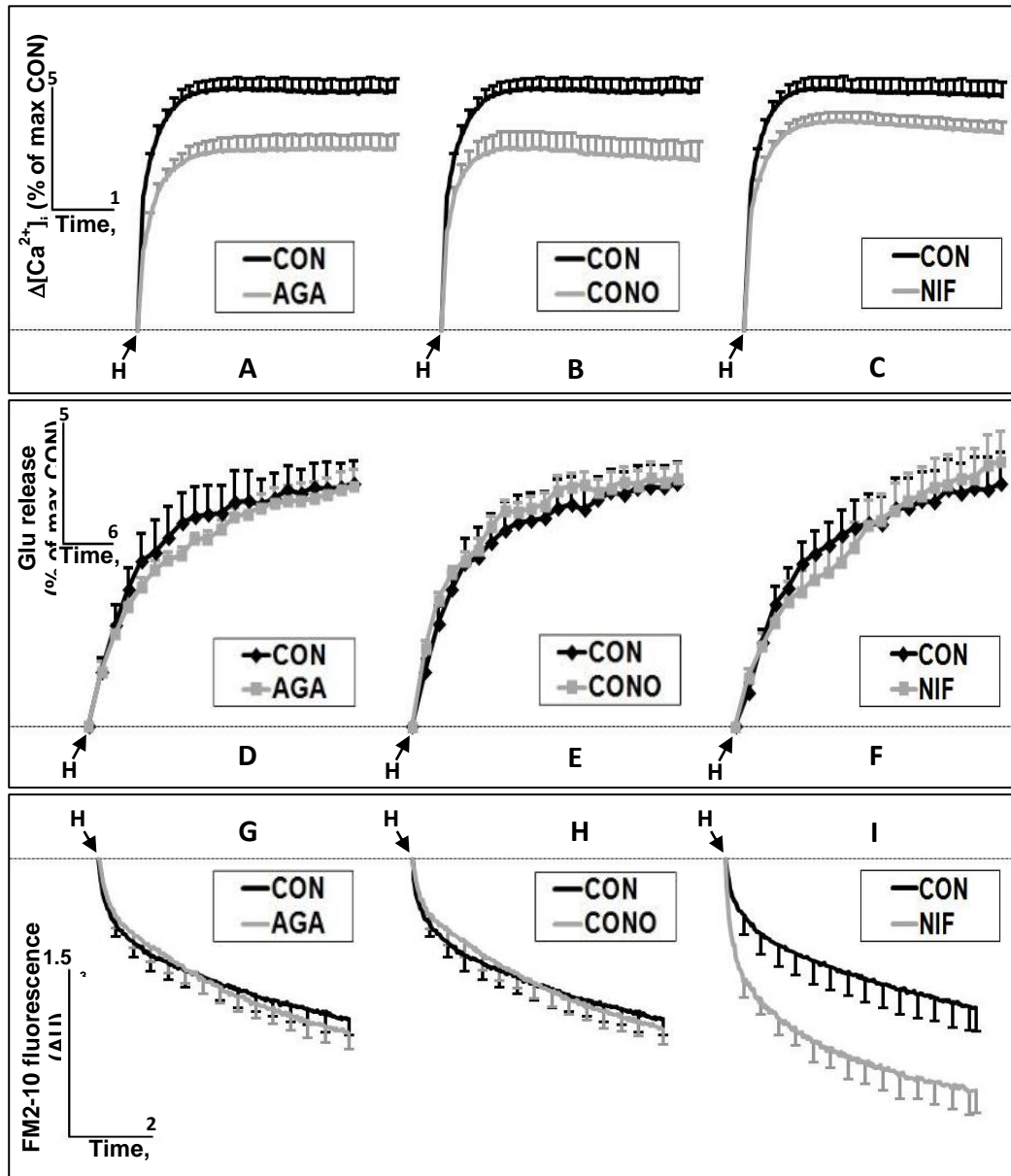


Figure 5.10. L-type Ca^{2+} channel regulates NM-II dependent KR pathway. HK5C evoked changes in a-c) $\Delta[\text{Ca}^{2+}]_i$; d-f) GLU, and g-i) FM dye in the absence or presence of 50 nM AGA, 1 μM CONO, and 1 μM NIF. Data are mean \pm SEM; $P > 0.05$ for a, b, c, i and $P < 0.05$ for d, e, f, g, h. Note that there was a significant difference between NIF treated condition and control for FM dye release representing the switch of releasing mode from KR to FF following L-type calcium channel inhibition. Note this data was produced by A.Ashton and is included here for comparison with HK5C stimulation in the presence of Go6983. It could have been included in the appendix but it was felt that it was easier to compare this with Fig 5.11, 5.12 and 5.13 if shown in this location.

5.5.1 HK5C evoked $\Delta[\text{Ca}^{2+}]_i$ is reduced by specific calcium channel blockers in Go6983 treated terminals

Inhibition of P/Q-type (Fig 5.11 a), N-type (Fig 5.11 b), or L-type (Fig 5.11 c) calcium channels in Go6983 treated terminals resulted in the reduction of HK5C evoked $\Delta[\text{Ca}^{2+}]_i$ compared to terminals just treated only with Go6983. These data are similar to results shown above (Fig 5.10 a-c), and this suggests that the presence of Go6983 does not change the calcium channel blocker action.

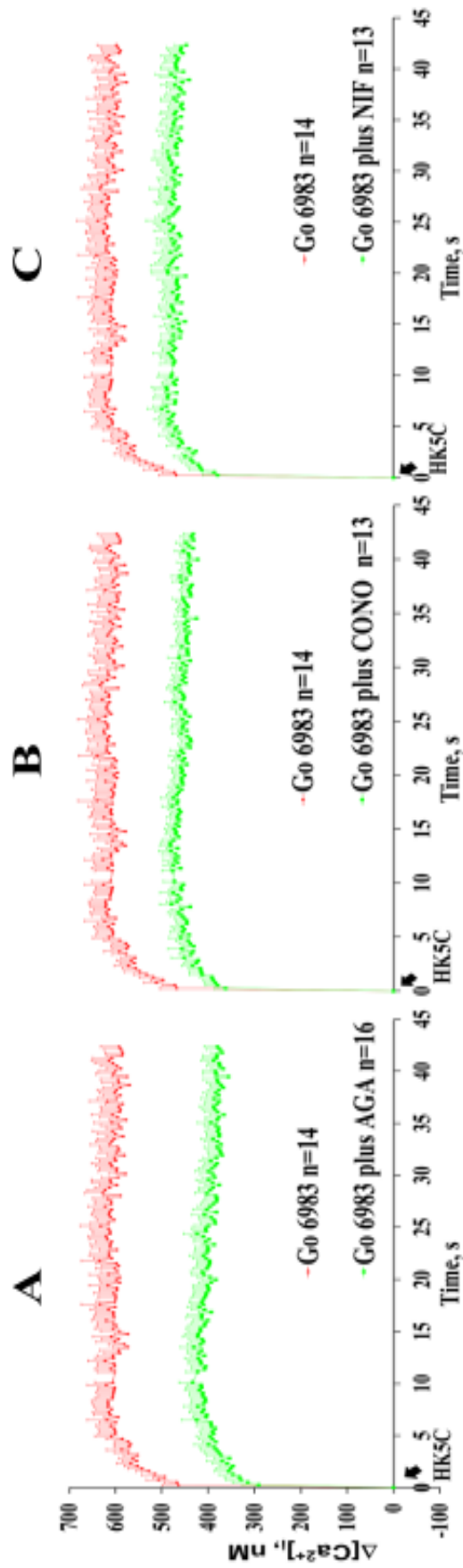


Figure 5.11. HK5C evoked $\Delta[Ca^{2+}]_i$ is reduced by all Ca^{2+} channel blockers in Go6983 treated terminals. HK5C evoked $\Delta[Ca^{2+}]_i$ in terminals treated with 1 μM Go6983 alone or 1 μM Go6983 plus a) 50 nM AGA b) 1 μM CONO c) 1 μM NIF. Data are mean \pm SEM, N=3 independent experiments; Ca^{2+} channel blockers significantly reduced ($P < 0.05$) the HK5C evoked $\Delta[Ca^{2+}]_i$ compared to Go6983 alone condition.

5.5.2 Calcium channel inhibition did not affect the HK5C evoked GLU release in Go6983 treated terminals

P/Q-type calcium channel inhibition with AGA (Fig 5.12 a) in the presence of Go6983 did not perturb the HK5C evoked GLU release as the release amount was similar to that in terminals only treated with Go6983. This was also found when N-type calcium channels were blocked with CONO (Fig 5.12 b) or when L-type calcium channels were blocked with NIF (Fig 5.12 c). These data are similar to that previous found in terminals not treated with Go6983 (Fig 5.10 d-f). Thus the PKC inhibition does not produce variation on the action of blockade of these Ca²⁺ channels on HK5C evoked GLU release.

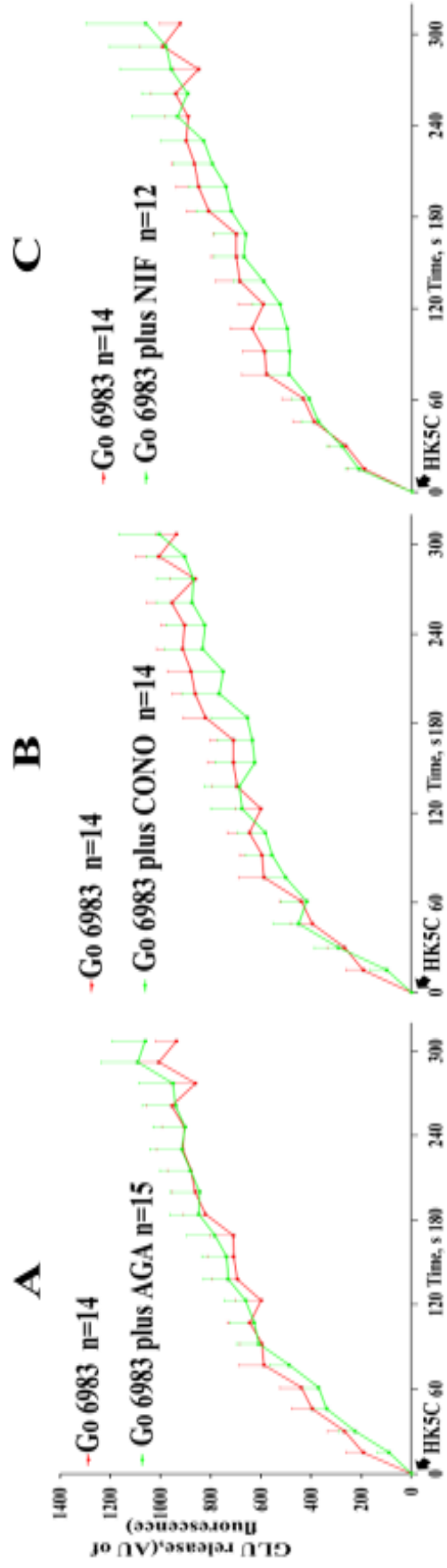


Figure 5.12. Ca²⁺ channel inhibition did not affect the HK5C evoked GLU release in Go6983 treated terminals. HK5C evoked GLU release in 1 μ M Go6983 treated or 1 μ M Go6983 plus a) 50 nM AGA b) 1 μ M CONO c) 1 μ M NIF. Data are mean \pm SEM, N=4 independent experiments; Significance is regarded if this value of P is obtained P <0.05. Note that there was no significant difference of release with or without Ca²⁺ channel blocker.

5.5.3 P/Q type calcium channel inhibition changed Dyn dependent HK5C evoked release from KR mode to FF

HK5C evoked FM dye release was measured in synaptosomes treated with Go6983 and each type of calcium channel blocker. In the presence of AGA with Go6983 (Fig 5.13 a), HK5C evoked FM dye release was significantly increased, whilst inclusion of CONO (Fig 5.13 b) or NIF (Fig 5.13 c) produced virtually the same amounts of release relative to treatment with Go6983 alone (control). These data demonstrate that under Go6983 treatment, when HK5C is now regulating Dyn dependent KR mode, only P/Q-type calcium channel inhibition has led to the changing of the releasing mode from KR to FF. Thus, it would appear that the Dyn dependent KR mode is regulated by P/Q-type calcium channels. Taken together, these results in combination with the data obtained from condition in the absence of Go6983, wherein HK5C is regulating NM-II dependent KR mode, allows one to propose that NM-II dependent KR is regulated through L-type calcium channel whilst P/Q-type calcium channel is mediating Dyn dependent KR mode. This is extremely important as these two distinction between these 2 KR modes may indicate that they are separate KR modes and that Dyn and NM-II are not working to regulate the same pathway.

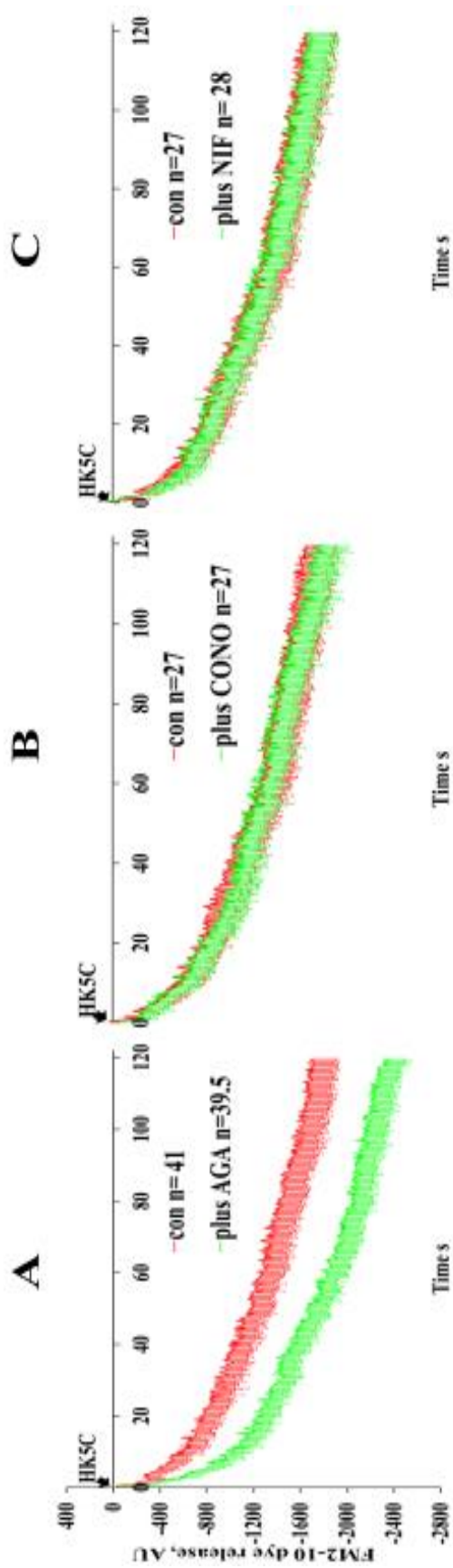


Figure 5.13. P/O-type Ca^{2+} channel inhibition changed Dyn dependent HK5C evoked FM release from KR mode to FF. HK5C evoked FM dye release in

the presence of 1 μ M Go6983 or 1 μ M Go6983 plus a) 50 nM AGA b) 1 μ M CONO c) 1 μ M NIF. Data are mean \pm SEM, N=6 independent experiments for

a; N=4 independent experiments for b and c; Note that there was significant difference ($P < 0.05$) of release between Go6983 and Go6983 plus P/Q-type

calcium channel evoked representing switch of the exocytotic mode from KR to FF, but there was no difference found between conditions in b or c.

5.5.4 Go6983 treatment does not interfere with switching of the RRP mode

HK5C evoked FM dye release was discovered to only increase when L-type calcium channels is inhibited, whilst in the presence of Go6983 only perturbation of P/Q-type calcium channels have produced similar phenomenon. These results can be interpreted as that when HK5C is regulating KR through NM-II dependent pathway, L-type calcium channel is required, but when HK5C is regulating through Dyn dependent pathway, P/Q-type calcium channel is needed. Nevertheless, there is still a possibility that PKC inhibition might interfere with switching of the RRP mode, meaning the result might not represent the calcium channel dependent regulation of the releasing modes.

Luckily, this can be checked using Okadaic acid (OA), a phosphatase inhibitor that has been found to increase the SV mobility in the terminal (i.e. Betz and Henkel, 1994). It was also shown to switch all RRP SVs exocytosis from a KR to a FF mode (Bhuva, 2015; Singh, 2017; see also appendix 1 Fig A5, A6). OA inclusion in Go6983 treated synaptosomes vs Go6983 alone control have revealed that there was an increase in the FM dye release in the presence of OA (Fig 5.14), reflecting that treatment with OA has changed the RRP SV mode to undergo FF. Clearly, Go6983 does not interfere with OA induced FF mode. Furthermore, OA treatment still allows FF of the RRP in Go6983 treated terminals treated with CONO (Fig 5.15), and NIF (Fig 5.16). Lastly, comparison between Go6983 plus OA versus Go6983 plus OA plus AGA (Fig 5.17) shows that OA and AGA work on the same RRP SVs as both treatments induced maximum release of the FM dye, confirming there is no additivity of effect when both treatments are applied and indicating that they work on the same pool.

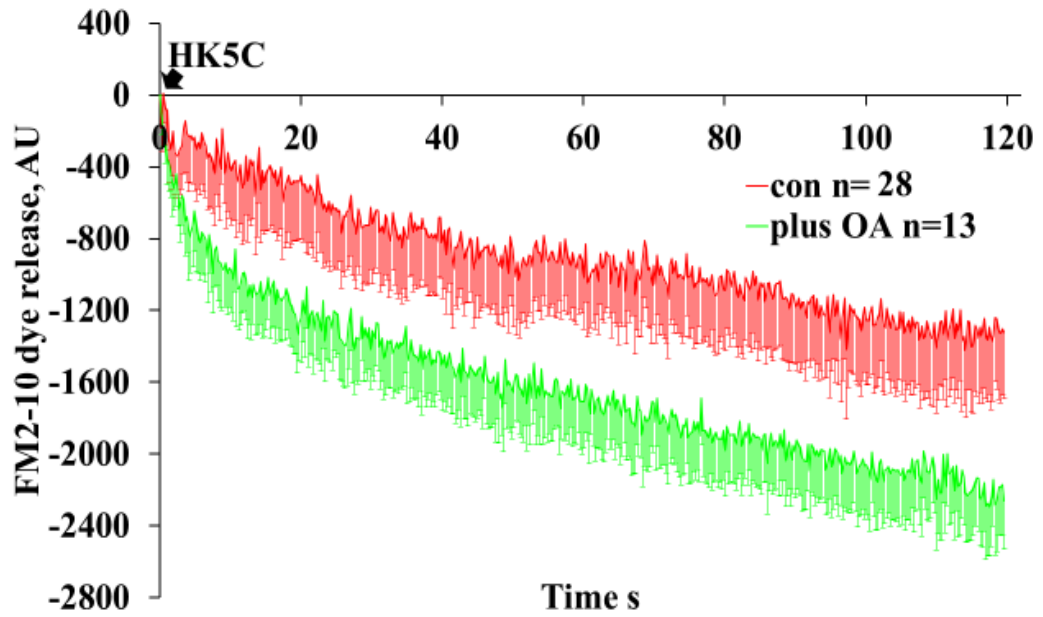


Figure 5.14. OA treatment switches FM dye release mode to FF. HK5C evoked FM dye release in terminals treated with 1 μ M Go6983 (control) or 1 μ M Go6983 plus 0.8 μ M OA. Data are mean \pm SEM, N=3 independent experiments; P<0.05.

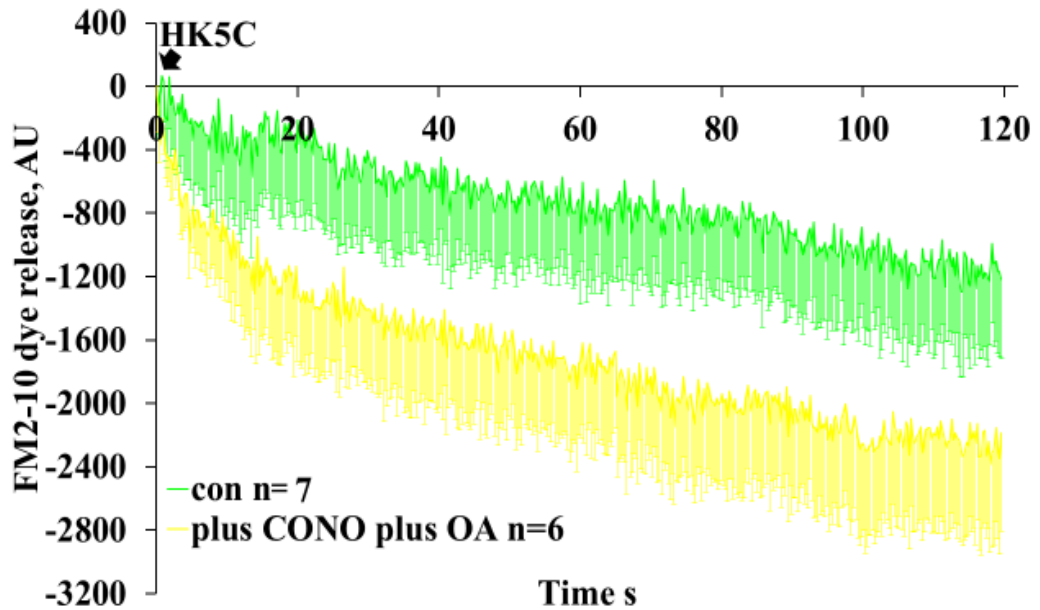


Figure 5.15. The RRP SVs can be switched to FF when OA is included in Go6983 plus CONO treated terminals. HK5C evoked FM dye release in the presence of 1 μ M Go6983 (control) or 1 μ M Go6983 plus 0.8 μ M OA plus 1 μ M CONO. Data are mean \pm SEM, N=1 independent experiments; This is a representative experiment.

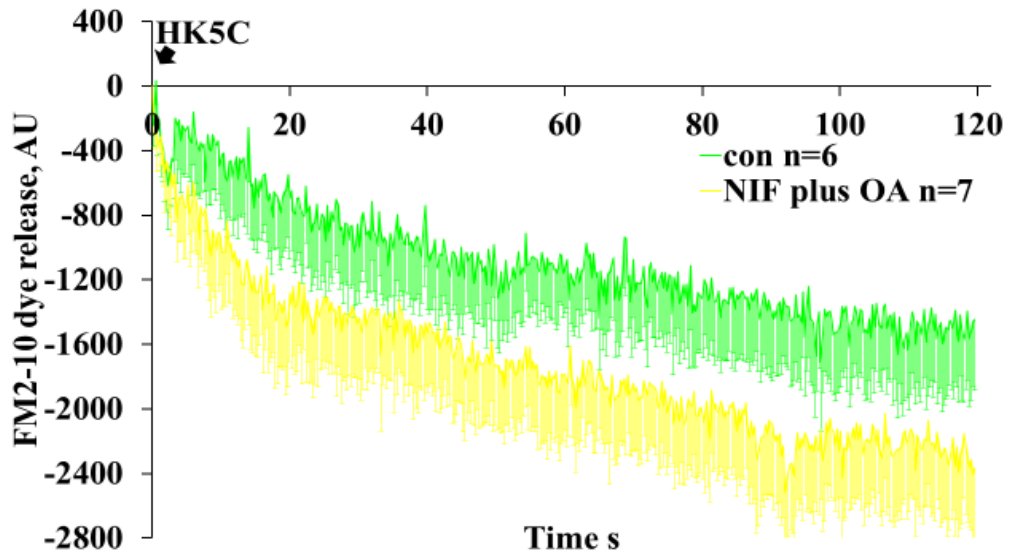


Figure 5.16. The RRP SVs can be switched to FF when OA is included in Go6983 plus NIF treated terminals. HK5C evoked FM dye release in the presence of 1 μM Go6983 (control) or 1 μM Go6983 plus 0.8 μM OA plus 1 μM NIF. Data are mean \pm SEM, N=1 independent experiments; This is a representative experiment.

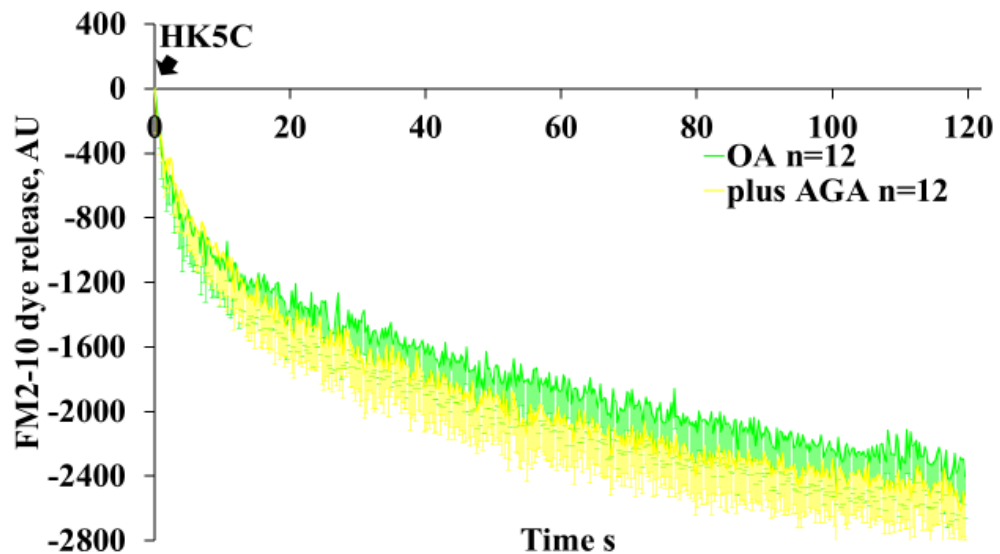


Figure 5.17. Synaptosomes treated with Go6983 plus AGA were already releasing in FF mode. HK5C evoked FM dye release in the presence of 1 μM Go6983 plus 0.8 μM OA or 1 μM Go6983 plus 50 nM AGA. Data are mean \pm SEM, N=2 independent experiments. Note that there is not much difference in the release between OA plus Go6983 condition and Go6983 plus AGA.

5.6 Bioenergetics

Several drugs have been employed in this chapter whilst investigating the properties of the exocytotic mode; MITMAB, KT5720; Go6983; AGA; CONO; NIF; OA. It is important to ascertain that these drugs do not have non-specific off-target effects that may disturb the bioenergetics of the nerve terminals. We carried out an XF Cell Mito stress test using the Seahorse XFp machine on each drug treated condition. Through comparison with non-drug treated condition, such protocols can reveal whether a drug treatment had any impact on the bioenergetics of synaptosomes.

5.6.1 MITMAB

The acute treatment with 30 μM MITMAB for 5 min failed to significantly disturb any of the parameters except from a small effect on non-mitochondrial respiration (Fig 5.18, Fig 5.19 a-f) which has nothing to do with the normal mitochondrial respiratory capacity.

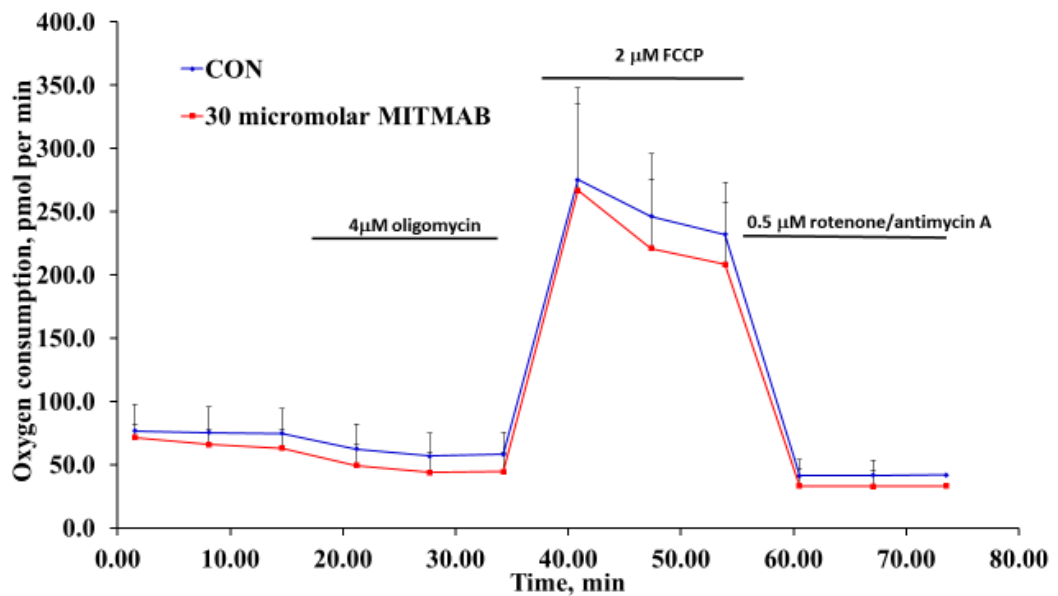


Figure 5.18. Synaptosomal bioenergetics were unaffected by 30 μM MITMAB treatment.

The effect of 30 μM MITMAB on the bioenergetics of synaptosomes. The experiment was done three times and the mean values represent an average of 9 independent measurements and error bars represent the SD; $P > 0.05$.

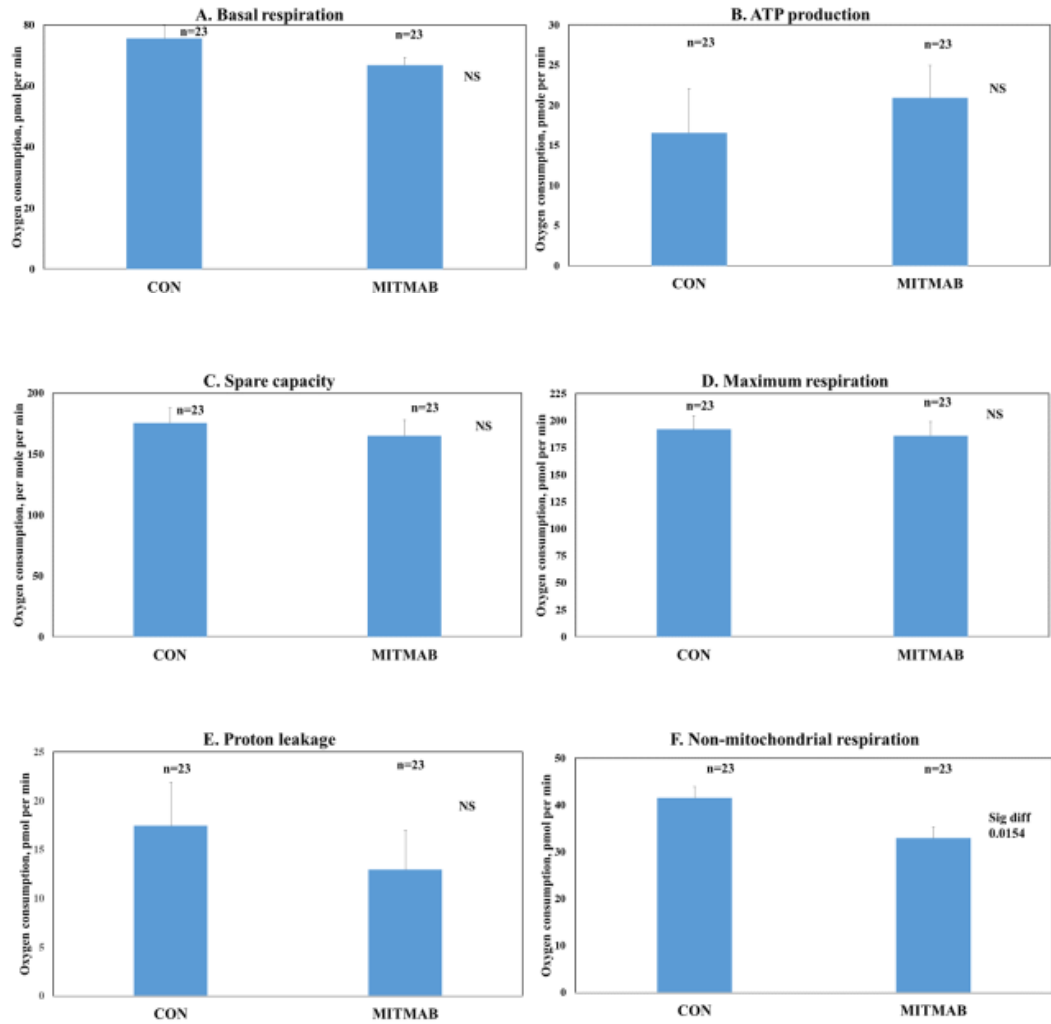


Figure 5.19. 30 μ M MITMAB treatment did not perturb most of bioenergetics parameters measured as it looks similar to those for the controls. The effect of a 5 min pre-incubation with 30 μ M MITMAB on (A) basal respiration, (B) ATP production, (C) spare capacity, (D) maximal respiration, (E) Proton leakage, and (F) Non-mitochondrial respiration in synaptosomes. The histograms represent the mean and the error bar shows the SEM.

5.6.2 KT5720

Treatment with KT5720 had a small effect on basal respiration, however, all other parameters remained at similar level with the non-drug treated condition (Fig 5.20, Fig 5.21 a-f) and as such this drug does not really perturb the nerve terminals.

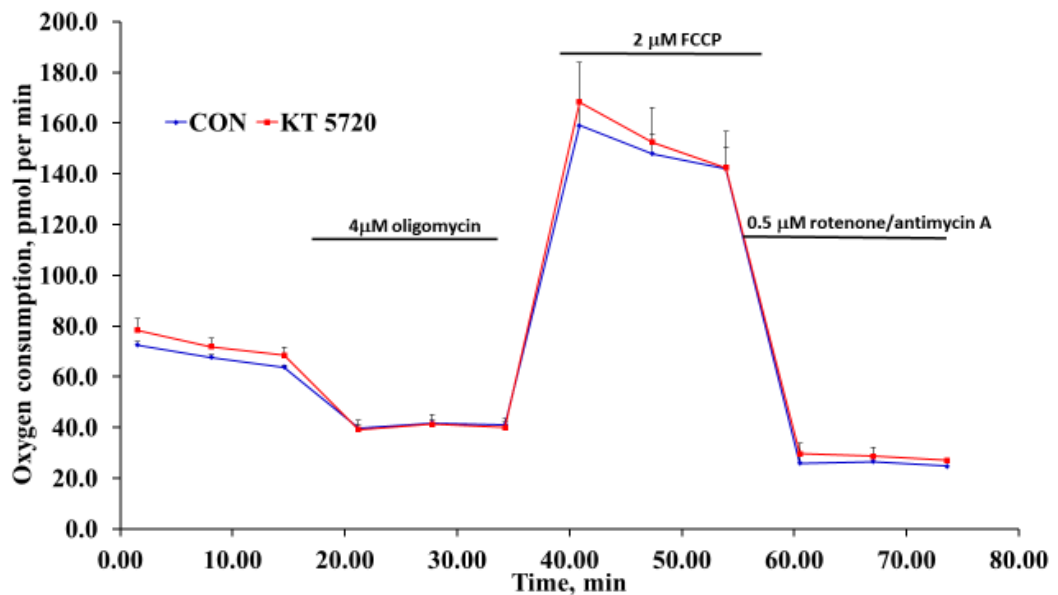


Figure 5.20. Synaptosomal bioenergetics were unaffected by 2 μM KT5720 treatment. The effect of 2 μM KT5720 on the bioenergetics of synaptosomes performed at 37°C. The experiment was done three times and the mean values represent an average of 9 independent measurements and error bars represent the SD; P>0.05.

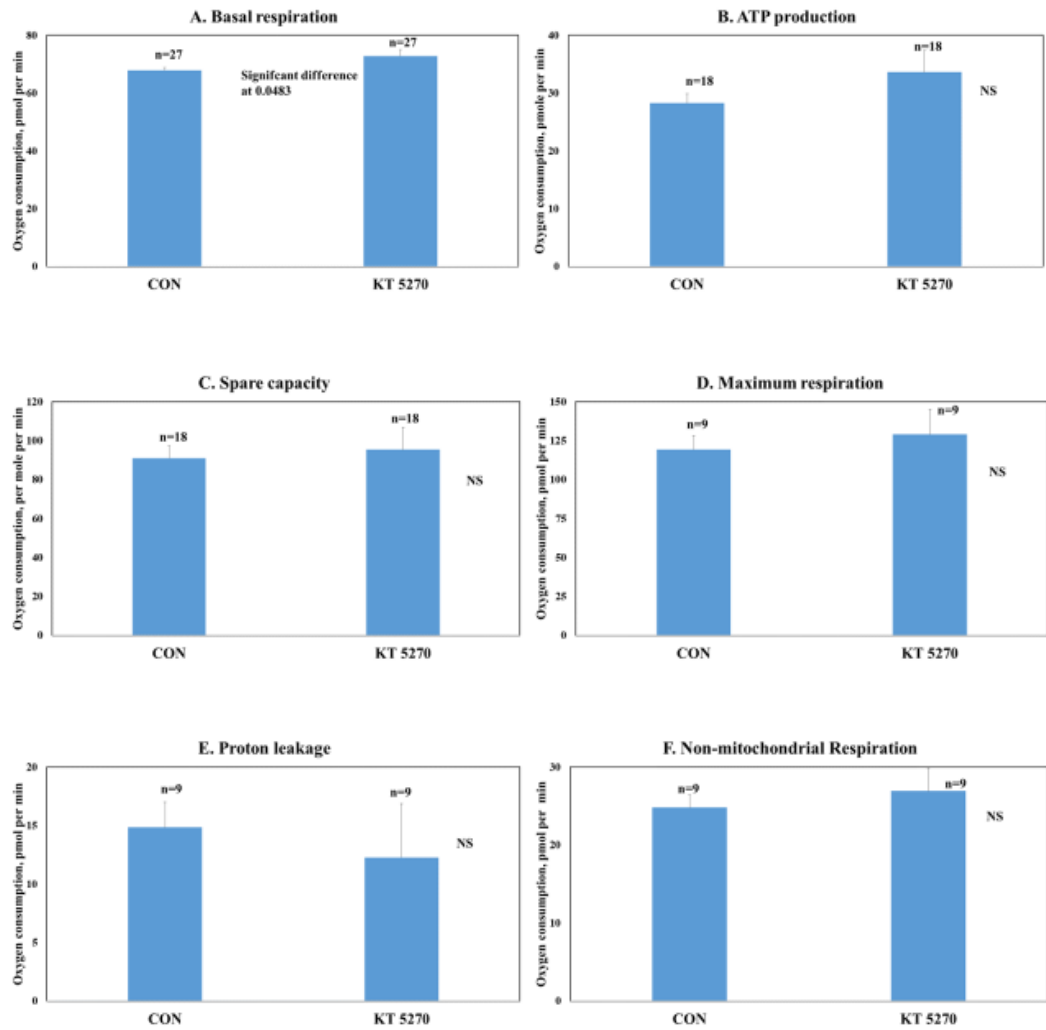


Figure 5.21. 2 μ M KT5720 treatment did not perturb most of bioenergetics parameters measured as it looks similar to those for the controls. The effect of 2 μ M KT5720 on (A) basal respiration, (B) ATP production, (C) spare capacity, (D) maximal respiration, (E) Proton leakage, and (F) Non-mitochondrial respiration in synaptosomes. The histograms represent the mean and the error bar shows the SEM.

5.6.3 Go6983 plus KT5720

Treatment with Go6983 alone has been shown in chapter 3 to have no effect on the bioenergetics (see Fig 3.38 and 3.39). The dual treatment of 1 μM Go6983 with 2 μM KT5720 did not disturb any of the bioenergetics parameters of the synaptosomes (Fig 5.22, Fig 5.23 a-f).

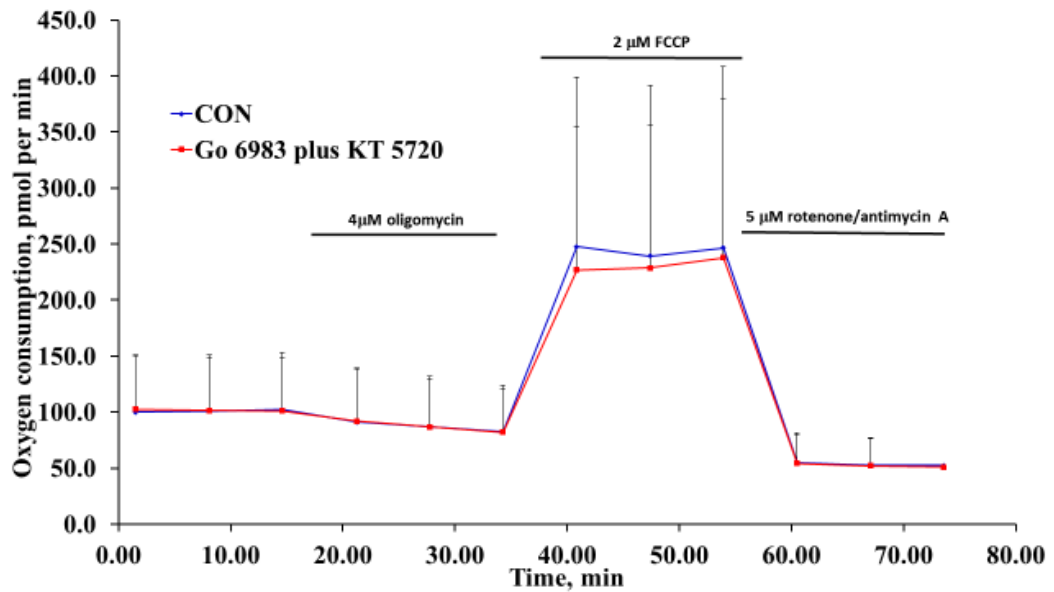


Figure 5.22. Synaptosomal bioenergetics were unaffected by dual treatment of 1 μM Go6983 and 2 μM KT5720. The effect of 1 μM Go6983 plus 2 μM KT5720 on the bioenergetics of synaptosomes. The experiment was done three times and the mean values represent an average of 7-8 independent measurements and error bars represent the SD; $P > 0.05$.

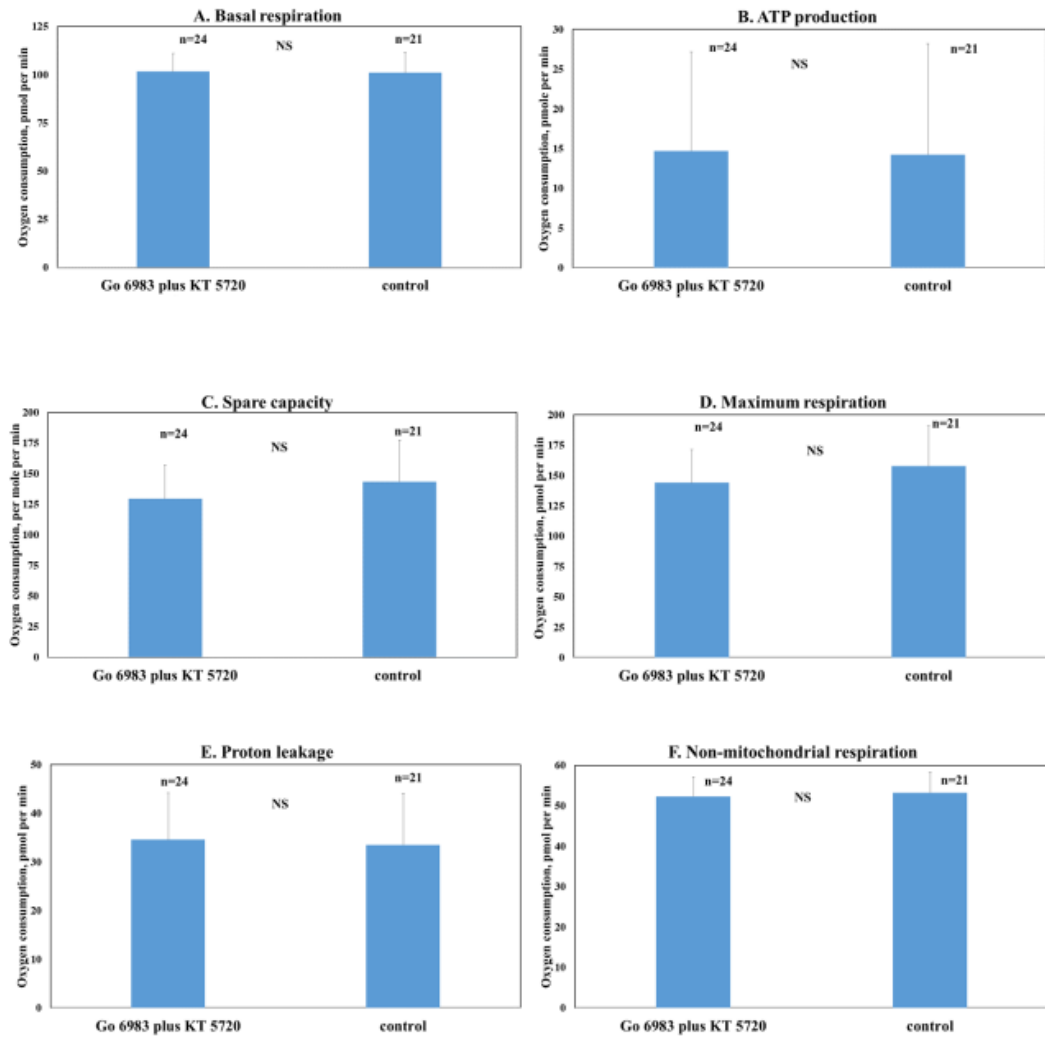


Figure 5.23. 1 μM Go6983 and 2 μM KT5720 dual treatment did not perturb any bioenergetics parameters measured as it looks similar to those for the controls. The effect of 1 μM Go6983 plus 2 μM KT5720 on (A) basal respiration, (B) ATP production, (C) spare capacity, (D) maximal respiration, (E) Proton leakage, and (F) Non-mitochondrial respiration in nerve terminals. The histobars represent the mean and the error bar shows the SEM.

5.6.4 Go6983 plus AGA

Treatment of synaptosomes with both 1 μM Go6983 and 50 nM AGA failed to significantly change any of the parameters (Fig 5.24, Fig 5.25 a-f).

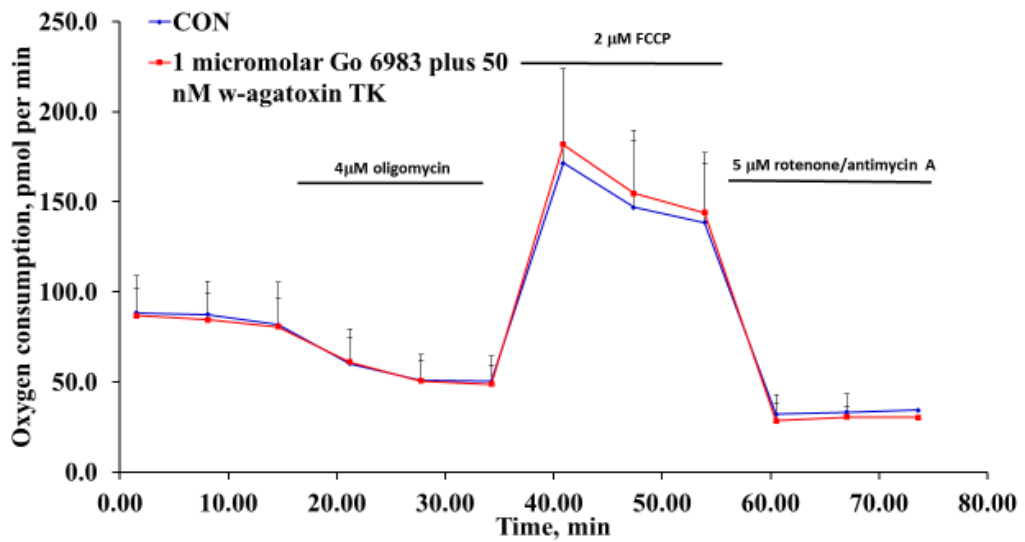


Figure 5.24. Synaptosomal bioenergetics were unaffected by 1 μM Go6983 and 50 nM AGA dual treatment. The effect of 1 μM Go6983 plus 50 nM AGA on the bioenergetics of synaptosomes. The experiment was done three times and the mean values represent an average of 8 independent measurements and error bars represent the SD; $P > 0.05$.

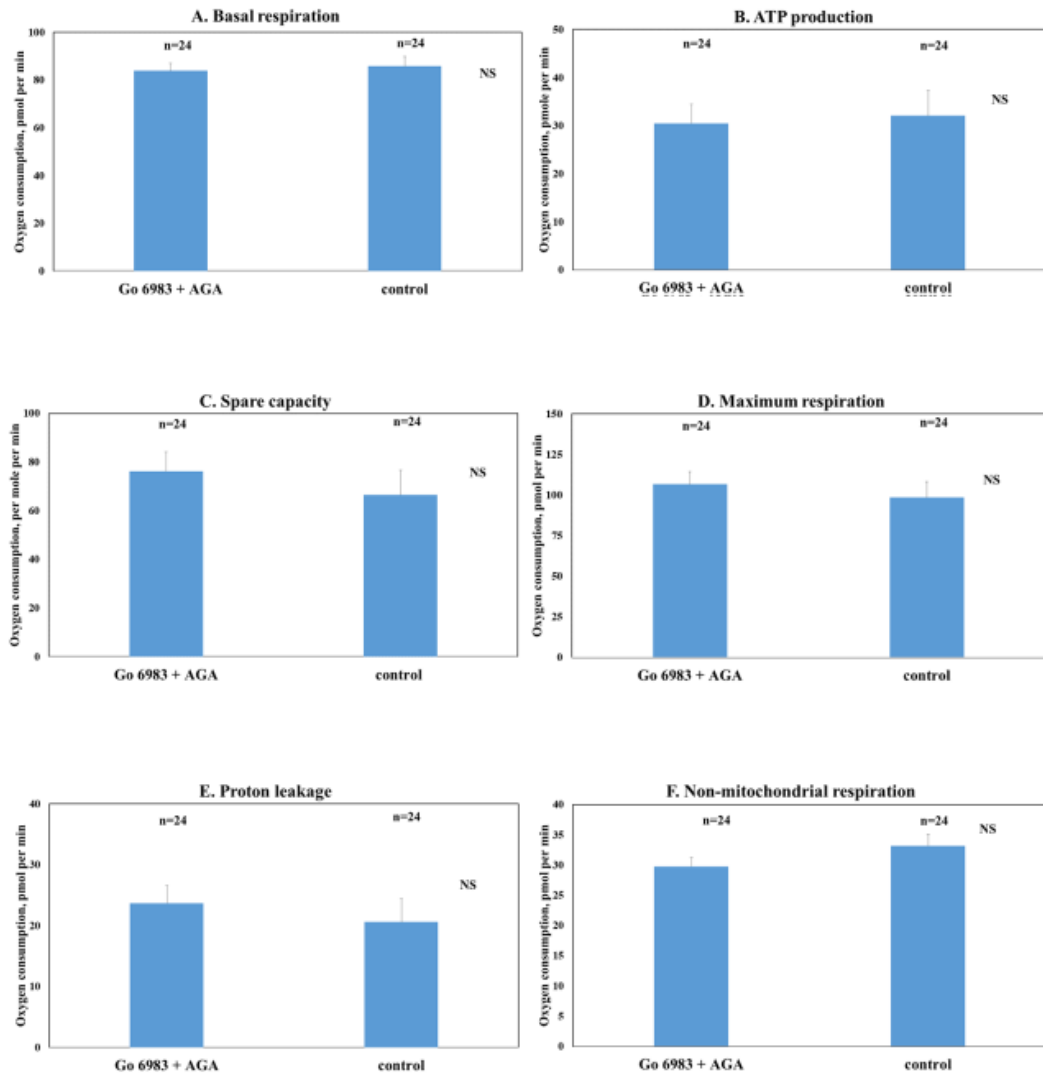


Figure 5.25. 1 μ M Go6983 and 50 nM AGA dual treatment did not perturb any bioenergetics parameters measured as it looks similar to those for the controls. The effect of 1 μ M Go6983 plus 50 nM AGA on (A) basal respiration, (B) ATP production, (C) spare capacity, (D) maximal respiration, (E) Proton leakage, and (F) Non-mitochondrial respiration on synaptosomes. The histograms represent the mean and the error bar shows the SEM.

5.6.5 Go6983 plus NIF

Bioenergetics of synaptosomes are unaffected by the double treatment of 1 μM Go6983 and 1 μM NIF as none of the parameters measured were significantly changed compared to control following the drug treatment (Fig 5.26, Fig 5.27 a-f).

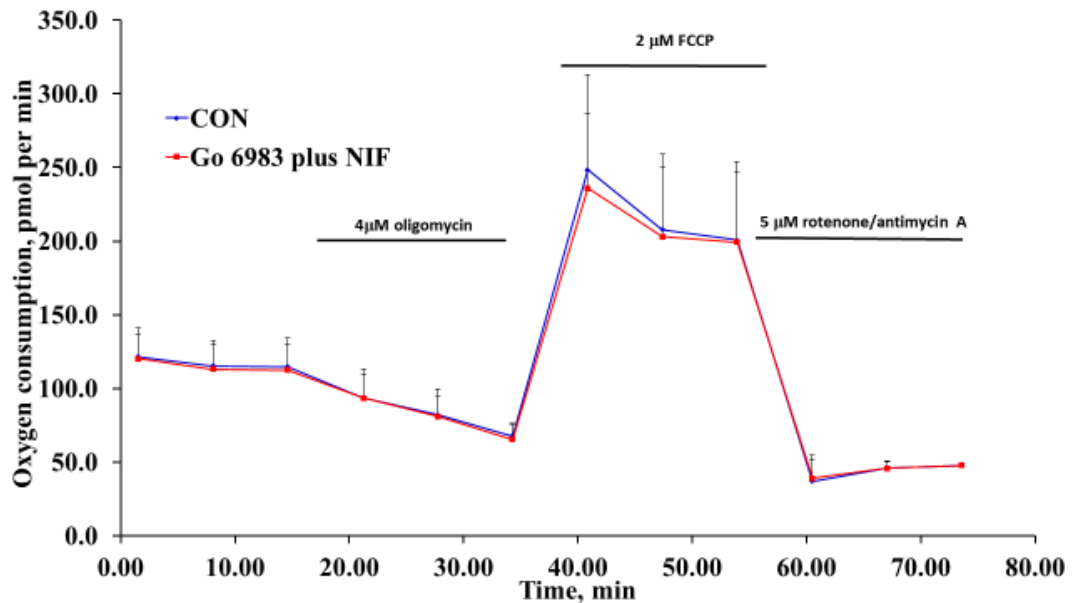


Figure 5.26. Synaptosomal bioenergetics were unaffected by 1 μM Go6983 and 1 μM NIF dual treatment. The effect of 1 μM Go6983 plus 1 μM NIF on the bioenergetics of synaptosomes. The experiment was done three times and the mean values represent an average of 9 independent measurements and error bars represent the SD; $P > 0.05$.

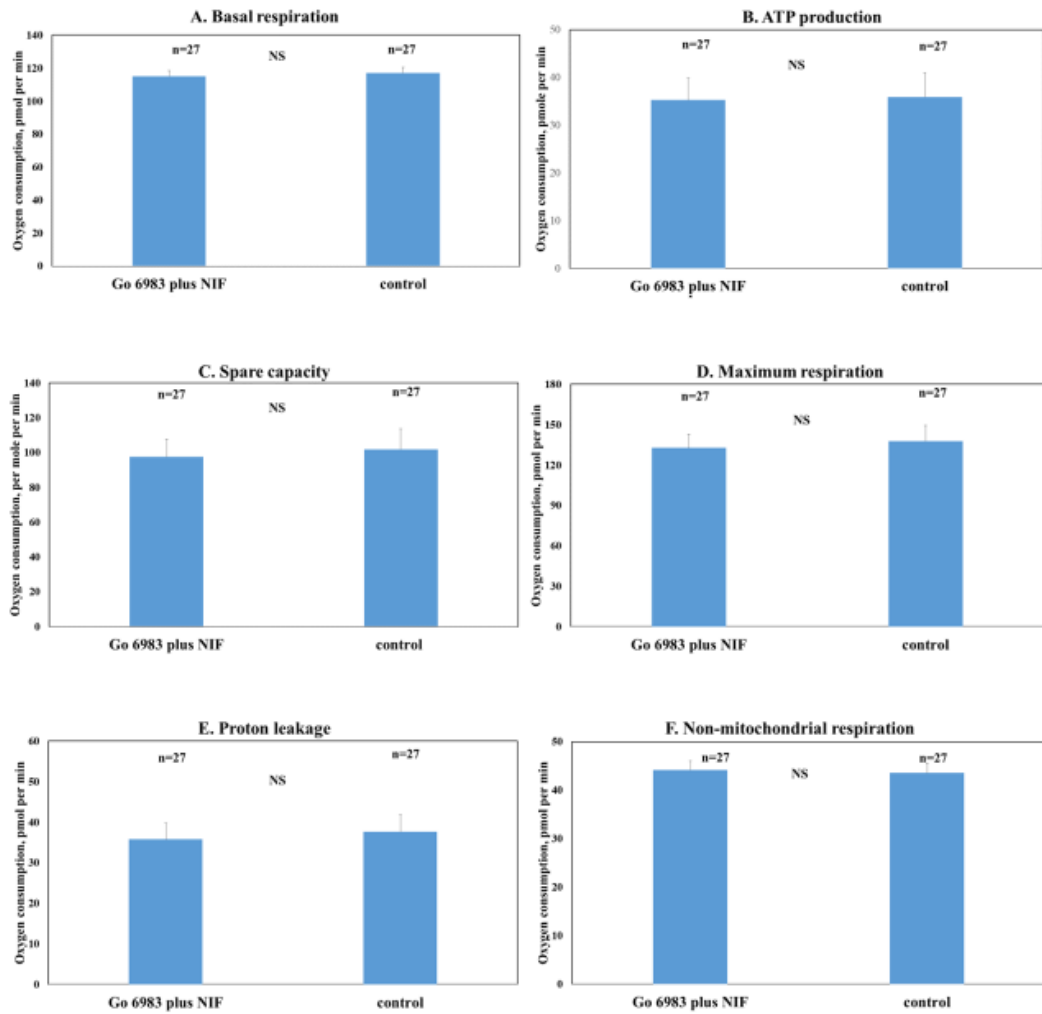


Figure 5.27. 1 μM Go6983 and 1 μM NIF dual treatment did not perturb any bioenergetics parameters measured as it looks similar to those for the controls. The effect of 1 μM Go6983 plus 1 μM NIF on (A) basal respiration, (B) ATP production, (C) spare capacity, (D) maximal respiration, (E) Proton leakage, and (F) Non-mitochondrial respiration in synaptosomes. The histobars represent the mean and the error bar shows the SEM.

5.6.6 OA

The acute treatment with OA slightly affected basal respiration of the synaptosomes, however all the other parameters were remained at the similar level with control condition (Fig 5.28, Fig 5.29 a-f) and overall the synaptosomes were very similar in the drug treated and non-treated terminals.

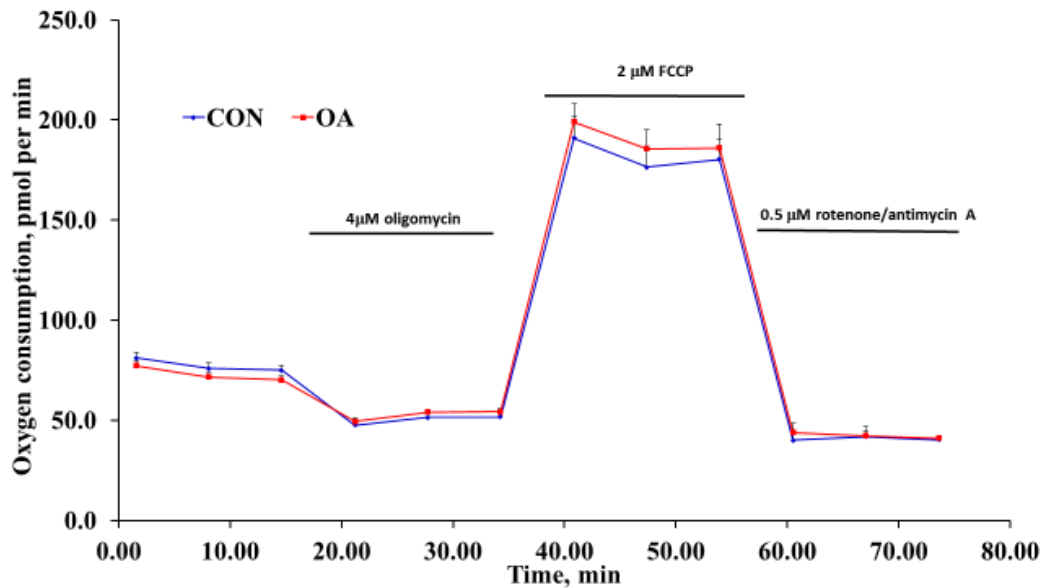


Figure 5.28. Synaptosomal bioenergetics were unaffected by 0.8 μM OA treatment. The effect of 0.8 μM OA on the bioenergetics of synaptosomes. The experiment was done three times and the mean values represent an average of 6 independent measurements and error bars represent the SD; P>0.05.

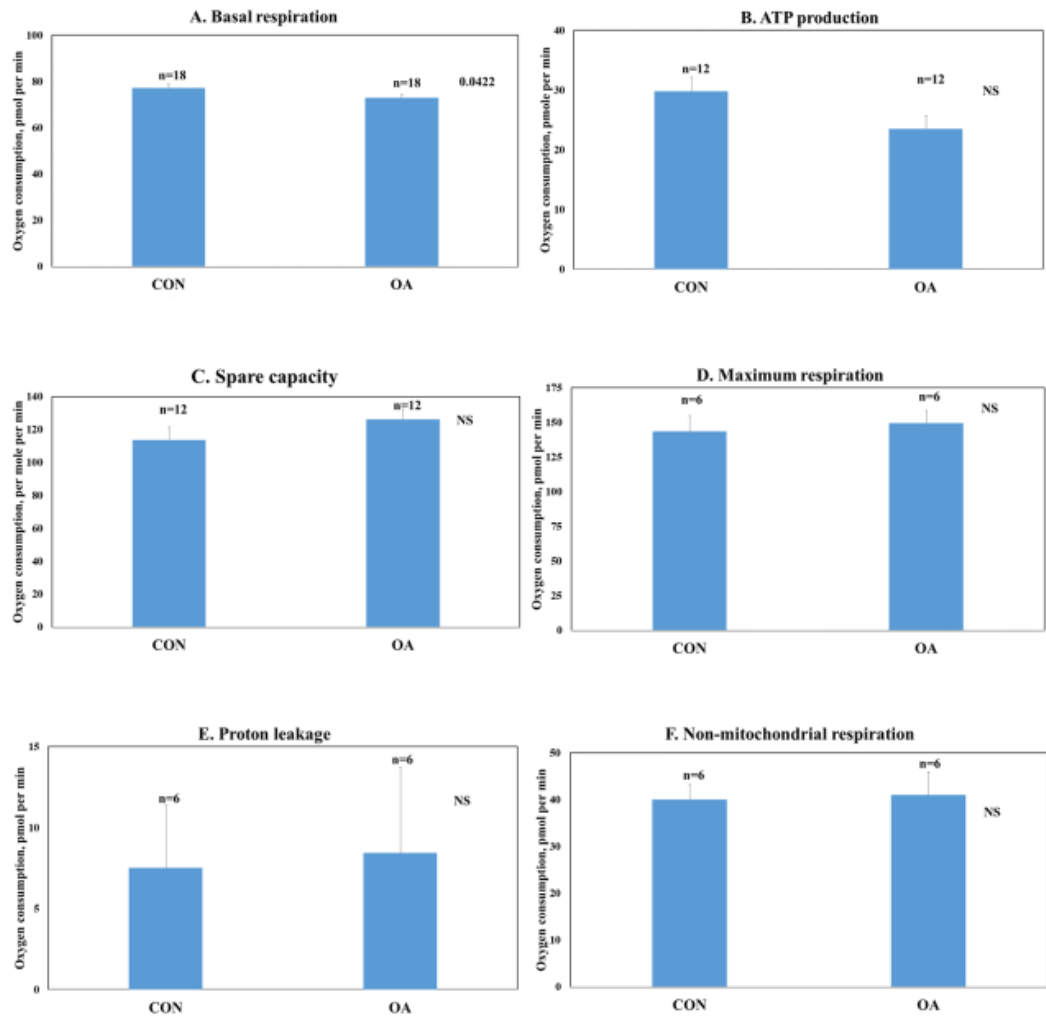


Fig 5.29. 0.8 μ M OA treatment did not perturb most of bioenergetics parameters measured as it looks similar to those for the controls. The effect of 0.8 μ M OA on (A) basal respiration, (B) ATP production, (C) spare capacity, (D) maximal respiration, (E) Proton leakage, and (F) Non-mitochondrial respiration in synaptosomes. The histograms represent the mean and the error bar shows the SEM.

5.6.7 Go6983 plus OA

The acute treatment of synaptosomes with 1 μM Go6983 plus 0.8 μM OA failed to disturb any of the bioenergetics parameters (Fig 5.30, Fig 5.31 a-f).

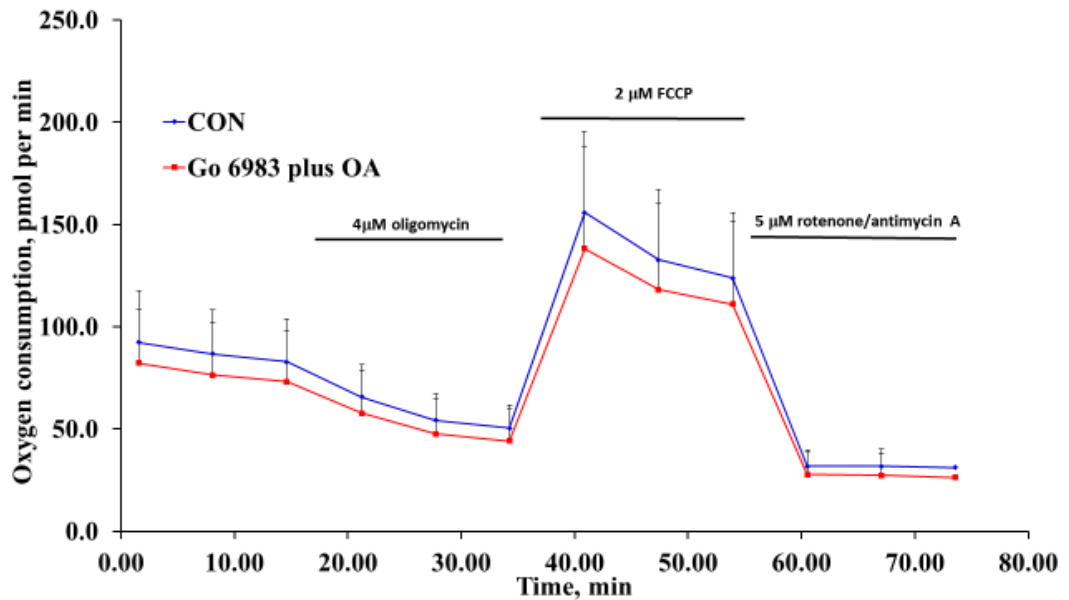


Figure 5.30. Synaptosomal bioenergetics were unaffected by 1 μM Go6983 and 0.8 μM OA dual treatment. The effect of 1 μM Go6983 plus 0.8 μM OA on the bioenergetics of synaptosomes. The experiment was done two times and the mean values represent an average of 5 independent measurements and error bars represent the SD; $P > 0.05$.

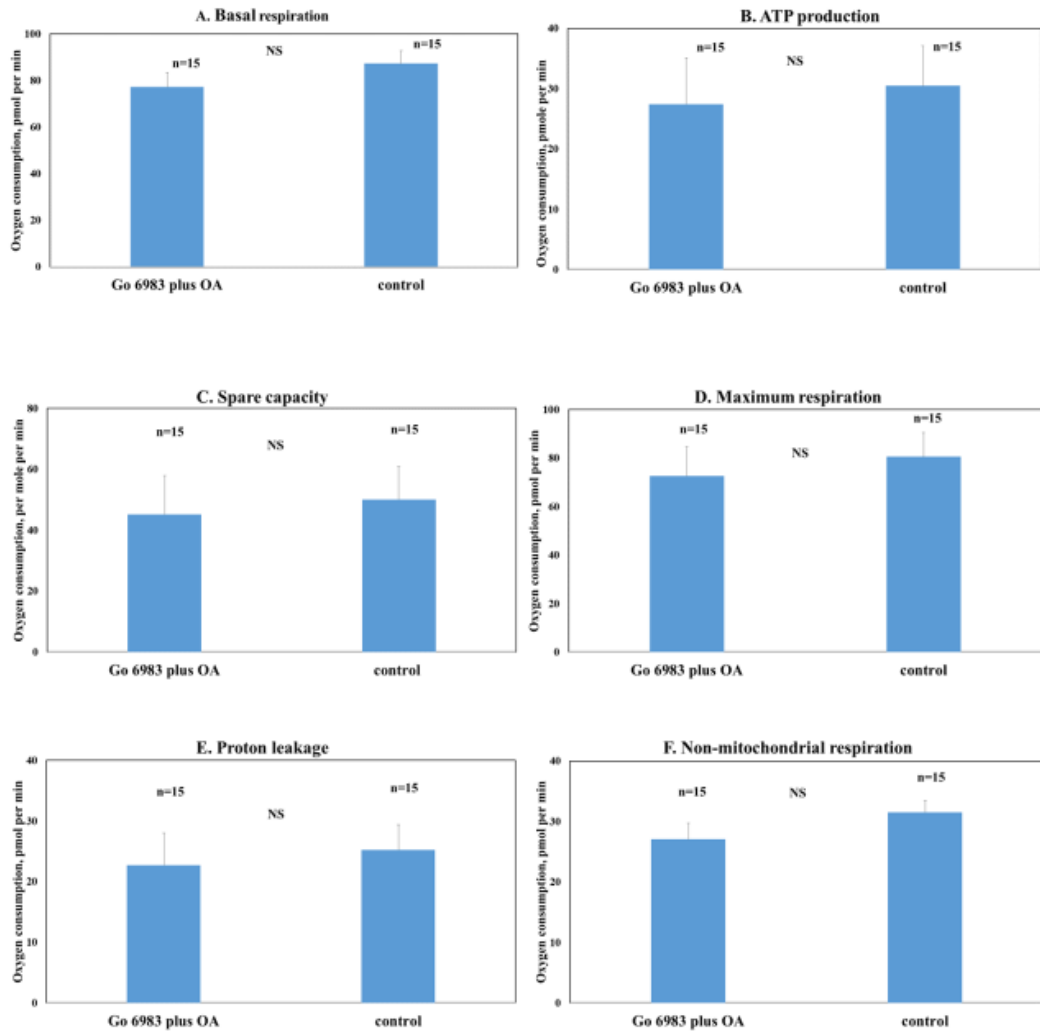


Figure 5.31. 1 μ M Go6983 and 0.8 μ M OA dual treatment did not perturb any bioenergetics parameters measured as it looks similar to those for the controls. The effect of 1 μ M Go6983 plus 0.8 μ M OA on (A) basal respiration, (B) ATP production, (C) spare capacity, (D) maximal respiration, (E) Proton leakage, and (F) Non-mitochondrial respiration in synaptosomes. The histobars represent the mean and the error bar shows the SEM.

#	Figure #	Assays	Stimulus	Drugs employed (conc.)	Key findings
1	5.1-5.4	GLU, FM, Fura-2	HK5C, ION5C	MITMAB (30 μ M)	Inhibition of Dyn translocation with MITMAB treatment produced no difference in all assays employed. This means, Dyn, already present on membrane, regulates the KR mechanism of exocytosis.
2	5.5-5.7	GLU, FM, Fura-2	4AP5C, HK5C, ION5C	KT5720 (2 μ M) Dynasore (160 μ M)	Inhibition of endogenous PKA with KT5720 perturbs the Dyn dependent KR (stimulated with ION5C) mechanism for the RRP SVs but not the NM-II dependent KR pathway (stimulated with HK5C). Similar results were previously found when Dyn was inhibited with Dynasore and stimulated with various stimulus. Thus, the hypothesis was made predicting that the inhibition of endogenous PKA leads to a switch of the Dyn dependent KR to FF, which explains why HK5C action on NM-II KR is not perturbed.
3	5.8-5.9	GLU, FM, Fura-2	HK5C	KT5720 (2 μ M), Go6983 (1 μ M)	Go6983 was used to switch HK5C to work through Dyn dependent KR pathway instead of NM-II dependent KR pathway. It was found that pre-treatment with Go6983 and KT5720 changed the mode of release to FF, confirming the suggestion that PKA only affect the Dyn dependent KR pathway. It also indicates that FM results were not limited to a particular action of a specific stimulus.
4	5.10-5.17	GLU, FM, Fura-2	HK5C	CONO (1 μ M), AGA (50 nM), NIF (1 μ M), Go6983 (1 μ M), OA (0.8 μ M)	HK5C evoked FM dye release was discovered to only increase when L-type calcium channels is inhibited, whilst in the presence of Go6983, only perturbation of P/Q-type calcium channels have produced similar phenomenon. These results may imply that L-type is required for NM-II dependent KR pathway whilst P/Q-type is needed for Dyn dependent KR pathway. This was also ascertained using OA.
5	5.18-5.31	Bio		All drugs tested in this chapter	Under any drug treatment, the bioenergetics parameters were virtually at the similar level to that of the control, meaning no disturbance of bioenergetics from the drugs employed were identified.

Figure 5.32. Summary of the findings in chapter 5.

5.7 Discussion

The mode of release is dependent on various protein activities. For instance, when a SV is releasing in a KR mode, fission of the FP should be performed so that the vesicle does not fully flatten into the membrane. This fission maybe involve Dyn activity. Dyn may aid in the scissoring of the FP formed between SV and PM by oligomerising into a spiral around the FP as it does for forming clathrin pits in CME following FF. However Dyn's precise role in KR has not been elucidated. Several lines of evidence have found that in the absence of Dyn, the KR mode of exocytosis is attenuated. In this chapter, investigation into several properties of the mode of release of the RRP have been described. We have employed several drugs, such as as MITMAB, KT5720, Go6983, AGA, CONO, NIF, and OA to explore how activity of various proteins could affect the regulation of the mode.

5.7.1 MITMAB

Dyn is important in regulating one type of KR mode for SV exocytosis. For investigation of the role of this protein, Dynasore, which blocks GTPase activity of Dyn and thereby pharmacologically inhibit its action, can be used. It has been previously found by Ashton's group that Dynasore treatment has led to switch of Dyn dependent mode from KR to FF, demonstrating pivotal role of Dyn in controlling the KR mode of the release. However, it was unclear whether Dyn had to translocate to a membrane compartment (either the PM or the vesicle membrane) prior to the fusion or whether Dyn already present on the membrane could regulate the mode. MITMAB is a drug that stops Dyn translocating from cytosol to membranes by stopping Dyn binding to the phospholipid in membranes (Quan *et al*, 2007). Therefore this drug was employed to test whether it would interfere with the Dyn dependent KR mode of exocytosis. MITMAB treatment was found not to affect the GLU release stimulated using HK5C, ION5C, and 4AP5C. Further, it was clear that the drug does not interfere with Dyn dependent KR pathway when FM dye release was measured. In addition, MITMAB treatment had negligible effects on evoked $\Delta[\text{Ca}^{2+}]_i$.

These findings suggest that Dyns are not required to translocate to a membrane compartment from the cytosol prior to SV exocytosis of the RRP via KR. These results do not indicate where exactly Dyn is localised to mediate the FF closure – during Dyn dependent KR - but some of the potential locations include the membrane of the SVs themselves or at the PM in the AZ. In unpublished observations, A. Ashton has shown that MITMAB does prevent the recycling of those SV that undergo FF indicating that the drug is active (as was shown by Quan *et al*, 2007).

5.7.2 PKA

Clearly, Dyn can play a role in the regulation of a KR mode of the RRP of SVs as inhibiting its GTPase activity induces Dyn dependent KR to switch to FF. Thus it is important to investigate processes that allowed Dyn to regulate the mode of release. Dyn is a substrate of numerous kinases, and one approach that could be undertaken would be the investigation of which kinases may cause switch in the Dyn dependent KR mode. Apart from PKC (see thesis by Bhuva, 2015; Singh, 2017) PKA could potentially regulate Dyn I activity as regards KR. Towards this, we employed KT5720, an inhibitor of endogenous PKA, to investigate the mode of release. 4AP5C and ION5C evoked FM dye releases were significantly increased in the presence of KT5720, reflecting the changes of mode from KR to FF. However, HK5C evoked release remained unchanged. These data demonstrate that PKA inhibition does not affect HK5C evoked FM dye release. This is intriguing because it is known that ION5C regulates KR through a Dyn dependent pathway whilst HK5C works via a NM-II dependent pathway. Thus, it would appear that endogenous PKA activity only affects the Dyn dependent KR pathway and not the NM-II dependent KR mode. This interpretation is due to the fact that HK5C evoked FM dye release is not affected when Dyn is inhibited with Dynasore, whilst 4AP5C and ION5C evoked release is switched to FF. This idea was further tested by measuring HK5C evoked FM dye release in the presence of Go6983 as when PKC is inhibited, HK5C now regulate the KR mode of the RRP SVs through the Dyn dependent pathway. Treatment of synaptosomes with

Go6833 plus KT5720 did not affect the HK5C evoked GLU release but such conditions increased the FM dye release relative to control, meaning the RRP SVs mode of release had switched from KR to FF. Thus, this proves that whilst KT5720 does not regulate the NM-II mode of exocytosis when HK5C regulates the KR mode via the Dyn dependent pathway PKA inhibition can regulate this latter mode. Clearly, PKA activity only affects Dyn dependent KR mode but not the NM-II dependent KR mode.

5.7.3 Calcium channel dependency of KR

Extracellular and intracellular calcium levels have been long considered as one of the major mediators for the KR mode of exocytosis (Neher and Sakaba, 2008). Thus it was obvious to consider the link between changes in calcium levels and the releasing mode. Calcium enters the nerve terminal through voltage-gated calcium channels (VGCC), and subsequently initiates neurotransmission. VGCC, therefore, have an important role in neurotransmission via regulation of intracellular calcium levels (Catterall, 2011). Preliminary research from A.Ashton's group had shown that inhibition of each type of calcium channels with specific toxin (AGA for P/Q-type, CONO for N-type, NIF for L-type) has determined that whilst inhibition of N-type and P/Q-type calcium channels does not affect the HK5C evoked FM dye release, disabling L-type channel function has led to dramatic increase in the HK5C evoked FM dye release. Thus, it was concluded that L-type calcium channel regulate the KR mode of release of the RRP. However, this result applies only to NM-II dependent KR mode since HK5C usually works through this pathway. Hence, there was a possibility that when KR is regulated through Dyn dependent pathway, another type of channel might be involved. Although, ION5C acts through the Dyn dependent KR mode, this ionophore bypasses the role of calcium channels and so cannot be employed for such investigation. However, a PKC inhibitor, Go6983, induces HK5C to operate through the Dyn dependent pathway, so we can measure HK5C evoked FM dye release in Go6983 treated terminals in the presence of the various calcium channel blockers. Intriguingly, whilst the treatment with any of the specific Ca²⁺ channel blockers

does not affect the HK5C evoked GLU release in Go6983 treated terminals, only AGA treatment led to an increase in the HK5C evoked FM dye release in such terminals. This data indicates that when HK5C evoked RRP SV release has changed to the Dyn dependent pathway, only P/Q type calcium channel inhibition can switch the mode. Overall, such results suggest that the NM-II dependent KR mode is regulated through L-type calcium channel whilst Dyn dependent release is regulated by P/Q type calcium channel. OA treatment, a drug that is known to switch the RRP SVs to FF for either mode of release, confirmed that Go6983 treatment does not prevent switching of the RRP mode. Thus, the difference in Ca²⁺ channel requirement for Dyn and NM-II dependent KR may indicate that these operates as two distinct KR processes rather than one that can be acted upon by these two proteins.

5.7.4 Bioenergetics

Bioenergetics experiments were done on drugs employed in this chapter using Seahorse XF analyser, and it was established that under any drug treatment, the bioenergetics parameters were virtually at the similar level to that of the control. These results imply that there were no disturbances of bioenergetics for such drug treatments used in this chapter, proving that the data we have obtained in this chapter are not due to non-specific effects of the drug on bioenergetics integrity. This is an important aspect of the study because it indicates that any drug induced actions are purely due to their effect on the release and it is not on disturbance of bioenergetics within the terminal.

5.8 Conclusion

In conclusion, various properties of the mode of the RRP of SVs have been studied in this chapter. Inhibition of translocation of Dyn from cytosol to membranes with MITMAB was found not to interfere with Dyn dependent KR mode. Thus, this demonstrates that Dyns are already present on membranes (either on SV or the PM) prior to exocytosis of vesicles at the AZ fusion site. Furthermore, inhibition of endogenous PKA activity only

affected Dyn dependent KR mode, revealing that PKA only regulate the KR mode of release through Dyn dependent pathway but not NM-II dependent pathway. Lastly, Dyn dependent KR mode was found to be regulated through P/Q-type calcium channel, and this in combination with previous results showing NM-II dependent pathway is regulating KR through L-type calcium channels, represents a calcium channel specificities in KR mode depending on whether Dyn or NM-II is regulating the FP.

Chapter 6:

The Effect of Actin Cytoskeleton Disassembly and Stabilisation on the Mode of SV Release

6.1 Introduction

The actin cytoskeleton may contribute to the regulation of the mode of exocytosis and to the release of the distinct pools of SVs. The cytoskeleton is involved in virtually every cell biological process in eukaryotes, ranging from cell division and motility to vesicle trafficking. The cytoskeleton is mainly composed of three types of protein filaments; actin, microtubules, and intermediate filaments (Dillon and Goda, 2005). The actin cytoskeleton is a main structural component of both pre- and postsynaptic components of the synapse. However, the precise role of the actin cytoskeleton in neurotransmission is yet to be fully elucidated. In regulated exocytosis, it was proposed to work either positively or negatively and this depended upon the secretory system under examination (Porat-Shliom *et al*, 2012). At the centre of the bouton terminal where SVs are distal from the AZ region of the PM, actin appears to interact with short filaments of Syn I, forming an actin-Syn I-SV meshwork. It has been suggested that it is this meshwork that sequesters the SVs that are distal to the AZ. Following elevated neuronal activity, phosphorylation of Syn I at specific sites may cause the disattachment and freeing of the SV and these mobilised SVs can replenish the RRP. At the AZ, actin is suggested to have dual functions. It might direct the arriving SVs and allow them to dock at the AZ, thereby positively controlling the size of the RRP. It could also form a physical and molecular barrier for priming reactions required for SNARE mediated exocytosis, and this may prevent facile fusion of vesicles (Cingolani and Goda, 2008).

The actin cytoskeleton is also proposed to interact with Dyn and myosin in the regulation of neurotransmission (Papadopoulos, 2017). In the case of Dyn, Gu *et al* (2010) reported that short actin filaments promoted Dyn self-assembly *in vitro* through direct Dyn-actin interaction. Such assembled Dyn was able to displace the capping protein (CP) gelsolin (Gsn) from barbed ends of actin filaments, and this resulted in the elongation of such filaments (Gu *et al*, 2010). Kessels *et al* (2001) reported that *in vitro* the mammalian F-actin binding protein (Abp1) links the actin cytoskeleton to Dyn through its SH3 domain.

Excitingly, the actin cytoskeletal scaffold, in association with Dyn, contributes to the closing dynamics of exocytotic fusion pores measured in PC12 cells (Kessels *et al*, 2001). Others have suggested that actin can regulate the vesicular fraction released in an extended KR mode (Trouillon and Ewing, 2014).

Regarding vesicle release, actin is proposed to form an actomyosin complex with NM-II to provide the force to drive exocytosis to completion (Nightingale *et al*, 2012; Porat-Shliom *et al*, 2013). Further, it was found that a F-actin cell cortex plays a key role in stabilising the KR fusion under lower stimulation frequency, and under higher stimulation frequency, the actin cortex dependent FF mode of release was disrupted. These authors have indicated that, an absence of NM-II or MLCK under increased stimulation frequency inhibited the FP dilation and sustained the granule in KR mode of exocytosis (Doreian *et al*, 2008).

In the previous chapter of this thesis, we have reported that KR modes of SV exocytosis can be associated with Dyn and NM-II activities. As both these can associate with the actin cytoskeleton as highlighted above, this justifies the exploration of the actin cytoskeleton action on the exocytotic mode and its regulation.

6.2 The effect of disassembly of actin cytoskeleton on the evoked release and mode of exocytosis

6.2.1 LAT inhibits the release of the RP but not the RRP

To establish an effect of actin disassembly on neurotransmission, we have pre-treated the synaptosomes with Latrunculin (LAT), and measured HK5C, ION5C, and 4AP5C evoked GLU releases. LAT disrupts the organisation of microfilament by binding to the actin monomer and preventing them from polymerising (i.e. Coue *et al*, 1987; Richard *et al*, 2004). HK5C evoked release was significantly lower compared to control, meaning actin disassembly caused some reduction in the release (Fig 6.1a), LAT also caused a reduction of ION5C evoked release (Fig 6.1 b). Intriguingly, 4AP5C evoked release was unchanged following actin disassembly (Fig 6.1 c). As 4AP5C is a stimulus that work exclusively on the RRP, it would appear that LAT induced actin disassembly only affects the RP release.

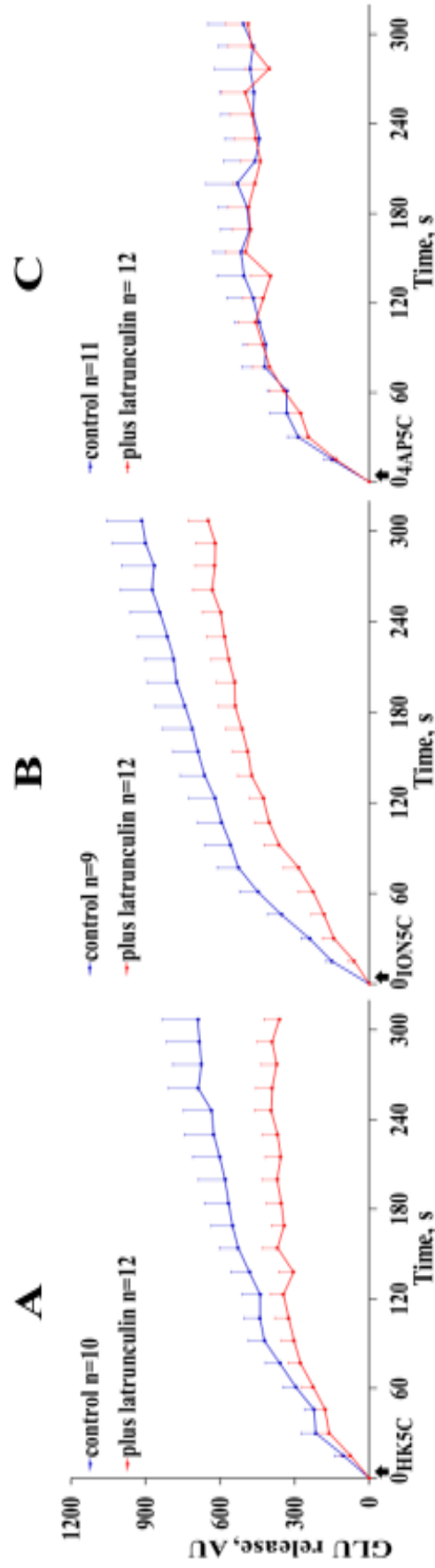


Figure 6.1. Actin disassembly only perturbs RP exocytosis. GLU release evoked by a) HK5C b) ION5C c) 4AP5C in control and 15 μ M LAT treated terminals. Data are mean \pm SEM, N=3 independent experiment. Note that for HK5C and ION5C evoked release, LAT significantly reduced ($P<0.05$) the release compared to control, but for 4AP5C stimulation, there was no significant difference ($P>0.05$) between the two conditions in the release suggesting that actin disassembly only perturbs the RP release.

6.2.2 LAT does not inhibit the FM dye release relative to control

LAT did not perturb the total FM dye content compared to control (appendix 3) proving that both the RRP and RP were still labelled with dye following microfilament disassembly. Furthermore, HK5C and ION5C (Fig 6.2) evoked FM dye release appears similar in LAT and non-drug treated terminals. However, it was shown above that the RP is not released in the presence of LAT and yet this is the pool that normally releases the FM dye because it undergoes FF. Normally the RRP does not release FM dye since it undergoes KR. Thus we have the situation that RRP SVs are being exocytosed and yet FM dye is also being released. This leads to the conclusion that disassembling actin microfilaments with LAT switches the RRP SVs to a FF mode of exocytosis. Okadaic acid (OA) (i.e. Bialojan and Takai, 1988) can switch the RRP SVs to FF (see earlier chapter and appendix 1) but application of OA to LAT treated terminals did not induce any further dye release clearly demonstrating that the RRP is already undergoing the FF mode of release (Fig 6.3).

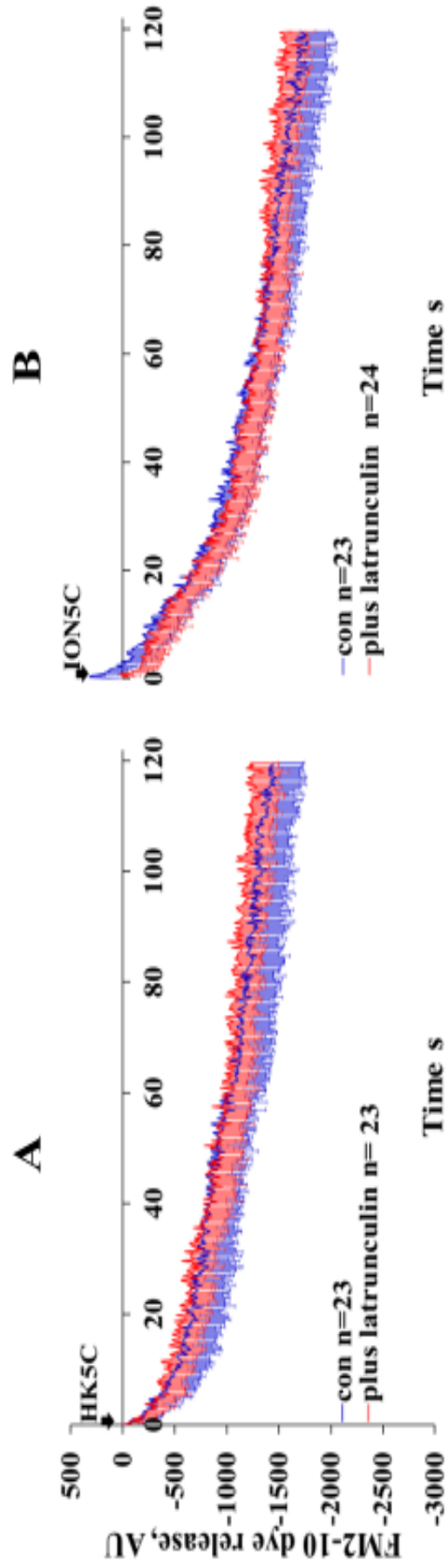


Figure 6.2. HK5C or ION5C evoked FM dye release in LAT treated synaptosomes were similar to non-drug treated control despite the fact that actin disassembly was found to perturb the RP exocytosis. FM dye release evoked by a) HK5C b) ION5C in the absence or presence of 15 μ M LAT. Data are mean \pm SEM, N=3 independent experiments; P<0.05 for significance. Note that there was no significant difference of release between control and drug treated conditions.

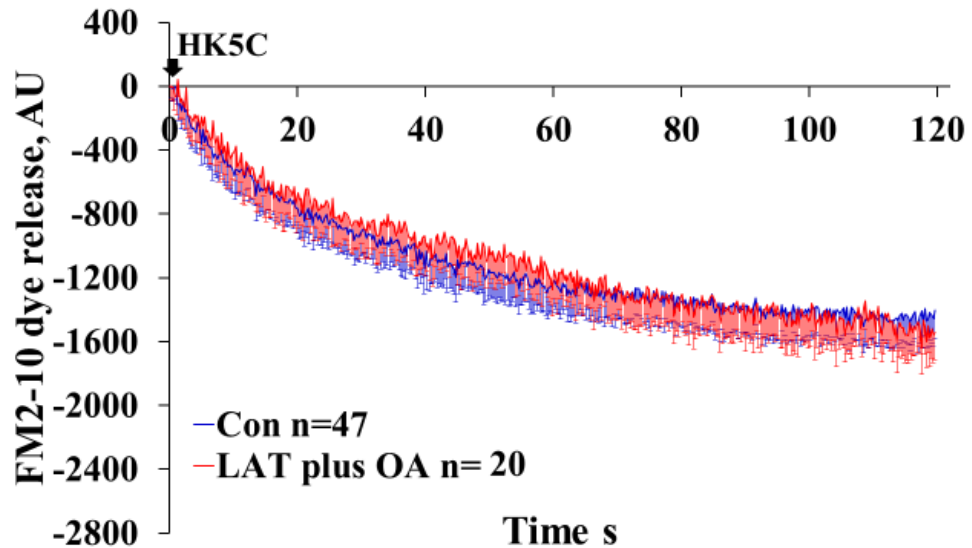


Figure 6.3. Actin disassembly allowed RRP to release in FF mode. HK5C evoked FM dye release in control or 15 μM LAT plus 0.8 μM OA treated synaptosomes. Data are mean \pm SEM, N=7 independent experiments; P <0.05 for significance. However, there was no significant difference of release between control and LAT plus OA treated terminals.

6.2.3 The action of LAT on evoked $\Delta[\text{Ca}^{2+}]_i$

Disassembly of actin with LAT inhibits RP release and leads to the RRP SVs switching to a FF mode of exocytosis for both HK5C and ION5C stimulation. One reason this could occur is that disassembly of the actin cytoskeleton may reduce the evoked $\Delta[\text{Ca}^{2+}]_i$. There was a significant drop in HK5C evoked $\Delta[\text{Ca}^{2+}]_i$ in LAT treated relative to control terminals (Fig 6.4). In contrast, ION5C evoked $\Delta[\text{Ca}^{2+}]_i$ was similar in drug free and drug treated terminals (Fig 6.5). Thus the action of LAT on ION5C evoked GLU containing SV RP release and its action on ION5C evoked FM dye release from the RRP SVs are not related to any changing in evoked $\Delta[\text{Ca}^{2+}]_i$. However, the action of LAT on HK5C evoked GLU and FM release could be explained by changing in $\Delta[\text{Ca}^{2+}]_i$ levels. Since, HK5C acts through NM-II dependent KR pathway for the RRP whilst ION5C operates via the Dyn dependent KR pathway for such vesicles, this could suggest that whilst intact actin

microfilaments could have a direct effect on the Dyn dependent KR mode (via regulation of the closure of the FP) this cytoskeletal component may not have direct effect on the NM-II dependent KR mode.

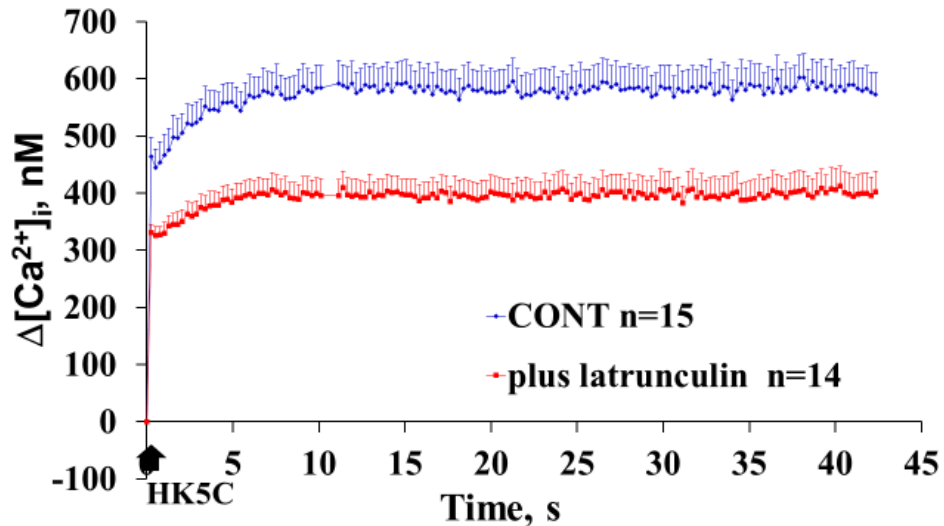


Figure 6.4. Actin disassembly reduce HK5C evoked $\Delta[Ca^{2+}]_i$. Change in $\Delta[Ca^{2+}]_i$ induced by HK5C in control and 15 μ M LAT treated terminals. Data are mean \pm SEM, N=3 independent experiments; Note that LAT significantly reduced the calcium entry compared to control ($P<0.05$).

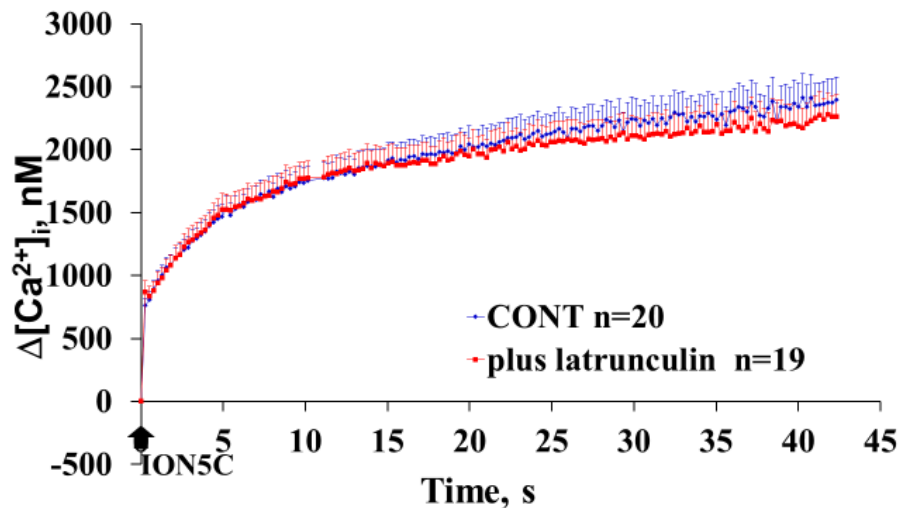


Figure 6.5. ION5C evoked $\Delta[Ca^{2+}]_i$ is unaffected by actin disassembly. Change in $\Delta[Ca^{2+}]_i$ induced by ION5C in control and 15 μ M LAT treated terminals. Data are mean \pm SEM, N=4 independent experiments. Note that there was no significant difference ($P>0.05$) between control and LAT treated terminals.

6.2.4 Higher $[Ca^{2+}]_e$ did not rescue the LAT induced inhibition of evoked RP exocytosis

It was evident in the above section that changes in HK5C evoked $\Delta[Ca^{2+}]_i$ maybe involved in the LAT induced inhibition of the RP evoked by this stimulation. An obvious question was whether using higher $[Ca^{2+}]_e$, one could prevent the effect of LAT. Therefore, HK20C evoked GLU release from synaptosomes was determined in the presence of LAT, but this stimulus failed to overcome the LAT block of the RP (Fig 6.6).

It is possible that our results demonstrate two separate actions of LAT, one involving inhibiting action of the drug on the release of the RP SVs, and another action that can regulate the mode of release. Therefore, future experiments would measure HK20C evoked FM dye release in the LAT treated synaptosomes.

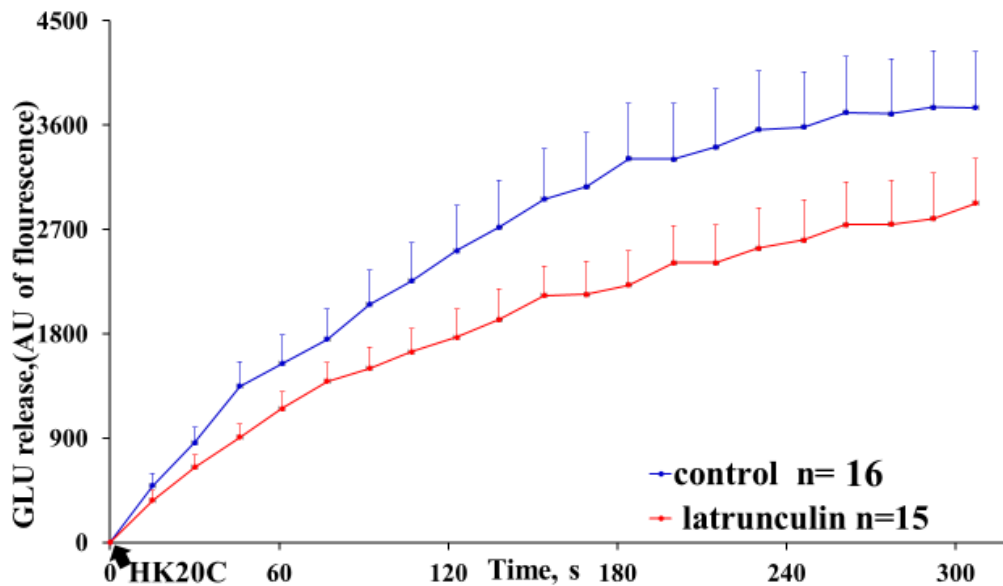


Figure 6.6. Higher $[Ca^{2+}]_e$ did not rescue the LAT induced inhibition of evoked RP exocytosis.

HK20C evoked GLU release in control and 15 μ M LAT treated terminals. Data are mean \pm SEM, N=6 independent experiments, P <0.05 was considered as a significant difference. LAT treatment has led to significant reduction in the release compared to control.

6.2.5 PKC inhibition reversed LAT effect on HK5C evoked release

It is clear that LAT treatment produced varying results depending on the stimulus employed. This might suggest that the effect of the actin cytoskeleton could depend upon whether Dyn or NM-II are regulating the FP during KR of the RRP SVs. HK5C normally acts on the NM-II dependent KR but inhibiting PKCs with Go6983 allows this stimulus to act on the Dyn dependent pathway instead (as discussed in earlier chapters). Thus, HK5C evoked release in Go6983 treated terminals in the presence or absence of LAT was measured.

PKC inhibition with Go6983 actually prevented the LAT induced reduction in the release as Go6983 (which behaves same as non-drug treated samples) and Go6983 plus LAT revealed no significant difference in HK5C evoked GLU release (Fig 6.7). It was also found that HK5C evoked FM dye release (Fig 6.8) and HK5C evoked $\Delta[\text{Ca}^{2+}]_i$ (Fig 6.9) that were previously changed by pre-treatment with LAT were no longer affected following PKC inhibition with Go6983. If LAT regulated the FP of RRP SV KR similarly for both HK5C and ION5C, then one might have expected that HK5C would work on the Dyn dependent pore in response to PKC attenuation with Go6983, whereas this does not appear to be the case even though ION5C acting on the Dyn dependent pore is sensitive to disassembly of microfilament. One possible interpretation is that the action of LAT on HK5C evoked release involves in some way the activation of PKCs since when these are blocked, the drug did not induce any effect.

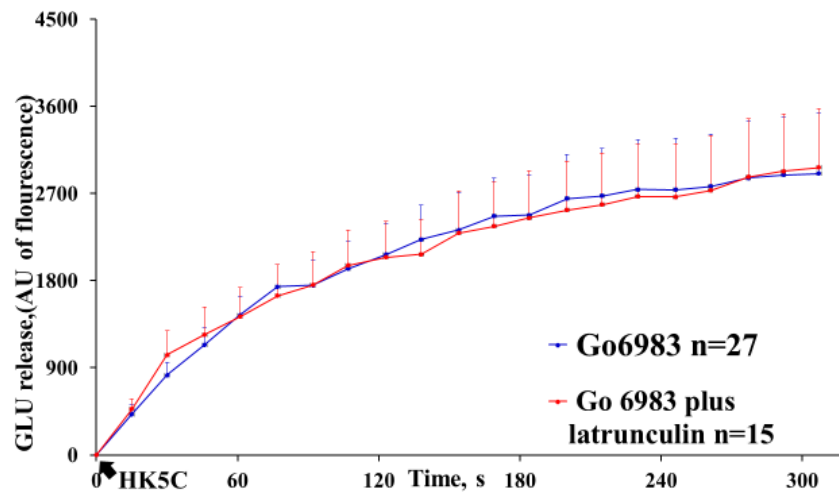


Figure 6.7. PKC inhibition reversed LAT effect on HK5C evoked GLU release. HK5C evoked GLU release in 1 μ M Go6983 or 1 μ M Go6983 plus 15 μ M LAT treated terminals. Data are mean \pm SEM, N=5 independent experiments. Note Go6983 plus LAT condition showed no significant difference ($P>0.05$) to Go6983 alone. Note that Go6983 treatment has been previously shown by Ashton's group not to effect HK5C evoked GLU release compared to non-drug treated samples.

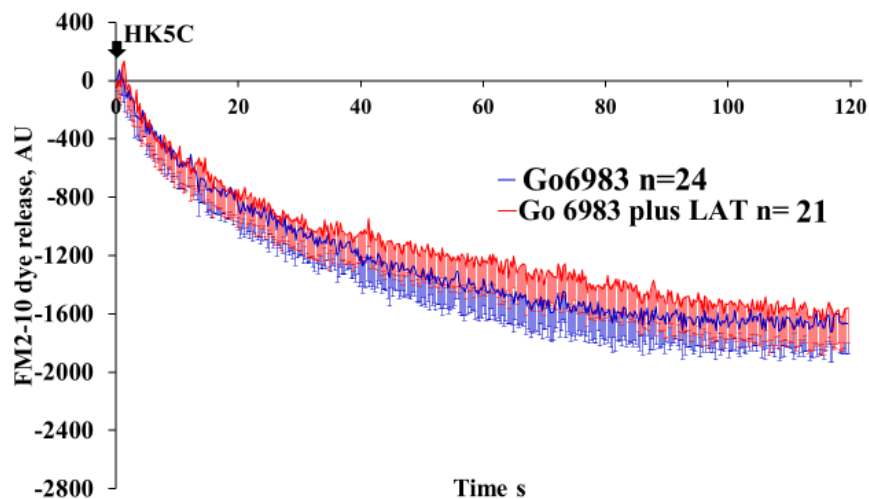


Figure 6.8. PKC inhibition reversed LAT effect on HK5C evoked FM dye release. HK5C evoked FM dye release from 1 μ M Go6983 or 1 μ M Go6983 plus 15 μ M LAT treated terminals. Data are mean \pm SEM, N=3 independent experiments. Note that there was no significant difference ($P>0.05$) in release between Go6983 and Go6983 plus LAT treated terminals. Note that Ashton and colleagues have previously shown that there is no difference in FM dye release between control and Go6983 treated terminals.

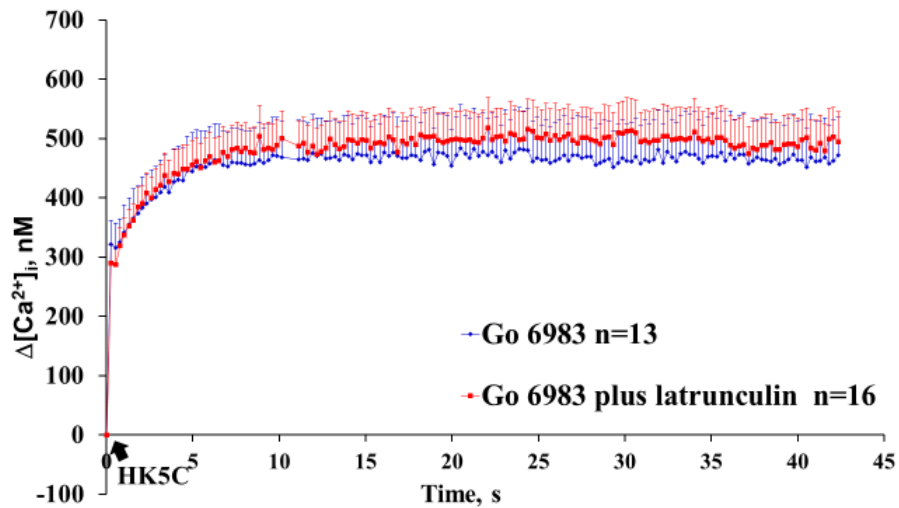


Figure 6.9. PKC inhibition reversed LAT effect on HK5C evoked $\Delta[Ca^{2+}]_i$. Change in $\Delta[Ca^{2+}]_i$ induced by HK5C in 1 μ M Go6983 and 1 μ M Go6983 plus 15 μ M LAT treated terminals. Data are mean \pm SEM, N=4 independent experiments; Note that there is no significant difference ($P>0.05$) in the change in $\Delta[Ca^{2+}]_i$ between Go6983 and Go6983 plus LAT treated terminals. Also note that previously Ashton and colleagues showed that Go6983 did not perturb HK5C evoked $\Delta[Ca^{2+}]_i$ relative to non-drug treated control.

An important control for these experiments is to test whether LAT induces its effects when ION5C is the stimulus and Go6983 treatment is also used, if this is the case, then it is clear that the LAT effect is different for the two distinct stimuli. Indeed, ION5C evoked GLU release in the synaptosomes treated with LAT plus Go6983 compared to Go6983 treatment alone clearly demonstrated that when PKCs are inhibited, LAT perturbed the ION5C evoked release of the RP of GLU containing SVs (Fig 6.10). Recently, Ashton and his colleagues have checked whether LAT could switch the ION5C evoked Dyn dependent RRP KR to FF when PKCs were blocked. Disassembly of the microfilaments did switch the mode even in the presence of Go6983. This highlights a big difference in the action of the 2 stimuli (A.Ashton, unpublished manuscript).

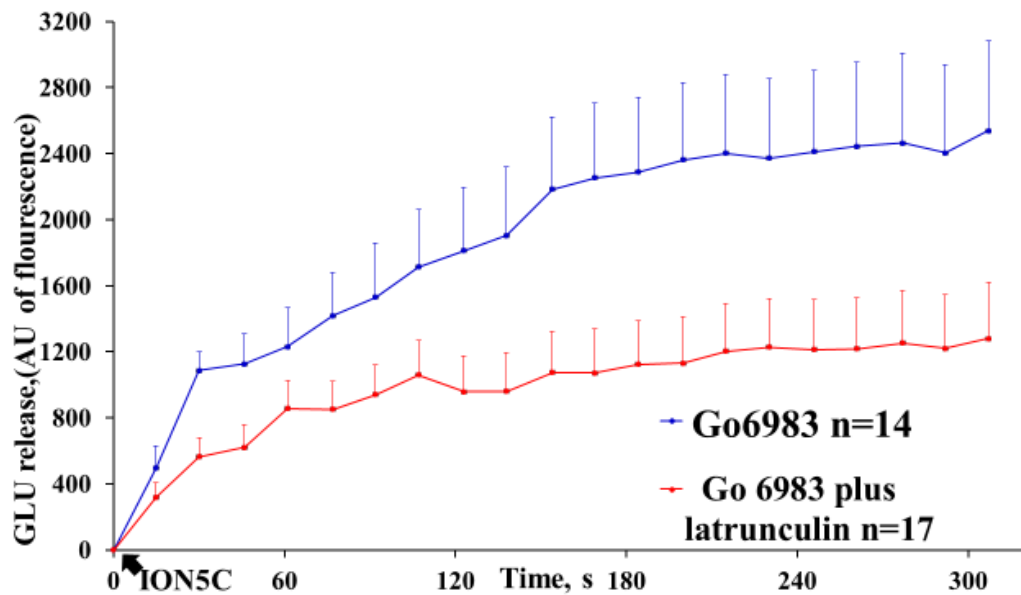


Figure 6.10. PKC inhibition failed to reverse LAT effect on ION5C evoked GLU release. ION5C evoked GLU release in 1 μ M Go6983 and 1 μ M Go6983 plus 15 μ M LAT treated terminals. Data are mean \pm SEM, N=4 independent experiments. Note that there was significant difference in release ($P < 0.05$) between Go6983 plus LAT condition and Go6983 alone.

6.3 Stabilisation of Actin

Disassembly of the actin cytoskeleton with LAT was shown to have effects on SV exocytosis and on release of distinct pools. However, it is possible that stabilisation of actin microfilament may also have an effect. Jasplakinolide (JASP) can be applied to promote actin stabilisation. It stimulates actin filament nucleation, thereby promoting actin polymerisation (i.e. Bubb et al, 1994, 2000). Thus, by performing the equivalent experiment to LAT, we can investigate how stabilisation of actin would impact on the releasing mode of the SVs.

6.3.1 Actin stabilisation does not affect evoked GLU and FM dye release, nor evoked $\Delta[\text{Ca}^{2+}]_i$

Synaptosomes were pre-treated with JASP and HK5C evoked GLU release, FM 2-10 dye and $\Delta[\text{Ca}^{2+}]_i$ were measured. GLU release was found not to be affected in response to actin stabilisation (Fig 6.11). Thus, whilst actin disassembly prevents the release of the RP, actin stabilisation with JASP does not affect the release of this pool. There was no difference in HK5C evoked FM 2-10 dye release between control and JASP treated condition (Fig 6.12) and since the RP of SVs are undergoing exocytosis this would suggest that stabilisation of actin microfilaments does not prevent RRP SVs from undergoing KR. When HK5C evoked $\Delta[\text{Ca}^{2+}]_i$ was measured it was found that JASP treatment actually increased the $\Delta[\text{Ca}^{2+}]_i$ induced by the stimulus (Fig 6.13).

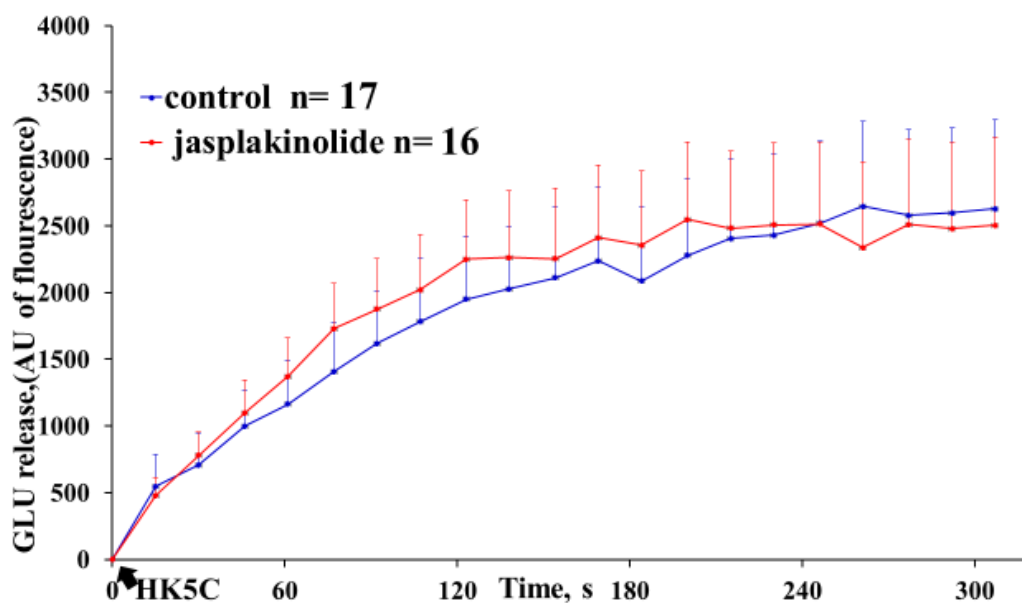


Figure 6.11. Actin stabilisation does not affect HK5C evoked GLU release. HK5C evoked GLU release in control and 2.5 μM JASP treated terminals. Data are mean \pm SEM, N=4 independent experiments; P >0.05. Note that JASP treatment does not affect the HK5C evoked release.

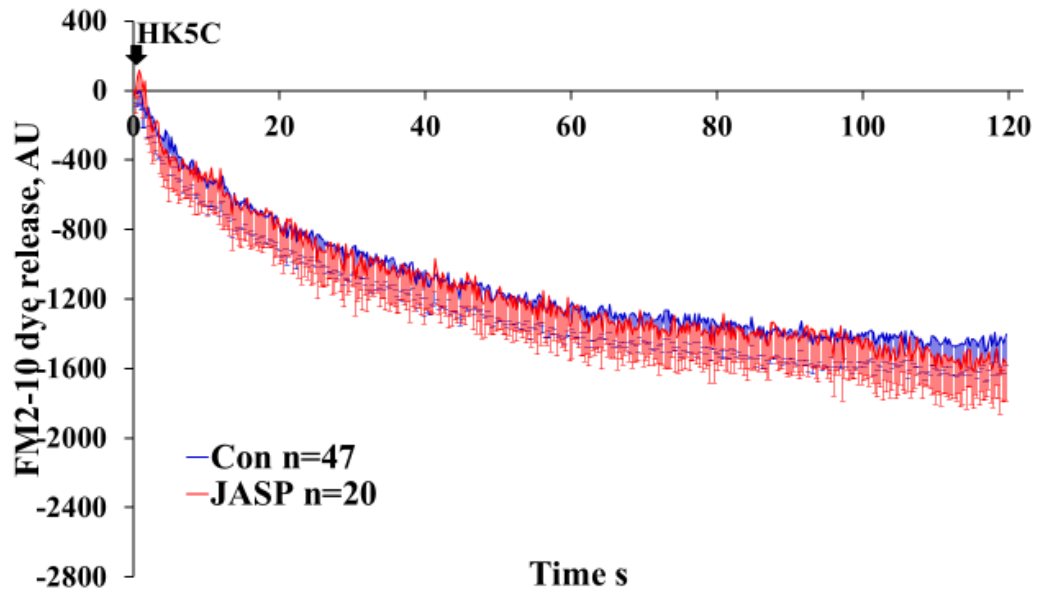


Figure 6.12. Actin stabilisation does not affect HK5C evoked FM dye release. HK5C evoked FM dye release in control and 2.5 μM JASP treated terminals. Data are mean \pm SEM, N=7 independent experiments. Note that there was no apparent significant difference ($P>0.05$) in the release between control and JASP treated synaptosomes.

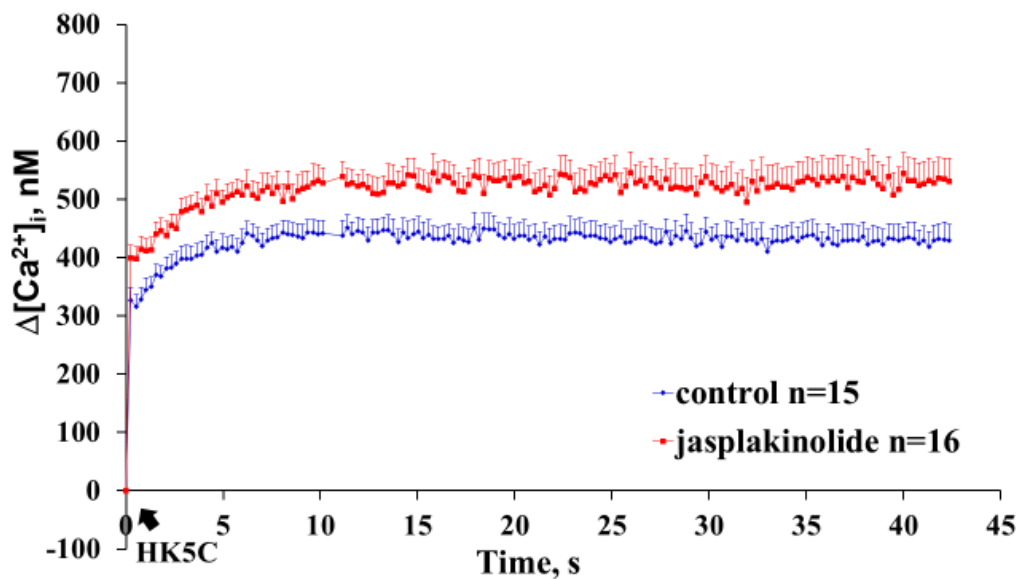


Figure 6.13. Actin stabilisation increase HK5C evoked $\Delta[\text{Ca}^{2+}]_i$. HK5C evoked $\Delta[\text{Ca}^{2+}]_i$ in control and 2.5 μM JASP treated terminals. Data are mean \pm SEM, N=6 independent experiments; Note that the JASP application has actually led to significant increase ($P<0.05$) in the $\Delta[\text{Ca}^{2+}]_i$.

ION5C evoked GLU and FM2-10 release and $\Delta[\text{Ca}^{2+}]_i$ were also measured in the presence of JASP. JASP did not perturb the ION5C evoked release of the RRP and RP of GLU containing SVs (Fig 6.14) nor did it affect the release of FM2-10 dye (Fig 6.15). Finally, stabilisation of actin microfilaments did not perturb the ION5C evoked $\Delta[\text{Ca}^{2+}]_i$ (Fig 6.16). This indicates that the Dyn dependent KR mode of the RRP SVs can still occur when actin microfilaments are stabilised such that you neither get disassembly nor assembly of such filament.

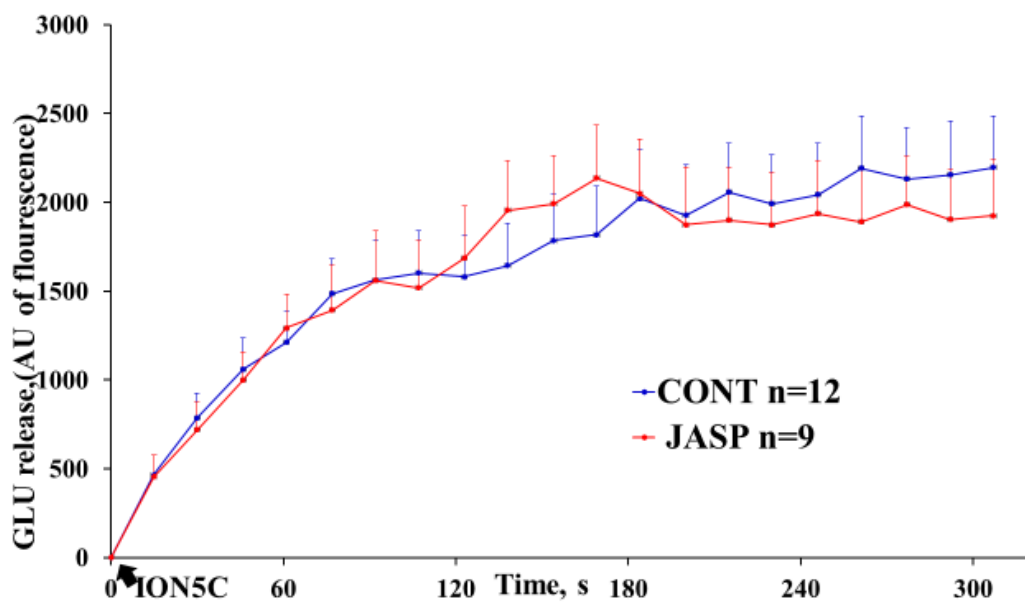


Figure 6.14. Actin stabilisation does not affect ION5C evoked GLU release. ION5C evoked GLU release in control and 2.5 μM JASP treated terminals. Data are mean \pm SEM, N=3 independent experiments. $P > 0.05$. Note that JASP treatment does not affect the ION5C evoked release.

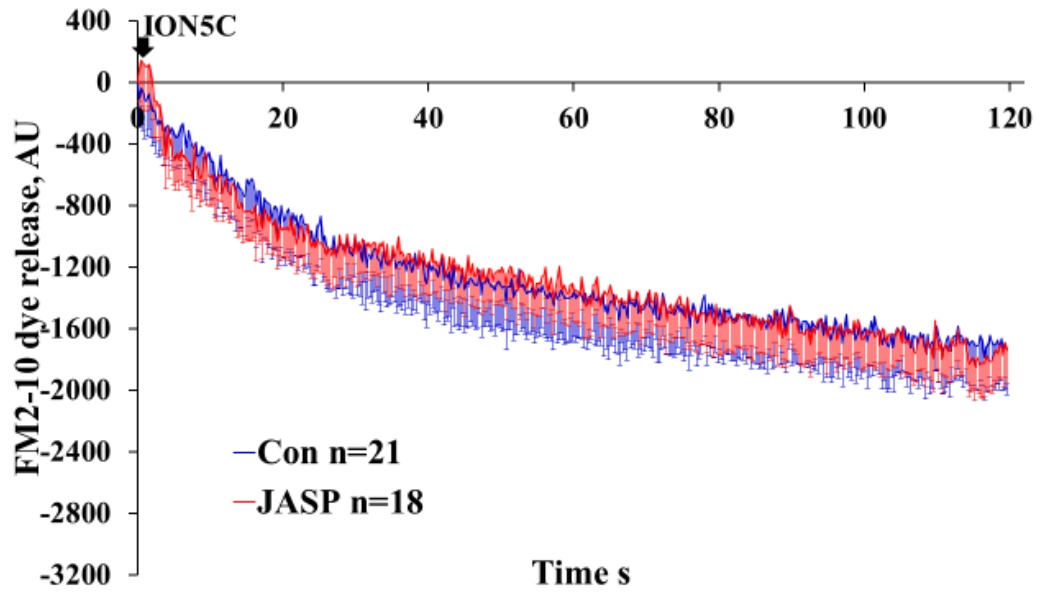


Figure 6.15. Actin stabilisation does not affect ION5C evoked FM dye release. ION5C evoked FM dye release in control and 2.5 μM JASP tested terminals. Data are mean \div SEM, N=3 independent experiments. Note that there was no significant difference ($P>0.05$) in the release between control and JASP treated synaptosomes.

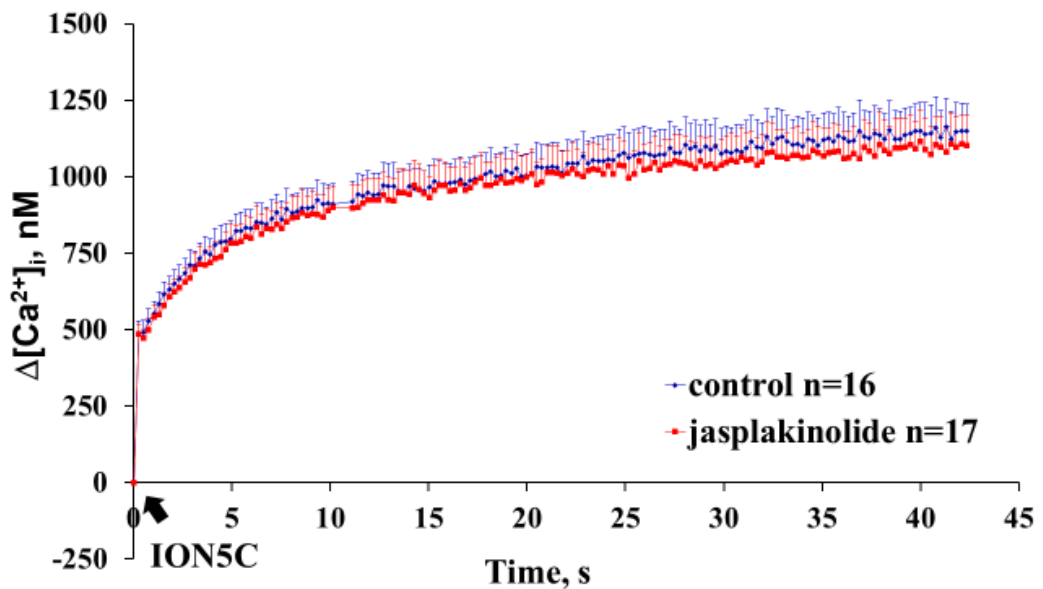


Figure 6.16. Actin stabilisation does not affect ION5C evoked $\Delta[\text{Ca}^{2+}]_i$. ION5C evoked $\Delta[\text{Ca}^{2+}]_i$ in control and 2.5 μM JASP treated terminals. Data are mean \pm SEM, N=6 independent experiments; $P>0.05$; Note that there was no significant difference in the release between control and JASP treated terminals.

6.3.2 JASP treatment reverse LAT's action

As synaptosomes were found to be releasing normally after JASP treatment, this enabled one to check whether any LAT action is truly due to disassembly of actin microfilaments. This is because prior stabilisation of microfilaments with JASP prevents subsequent disassembly of such filament by LAT. Synaptosomes were pre-treated with JASP prior to LAT addition and then GLU release was evoked by HK5C or ION5C. HK5C (Fig 6.17) and ION5C (Fig 6.18) evoked GLU release consisted of the exocytosis of the RRP and RP of SVs after the stabilisation of the actin cytoskeleton indicating that LAT no longer could disassemble such microfilaments. This proves that the previous effects of LAT were due to disassembly of such filaments and were not due to a non-specific secondary effect of this drug.

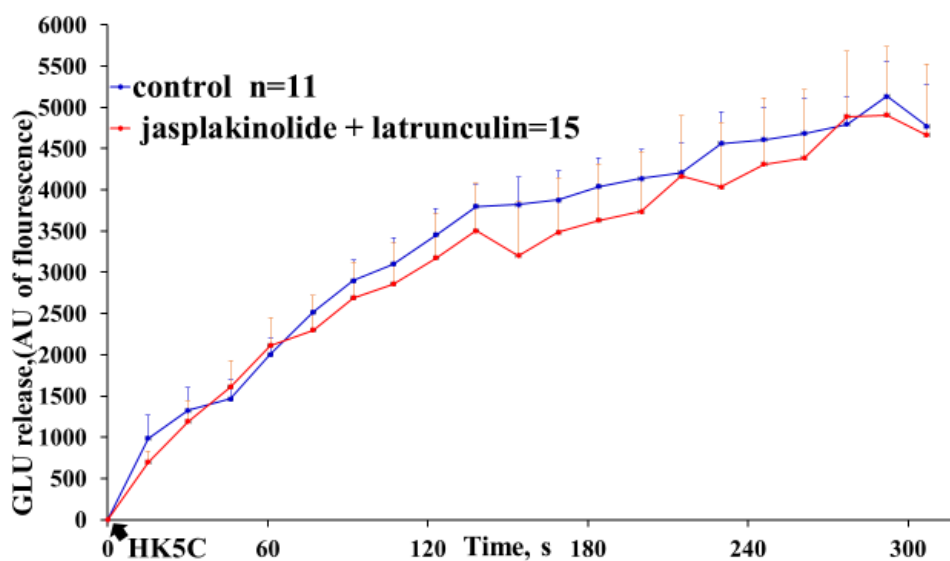


Figure 6.17. Actin stabilisation reverses LAT effect on HK5C evoked GLU release. HK5C evoked GLU release in control and 2.5 μ M JASP plus 15 μ M LAT treated terminals. Data are mean \pm SEM, N=3 independent experiments; P<0.05 for significance. Note that JASP plus LAT treatment does not significantly perturb the release of the RRP and the RP.

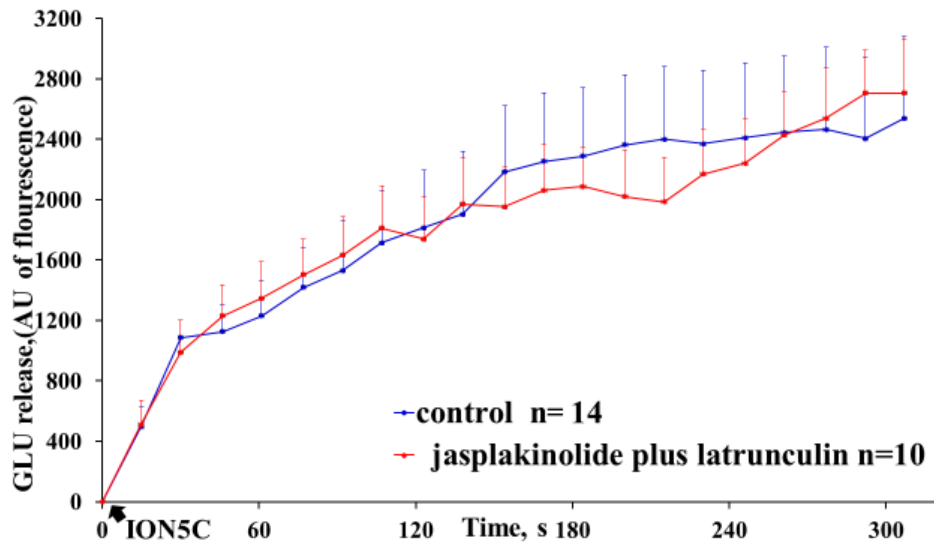


Figure 6.18. Actin stabilisation reverses LAT effect on ION5C evoked GLU release ION5C evoked GLU release in control and 2.5 μ M JASP plus 15 μ M LAT treated terminals. Data are mean \pm SEM, N=4 independent experiments. There is no significant difference ($P>0.05$) between control and JASP plus LAT treated terminals indicating that stabilisation of microfilaments prevents their disassembly by LAT.

6.3.3 LAT does not perturb the HK5C evoked calcium entry in the presence of JASP

Next, we wanted to see how evoked $\Delta[Ca^{2+}]_i$ is affected when LAT is applied to the nerve terminal following JASP pre-treatment. A comparison between LAT alone vs JASP plus LAT condition shown that in the latter condition HK5C produced a significantly higher $\Delta[Ca^{2+}]_i$, implying that truly actin disassembly does reduce the HK5C evoked changes in calcium level but this is prevented by JASP treatment (Fig 6.19b). Indeed, as we saw with JASP alone, there is a slight increase in the HK5C evoked $\Delta[Ca^{2+}]_i$ in the presence of both drugs (Fig 6.19a).

Note, as LAT had no effect on ION5C evoked $\Delta[Ca^{2+}]_i$, there was no reason to do the equivalent experiment.

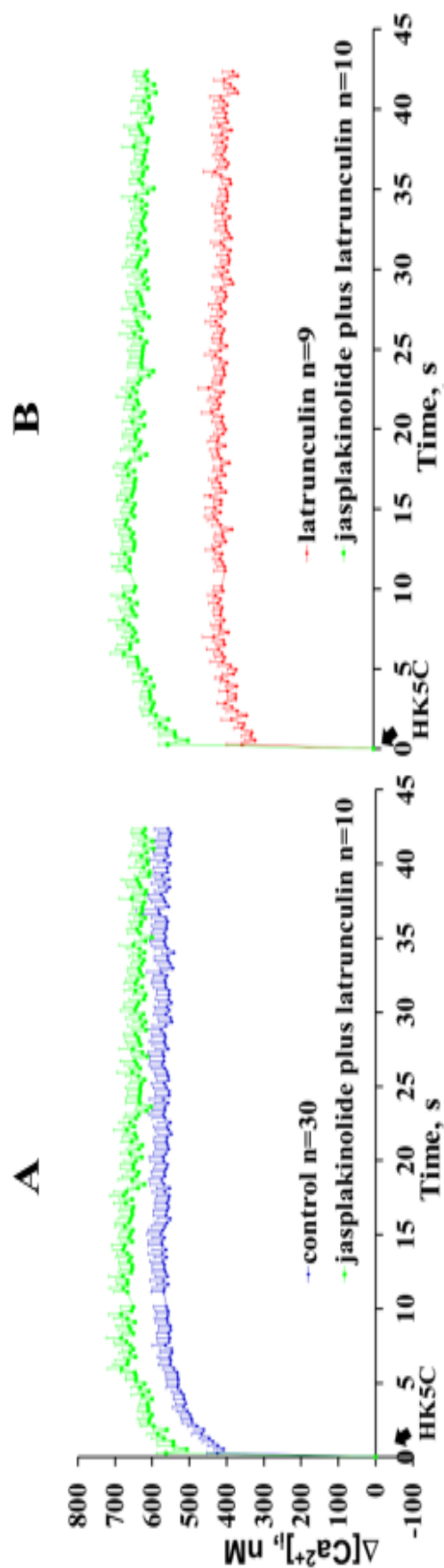


Figure 6.19. Actin stabilisation prevents LAT action on perturbation of HK5C evoked $\Delta[Ca^{2+}]_i$. HK5C evoked $\Delta[Ca^{2+}]_i$ in a) control and 2.5 μ M JASP plus 15 μ M LAT treated terminals b) 15 μ M LAT and 2.5 μ M JASP plus 15 μ M LAT treated terminals. Data are mean \pm SEM, N=4 independent experiments; P>0.05 in a and P<0.05 in b; JASP plus LAT treated terminals exhibit a slightly higher $\Delta[Ca^{2+}]_i$ than control whilst compared to LAT alone, there is a substantially larger $\Delta[Ca^{2+}]_i$ highlighting the fact that JASP treatment has prevented LAT's action on HK5C evoked $\Delta[Ca^{2+}]_i$.

6.3.4 JASP treatment prevents LAT action on evoked FM dye release

The action of LAT in inducing a switch in the RRP SVs from KR to FF for both HK5C and ION5C may not have been due to disassemble of the actin microfilament. However, this was checked by preventing LAT's action by pre-treatment with JASP. As such treatment allowed the RP SVs to be released, we measured the FM dye release under such condition. JASP treatment appeared to prevent LAT action on HK5C evoked FM dye release (Fig 6.20) or ION5C evoked dye release (Fig 6.21).

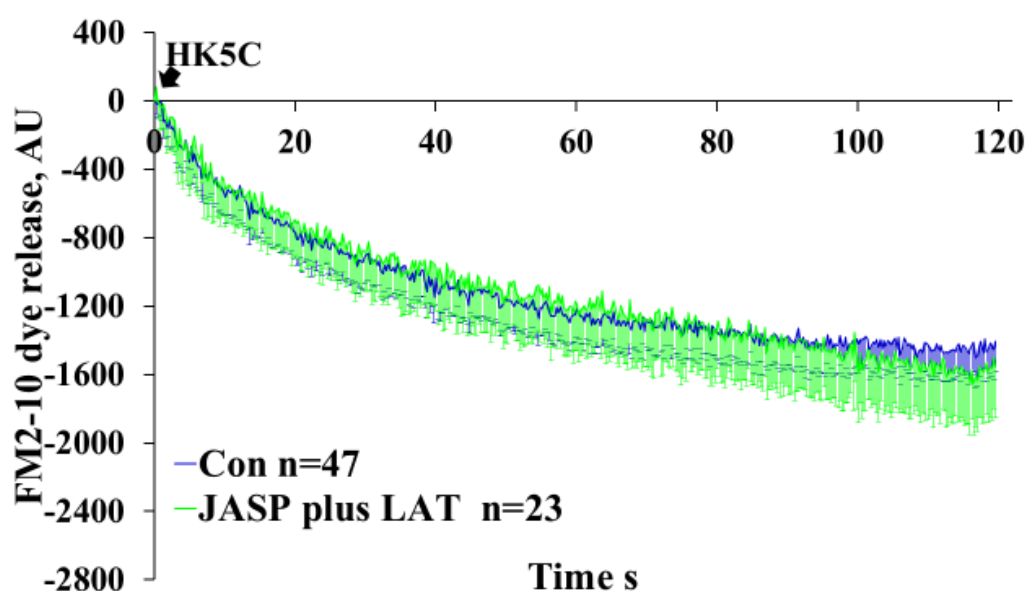


Figure 6.20. Actin stabilisation prevents LAT action on HK5C evoked FM dye release. HK5C evoked FM dye release in control and 2.5 μ M JASP plus 15 μ M LAT treated terminals. Data are mean \pm SEM, N=7 independent experiments; P <0.05 for significant difference. Note that there was no significant difference in the release between control and JASP plus LAT treated synaptosomes.

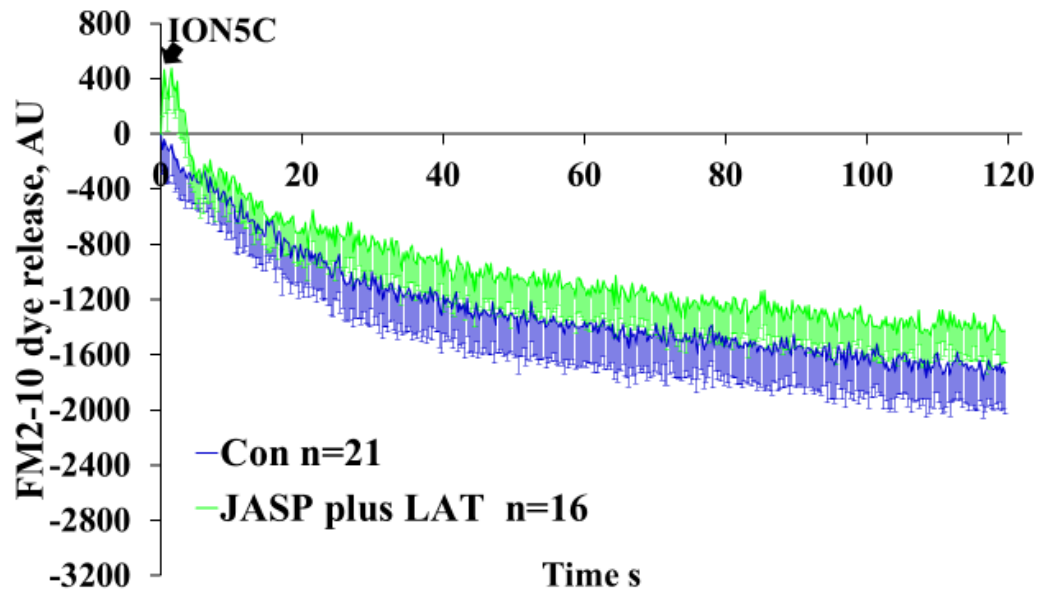


Figure. 6.21 Actin stabilisation prevents LAT action on ION5C evoked FM dye release.
 ION5C evoked FM dye release in control and 2.5 μ M JASP plus 15 μ M LAT treated terminals.
 Data are mean \pm SEM N=3 independent experiments. Note that there was no significant
 difference ($P>0.05$) in the release between control and JASP plus LAT treated synaptosomes.

However, whilst the FM dye release looks similar to the control release in these conditions (Fig 6.20, Fig 6.21), one could argue that this is also the case for LAT alone and so we needed to show that following JASP plus LAT, the RP is releasing via FF and the RRP is releasing via KR whereas for LAT alone, the RP is not releasing and the RRP is releasing via FF. Fortunately, it is possible to test whether the RRP is releasing by KR or FF by also treating the synaptosomes with OA since this drug will switch the RRP undergoing KR to FF (as discussed earlier) whereas it will have no effect on dye release if the RRP is already releasing by FF.

Indeed, JASP plus LAT plus OA was found to allow HK5C (Fig 6.22a) or ION5C (Fig 6.23a) to evoke more FM dye release compared to control, similarly, this further exhibited more HK5C evoked (Fig 6.22b) or ION5C evoked (Fig 6.23 b) FM dye in terminal treated with LAT plus JASP. Finally, the triple treated terminals exhibited more FM dye release evoked by HK5C (Fig 6.22c) or ION5C (Fig 6.23 c) then in LAT plus OA treated synaptosomes.

These results are convincing because it indicates that JASP prevents the LAT from removing the RP of SVs and that these undergo normal FF, whilst RRP of the SVs now undergo KR. This is demonstrated by a comparison between JASP plus LAT and JASP plus LAT plus OA treated terminals, in which more release was measured in the latter treatment condition. Likewise, it is clear that LAT does remove the RP from releasing and switches the RRP to FF since LAT plus OA produces no extra release evoked by either stimuli. Very recently, it was shown by A.Ashton's group that this inclusion of OA with any of these other treatments did not change the amount of HK5C or ION5C evoked GLU release. This was assumed to be the case in the studies repeated herein but this has now been verified.

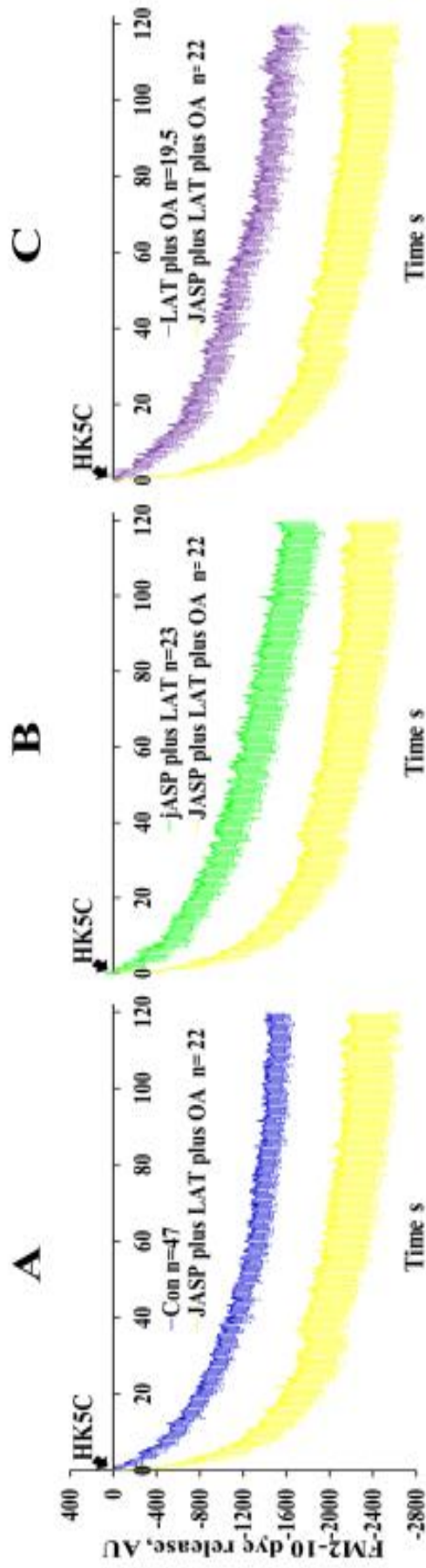


Figure 6.22. Actin stabilisation prevents the LAT from inducing RRP to undergo KR. HK5C evoked FM dye from terminal treated with a) no-drug (control) and 2.5 μM JASP plus 15 μM LAT plus 0.8 μM OA b) 2.5 μM JASP plus 15 μM LAT and 2.5 μM JASP plus 15 μM LAT plus 0.8 μM OA c) 15 μM LAT plus 0.8 μM OA and 2.5 μM JASP plus 15 μM LAT plus 0.8 μM OA. Data are mean \pm SEM, N=7 independent experiments. Note that there were significant difference ($P < 0.05$) in all sets of data. JASP plus LAT plus OA in all conditions released higher level of FM dye meaning the presence of OA induced switch of the mode to FF except from treatment with LAT where LAT has already switched the RRP to a FF mode.

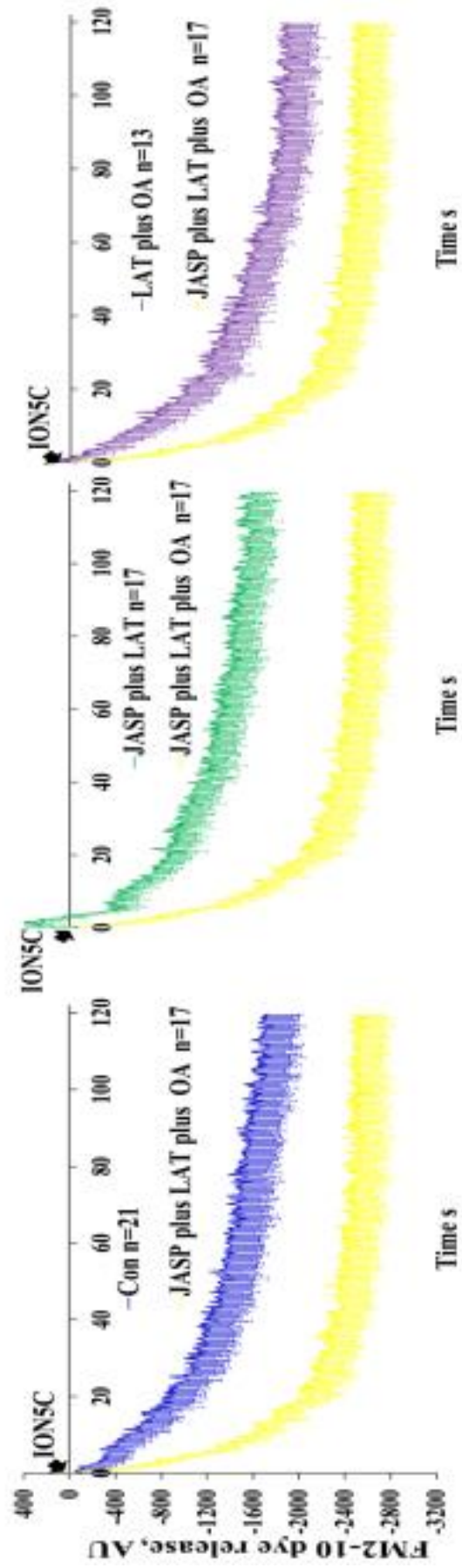


Figure 6.23. . Actin stabilisation prevents the LAT from inducing RRP to undergo KR_ION5C evoked FM dye from terminal treated with a) no-drug (control) and 2.5 μ M JASP plus 15 μ M LAT plus 0.8 μ M OA b) 2.5 μ M JASP plus 15 μ M LAT and 2.5 μ M JASP plus 15 μ M LAT plus 0.8 μ M OA c) 15 μ M LAT plus 0.8 μ M OA and 2.5 μ M JASP plus 15 μ M LAT plus 0.8 μ M OA. Data are mean \pm SEM, N=3 independent experiments. Note that there were significant difference ($P < 0.05$) in all sets of data. JASP plus LAT plus OA in all conditions released higher level of FM dye meaning the presence of OA induced switch of the mode to FF except from treatment with LAT where LAT has already switched the RRP to a FF mode.

6.4 Bioenergetics

6.4.1 LAT

The Synaptosomes were treated with 15 μM LAT for 5-10 min at 37°C in order to allow actin microfilament disassembly. However, such treatment failed to disturb any of the bioenergetics parameters measured, confirming that the drug does not have non-specific effect on the bioenergetics (Figure 6.24, Figure 6.25a-f).

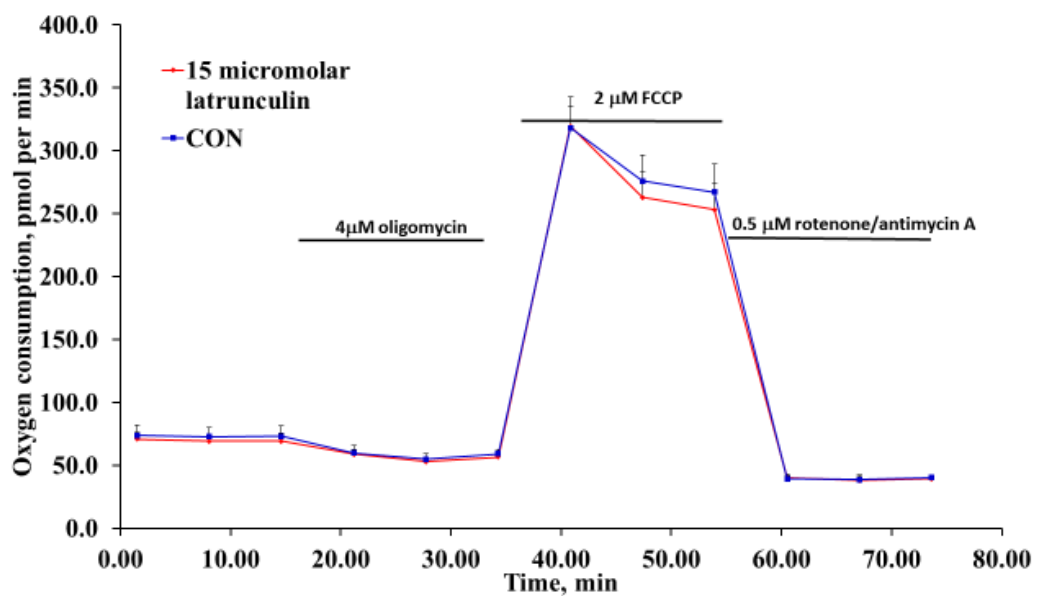


Figure 6.24. Synaptosomal bioenergetics were unaffected by 15 μM LAT treatment. The effect of 15 μM LAT on the bioenergetics of synaptosomes. The experiment was conducted twice and the mean values represent an average of 6 independent measurements and error bars represent the SD.

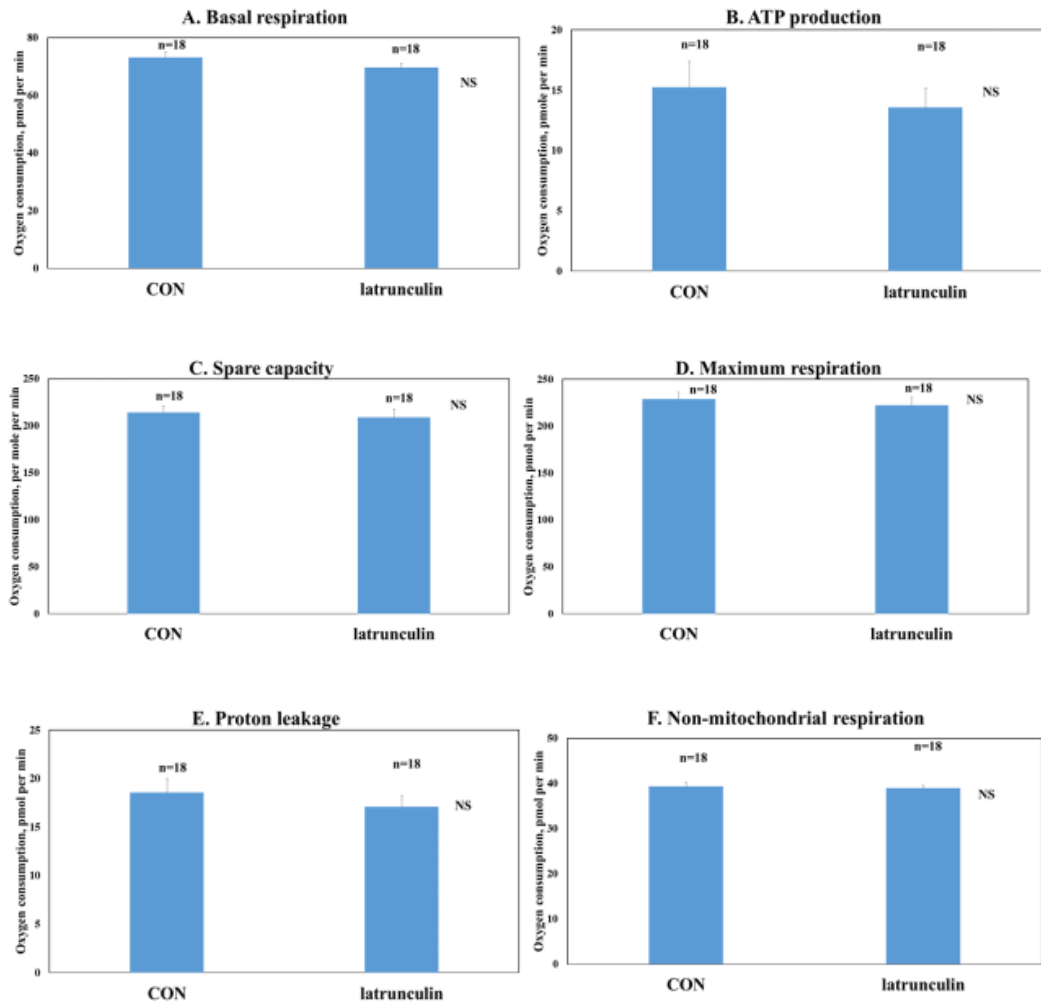


Figure 6.25. 15 μ M LAT treatment did not perturb any bioenergetics parameters measured as it looks similar to those for the controls. The effect of 15 μ M LAT on (A) basal respiration, (B) ATP production, (C) spare capacity, (D) maximal respiration, (E) Proton leakage, and (F) Non-mitochondrial respiration in synaptosomes. The histobars represent the mean and the error bar shows the SEM.

6.4.2 Go6983 plus LAT

The double drug treatment of synaptosomes with Go6983 and LAT failed to perturb in any of the bioenergetics parameters measured (Figure 6.26, Figure 6.27 a-f).

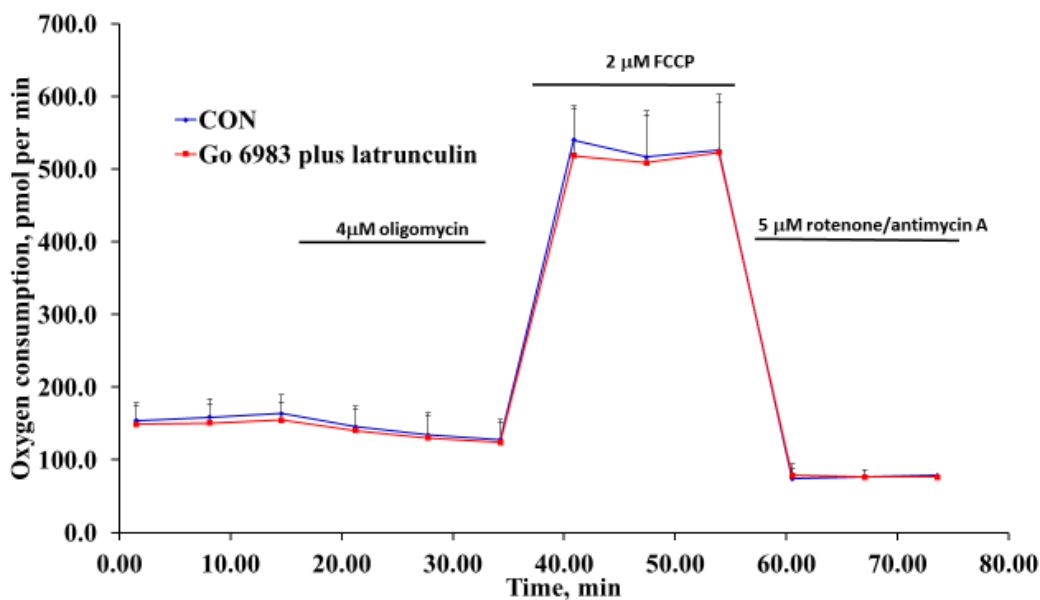


Figure 6.26. Synaptosomal bioenergetics were unaffected by dual treatment of 1 μM Go6983 and 15 μM LAT treatment. The effect of 1 μM Go6983 plus 15 μM LAT treatment on the bioenergetics of synaptosomes compared to nondrug treated control. The experiment was conducted three times and the mean values represent an average of 8 independent measurements and error bars represent the SD; P>0.05.

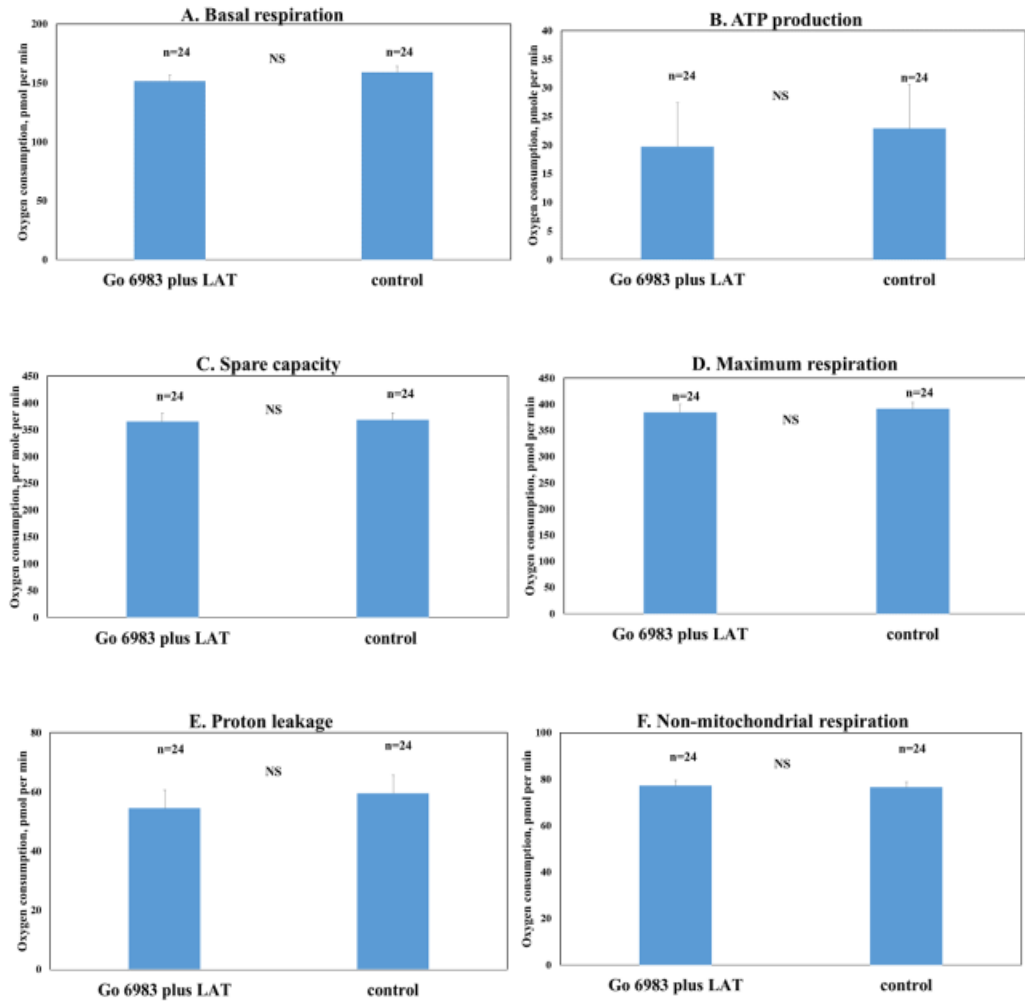


Figure 6.27. 1 μ M Go6983 and 15 μ M LAT double treatment did not perturb any bioenergetics parameters measured as it looks similar to those for the controls. The effect of 1 μ M Go6983 plus 15 μ M LAT on (A) basal respiration, (B) ATP production, (C) spare capacity, (D) maximal respiration, (E) Proton leakage, and (F) Non-mitochondrial respiration of synaptosomes compared to non-drug treated terminal. The histograms represent the mean and the error bar shows the SEM.

6.4.3 JASP

Treatment of synaptosomes with 2.5 μM JASP for 10-20 min at 37°C was found to produce a slight difference in non-mitochondrial respiration compared to control. However, the change was minor and it failed to disturb any of the other bioenergetics parameters (Figure 6.28, Figure 6.29 a-f).

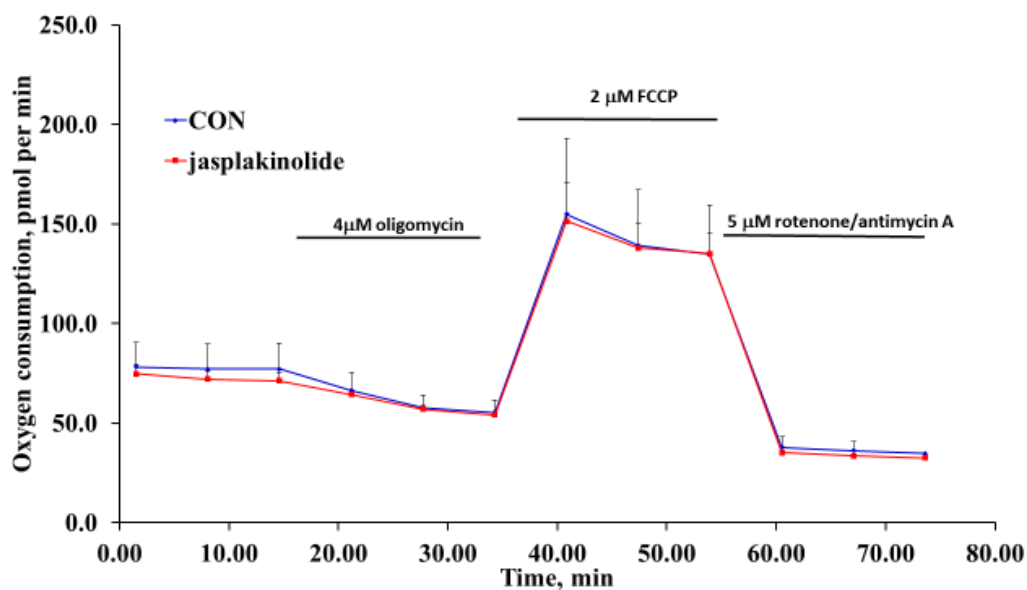


Figure 6.28. Synaptosomal bioenergetics were unaffected by 2.5 μM JASP treatment. The effect of 2.5 μM JASP on the bioenergetics of synaptosomes. The experiment was conducted three times and the mean values represent an average of 6-7 independent measurements and error bars represent the SD; $P > 0.05$.

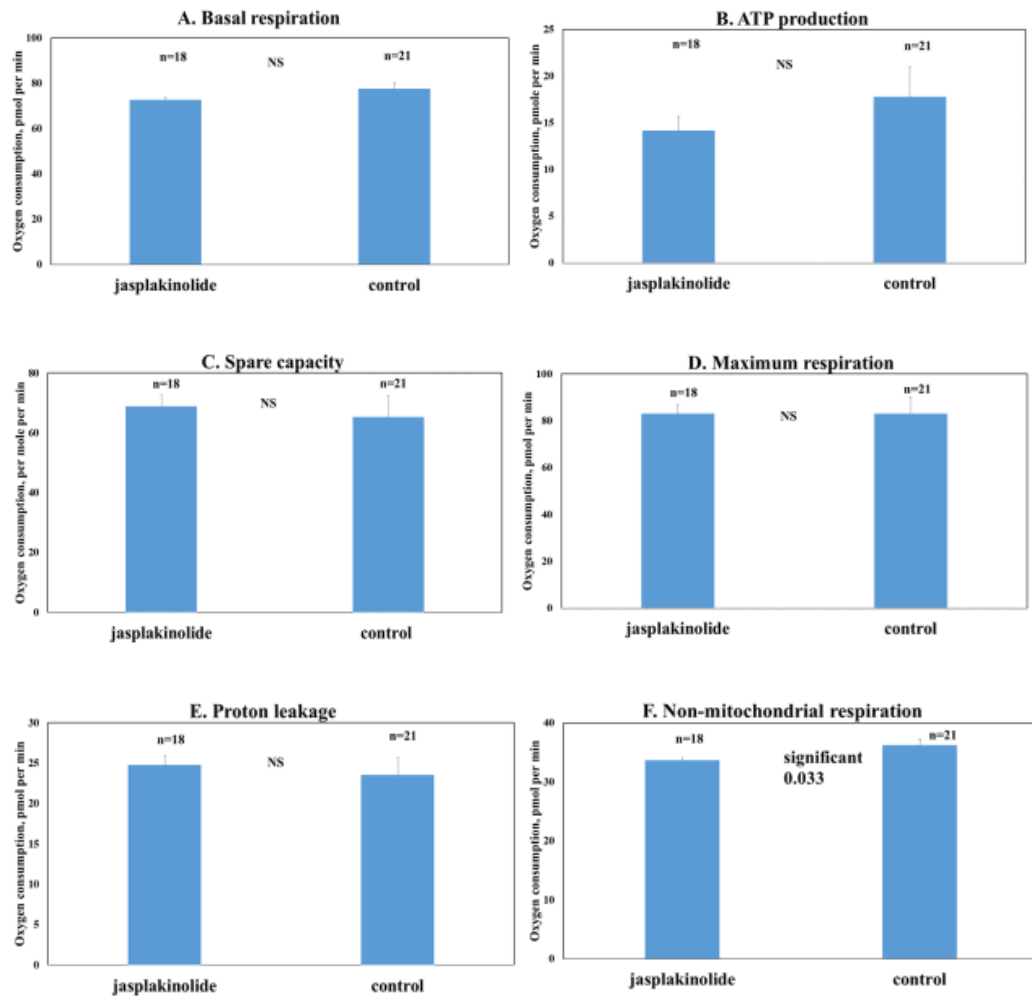


Figure 6.29. 2.5 μ M JASP treatment did not perturb most of bioenergetics parameters measured as it looks similar to those for the controls. The effect of 2.5 μ M JASP on (A) basal respiration, (B) ATP production, (C) spare capacity, (D) maximal respiration, (E) Proton leakage, and (F) Non-mitochondrial respiration in synaptosomes compared to non-drug treated control. The histograms represent the mean and the error bar shows the SEM.

6.4.4 JASP plus LAT

Synaptosomes were pre-treated with 2.5 μM JASP for 20 min at 37°C and LAT (for the last 10 min of this incubation). Such conditions failed to disturb any of the bioenergetics parameters measured (Figure 6.30, Figure 6.31 a-f)

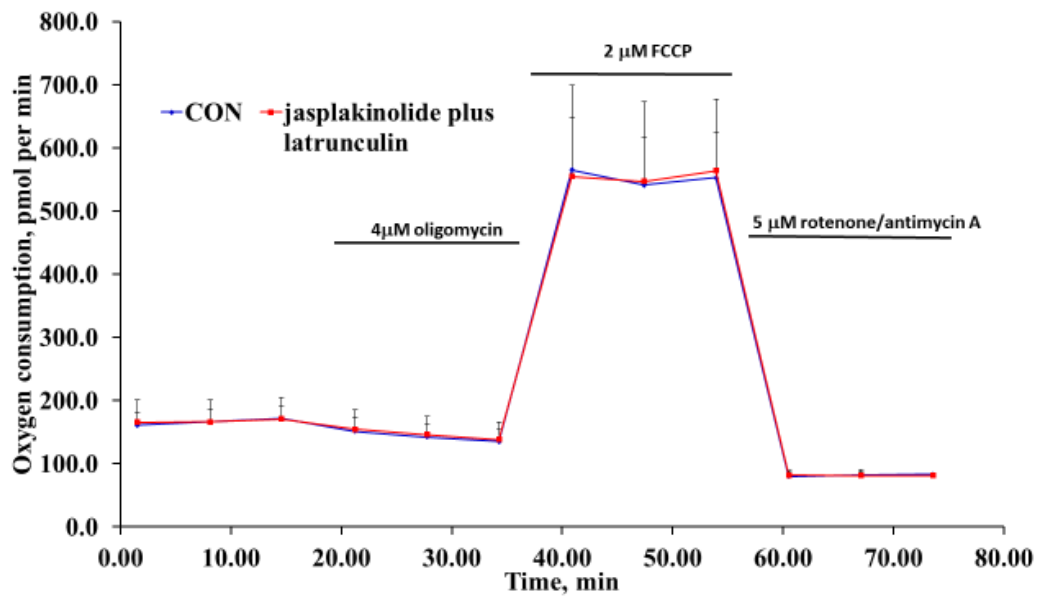


Figure 6. 30. Synaptosomal bioenergetics were unaffected by 2.5 μM JASP and 15 μM LAT double treatment. The effect of 2.5 μM JASP plus 15 μM LAT treatment on the bioenergetics of synaptosomes. The experiment was conducted three times and the mean values represent an average of 8 independent measurements and error bars represent the SD; $P > 0.05$.

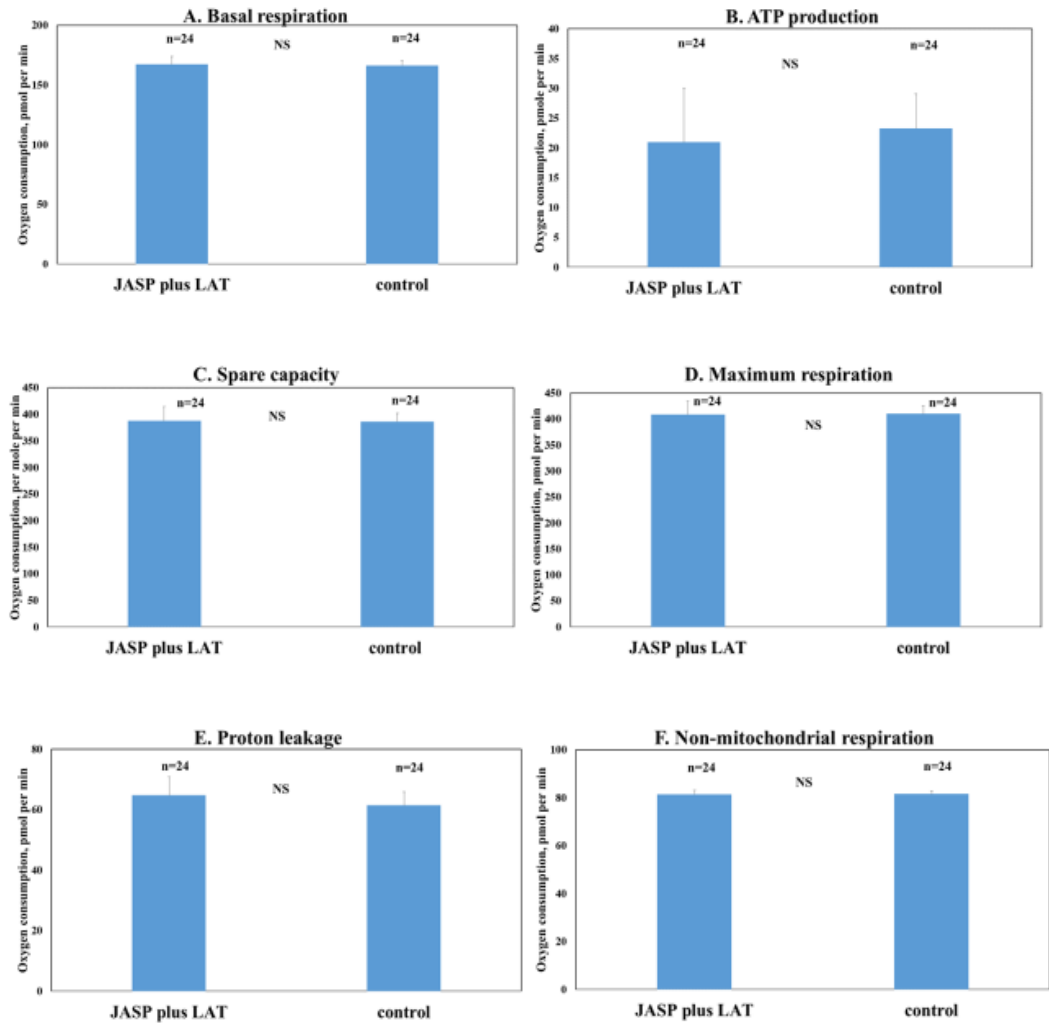


Figure 6.31. 2.5 μ M JASP and 15 μ M LAT double treatment did not perturb any bioenergetics parameters measured as it looks similar to those for the controls. The effect of 2.5 μ M JASP plus 15 μ M LAT treatment on (A) basal respiration, (B) ATP production, (C) spare capacity, (D) maximal respiration, (E) Proton leakage, and (F) Non-mitochondrial respiration in synaptosomes compared to non-drug treated control. The histograms represent the mean and the error bar shows the SEM.

6.4.5 LAT plus JASP plus OA

The Triple drug treatment of synaptosomes with 2.5 μM JASP for 10 min at 37°C followed by a further 10 min at 37°C with 15 μM LAT and 0.8 μM OA failed to produce any changes in the bioenergetics parameters of the treated terminals. Note that last 3 points were not present for one of the experiment and so these values could not be averaged. Consequently, protein leakage and non-mitochondrial respiration values are missing (Figure 6.32, Figure 6.33).

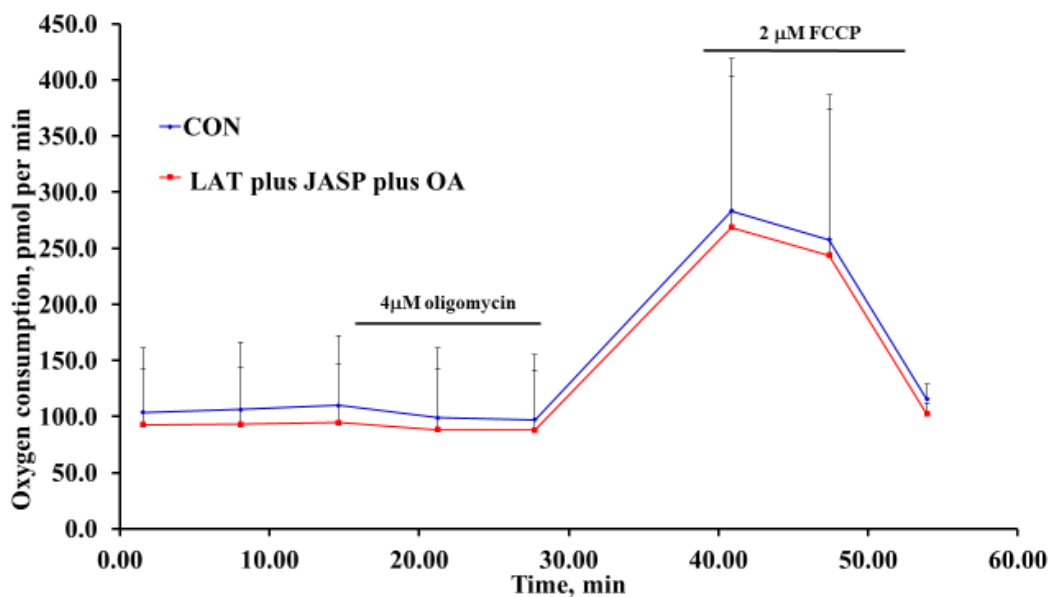


Figure 6.32. Synaptosomal bioenergetics were unaffected by 15 μM LAT, 2.5 μM JASP and 0.8 μM OA triple treatment. The effect of 15 μM LAT plus 2.5 μM JASP plus 0.8 μM OA on the bioenergetics of synaptosomes. The experiment was conducted twice and the mean values represent an average of 6 independent measurements and error bars represent the SD. Note that last three points were not present in one of the experiments, and thus these values were not averaged.

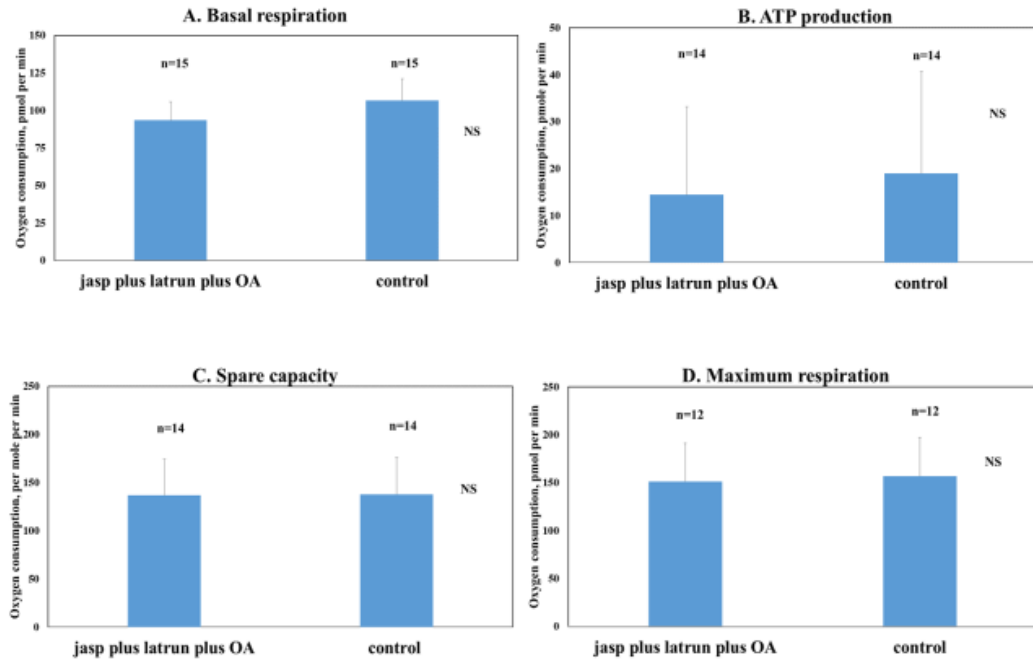


Figure 6.33. 2.5 μ M JASP, 15 μ M LAT and 0.8 μ M OA triple drug treatment did not perturb any bioenergetics parameters measured as it looks similar to those for the controls. The effect of triple drug treatment of 2.5 μ M JASP plus 15 μ M LAT plus 0.8 μ M OA on (A) basal respiration, (B) ATP production, (C) spare capacity, (D) maximal respiration in synaptosomes compared to non-drug treated control. The histobars represent the mean and the error bar shows the SEM.

#	Figure #	Assays	Stimulus	Drugs employed (conc.)	Key findings
1	6.1	GLU	4AP5C HK5C, ION5C	LAT (15 μ M)	The RP release is perturbed when actin is disassembled.
2	6.2- 6.3	FM	HK5C, ION5C	LAT (15 μ M), OA (0.8 μ M)	The mode of RRP release has changed to FF and this was confirmed by including OA.
3	6.4- 6.5	Fura-2	HK5C, ION5C	LAT (15 μ M)	LAT treatment reduced the HK5C evoked $\Delta[Ca^{2+}]_i$ but not ION5C evoked $\Delta[Ca^{2+}]_i$. Thus the action of LAT on ION5C evoked GLU containing SV RP release and its action on ION5C evoked FM dye release from the RRP SVs are not related to any changing in evoked $\Delta[Ca^{2+}]_i$. Although, the action of LAT on HK5C evoked GLU and FM release could be explained by changing in $\Delta[Ca^{2+}]_i$.
4	6.6	GLU	HK20C	LAT (15 μ M)	Higher $[Ca^{2+}]_e$ did not rescue the LAT effect on the RP release.
5	6.7- 6.10	GLU, FM, Fura-2	HK5C, ION5C	LAT (15 μ M), Go6983 (1 μ M)	PKC inhibition prevented the LAT induced effect in all release parameters for HK5C but not ION5C. One possible interpretation is that the action of LAT on HK5C evoked release involve in some way the activation of PKCs, since when these are blocked, the drug did not induce any effect.
6	6.11- 6.16	GLU, FM, Fura-2	HK5C, ION5C	JASP (2.5 μ M)	Actin stabilisation does not affect evoked GLU, FM dye release, nor evoked $\Delta[Ca^{2+}]_i$
7	6.17- 6.19	GLU, Fura-2	HK5C, ION5C	JASP (2.5 μ M) LAT (15 μ M)	JASP treatment reverse LAT's action on evoked GLU release and evoked $\Delta[Ca^{2+}]_i$. This proves that the previous effects of LAT were due to disassembly of such filaments and were not due to non-specific secondary effect of this drug.
8	6.20- 6.23	FM	HK5C, ION5C	JASP (2.5 μ M), LAT (15 μ M), OA (0.8 μ M)	<ul style="list-style-type: none"> - JASP treatment prevented LAT action on HK5C evoked FM dye release or ION5C evoked dye release. - OA was used to test whether RRP is releasing by KR or FF. Indeed, OA inclusion to JASP plus LAT condition was found to evoke more FM dye release compared to control and in terminal treated with LAT plus JASP. - Also, the triple treated terminals exhibited more evoked FM dye release compared to LAT plus OA treated synaptosomes. These results indicate that JASP prevents the LAT from removing the RP of SVs and that these undergo normal FF, whilst RRP of the SVs now undergo KR. - Likewise, it is clear that LAT does remove the RP from releasing and switches the RRP to FF
9	6.24- 6.33	BIO		All drugs tested	Majority of bioenergetics parameters in drug treated synaptosomes were unaltered compared to control.

Figure 6.33. Summary of the findings in chapter 6.

6.5 Discussion

In this chapter, we have investigated the role of the actin cytoskeleton on regulating both the release of the SV content and SV mode of exocytosis. We have investigated this using ION5C (a stimuli known to induce Dyn dependent KR) and HK5C (a stimuli known to induce NM-II dependent KR) to stimulate on terminals in which LAT treatment has induced actin disassembly or in terminal in which microfilament have been stabilised by JASP pre-treatment.

6.5.1 Effect of actin disassembly on the release of SV pools and on the exocytotic mode

Disassembly of actin with LAT was found to inhibit some HK5C and ION5C evoked GLU release. As GLU released by 4AP5C stimulation was not perturbed, it would appear that LAT perturbs the RP release but not the RRP release. However, such drug treatment would appear not to inhibit any FM dye release (note the RRP and RP are labelled normally with the dye). This result is misleading because we know that the RP, that normally releases FM2-10 dye because it undergoes FF, is not being released. Therefore, the dye release measured must be from RRP undergoing FF, whereas under control conditions the RRP does not release the dye since it undergoes KR. The conclusion must be that following the disassembly of actin microfilament with LAT, RRP SVs evoked to release by HK5C or ION5C are switched to FF. Proof for this was provided by the fact that OA added to LAT treated terminals did not allow any HK5C or ION5C evoked the further FM dye release indicating that the RRP was already releasing through the FF mode of exocytosis.

$\Delta[\text{Ca}^{2+}]_i$ evoked by HK5C stimulation, but not that evoked by ION5C, was reduced in LAT treated synaptosomes. This indicates that the action of LAT in blocking ION5C evoked RP release and on switching the ION5C release of the RRP to FF are not related to the change in ION5C evoked $\Delta[\text{Ca}^{2+}]_i$ whilst the results for HK5C may be explained by

a reduction in the HK5C evoked $\Delta [Ca^{2+}]_i$. This leads to the idea that whilst actin microfilaments could have a direct effect on the Dyn dependent KR mode (induced by ION5C stimulation) by regulating the closure of the FP, this cytoskeleton might not have a direct effect on the NM-II dependent KR mode (triggered by HK5C stimulation) and the results could be simply due to a reduction in evoked $\Delta[Ca^{2+}]_i$. However, the use of a higher $[Ca^{2+}]_e$ level (20 mM) by employing a HK20C stimulus failed to reverse the action of LAT on the block of the RP. Note Ashton and colleagues have demonstrated that the RRP SV undergoing KR depends on the $[Ca^{2+}]_i$ (A.Ashton *et al*, unpublished) and, indeed, this explains why 4AP5C only induces some KR since it does not induce a high enough $\Delta[Ca^{2+}]_i$ (see appendix 1 Fig A5 and A6). Furthermore, too low of $\Delta[Ca^{2+}]_i$ is unable to release the RP of SVs as determined with 4AP5C (appendix 1 Fig A1, A5, and A6)

We tried to establish whether it could be that the actin cytoskeleton effects seen depend on whether Dyn or NM-II are regulating the FP because Go6983 causes HK5C to act on the Dyn dependent pathway. We measured HK5C evoked release in Go6983 treated terminals in the presence or absence of LAT. If LAT exerted its effects on the FP similarly for both HK5C and ION5C stimuli then one might expect that HK5C would work on the Dyn dependent pathway following PKC blocking with Go6983 in a similar manner to ION5C. However, this was not the case and it would appear that the effect of LAT on HK5C evoked release involves in some way the activation of PKCs, because following blockade of these enzymes, LAT failed to affect the release of the RP and the mode of exocytosis of the RRP. However, for the ION5C stimulation LAT still induced the changes expected in terminals also treated with Go6983 treatment. Therefore, it would appear that the effect of LAT action differs for the two stimuli.

6.5.2 The effect of stabilisation of the actin cytoskeleton on the release of the pools of SVs and on their release mode

We employed JASP, a drug that promotes the stabilisation of actin microfilaments, to test how it would affect the pools of SVs and their mode of release. JASP was found not to perturb HK5C or ION5C evoked GLU release or FM dye release. Intriguingly, JASP pre-treatment led to a slight increase in HK5C evoked $\Delta[\text{Ca}^{2+}]_i$. We also checked whether stabilisation of actin microfilaments (by pre-treatment with JASP) could prevent the actions of LAT. This test demonstrates whether any LAT action is truly due to microfilament disassembly. After the actin cytoskeleton is stabilised by JASP, LAT no longer exerts any action as both HK5C and ION5C evoked GLU release of both the RRP and the RP of SVs. Thus, the action of LAT in blocking the evoked release of RP was truly due to the disassembly of actin microfilaments. Furthermore, it was apparent that actin disassembly did reduce the HK5C evoked $\Delta[\text{Ca}^{2+}]_i$ because JASP reversed this action of LAT. In fact, there was a slight elevation in the HK5C evoked $\Delta[\text{Ca}^{2+}]_i$ in the presence of both drugs to a similar extent to that seen with JASP alone. Although, FM dye release evoked by HK5C or ION5C appeared to be similar to control release in JASP plus LAT treated terminals but unlike LAT treatment alone, it was assumed that this was due to the RP being released by FF whilst the RRP is releasing KR. We treated synaptosomes with OA to prove this, as if the RRP was undergoing KR it should now switch to FF and so more dye would be released. By comparing synaptosomes treated with JASP plus LAT with or without OA, the results clearly demonstrated that JASP stops the LAT removing the RP of SVs and that these undergo normal FF, whilst RRP of SVs now undergo KR but OA switches this. Likewise, it was apparent that LAT treatment does remove the RP from releasing and switches the RRP to FF since the pre-treatment with LAT followed by OA does not allow any further FM dye release. Whilst we can suggest that actin microfilaments may play a role in the Dyn mediated closure of the KR FP, we actually cannot make a conclusion about the role of this cytoskeletal component for NM-II mediated KR because

LAT actually perturbs the HK5C stimulus. One possible future experiment would be to switch ION5C action to the NM-II pathway by including 40 nM PMA in the experiment (previously shown by Asthon's group e.g. Bhuva, 2015; Singh, 2017; see appendix 1 Fig A14 and A15). Then one could measure the effect of LAT on this stimulus. This maybe complicated because of the suggestion that PKCs themselves maybe affected by LAT.

6.5.3 Bioenergetics

The Drug treatments employed in this chapter include LAT, Go6983, JASP, LAT plus JASP, LAT plus JASP plus OA. Although, the results obtained from performing such drug treatments appeared to be specific and could be explained by action on the pools and modes of SVs, it was important to ascertain that none of these drug treatment induced non-specific effects. One possible non-specific action could be to perturb the bioenergetics of the terminals as this would clearly Affect SV release. We tested this using Seahorse XFp analyser and the mito stress test. By carrying out such measurements, we found that the majority of bioenergetics parameters in drug treated synaptosomes were unaltered compared to non-drug treated terminals. Any changes seen were very minor and unlikely to affect the SV exocytosis. Overall, such data confirm that the effects of all drug treatments identified in this chapter were not from detrimental effects of the drugs on the bioenergetics of the synaptosomes.

6.6 Conclusion

In conclusion, the role of the actin cytoskeleton in regulating both the release of SV pools and the exocytotic mode of such vesicles has been investigated in this chapter. Disassembly of actin microfilament with LAT was discovered to inhibit the HK5C and ION5C evoked RP release, and it was also shown to change the mode of RRP release from KR to FF. However, whilst LAT treatment led to a significant reduction in HK5C $\Delta[\text{Ca}^{2+}]_i$; this did not perturb ION5C stimulation of $\Delta[\text{Ca}^{2+}]_i$. This could mean that whilst the actin microfilaments could have a direct effect on the Dyn dependent KR mode (induced by

ION5C stimulation) regarding to the closure of the FP, actin microfilament might not have a direct effect on the NM-II dependent KR mode (triggered by HK5C stimulation). A difference in the action of LAT with these 2 stimuli was further shown by dual treatment with LAT and Go6983 (that inhibits PKCs) because whilst this did not prevent the action of microfilament disassembly on ION5C evoked events it totally reversed any action of LAT on HK5C evoked GLU release, FM dye release, and $\Delta[\text{Ca}^{2+}]_i$. This suggests that the actual mechanism whereby HK5C induces SV exocytosis may be perturbed by disrupting actin microfilaments.

Actin stabilisation with JASP was also tested. In contrast to disassembly, stabilisation of actin was found not to reduce HK5C or ION5C evoked GLU release or disturb the mode of SV exocytosis as measured by FM dye release. JASP treatment was also found to antagonise LAT effect, proving the actions of LAT measured were truly due to disassembly of microfilaments. This result with JASP is interesting as it means that neither the release of the pools or the modes of exocytosis require changes in actin assembly at the point of SV fusion. This is because, by stabilising microfilament, no new microfilament was allowed to assemble.

Chapter 7:

General Discussion

7.1 Results

Synaptic transmission is the basis of neuronal networking and disturbances of this process are associated with the pathophysiology of numerous neuronal and psychiatric disorders. Therefore, it is important to elucidate the molecular mechanism of synaptic vesicle (SV) exocytosis. SVs are small, electron-lucent vesicles that are clustered at presynaptic terminal. They store neurotransmitters and release them by calcium triggered exocytosis (Takamori, 2009). In the nerve terminal, they are organised in three distinct pools; readily releasable pool (RRP), reserve pool (RP), and silent pool (SP) (Tsien and Alabi, 2012). Despite the importance of these pools, understanding about their properties are far from fully understood. Herein we have investigated various properties of SV pools in synaptic transmission, including the SP exocytosis following Roscovitine (Cdk5 inhibitor) (Chapter 3) or Fluoxetine (SSRI drug) (Chapter 4) treatment, and also the effect of PKA and Calcium channels (Chapter 5), and the actin cytoskeleton (Chapter 6) on properties of the SV exocytotic modes.

7.1.1 Roscovitine

The SP is known to contain the majority of the SVs in certain type of experimental models, such as rodent hippocampal cultured cells. Interestingly, despite this characteristic, the SP rarely contributes to neurotransmission under normal physiological conditions (Sudhof, 2004). The reason why such a large number of SVs, that could theoretically take part in the synaptic transmission, are reluctant to release has been a major question.

Recently, Kim and Ryan (2010) used the Cdk5 inhibitor, Roscovitine, to successfully induce an extra release of SVs from mammalian hippocampal cell cultures and such release is from the SP. These authors have reported that treatment with Roscovitine allowed a 100-AP stimulation to trigger release of virtually all of the SVs in the terminal. They concluded that Cdk5 inhibition has increased the size of the available SV pool by allowing SP SVs to now become releasable (Kim and Ryan, 2010, 2013). We have now

employed Roscovitine to investigate the properties of the SP rat cerebral cortical synaptosomes.

Roscovitine treatment dose dependently increased the evoked GLU release from the nerve terminals with the maximum effect being identified at 100 μM . Under the stimulation conditions employed (HK5C or ION5C) the synaptosomes only undergo one round of SV release. However, under conditions where the SV recycling machineries were pharmacologically blocked with Dynasore and Pitstop2TM, Roscovitine still triggered extra release with the stimuli. This means that the release observed has occurred from SVs from a different pool other than the RRP and the RP, and this must be the SP. ION5C stimulation could also release the SP in the presence of Roscovitine, and as ION5C is an ionophore that bypasses any Ca^{2+} channel requirement, such result suggests that the level of Ca^{2+} influx through specific channels might not play an important role in the release of the SP providing there is a sufficient increase in $[\text{Ca}^{2+}]_i$. Indeed, whilst 100 μM Roscovitine allows the HK5C to evoke the SP release, it does not affect the evoked $\Delta[\text{Ca}^{2+}]_i$.

Although it was clear that $[\text{Ca}^{2+}]_i$ was unchanged with the treatment of Roscovitine, it was possible that additional $[\text{Ca}^{2+}]_e$ could induce further release in the presence of Roscovitine i.e. the condition being used did not maximally release the SP. This was found not to be the case as following Roscovitine pre-treatment HK10C and HK20C was actually unable to release the SP, indicating that higher $[\text{Ca}^{2+}]_e$ actually does not support the release of the SP. Intriguingly, the evoked $\Delta[\text{Ca}^{2+}]_i$ was reduced with HK10C or HK20C stimulation following Roscovitine treatment compared to that induced by HK5C, clearly there are some very precise requirements involving changes in $[\text{Ca}^{2+}]_i$ that are involved in the regulation of the SP release. There was also some specific PKC requirements as determined by using PMA and Go6983. Supramaximal activation of PKC with 1 μM PMA actually blocks the SP release evoked in Roscovitine treated terminals. However, inhibition of PKCs by Go6983 did not prevent the SP being released by HK5C in Roscovitine treated synaptosomes. However, HK10C and HK20C evoked release in the

presence of both Roscovitine and Go6983 failed to release the SP indicating that the higher $[Ca^{2+}]_e$ was not activating PKCs to the same extent as 1 μ M PMA since otherwise, as PKCs are blocked, one might have expected the SP to be released. All the experiments outlined in this paragraph are novel and the precise mechanisms involved will need to be elucidated in the future.

We next investigated whether SP release is dictated by specific types of voltage dependent Ca^{2+} channel. For this, toxins targeting and blocking specific types of Ca^{2+} channels were employed (CONO for N-type Ca^{2+} channels, AGA for P/Q type Ca^{2+} channels, NIF for L-type Ca^{2+} channels). It was apparent from the results that SP release requires a certain amount of Ca^{2+} influx through Ca^{2+} channels and SP exocytosis was perturbed by blocking any of these three types of Ca^{2+} channel. Thus, in rat cortical synaptosomes the SP regulated by entry of Ca^{2+} through voltage dependent Ca^{2+} channels but there is no one specific channel linked to this release. This may have been predicted as ION5C bypasses these channels but allows the SP to release in Roscovitine treated terminals.

The actin cytoskeleton has been suggested to play a role in regulation of synaptic transmission via scaffolding the SVs (Cingolani and Goda, 2008; Porat-Shliom *et al.*, 2012). The actin cytoskeleton must restrain the mobility of SVs, so that they remain distal from the AZ; a feature that overlaps with the reluctant release of the SP (Dillon and Goda, 2005). Therefore, the actin cytoskeleton might contribute to the SP regulation. Actin microfilaments were stabilised with JASP in Roscovitine treated terminals and HK5C still evoked release of the SP. Therefore, actin stabilisation with JASP was found not to affect the SP exocytosis. This is intriguing since it is clear that the actin microfilaments cannot act as barrier to unattached SP SVs, Roscovitine could still physically disattach the SVs from this cytoskeleton and such vesicles maybe now available for release.

Roscovitine treatment has been established in this study to allow HK5C and ION5C to evoke the SP exocytosis and this presumably involves Cdk5 inhibition. However, a precise mechanism of how inhibition of Cdk5 has led to the SP release is unknown. Cdk5 is a

kinase that has numerous substrates in the nerve terminal, such as Syn I. Benfenati's group has previously reported that Cdk5 phosphorylation of Syn I at Ser-551 site restrains the mobility of the SVs through association with actin cytoskeleton (Verstegen *et al*, 2014). Therefore, it is possible that Syn I phosphorylation might have been modified following Cdk5 inhibition with Roscovitine, and this allows previously immobilised SVs to exocytose. To investigate this, the specific phosphorylation of certain sites on Syn I were explored using western blotting experiments.

Semi-quantitative analysis of Syn I phospho-Ser-553 probed blots indicated that Roscovitine may have reduced the phosphorylation of this site. Additionally, phospho-Ser-9 and Ser-603 probed blots have shown increased phosphorylation following Roscovitine application relative to drug free control. Thus, it would appear that Roscovitine treatment leads to decreased phosphorylation of Syn I at Ser-553 site, whereas Ser-9 and Ser-603 site phosphorylation increases, and these changes may allow the stimuli to evoke the SP exocytosis. Importantly, in the previous literature it was shown that Cdk5 phosphorylation restricts the mobility of SVs by anchoring it with actin cytoskeleton (Verstegen *et al*, 2014), whereas PKA and CaMK II phosphorylation dissociates Syn I with SVs, thereby facilitate the SV exocytosis (Llinas *et al*, 1985, 1991; Petrucci and Morrow, 1987; Valtorta *et al*, 1991; Ceccaldi *et al*, 1995; Menegon *et al*, 2006; Wang *et al*, 2008). Therefore, results from current study match with findings from previous research. However, careful comparison between 4AP5C induced changes and HK5C and ION5C induced changes may highlight that the PKA site Ser-9 might not be involved (as ION5C does not change this phosphorylation in Roscovitine treated terminals) and that large changes in phosphorylation of Ser-553 and Ser-603 are required because 4AP5C can induce some change. As this is still preliminary data, many more repeats of these experiments are required to ascertain the validity of these statements.

7.1.2 Fluoxetine

Roscovitine treatment and subsequent stimulation with HK5C and ION5C have successfully induced the SP release. Nevertheless, considering the complexity of neurotransmission, it is unlikely that Cdk5 inhibition is the only approach that would allow one to study this pool of SVs. Hence, we attempted to find an alternative method that could allow the SP of SVs to be released extra release. One of the possible candidate was Fluoxetine, a commonly prescribed antidepressant drug. Recently, Jung *et al* (2014) reported that 1 μ M Fluoxetine increased the size of the recycling pools at the expense of the SP, in hippocampal cultured cells. Thus, we have tested whether Fluoxetine could also support the release of glutamatergic SVs from the SP.

Synaptosomes were treated with various concentrations (1 μ M, 200 nM, 100 nM, and 50 nM) of Fluoxetine for 5 min and its GLU release was evoked by HK5C. None of the concentrations applied were found to allow HK5C to evoke an extra release, and in fact 1 μ M Fluoxetine actually inhibited some release. This was analogous to the finding that 8 μ M Fluoxetine inhibited release in the study by Jung *et al* (2014). Synaptosomes were then treated with different concentrations (1 μ M, 200 nM, 100 nM, 50 nM, 40 nM, 20 nM, and 5 nM) of Fluoxetine for an extended period of incubation (20 min) to determine if this provided better conditions. The release was still reduced with 1 μ M Fluoxetine as it was with 200 nM and 100 nM Fluoxetine, indicating that these dosages of the drug perturb release. Remarkably, 40 nM Fluoxetine induced extra evoked release of GLU as did 20 nM, although this was a smaller effect. However, 5 nM failed to effect evoked release. Therefore, it would appear that maximum release of the SP was produced following 40 nM Fluoxetine treatment for 20 min at 37°C prior to stimulation. A comparison with 100 μ M Roscovitine treatment demonstrated that 40 nM Fluoxetine treatment allowed HK5C to evoke a similar amount of SP release. Further, dual treatment of Roscovitine and Fluoxetine was found not to induce any further increase in release, confirming that the

maximum release of the SP has been achieved. 40 nM Fluoxetine can also allow ION5C to evoke the SP release so again this suggests that the action of Fluoxetine is independent of any specific voltage dependent Ca^{2+} channels.

Even though this study obtained extra evoked GLU release with Fluoxetine using ION5C or HK5C stimuli, there was still a possibility that the drug, through unknown mechanism, might actually promote a recycling of the RRP and RP and the re-release during the stimulus period. So that this study was observing a recycling of these two pools rather than release of the SP. However, this was found not to be the case since even after the inhibition of the recycling machineries involving Dyn and clathrin, Fluoxetine was still able to allow ION5C and HK5C to evoke the SP release.

40 nM Fluoxetine with 20 min incubation was found to be an ideal condition to allow evoked release of the SP release. However, there was a noticeable decrease in the evoked release when 1 μM Fluoxetine was applied, indicating that this concentration of the drug is perturbing some release from the RRP and RP. One of the possible explanations for perturbation of release following 1 μM Fluoxetine treatment may be due to a reduction in evoked $\Delta[\text{Ca}^{2+}]_i$. Indeed, 1 μM Fluoxetine application did reduce evoked $\Delta[\text{Ca}^{2+}]_i$ compared to non-drug treated control, suggesting that an inhibition effect derived from 1 μM Fluoxetine treatment may be from a reduction in the evoked $\Delta[\text{Ca}^{2+}]_i$ level.

7.1.3 Effect of PKA and Calcium channel on regulation of SV releasing modes

From previous research in Ashton's group, it was established that regulation of releasing modes is dependent on various protein activities (Bhuva, 2015; Singh, 2017). Herein we are discussing the regulation of releasing modes dependent on activities of various proteins; Dyn, PKA, and Ca^{2+} channels.

Dyn plays an important role in the regulation of some type of KR mode of exocytosis as inhibition of its GTPase activity with Dynasore has shown to change the mode to FF. However, it was unknown whether Dyn has to be translocated to a membrane compartment prior to SV fusion or whether Dyn already present on such membranes regulates the KR mode of exocytosis. This was investigated using MITMAB, a drug that inhibits the translocation of Dyn from the cytosol to membranes as it prevents membrane binding. Evoked GLU and FM dye release and $\Delta[\text{Ca}^{2+}]_i$ were found to be unchanged following MITMAB treatment compared to non-drug treated control, indicating that this drug does not interfere with the Dyn dependent KR pathway. These results suggest that Dyn that is already present on membranes can regulate the mode of release. In recent experiment (Ashton *et al*, unpublished), it was shown that MITMAB can prevent the recycling of those SVs undergoing FF. Thus, as previously characterised, this CDE does require Dyn to bind to membrane. Further, it also proves that MITMAB is active.

Dyn is a substrate of PKC but, although it is speculated that PKC mediated Dyn I phosphorylation regulates the KR mode, it was hard to block changes in site specific phosphorylation in Dyn using PKC inhibitors. Thus, other kinases may also play a role (Singh, 2017). Dyn I is also proposed to be phosphorylated by other kinases, including PKA. Thus, we tested whether absence of endogenous PKA activities induced by its inhibition by KT5720 would affect the releasing mode. 4AP5C and ION5C evoked FM dye releases were found to be increased following KT5720 treatment, demonstrating that the mode of release has changed from KR to FF. Intriguingly, KT5720 treatment did not perturb the KR mode of the RRP evoked by HK5C. Such results are identical to what occurs when Dynasore inhibits the Dyn dependent KR mode. Thus, it would appear that endogenous PKA inhibition is only affecting the Dyn dependent KR mode, whereas HK5C evoked release operating through NM-II dependent pathway is not affected by the treatment with KT5720. Excitingly one can change HK5C to act on the Dyn dependent KR by inhibiting PKCs with Go6983. Under such circumstance, KT5720 can now switch

the HK5C evoked RRP SVs from KR to FF. Clearly, the Dyn dependent but not NM-II dependent KR has a requirement for endogenous PKA activity.

In a preliminary study from A.Ashton's group, it was discovered that HK5C evoked FM dye release from the RRP was induced following L-type Ca^{2+} channel inhibition, suggesting that the KR mode is regulated through L-type Ca^{2+} channels. However, this data only applies to the NM-II dependent KR pathway since HK5C works through this pathway. ION5C is the stimulus that acts on the Dyn dependent KR mode but as this stimulus bypasses Ca^{2+} channel requirements, one cannot use this stimuli to investigate possible specific Ca^{2+} channel requirement. Since Go6983 can change the HK5C to work through Dyn dependent KR, we measured HK5C evoked FM dye release in the presence of Go6983 with different Ca^{2+} channel inhibitors. Intriguingly, only the P/Q type Ca^{2+} channel inhibitor, AGA, changed the releasing mode of the RRP SVs from KR to FF, whereas, CONO (N-type Ca^{2+} channel inhibitor) and NIF (L-type Ca^{2+} channel inhibitor) failed to induce any changes in mode of release. Importantly, these results demonstrate that the NM-II dependent KR is regulated by L-type Ca^{2+} channels whilst the Dyn dependent KR mode is mediated through P/Q-type Ca^{2+} channels. This result has now led us to the idea that rather than us studying one KR mode that can be regulated by either Dyn or NM-II (dependent on the stimulation conditions) we are studying two independent KR modes: one regulated by Dyn and P/Q type channels and one regulated by NM-II and L-type channels. As these channels may be localised to distinct regions on the AZ, it could be that these two modes occur at distinct regions herein. This may also now explain difference in certain properties e.g. PKA's maybe localised near to the Dyn dependent KR SVs and regulated this but not near the NM-II dependent KR SVs.

7.1.4 Effect of Actin cytoskeleton on the releasing mode

At the AZ, the actin cytoskeleton is suggested to have a dual function. It might direct the arriving SVs to dock at the AZ, thereby positively controlling the size of the RRP. It could

also form a physical and molecular barrier for priming reaction, and thereby prevent facile fusion of vesicles (Cingolani and Goda, 2008; Porat-Shliom *et al*, 2012). The actin cytoskeleton can interact with Dyn and NM-II (Papadopulos, 2017) suggesting the possibility of its role as a regulator of Dyn and NM-II dependent KR mode. Herein, we have investigated the properties of KR mode depending on the actin cytoskeleton activity.

Actin microfilament disassembly due to LAT treatment prevented the release of RP GLU containing SV. If LAT does not perturb the modes of release, then one should expect the HK5C or ION5C should induce little FM dye because RRP normally undergoes KR so it does not release the dye and the RP SVs are blocked. However, HK5C and ION5C released FM dye and this was comparable to that found in non-drug treated controls. A possible explanation is that actin disassembly switches the RRP SVs to a FF mode. This idea was found to be correct because OA – which normally switches the RRP SVs to FF failed to produce any further FM dye release in LAT treated terminals, indicating that the RRP had been switched to the FF mode of exocytosis by disassembling actin microfilaments.

These results would initially suggest that both the Dyn dependent FP closure for KR and the NM-II dependent FP closure for KR may also require intact microfilaments. These may help to close the FP. However, we have found some difference between HK5C and ION5C that means that both KR modes FP may not both be directly affected by microfilament. HK5C evoked $\Delta[Ca^{2+}]_i$ levels were found to be reduced following disassembly of actin cytoskeleton, suggesting that a reduction in $[Ca^{2+}]_i$ level by microfilament of this cytoskeleton component may explain the switch of the RRP KR to FF and further, this could also explain why there is no release from the RP. However, actin disassembly action on ION5C evoked RP release and on ION5C RRP SVs mode of release were not connected to changes in ION5C evoked $\Delta[Ca^{2+}]_i$. One possibility is that actin microfilaments have an indirect involvement on the NM-II dependent KR mode (represented with HK5C stimulation), potentially through the regulation of calcium level,

but this cytoskeleton may directly mediate the Dyn dependent pathway (represented with ION5C stimulation).

We have also found that higher $[Ca^{2+}]_e$ using HK20C did not prevent the LAT induced perturbation of the RP GLU containing SV release. However, this has to be tested on the FM dye release assay to see whether HK20C can switch the RRP mode of release back to KR. If the results appears that higher $[Ca^{2+}]_i$ could reverse the change in the mode induced by actin disassembly, it will prove that we are actually looking at the two distinctive effects of LAT application.

We have used ION5C to work on the Dyn dependent KR pathway and HK5C to work on the NM-II dependent KR pathway. However, as we have found that these stimuli may also be perturbed by actin disassembly, we sought to check the specificity of our findings for the KR mode independent of the stimulus employed. We treated terminals with Go6983 to change the HK5C to a Dyn dependent KR mode and then disassembled microfilament with LAT. However, surprisingly the Go6983 treatment led to recovery of RP containing GLU SV release evoked by HK5C. Likewise, the LAT action on HK5C evoked $\Delta[Ca^{2+}]_i$ level has also found to be reversed in the presence of Go6983. Previously, it was proposed that LAT action on RP inhibition for HK5C is derived from the reduction in evoked $\Delta[Ca^{2+}]_i$ level and the results with Go6983 suggest that this is correct because this allows normal HK5C evoked $\Delta[Ca^{2+}]_i$ level, and normal release of the RP. These results may indicate that active PKCs are important for the effect of actin disassembly on release. To check this one will have to conduct similar experiments using the ION5C stimulation. However, initial results suggest that the release of RP of GLU containing SVs is still blocked using ION5C stimulation following treatment with LAT and Go6983. This suggests that PKCs may not play a role for the regulation of SV release by ION5C in LAT treated terminals.

The properties of the actin cytoskeleton can be further investigated by stabilising microfilament with JASP. JASP treatment does not perturb the HK5C or ION5C evoked GLU release and FM dye release, although it induces a slight increase in the HK5C evoked $\Delta[\text{Ca}^{2+}]_i$.

As JASP treatment does not perturb release, we can use it to show that the LAT actions is related to actin disassembly as JASP prevents this action of LAT. Indeed, JASP pre-treatment followed by LAT prevents the effect of LAT so the latter does work by actin disassembly. FM dye release in the presence of both drugs were found to produce similar result to when LAT was treated alone but this can be shown to be due to the RP now releasing by FF and the RRP releasing by KR. OA treatment of the JASP plus LAT treated terminals allowed more FM dye release proving that the RRP was originally undergoing KR but is now undergoing FF.

7.2 Future Studies

Finding from this thesis contributes to the understanding of the properties of distinct pool and their release. In particular, it has been discussed herein that the Roscovitine and Fluoxetine can allow stimulus to induce SP release. Additionally, effect of different protein activities including Dyn, PKA, Ca^{2+} channels, and actin cytoskeleton, on the mode of release were demonstrated. Nevertheless, there are still areas that are required to be studied in the future research in order to achieve the full understanding of the field. Likewise, some of the experiments proposed in this section may aid current knowledge and expand the understanding surrounding SV exocytosis in neurons.

- Reversibility of Roscovitine and Fluoxetine - Roscovitine and Fluoxetine have been established to allow HK5C or ION5C to induce the SP release. The use of FM2-10 dye to study the releasing mode of SP exocytosis has not been performed in this study. This is due to the fact that in order to load up the SP SVs with dye, one has to pre-treat the terminals with either Fluoxetine or Roscovitine so that the

SP is released and so it can be labelled with the Fluorescence dye, so that following its recycling, one would have labelled SP SVs. Subsequently in Fluoxetine or Roscovitine treated terminals, one can then allow HK5C or ION5C to evoke the release of FM dye from the exocytosing SP of SVs. However, one problem is that these drugs may perturb the SV recycling cycle, such that one may not be able to label SP SVs by this method e.g. Cdk5 phosphorylates Dyn following CDE, but blocking this may perturb parts of the SV recycling pathway. If drug actions are reversible, then one could allow the SP to be stimulated and labelled with dye and then the drug could be removed, if its action is really reversible, this may allow for fully functional recycling. Subsequently, fully labelled SP SVs could be induced to release by treating with one of these drugs. In the ideal world, one could test Roscovitine for pre-stimulation, its removed, and then Fluoxetine for stimulation or vice versa.

- PKA dependency of Roscovitine – In the current study, SP release in Roscovitine treated terminals has been discovered to be strongly dependent upon PKC as 1 μ M PMA prevents this, however, other kinases that are known to have important role in neurotransmission, such as PKA, were not investigated herein. Thus one could investigate whether PKA is a potential regulator of the SP exocytosis. We could study this by pharmacologically promoting PKA activity with c-BIMPs, or attenuating its activity with KT5720. This is analogous to the PKC studies where we supramaximally activated PKCs with 1 μ M PMA or inhibited PKCs with Go6983.
- More experiments with ION5C – Some of the experiments presented in this thesis only employed HK5C and there is a need to test these using ION5C as the stimulus. For example, whilst ION5C evoked GLU release is already performed for treatment with Go6983 plus LAT, one needs to study ION5C evoked FM dye release in the presence of LAT and Go6983. Thus, it is important to investigate

the conditions under ION5C stimulation. Additionally, ION5C evoked GLU release under Dynasore, Pitstop2TM, JASP, Blebbistatin, and Cys A treatment in the presence of Roscovitine need to be checked as was done for HK5C (see chapter 3). Also, the action for 40 nM Fluoxetine (chapter 4) with 20 min incubation on ION5C evoked GLU release also needs to be investigated.

- Fluoxetine with Serotonergic receptor agonists and antagonists – Fluoxetine has been discovered herein to allow HK5C and ION5C to evoke the release of the SP. This is intriguing result because Fluoxetine is known as SSRI, but it can also allow extra exocytosis of GLU containing SVs from glutamatergic nerve terminals. Therefore, it is possible that part of the antidepressant effect of drug may be derived from elevating the number of NT vesicles that can be stimulated to release and these effects would not be restricted to serotonergic terminals. There is a minimal number of serotonergic terminals in the cerebrocortical synaptosomes preparation which is over 80% glutamatergic. Thus it can be argued that Fluoxetine blocking reuptake of serotonin could not possibly act on all these glutamatergic terminals. There would not be enough present to do this and further, not all glutamatergic synaptosomes would have serotonin presynaptic receptors to produce this substantial increase in GLU release. However, for completion, one should add well characterised serotonin receptor agonists and antagonists and see what possible effect these could have on evoked GLU release alone. More importantly, these could be used in conjunction with Fluoxetine to show that the Fluoxetine affect is not due to serotonin levels.
- Calcium dependency of Fluoxetine action - It is necessary to investigate the changes in evoked $\Delta[Ca^{2+}]_i$ in the condition where Fluoxetine has successfully allowed HK5C and ION5C to induce SP release (40 nM for 20 min incubation at 37°C). This result, in combination with SP release observed at Roscovitine treated terminals, will represent the Calcium dependency of the SP regulation. As was

done for Roscovitine, it will be important to see whether Fluoxetine action depends on one of the three voltage dependent Ca^{2+} channels that we have tested.

- Western blotting – Western blotting results presented in Chapter 3 attempted to demonstrate that changes in the specific phosphorylation sites in Syn I following Roscovitine treatment, are related to the release of the SP. However, this was, by necessity, only a preliminary finding and more repeats need to be performed. Furthermore, the exact analogous experiment needs to be performed using Fluoxetine treated terminals. This may allow us to find some commonalities and differences and ascertain those phosphorylations that are truly required for release of the SP.
- FM experiments for HK20C in the presence of LAT – In chapter 6, disassembly of actin cytoskeleton with LAT has led to inhibition of HK5C evoked RP release and following effect appear to be directly associated with the reduction of $[\text{Ca}^{2+}]_i$, showcasing an importance of $[\text{Ca}^{2+}]_i$ in LAT activity on RP release. Hence, it will be important to investigate if higher $[\text{Ca}^{2+}]_e$ with HK20C would overcome the LAT effect. The GLU release experiment has revealed that it failed to reverse the effect but this also have to be tested under FM dye assay to see if there is any difference in the releasing mode.
- Specificity of calcium channel for LAT induced effect – HK5C evoked GLU release in the presence of LAT and Go6983 was found to recover the RP release. Furthermore, calcium level was found to be at the equal level with the control condition where LAT alone was applied, thus it would be appear that recovery of the RP release is linked to recovery of Calcium level. This finding highlights the importance of calcium level in LAT action on HK5C evoked release. This could be further tested by using various toxins that inhibit specific calcium channel. Following experiment will reveal any specificity of calcium channel involved in LAT induced effect.

- Does OA induced the FF of the RRP SVs following HK5C evoked dye release in LAT and Go6983 treated terminals? – The level of FM dye release was discovered to be equal to control in LAT and Go6983 treated terminals. However, it is not yet certain whether this means RP is releasing in KR and RRP has returned back to FF. This could be tested by including the OA in the drug treatment. OA will induce FF, thus if any extra release is observed in the following experiment, this will confirm that LAT effect has been reversed with the treatment of Go6983.

Chapter 8:
Reference and Appendix

Reference

- Afuwape, O. A., Wasser, C. R., Schikorski, T. and Kavalali, E. T. (2017). Synaptic vesicle pool-specific modification of neurotransmitter release by intravesicular free radical generation. *The Journal of Physiology*, 595(4), 1223-1238.
- Akbergenova, Y. and Bykhovskaia, M. (2007). Synapsin maintains the reserve vesicle pool and spatial segregation of the recycling pool in *Drosophila* presynaptic boutons. *Brain Research*, 1178, 52-64.
- Akbergenova, Y., Bykhovskaia, M. (2010). Synapsin regulates vesicle organisation and activity dependent recycling at *Drosophila* motor boutons. *Neuroscience*, 170(2), 441-452.
- Alabi, A. R. A. and Tsien, R. W. (2012). Synaptic vesicle pools and dynamics. *Cold Spring Harbor Perspective in Biology*, 4, 1-18.
- Alabi, A. R. A. and Tsien, R. W. (2013). Perspective on Kiss-and-Run: role in exocytosis, endocytosis, and neurotransmission. *The Annual Review of Physiology*, 75, 393-422.
- Alboghobeish, S., Naghizadeh, B., Kheirollah, A., Ghorbanzadeh, B., Mansouri, M. T. (2019), Fluoxetine increases analgesic effects of morphine, prevents development of morphine tolerance and dependence through the modulation of L-type calcium channels expression in mice. *Behavioural Brain Research*, 361, 86-94.
- Ales, E., Tabares, L., Poyato, J. M., Valero, V., Lindau, M. and de Toledo, G. A. (1999) High calcium concentrations shift the mode of exocytosis to the kiss-and-run mechanism. *Nature Cell Biology*, 1.
- Anantharam, A., Bittner, M. A., Aikman, R. L., Stuenkel, E. L., Schmid, S. L., Axelrod, D., Holz, R. W. (2011). A new role for the dynamin GTPase in the regulation of fusion pore expansion. *Molecular Biology of the Cell*, 22, 1907-1918.
- Aravanis, A. M., Pyle, J. L., Harata, N. C. and Tsien, R. W. (2003). Imaging single synaptic vesicles undergoing repeated fusion events: kissing, running, and kissing again. *Neuropharmacology*, 45, 797-813.
- Armbruster, M., Messa, M., Ferguson, S.M., De Camilli, P. and Ryan, T.A. (2013). Dynamin phosphorylation controls optimization of endocytosis for brief action potential bursts. *eLife* 2013,2:e00845.
- Ashton, A.C. and Ushkaryov, Y.A. (2005). Properties of synaptic vesicle pools in mature central nerve terminals. *Journal of Biological Chemistry*, 280, 37278-37288.
- Ashton, A.C., Babar, P.M. and Sihra, T.S. (2009). Changes in protein phosphorylation and calcium regulate switching between distinct modes of synaptic vesicle exocytosis. *Annual Society of Neuroscience Conference*.

- Ashton, A.C., Patel, M.H., Bhuva, D.A. and Sihra T.S. (2011). Regulation of modes of synaptic vesicle release in control and diabetic nerve terminals. *Annual Society of Neuroscience Conference*. 445.17/D42.
- Ashton, A.C., Bhuva, D.A., Singh, D.S. and Sihra, T.S. (2013). The role of dynamin and myosin 2 in regulating the mode of synaptic vesicle exocytosis. *Annual society of Neuroscience Conference*. 424.14/G51.
- Bahring, R. and Covarrubias, M. (2011). Mechanisms of closed-state inactivation in voltage-gated ion channels. *Journal of Physiology*, 589, 461-479.
- Baldwin, M. L. Rostas, J. A. P. and Sim, A. T. R. (2003). Two modes of exocytosis from synaptosomes are differentially regulated by protein phosphatase types 2A and 2B. *Journal of Neurochemistry*, 85, 1190-1199.
- Beach, J.R., Licate, L.S., Crish, J.F. and Egelhoff, T.T. (2011). Analysis of the role of Ser1/Ser2/Thr9 phosphorylation on myosin II assembly and function in live cells. *BMC cell biology*, 12, 52.
- Becherer, U. and Rettig, J. (2006). Vesicle pools, docking, priming, and release, *Cell and Tissue Research*, 326, 393-407.
- Bellani, S., Sousa, V. L., Ronzitti, G., Valtorta, F., Meldolesi, J., Chiergatti, E. (2010). The regulation of synaptic function by α -synuclein. *Communicative and Integrative Biology*, 3(2), 106-109.
- Benfenati, F., Neyroz, P., Bahler, M., Masotti, L. and Greengard, P. (1990). Time-resolved fluorescence study of the neuron-specific phosphorprotein synapsin I. Evidence for phosphorylation-dependent conformational changes. *The Journal of Biological Chemistry*, 265(21), 12584-12595.
- Berberian, K., Torres, A. J., Fang, Q, H., Kisler, K. and Lindau, M. (2009). F-actin and Myosin II accelerate catecholamine release from chromaffin granules. *The Journal of Neuroscience*, 29(3), 863-870.
- Betz, W. J. and Henkel, A. W. (1994). Okadaic acid disrupts clusters of synaptic vesicles in frog motor nerve terminals. *The Journal of Cell Biology*, 124(5), 843-854.
- Bhat, P. and Thorn, P. (2009). Myosin 2 maintains an open exocytic fusion pore in secretory epithelial cells. *Molecular Biology of the Cell*, 20, 1795-1803.
- Bhat, S., Dao, D. T., Terrillion, C. E., Arad, M. Smith, R. J., Soldatov, N. M., Gould, T. D. (2012), CACNA1C (Ca_v1.2) in the pathophysiology of psychiatric disease. *Progress in Neurobiology*, 99, 1-14.

- Bhuva, D. (2015). Dynamins and myosin-II regulate the distinct modes of synaptic vesicle exocytosis in mature cerebrocortical nerve terminals and this involves calcium dependent phosphorylations. Doctoral thesis, UCLan, Preston.
- Bialojan, C. and Takai, A. (1988). Inhibitory effect of a marine-sponge toxin, Okadaic acid, on protein phosphatases. Specific and kinetic. *Biochemical Journal*, 256, 283-290.
- Bloom, O., Evergren, E., Tomilion, N., Kjaerulff, O., Low, P., Brodin, L., Pieribone, V.A., Greengard, P., Shupliakov, O. (2003). Colocalisation of synapsin and actin during synaptic vesicle recycling. *The Journal of Cell Biology*, 161, 737-747.
- Bonanomi, D., Menegon, A., Miccio, A., Ferrari, G., Corradi, A., Kao, H. T., Benfenati, F., Valtorta, F. (2005) Phosphorylation of synapsin I by cAMP-dependent protein kinase controls synaptic vesicle dynamics in developing neurons. *The Journal of Neuroscience*, 25(32), 7299-7308.
- Brodin, L., Low, P. and Shupliakov, O. (2000). Sequential steps in clathrin-mediated synaptic vesicle endocytosis. *Current opinion in Neurobiology*, 10(3), 312-320.
- Bubb, M. R., Senderowicz, A. M. J., Sausville, E. A., Duncan, K. L. K., Korn, E. D. (1994). Jasplakinolide, a cytotoxic natural product, induces actin polymerisation and competitively inhibits the binding of phalloidin to F-actin. *The Journal of Biological Chemistry*, 269 (21), 14869-14871.
- Bubb, M. R., Spector, I., Beyer, B. B., Fosen, K. M. (2000). Effects of Jasplakinolide on the kinetics of actin polymerisation. An explanation of certain *in vivo* observations. *The Journal of Biological Chemistry*, 275 (7), 5163-5170.
- Bykhovskaia, M. (2011) Synapsin regulation of vesicle organization and functional pools. *Seminars in Cell and Developmental Biology*, 22, 387-392.
- Bymaster, F. P., Zhang, W., Carter, P. A., Shaw, J., Chernet, E., Phebus, L., Wong, D. T., Perry, K. W. (2002), Fluoxetine, but not other selective serotonin uptake inhibitors, increases norepinephrine and dopamine extracellular levels in prefrontal cortex. *Psychopharmacology*, 160, 353-361.
- Cabin, D.E., Shimazu, K., Murphy, D., Cole, N.B., Gottschalk, W., McIlwain, K.L., Orrison, B., Chen, A., Ellis, C.E., Paylor, R., Lu, B. and Nussbaum, R.L. (2002). Synaptic vesicle depletion correlates with attenuated synaptic responses to prolonged repetitive stimulation in mice lacking alpha-synuclein. *Journal of Neuroscience*, 22. 8797-8807.
- Cardenas, A. M. and Marengo, F. D. (2016). How the stimulus defines the dynamics of vesicle pool recruitment, fusion mode, and vesicle recycling in neuroendocrine cells. *Journal of Neurochemistry*, 137, 867-879.
- Catterall, W. A., Leal, K., Nanou, E. (2013). Calcium channels and short term synaptic plasticity. *The Journal of Biological Chemistry*, 288(15), 10742-10749.

- Cazares, V. A., Njus, M. M., Manly, A., Saldate, J. J., Subramani, A., Ben-Simon, Y., Sutton, M. A., Ashery, U. and Stuenkel, E. L. (2016). Dynamic partitioning of synaptic vesicle pools by the SNARE-binding protein Tomosyn. *The Journal of Neuroscience*, 36(44), 11208-11222.
- Ceccaldi, P. E., Grohovaz, F., Benfenati, F., Chierigatti, E., Greengard, P., Valtorta, F. (1995). Dephosphorylated synapsin I anchors synaptic vesicles to actin cytoskeleton: an analysis by videomicroscopy. *The Journal of Cell Biology*, 128, 905-912.
- Ceccarelli, B., Hurlbut, W. P. and Mauro, A. (1973). Turnover of transmitter and synaptic vesicles at the frog neuromuscular junction. *Journal of Cell Biology*, 57, 499-524.
- Cesca, F., Baldelli, P., F. Valtorta, F. and Benfenati, F. (2010). The synapsins: Key actors of synapse function and plasticity. *Progress in Neurobiology*, 91, 313-348.
- Chamberland, S. and Toth, K. (2016). Functionally heterogeneous synaptic vesicle pools support diverse synaptic signalling. *Journal of Physiology*, 594(4), 825-835.
- Chan, S. A., Doreian, B., Smith, C. (2010). Dynamin and Myosin regulate differential exocytosis from mouse adrenal chromaffin cells. *Cellular and Molecular Neurobiology*, 30(8), 1351-1357.
- Charles, E., Hammadi, M., Kischel, P., Delcroix, V., Demaurex, N., Castelbou, C., Vacher, A. M., Devin, A., Ducret, T., Nunes, P., Vacher, P. (2017), The antidepressant fluoxetine induces necrosis by energy depletion and mitochondrial calcium overload. *Oncotarget*, 8(2), 3181-3196.
- Cheung, G., Jupp, O. J. and Cousin, M. A. (2010). Activity-dependent bulk endocytosis and clathrin-dependent endocytosis replenish specific synaptic vesicle pools in central nerve terminals. *Journal of Neuroscience*, 30, 8151-8161.
- Cingolani, L. A. and Goda, Y. (2008). Actin in action: the interplay between the actin cytoskeleton and synaptic efficacy. *Nature Reviews*, 9, 344-356
- Clayton, D.F. and George, J.M. (1999). Synucleins in synaptic plasticity and neurodegenerative disorders. *Journal of Neuroscience Research*, 58, 120-129.
- Clayton, E. L. and Cousin, M. A. (2008). Differential labelling of bulk endocytosis in nerve terminals by FM dyes. *Neurochemistry International*, 53, 51-55.
- Clayton, E.L. and Cousin, M.A. (2009). The molecular physiology of activity-dependent bulk endocytosis of synaptic vesicles. *Journal of Neurochemistry*, 111, 901-914.
- Clayton, E.L., Sue, N., Smillie, K.J., O'Leary, T., Bache, N., Cheung, G., Cole, A.R., Wyllie, D.J., Sutherland, C. and Robinson, P.J. (2010). Dynamin I phosphorylation by GSK3 controls activity-dependent bulk endocytosis of synaptic vesicles. *Nature Neuroscience*, 13, 845-851.
- Clevenger, S. S., Malhortra, D., Dang, J., Vanle, B., IsHak, W. W. (2018), The role of selective serotonin reuptake inhibitors in preventing relapse of major depressive disorder. *Therapeutic Advances in Psychopharmacology*, 8(1), 49-58.

- Cole, J. C., Villa, B. R. S., Wilkinson, R. S. (2000). Disruption of actin impedes transmitter release in snake motor terminals. *The Journal of Physiology*, 525(3), 579-586.
- Cotter, K., Stransky, L., McGuire, C. and Forgac, M. (2015). Recent insights into the structure, regulation and function of the V-ATPases. *Trends in Biochemical Sciences*, 40, 611-622.
- Coue, M., Brenner, S. L., Spector, I., Korn, E. D. (1987). Inhibition of actin polymerisation by Latrunculin A. *FEBS Letters*, 213 (2), 316-318.
- Crawford, D.C. and Kavalali, E.T. (2015). Molecular Underpinnings of Synaptic Vesicle Pool Heterogeneity. *Traffic*, 16, 338-364.
- Dale, E., Andersen, B. B., Sanchez, C. (2015), Emerging mechanisms and treatments for depression beyond SSRIs and SNRIs. *Biochemical Pharmacology*, 95, 81-97.
- De Camilli, P., Takei, K. and McPherson, P. (1995). The function of dynamin in endocytosis. *Current Opinion in Neurobiology*, 5, 559-565.
- Deak, F., Lasztocki, B., Pacher, P., Petheo, G. L., Kecskemeti, V. and Spat, A. (2000). Inhibition of voltage-gated calcium channels by fluoxetine in rat hippocampal pyramidal cells. *Neuropharmacology*, 39, 1029-1036.
- Denker, A. and Rizzoli, S. O. (2010). Synaptic vesicle pools: an update. *Frontiers in Synaptic Neuroscience*, 2(135), 1-12.
- Denker, A., Bethani, I., Krohnert, K., Korber, C., Horstmann, H., Wilhelm, B. G., Barysch, S. V., Kuner, T., Neher, E. and Rizzoli, S. O. (2011). A small pool of vesicles maintains synaptic activity in vivo. *PNAS*, 108(41), 17177-17182.
- Denker, A., Krohnert, K., Buckers, J., Neher, E., and Rizzoli, S.O. (2011). The reserve pool of synaptic vesicles acts as a buffer for proteins involved in synaptic vesicle recycling. *PNAS*, 108, 17183-17188.
- Di Maio, V. (2008). Regulation of information passing by synaptic transmission: a short review. *Brain Research*, 1225, 26-38.
- Dillon, C. and Goda, Y. (2005). The actin cytoskeleton: integrating form and function at the synapse. *Annual Review of Neuroscience*, 28, 25-55.
- Ding, J. J., Zou, R. X., He, H. M., Lou, Z. Y., Xu, Y., Wang, H. L. (2018) Pb inhibits hippocampal synaptic transmission via cyclin-dependent kinase 5 dependent synapsin I phosphorylation. *Toxicology Letter*, 296, 125-131.
- Doreian, B. W., Fulop, T. G., Smith, C. B. (2008). Myosin II activation and actin re-organisation regulate the mode of quantal exocytosis in mouse adrenal chromaffin cells. *Journal of Neuroscience*, 28(17), 4470-4478.

Doreian, B.W., Fulop, T.G., Meklemburg, R.L., and Smith, C.B. (2009). Cortical F-actin, the exocytic mode, and neuropeptide release in mouse chromaffin cells is regulated by myristoylated alanine-rich C-kinase substrate and myosin II. *Molecular Biology of the Cell*, 20, 3142-3154.

Duman, R. S. and Aghajanian, G. K., (2012), Synaptic dysfunction in depression: potential therapeutic targets. *Science*, 338(6103), 68-72.

Dutta, D., Williamson, C. D., Cole, N. B. and Donaldson, J. G. (2012). Pitstop 2 is a potent inhibitor of Clathrin-independent endocytosis. *PLoS ONE*, 7(9).

Elhamdani, A., Palfrey, C. and Artalejo, C. R. (2001). Quantal size is dependent on stimulation frequency and calcium entry in calf chromaffin cells. *Neurons*, 31, 819-830.

Evans, G.J. and Cousin, M.A. (2007). Activity-dependent control of slow synaptic vesicle endocytosis by cyclin-dependent kinase 5. *The Journal of Neuroscience*, 27, 401-411.

Ferguson, S.M., Brasnjo, G., Hayashi, M., Wolfel, M., Collesi, C., Giovedi, S., Raimondi, A., Gong, L.W., Ariel, P. and Paradise, S. (2007). A selective activity-dependent requirement for dynamin 1 in synaptic vesicle endocytosis. *Science*, 316, 570-574.

Fernandez-alfonso, T. and Ryan, T. A. (2008). A heterogenous resting pool of synaptic vesicles that is dynamically interchanged across boutons in mammalian CNS synapses. *Brain Cell Biology*, 36(1-4), 87-100.

Fiumara, F., Giovedi, S., Menegon, A., Milanese, C., Merlo, D., Montarolo, P. G., Valtorta, F., Benfenati, F., Ghirardi, M. (2004). Phosphorylation by cAMP-dependent protein kinase is essential for synapsin-induced enhancement of neurotransmitter release in invertebrate neurons. *Journal of Cell Science*, 117(21), 5145-5154.

Fornasiero, E.F., Raimondi, A., Guarnieri, F.C., Orlando, M. Fesce, R. Benfenati, F. and Valtorta, F. (2012). Synapsin contribute to the dynamic spatial organisation of synaptic vesicles in an activity-dependent manner. *The Journal of Neuroscience*, 32(35), 12214-12227.

Fowler, M.W. and Staras, K. (2015). Synaptic vesicle pools: Principles, properties and limitations. *Experimental Cell Research*, 335, 150-156.

Fulop, T., Radabaugh, S. and Smith, C. (2005). Activity-dependent differential transmitter release in mouse adrenal chromaffin cell. *Journal of Neuroscience*, 25(32), 7324-32.

Gaydukov, A. E., Tarasova, E. O. and Balezina, O. P. (2013). Calcium-dependent phosphatase calcineurin downregulates evoked neurotransmitter release in neuromuscular junctions of mice. *Journal of Neurochemistry*, 7 (29), 29-33.

Gedalya, B.T., Loeb, V., Israeli, E., Altschuler, Y., Selkoe, D.J. and Sharon, R. (2009). Alpha-synuclein and polyunsaturated fatty acid promote clathrin mediated endocytosis and synaptic vesicle recycling. *Traffic*, 10, 218-234.

- Graham, M. E., O' Callaghan, D. W., McMahon, H. T. and Burgoyne, R. D. (2002) Dynamin-dependent and Dynamin-independent processes contribute to the regulation of single vesicle release kinetics and quantal size. *PNAS*, 99(10), 7124-7129.
- Graham, M. E., Anggono, V., Bache, N., Larsen, M. R., Craft, G. E. and Robinson, P. J. (2007). The *in vivo* phosphorylation sites of rat brain dynamin I. *The Journal of Biological Chemistry*, 282(20), 14695-14707.
- Granseth, B., Odermatt, B., Royle, S. J. and Lagnado, L. (2007). Clathrin-mediated endocytosis: the physiological mechanism of vesicle retrieval at hippocampal synapses. *The Journal of Physiology*, 585, 681-686.
- Granseth, B., Odermatt, B., Royle, S. J. and Lagnado, L. (2006). Clathrin-mediated endocytosis is the dominant mechanism of vesicle retrieval at hippocampal synapses. *Neuron*, 51, 773-786.
- Grynkiewicz, G., Poenie, M., Tsien, R.Y. (1985). A new generation of Ca²⁺ indicators with greatly improved fluorescence properties. *Journal of Biological Chemistry*, 260(6), 3440-3450.
- Gschwendt, M., Dieterich, S., Rennecke, J., Kittstein, W., Mueller, H. J. and Johannes, F. J. (1996). Inhibition of protein kinase C μ by various inhibitor: Differentiation from protein kinase c isoenzymes. *FEBS Letter*, 392, 77-80.
- Gu, C. K., Yaddanapudi, S., Weins, A., Osborn, T., Reiser, J., Pollak, M., Hartwig, J., Sever, S. (2010). Direct dynamin-actin interactions regulate the actin cytoskeleton. *The EMBO Journal*, 29, 3593-3606.
- Guarnieri, F. C. (2017). How do synaptic vesicles know which pool they belong to. *The Journal of Neuroscience*, 37(9), 2276-2278.
- Hamilton, T. J., Kwan, G. T., Gallup, J., Tresguerres, M. (2016), Acute fluoxetine exposure alters crab anxiety-like behaviour, but not aggressiveness. *Scientific Reports*, 6, 1-6.
- Hammond, J. W., Lu, S. M. and Gelbard, H. A. (2016). Platelet activating factor enhances synaptic vesicle exocytosis via PKC, elevated intracellular calcium, and modulation of synapsin 1 dynamics and phosphorylation. *Frontiers in Cellular Neuroscience*, 9(505), 1-13.
- Harata, N. C., Choi, S. W., Pyle, J. L., Aravanis, A. M. and Tsien, R. W. (2006) Frequency-dependent kinetics and prevalence of kiss-and-run and reuse at hippocampal synapses studied with novel quenching methods. *Neuron*, 49, 243-256.
- Harata, N. C., Aravanis, A. M. and Tsien, R. W. (2006) Kiss-and-run and full-collapse fusion as modes of exo-endocytosis in neurosecretion. *Journal of Neurochemistry*, 97, 1546-1570.
- Haviv, L., Gillo, D., Backouche, F., and Bernheim-Groswasser, A. (2008). A cytoskeletal demolition worker: myosin II acts as an actin depolymerization agent. *Journal of Molecular Biology*, 375, 325-330.

- He, L., Wu, X. S., Mohan, R. and Wu, L. G. (2006). Two modes of fusion pore opening revealed by cell-attached recordings at a synapse. *Nature*, 444, 102-105.
- Heuser, J. E. and Reese, T. S (1973). Evidences for recycling of synaptic vesicle membrane during transmitter release at the frog neuromuscular junction. *The Journal of Cell Biology*, 57, 315-344.
- Heuser, J. E. (1989). Review of electron microscopic evidence favouring vesicle exocytosis as the structural basis for quantal release during synaptic transmission. *Quality Journal of Experimental Physiology*, 74, 1051-1069.
- Hilfiker, S., Schwizer, F. E., Kao, H. T., Czernik, A. J., Greengard, P., Augustine, G. J. (1998). Two sites of action for synapsin domain E in regulating neurotransmitter release. *Nature neuroscience*, 1(1), 29-35.
- Hilfiker, S., Benfenati, F., Doussau, F., Nairn, A. C., Czernik, A. J., Augustine, G. J., Greengard, P. (2005). Structural domains involved in the regulation of transmitter release by synapsins. *The Journal of Neuroscience*, 25(10), 2658-2669.
- Hinshaw, J. E. and Schmid, S. L. (1995). Dynamin self assembles into rings suggesting a mechanism for coated vesicle budding. *Nature*, 374, 190-192.
- Hinshaw, J. E. (2000). Dynamin and its role in membrane fission. *Annual Review of Cell and Developmental Biology*, 16, 483-519.
- Hosaka, M., Hammer, R. E., Sudhof, T. S. (1999). A phosphor-switch controls the dynamic association of synapsins with synaptic vesicles. *Neuron*, 24, 377-387.
- Ikeda, K. and Bekkers, J. M. (2009). Counting the number of releasable synaptic vesicles in a presynaptic terminal. *PNAS*, 106, 2945-2950.
- Johri A. and Beal M.F. (2012). Mitochondrial dysfunction in neurodegenerative diseases. *Journal of Pharmacology and Experimental Therapeutics*, 342(3), 619-630.
- Jung, J., Loy, K., Schilling, E. M., Rother, M., Brauner, J. M., Huth, T., Schlotzer-Schrenhardt, U., Alzheimer, C., Kornhuber, J., Welzel, O., Groemer, T. W. (2014), The antidepressant Fluoxetine mobilise vesicles to the recycling pool of rat hippocampal synapses during high activity. *Molecular Neurobiology*, 49, 916-930.
- Katz, B. and Mildei, R. (1967). Ionic requirements of synaptic transmitter release. *Nature*, 215. 651.
- Katz, B. and Miledi, R. (1968). The role of calcium in neuromuscular facilitation. *The Journal of Physiology*, 195, 481-492.
- Kessels, M. M., Engqvist-Goldstein, A. E. Y., Drubin, D. G., Qalman, B. (2001). Mammalian Abp1, a signal-responsive F-actin-binding protein, links the actin cytoskeleton to endocytosis via the GTPase dynamin. *The Journal of Cell Biology*, 153(2), 351-366.

- Kim, S.H. and Ryan, T.A. (2010). CDK5 Serves as a Major Control Point in Neurotransmitter Release. *Neuron*, 67, 797–809.
- Kim, S.H. and Ryan, T.A. (2013). Balance of calcineurin Aa and Cdk5 activities set release probability at nerve terminals. *Journal of Neuroscience*, 33(21), 1-22.
- Kim, J. H., Kim, H. J., Yu, D. H., Kweon, H. S., Huh, Y. H., Kim, H. R. (2017). Changes in numbers and size of synaptic vesicles of cortical neurons induced by exposure to 835 MHz radiofrequency-electromagnetic field. *PLoS ONE*, 12(10), 1-12.
- Knononenko, N. L. and Haucke, V. (2015). Molecular mechanisms of presynaptic membrane retrieval and synaptic vesicle reformation. *Neurons*, 85, 484-496.
- Kokotos, A. C., Peltier, J., Davenport, E. C., Trost, M. and Cousin, M. A. (2018). Activity-dependent bulk endocytosis proteome reveals a key presynaptic role for the monomeric GTPase Rab 11. *PNAS*, 115 (43), 10177-10186.
- Kovacs, M., Toth, J., Hetenyi, C., Malnasi-Csizmadia, A., and Sellers, J.R. (2004). Mechanism of blebbistatin inhibition of myosin II. *The Journal of Biological Chemistry*. 279. 35557-35563.
- Kuromi, H. and Kidokoro, K. (1998). Two Distinct Pools of Synaptic Vesicles in Single Presynaptic Boutons in a Temperature-Sensitive Drosophila Mutant, shibire. *Neuron*, 20, 917–925.
- Kuromi, H. and Kidokoro, K. (2005). Exocytosis and Endocytosis of Synaptic Vesicles and Functional Roles of Vesicle Pools: Lessons from the Drosophila Neuromuscular Junction. *Neuroscientist*, 11, 138-147.
- Lavoie, N., Jeyaraju, D. V., Peralta III, M. R., Seress, L., Pellegrini, L. and Toth, K. (2011). Vesicular zinc regulates the Ca²⁺ sensitivity of a subpopulation of presynaptic vesicles at hippocampal mossy fiber terminals. *The Journal of Neuroscience*, 31(50), 18251-18265.
- Lee, S. J., Kim, H. W., Na, J. E., Kim, D. S., Kim, D. H., Ryu, J. R., Sun, W., Rhyu, I. J. (2018). Role of actin filament on synaptic vesicle pooling in cultured hippocampal neurons. *Applied Microscopy*, 48(3), 55-61.
- Levy, M. J. F., Boulle, F., Emerit, M. B., Poilbout, C., Steinbusch, H. W. M., Van den Hove, D. L. A., Kenis, G., Lanfumey, L. (2019), 5-HTT independent effects of fluoxetine on neuroplasticity. *Scientific Report*, 9, 1-11.
- Li, L., Chin, L. S., Shupliakov, O., Brodin, L., Sihra, T. S., Hvalby, O., Jensen, V., Zheng, D., McNamara, J. O., Greengard, P., Andersen, P. (1995b) *Proceeding of the National Academy of Sciences of the United States of America*, 92, 9235-9239.
- Linares-Clemente, P., Rozas, J. L., Mircheski, J., Garcia-Junco-Clemente, P., Martinez-Lopez, J. A., Nieto-Gonzalez, J. L., Vazquez, M. E., Pintado, C. O. and Fernandez-Chacon, R. (2015). Different dynamin blockers interfere with distinct phase of synaptic endocytosis during stimulation in motoneurons. *Journal of Physiology*, 13, 2867-2888.

- Llinas, R., McGuinness, T. L., Leonard, C. S. Sugimori, M. Greengard, P. (1985). Intraterminal injection of synapsin I or calcium calmodulin dependent kinase II alters neurotransmitter release at the squid giant synapse. *Proceeding of the National Academy of Sciences of the United States of America*, 82, 3035-3039.
- Llinas, R., Gruner, J. A., Sugimori, M., McGuinness, T. L., Greengard, P. (1991). Regulation by synapsin I and Ca²⁺-Calmodulin-dependent protein kinase II of transmitter release in squid giant synapse. *Journal of Physiology*, 436, 257-282.
- Ludowyke, R.I., Elgundi, Z., Kranenburg, T., Stehn, J.R., Schmitz-Peiffer, C., Hughes, W.E. and Biden, T.J. (2006). Phosphorylation of non muscle myosin heavy chain IIA on Ser1917 is mediated by protein kinase C beta II and coincides with the onset of stimulated degranulation of RBL-2H3 mast cells. *Journal of Immunology*, 177, 1492-1499.
- Luo, F., Dittrich, M., Cho, S. Y., Stiles, J. R., Meriney, S. D. (2015). Transmitter release is evoked with low probability predominately by calcium through single channel openings at the frog neuromuscular junction. *Journal of Neurophysiology*, 113, 2480-2489.
- Macia, E., Ehrlich, M., Massol, R., Boucrot, E., Brunner, C., and Kirchhausen, T. (2006). Dynasore, a cell-permeable inhibitor of dynamin. *Developmental Cell*, 10, 839-850.
- Marra, V., Burden, J.J., Thorpe, J.R., Smith, I.T., Smith, S.L., Hausser, M., Branco, T. and Staras, K. (2012). A preferentially segregated recycling vesicle pool of limited size supports neurotransmission in native central synapses. *Neuron*, 76, 579-589.
- Martensen, A., Schakman, O., Yerna, X., Dessy, C. and Morel, N. (2014). Myosin light chain kinase controls voltage dependent calcium channels in vascular smooth muscle. *Pflugers Archiv*, 466(7), 1377-1389.
- Meder, W., Fink, K. and Gothert, M. (1997). Involvement of different calcium channels in K⁺ - and ventridine-induced increases of cytosolic calcium concentration in rat cerebral cortical synaptosomes. *Nauyn-Schmiedeberg's Arch Pharmacol*, 356, 797-805.
- Menegon, A., Bonanomi, D., Albertinazzi, C., Lotti, F., Ferrari, G., Kao, H. T., Benfenati, F., Beldelli, P., Baltorta, F. (2006). Protein Kinase A-mediated synapsin I phosphorylation is a central modulator of Ca²⁺-dependent synaptic activity. *The Journal of Neuroscience*, 26(45), 11670-11681.
- Mellander, L. J., Trouillon, R., Svensson, M. I. and Ewing, A. G. (2012). Amperometric post spike feet reveal most exocytosis is via extended kiss-and-run fusion. *Scientific Report*, 2, 10.1038/srep00907.
- Morales, M., Colicos, M. A., Goda, Y. (2000). Actin-dependent regulation of neurotransmitter release at central synapses. *Neuron*, 27, 539-550.

- Morton, A., Marland, J. R. and Cousin, M. A. (2005). Synaptic vesicle exocytosis and increased cytosolic calcium are both necessary but not sufficient for activity-dependent bulk endocytosis. *Journal of Neurochemistry*, 134, 405-415.
- Murray, A. J. (2008). Pharmacological PKA inhibition. All may not be what it seems. *Science Signalling*, 1(22), 1-6.
- Neco, P., Gil, A., Frances, M. M., Viniegra, S., Gutierrez, L. M. (2002). The role of myosin in vesicle transport during bovine chromaffin cell secretion. *Biochemical Journal*, 368, 405-413.
- Neco, P., Giner, D., Viniegra, S., Borges, R., Villarroel, A., Gutierrez, L. M. (2004). New role of myosin II during vesicle transport and fusion in chromaffin cells. *The Journal of Biological Chemistry*, 279(26), 27450-27457.
- Neco, P., Fernandez-Peruchena, C., Navas, S., Gutierrez, L. M., de Toledo, G. A., Ales, E. (2008). Myosin II contribute to fusion pore expansion during exocytosis. *The Journal of Biological Chemistry*, 283 (16), 10949-10957.
- Neher, E. and Sakaba, T. (2008). Multiple roles of calcium ions in the regulation of neurotransmitter release. *Neuron*, 59, 861-872.
- Nemani, V. M., Lu, W., Berge, V., Nakamura, K., Onoa, B., Lee, M.K., Chaudhry, F.A., Nicoll, R. A. and Edwards, R. H. (2010). Increased expression of α -synuclein reduces neurotransmitter release by inhibiting synaptic vesicle reclustering after endocytosis. *Neuron*, 65, 66-79.
- Nestler, E.J. and Greengard, P. (1982) Distribution of protein I and regulation of its state of phosphorylation in the rabbit superior cervical ganglion. *The Journal of Neuroscience*, 2(8), 1011-1023.
- Neuland, K., Sharma, N. and Frick, M. (2014). Synaptotagmin-7 links fusion-activated Ca^{2+} entry and fusion pore dilation. *Journal of Cell science*, 127, 5218-5227.
- Nguyen, P.V. and Wo, N. H. (2003). Regulation of hippocampal synaptic plasticity by cyclic AMP-dependent protein kinases. *Progress in Neurobiology*, 71, 401-437.
- Nicholls, D.G., Sihra, T.S., Sanchez-Prieto, J. (1987). Calcium-dependent and independent release of glutamate from synaptosomes monitored by continuous fluorimetry. *Journal of Neurochemistry*, 47, 50-57.
- Nichols, R. A., Chilcote, T. J., Czernik, A. J., Greengard, P. (1992). Synapsin I regulates glutamate release from rat brain synaptosomes. *Journal of Neurochemistry*, 58(2), 783-785.
- Nicholson-fash, J. C., Kokotos, A. C., Gillingwater, T. H., Smillie, K. J. and Cousin, M. A. (2015). VAMP4 is an essential cargo molecule for activity dependent bulk endocytosis. *Neuron*, 88, 973-984.

- Nightingale, T. D., Cutler, D. F., Cramer, L. P. (2012). Actin coats and rings promote regulated exocytosis. *Trends in Cell Biology*, 22(6), 329-337
- Normann, C., Frase S., Haug, V., von Wolff, G., Clark, K., Munzer, P., Dorner, A., Scholliers, J., Horn, M., Van, T. V., Seifert, G., Serchov, T., Biber, K., Nissen, C., Klugbauer, N., Bischofberger, J. (2018), Antidepressants rescue stress-induced disruption of synaptic plasticity via serotonin transporter-independent inhibition of L-type calcium channels. *Biological Psychiatry*, 84, 55-64.
- Orenbuch, A., Shalev, L., Marra, V., Sinai, I., Lavy, Y., Kahn, J., Burden, J.J., Staras, K., Gitler, D. (2012). Synapsin selectively controls the mobility of resting pool vesicles at hippocampal terminals. *The Journal of Neuroscience*, 32(12), 3969-3980.
- Papadopoulos, A. (2017). Membrane shaping by actin and myosin during regulated exocytosis. *Molecular and Cellular Neuroscience*, 28, 93-99.
- Park, A. J., Havekes, R., Choi, J. H. K., Luczak, V., Nie, T., Huang, T. and Abel, T. (2014). A presynaptic role for PKA in synaptic tagging and memory. *Neurobiology of Learning and Memory*, 114, 101-112.
- Park, H. K., Li, Y. L., Tsien, R. W. (2012), Influence of synaptic vesicle position on release probability and exocytosis fusion mode. *Science*, 335, 1362-1366.
- Park, R. J., Shen, H., Liu, L., Liu, X., Ferguson, S.M., De Camilli, P. (2013). Dynamin triple knockouts reveal off target effects of commonly used dynamin inhibitors. *Journal of Cell Science*, 126, 5305-5312.
- Petrucci, T. C. and Morrow, J. S. (1987). Synapsin I: an actin-bundling protein under phosphorylation control. *The Journal of Cell Biology*, 105, 1355-1363.
- Porat-Shlion, N., Milberg, O., Masedunskas, A., Weigert, R. (2013). Multiple roles for the actin cytoskeleton during regulated exocytosis. *Cellular and Molecular Life Science*, 70, 2099-2121.
- Pollard, T. D. (2016). Actin and Actin-binding proteins. *Cold Spring Harbor Perspectives in Biology*, 8, 1-17.
- Polymeropoulos, M.S., Lavedan, C., Leroy, E., Ide, S.E., Dehejia, A., Dutra, A., Pike, B., Root, H., Rubenstein, J., Boyer, R., Senroos, E.S., Chandrasekharappa, S., Athanassiadou, A., Papapetropoulos, T., Johnson, W.G., Lazzarini, A.M., Duvoisin, R.C., Di Iorio, G., Golbe, L.I. and Nussbaum, R.L.(1997). Mutation in the alpha-synuclein gene identified in families with Parkinson's disease. *Science*, 276 (5321), 2045-2047.
- Powell, K. A., Valova, V. A., Malladi, C. S., Jensen, O. N., Larsen, M. R. and Robinson, P. J. (2000). Phosphorylation of dynamin I on Ser-795 by protein kinase C blocks its association with phospholipids. *Journal of Biological Chemistry*, 275, 11610-11617.
- Quan, A., McGeachie, A. B., Keating, D. J., van Dam, E. M., Rusak, J., Chau, N., Malladi, C. S., Chen, C., McCluskey, A., Cousin, M. A., Robinson, P. J. (2007). Myristyl trimethyl ammonium

bromide and octadecyl trimethyl ammonium bromide are surface active small molecule dynamin inhibitors that blocks endocytosis mediated by dynamin I or dynamin II. *Molecular Pharmacology*, 72(6), 1425-1439.

Rahn K. A., Cao, Y. J., Hendrix, C. W., Kaplin, A. (2015). The role of 5-HT1A receptors in mediating acute negative effects of antidepressants: implications in pediatric depression. *Translational Psychiatry*, 5, 1-8.

Raimondi, A., Ferguson, S.M., Lou, X., Armbruster, M., Paradise, S., Giovedi, S., Mess, M., Kono, N., Takasaki, J. and Cappello, V. (2011). Overlapping role of dynamin isoforms in synaptic vesicle endocytosis. *Neuron*, 70, 1100-1114.

Ramachandran, R. (2011). Vesicle Scission: Dynamin. *Seminars in Cell & Developmental Biology*, 22, 10-17.

Ratnayaka, A., Marra, V., Bush, D., Burden, J.J., Branco, T. and Staras, K. (2012). Recruitment of resting vesicles into recycling pools supports NMDA receptor-dependent synaptic potentiation in cultured hippocampal neurons. *The Journal of Physiology*, 590, 1585-1597.

Richards, D.A. (2009). Vesicular release mode shapes the postsynaptic response at hippocampal synapses. *The Journal of Physiology*, 587, 5073-5080.

Richards, D.A. (2010). Regulation of exocytic mode in hippocampal neurons by intra-bouton calcium concentration. *The Journal of Physiology*, 588, 4927-4936.

Richards, D. A., Rizzoli, S. O. and Betz, W. J. (2004). Effects of wortmannin and latrunculin A on slow endocytosis at the frog neuromuscular junction. *The Journal of Physiology*, 557(1), 77-91.

Rizzoli, S. O. and Betz, W. J. (2004). The structural organisation of the readily releasable pool of synaptic vesicles. *Science*, 303, 2037-2039.

Rizzoli, S. O. and Betz, W. J. (2005). Synaptic vesicle pools. *Nature Reviews Neuroscience*, 6, 57-69.

Rizzoli, S. O. and Jahn, R. (2007). Kiss-and-run, collapse and 'readily retrievable' vesicles. *Traffic*, 8, 1137-1144.

Rizzoli, S. O. (2014). Synaptic vesicle recycling: steps and principles. *The EMBO Journal*, 33(8), 788-822.

Robinson, P. J. (1991). Dephosphin, a 96,000 Da substrate of protein kinase C in synaptosomal cytosol, is phosphorylated in intact synaptosomes. *FEBS Lett*, 282, 388-392.

Robinson, P. J. (1992). Differential stimulation of protein kinase C activity by Phorbol Ester on calcium/phosphatidylserine *in vitro* and in intact synaptosomes. *Journal of Biological Chemistry*, 267, 21637-21644.

Robinson, P. J., Liu, K. A., Powell, K. A., Fyske, E. M. and Sudhof, T. C. (1994). Phosphorylation of dynamin and synaptic-vesicle recycling. *Trends in Neuroscieicne*, 17, 348-353.

Rostron, A. (2019). The role of dynamins in the fusion of synaptic vesicles and their subsequent recycling. Doctoral thesis, UCLan, Preston.

Ryan, T.A. (1999). Inhibitors of Myosin Light Chain Kinase Block Synaptic Vesicle Pool Mobilization during Action Potential Firing. *The Journal of Neuroscience*, 19, 1317–1323.

Sakurada K., Kato H., Nagumo H., Hiraoka H., Furuya K., Ikuhara T., Yamakita Y., Fukunaga K., Miyamoto E., Matsumura F., Matsuo Y.I., Naito Y., Sasaki Y. (2002). Synapsin I is phosphorylated at Ser603 by p21-activated kinases (PAKs) *in Vitro* and in PC12 cells stimulated with Bradykinin. *The Journal of Biological Chemistry*, 277(47), 45473-45479.

Samasilp, P., Chan, S. A., Smith, C. (2012) Activity-dependent fusion pore expansion regulated by a calcineurin0dependent dynamin-syndapin pathway in mouse adrenal chromaffin cells. *The Journal of Neuroscience*, 32(30), 10438-10447.

Samigullin, D. Bill, C. A., Coleman, W. L., Bykhovskia, M. (2004) Regulation of transmitter release by synapsin II in mouse motor terminals. *The Journal of Physiology*, 561.1, 149-158.

Sanborn, K.B., Mace, E.M., Rak, G.D., Difeo, A., Martignetti, J.A., Pecci, A., Bussel, J.B., Favier, R. and Orange, J.S. (2011). Phosphorylation of the myosin IIA tailpiece regulates single myosin IIA molecule association with lytic granules to promote NK-cell cytotoxicity. *Blood*, 118, 5862-5871.

Schiebler, W., Jahn, R., Doucet, J. P., Rothlein, J. and Greengard, P. (1986). Characterisation of synapsin I binding to small synaptic vesicles. *The Journal of Biological Chemistry*, 261(18), 8383-8390.

Scott, D. and Roy, S. (2012). α -synuclein inhibits intersynaptic vesicle mobility and maintains recycling-pool homeostasis. *The Journal of Neuroscience*, 32(30), 10129-10135.

Seahorse Bioscience. (n.d). XF Cell Mito Stress Test Kit: User Guide. *Seahorse Bioscience*

Segovia, M., Ales, E., Montes, M. A., Bonifas, I., Jemal, I., Lindau, M., Maximov, A., Sudhof, T. C. and de Toledo, G. A. (2010). Push-and-pull regulation of the fusion pore by synaptotagmin-7. *PNAS*, 107(44), 19032-19037.

Seino, S. and Shibasaki, T. (2005). PKA-dependent and PKA-independent pathways for cAMP-regulated exocytosis. *Physiological Review*, 85, 1303-1342.

Shu, S., Liu, X., Korn, E.D. (2005). Blebbistatin and blebbistatin-inactivated myosin II inhibit myosin II-independent processes in Dictyostelium. *Proceedings of the National Academy of Sciences of the United States of America*, 102, 1472-1477.

- Shupliakov, O., Haucke, V., Pechstein, A. (2011) How synapsin I may cluster synaptic vesicles. *Seminars in Cell and Developmental Biology*, 22, 393-399.
- Siksou, L., Rostaing, P., Lechaire, J. P., Boudier, T., Ohtsuka, T., Fejtova, A., Kao, H. T., Greengard, P., Gundelfinger, E. D., Triller, A., Marty, S. (2007) Three-dimensional architecture of presynaptic terminal cytomatrix. *The Journal of Neuroscience*, 27(26), 6868-6877.
- Sim, A.T., Herd, L., Proctor, D.T., Baldwin, M.L., Meunier, F.A., and Rostas, J.A. (2006). High throughput analysis of endogenous glutamate release using a fluorescence plate reader. *Journal of Neuroscience Method*. 153, 43-47.
- Simille, K. J. and Cousin. M. A. (2005). Dynamin I phosphorylation and the control of synaptic vesicle endocytosis. *Biochemical Society Symposia*, 72, 87-97.
- Singh, D. (2017). Phosphorylation sites on specific neuronal protein can control the mode of synaptic vesicle exocytosis and thereby regulate synaptic transmission. Doctoral thesis, UCLan, Preston.
- Smith, S. M., Renden, R. and von Gersdorff, H. (2008). Synaptic vesicle endocytosis: fast and slow modes of membrane retrieval. *Trends in Neuroscience*, 31(11), 559-568.
- Sobieski, C., Fitzpatrick, M. J. and Mennerick, S. J. (2017). Differential presynaptic ATP supply for basal and high-demeand transmission. *The Journal of Neuroscience*, 37(7). 1888-1899.
- Soykan, T., Maritzen, T. and Haucke, V. (2016). Modes and mechanisms of synaptic vesicle recycling. *Current Opinion in Neurobiology*, 39, 17-23.
- Spinelli, K.J., Taylor, J.K., Osterberg, V.R., Churchill, M.J., Pollock, E., Moore, C., Meshul, C.K. and Unni, V.K. (2014). Presynaptic α -synuclein aggregation in a mouse mode of Parkinson's Disease. *The Journal of Neuroscience*, 34(6), 2037-2050.
- Srinivasan, G., Kim, J.H. and von Gersdorff, H. (2008). The Pool of Fast Releasing Vesicles Is Augmented by Myosin Light Chain Kinase Inhibition at the Calyx of Held Synapse. *Journal of Neurophysiology*, 99, 1810-1824.
- Stevens, C. F. and Sullivan, J. M. (1998). Regulation of the readily releasable vesicle pool by protein kinase C. *Neuron*, 21, 885-893.
- Stevens, C. F. and Williams, J. H. (2000). Kiss and run exocytosis at hippocampal synapses. *PNAS*, 97(23), 12828-12833.
- Sudhof, T. C. (2004). The synaptic vesicle cycle. *Annual Review Neuroscience*, 27, 509-547.
- Sudhof, T. C. (2012). Calcium control of neurotransmitter release. *Cold Spring Harbor Perspectives in Biology*, 4, 1-15.
- Sumi M., Kiuchi K., Ishikawa T., Ishii A., Hagiwara M., Nagatsu T., and Hidaka H. (1991). The newly synthesized selective Ca^{2+} /calmodulin dependent protein kinase II inhibitor KN-93 reduces

dopamine contents in PC12h cells. *Biochemical and Biophysical Research Communications*, 181, 968-975.

Sweitzer, S. M. and Hinshaw, J. E. (1998). Dynamin undergoes a GTP-dependent conformational change causing vesiculation. *Cell*, 93, 1021-1029.

Takamori, S., Holt, M., Stenius, K., Lemke, E. A., Grønborg, M., Riedel, D., Urlaub, H., Schenck, S., Brügger, B., Ringler, P., Müller, S. A., Rammner, B., Gräter, F., Hub, J. S., De Groot, B. L., Mieskes, G., Moriyama, Y., Klingauf, J., Grubmüller, H., Heuser, J., Wieland, F. and Jahn, R. (2006). Molecular anatomy of a trafficking organelle. *Cell*, 127, 831-846.

Thomas, M. M., Puligandla, P. S. and Dunn, S. M. J. (1994). Effects of calcium channel blockers on the kinetics of voltage-dependent changes in synaptosomal calcium concentration. *Brain Research*, 635, 9-17.

Tokuoka, H. and Goda, Y. (2006). Myosin light chain kinase is not a regulator of synaptic vesicle trafficking during repetitive exocytosis in cultured hippocampal neurons. *Journal of Neuroscience*, 26, 11606-11614.

Tomizawa, K., Ohta, J., Matsushita, M., Moriwaki, A., Li, S. T., Takei, K., Matsui, H. (2002). Cdk5/p35 regulates neurotransmitter release through phosphorylation and downregulation of P/Q-type voltage-dependent calcium channel activity. *Journal of Neuroscience*, 22(7), 2590-2597.

Trouillon, R. and Ewing, A. G. (2014). Actin controls the vesicular fraction of dopamine released during extended kiss and run exocytosis. *ACS Chemical Biology*, 9, 812-820.

Tsou, K. and Greengard, P. (1982) Regulation of phosphorylation of proteins I, IIIa, and IIIb in rat neurohypophysis *in vitro* by electrical stimulation and by neuroactive agents. *Proceeding of the National Academy of Sciences of the United States of America*, 79, 6075-6079.

Vargas, K.J., Makani, S., Davis, T., Westphal, C.H., Catillo, P.E. and Chandra, S.S. (2014). Synuclein regulate the kinetics of synaptic vesicle endocytosis. *The Journal of Neuroscience*, 34(28), 9364-9376.

Valtorta, F., Greengard, P., Fesce, R., Chierigatti, E. and Benfenati, F. (1992). Effects of the neuronal phosphoprotein synapsin I on actin polymerisation. *The Journal of Biological Chemistry*, 267(16), 11281-11288.

Verstegen, A.M.J., Tagliatti, E., Lignani, G., Marte, A., Stoloro, T., Atias, M., Corradi, A., Valtorta, F., Gitler, D., Onofri, F., Fassio, A. and Benfenati, F. (2014). Phosphorylation of Synapsin I by Cyclin-Dependent Kinase-5 Sets the Ratio between the Resting and Recycling Pools of Synaptic Vesicles at Hippocampal Synapses. *The Journal of Neuroscience*, 34, 7266–7280.

Villanueva, J., Torres, V., Torregrosa-Hetland, C. J., Garcia-Martinez, V., Lopez-Font, I., Viniestra, S., Gutierrez, L. M. (2012). F-actin-Myosin II inhibitors affect chromaffin granule plasma

membrane distance and fusion kinetics by retraction of the cytoskeletal cortex. *Journal of Molecular Neuroscience*, 48, 328-338.

Virmani, T., Ertunc, M., Sara, Y., Mozhayeva, M., Kavalali, E.T. (2005). Phorbol esters target the activity-dependent recycling pool and spare spontaneous vesicle recycling. *The Journal of Neuroscience*, 25, 10922-10929.

Wang, S. J., Su, C. F., Kuo, Y. H. (2003), Fluoxetine depresses glutamate exocytosis in the rat cerebrocortical nerve terminals (synaptosomes) via inhibition of P/Q-type Ca²⁺ channels. *Synapse*, 48(4), 170-177.

Wang, L., Das, U., Scott, D.A., Tang, Y., McLean, P.J. and Roy, S.(2014). α -synuclein multimers cluster synaptic vesicles and attenuate recycling. *Current Biology*, 24, 2319-2326.

Wang, Z. W. (2008) Regulation of synaptic transmission by presynaptic CaMKII and BK channels. *Molecular Neurobiology*, 38(2), 153-166.

Warnock, D. E. and Schmid, S. L. (1996). Dynamin GTPase, a force-generating molecular switch. *BioEssays*, 18(11), 885-893.

Watanabe, S., Rost, B. R., Camacho-Perez, M., Davis, M. W., Sohl-Kielczynski, B., Rosenmund, C., Jorgensen, E. M. (2013). Ultrafast endocytosis at mouse hippocampal synapses. *Nature*, 504(7479), 242-247.

Watanabe, S., Trimbuch, T., Camacho-Perez, M., Rost, B. R., Brokowski, B., Sohl-Kielczynski, B., Felies, A., Davis, M. W., Rosenmund, C. and Jorgensen, E. M. (2014). Clathrin regenerates synaptic vesicle from endosomes. *Nature*, 515(7526), 228-233.

Watanabe, S. and Boucrot, E. (2017). Fast and ultrafast endocytosis. *Current opinion in Cell Biology*. 47, 64-71.

Wu, W. and Wu, L. G. (2007). Rapid bulk endocytosis and its kinetics of fission pore closure at a central synapse. *PNAS*, 104, 10234-10239.

Wu, Q. H., Zhang, Q. F., Liu, B., Li, Y. L., Wu, X., Kuo, S., Zheng, L. H., Wang, C. H., Zhu, F. P. and Zhou, Z. (2019). Dynamin I retrains vesicular release to a subquantal mode in mammalian adrenal chromaffin cell. *The Journal of Neuroscience*, 39(2), 199-211.

Xie, Z. L., Long, J. G., Liu, J. K., Chai, Z. Y., Kang, X. J., Wang, C. H. (2017). Molecular mechanisms for the coupling of endocytosis to exocytosis in neurons. *Frontier in Molecular Neuroscience*, 10(47), 1-8.

Yamagata Y. and Nairn A.C. (2015). Contrasting features of ERK1/2 activity and synapsin I phosphorylation at the ERK1/2-dependent site in the rat brain in status epilepticus induced by kainic acid *in vivo*. *Brain Research*. 1625, 314-323.

Zaltieri, M., Grigoletto, J., Longhena, F., Navarria, L., Favero, G., Castrezzati, S., Colivicchi, M.A., Corte, L.D., Rezzani, R., Pizzi, M., Benfenati, F., Spillantini, M.G., Missale, C., Spano, P.F. and Bellucci, A.(2015). α -synuclein and synapsin III cooperatively regulate synaptic function in dopamine neurons. *Journal of Cell Science*, 128, 2231-2243.

Zhang, Q., Cao, Y. Q. and Tsien, R. W. (2007). Quantum dots provide an optical signal specific to full collapse fusion of synaptic vesicles. *PNAS*, 104(45), 17843-17848.

Zhang, Q., Li, Y. and Tsien, R.W. (2009). The dynamic control of kiss-and-run and vesicular reuse probed with single nanoparticles. *Science*, 323, 1448-1453.

Appendix 1

A. 1.1 Review of Previous Research

Results in this section reflect previous research carried out by the Ashton group. These results were created whilst establishing optimal experimental conditions for use with the synaptosomes model, and are displayed here to aid understanding of new and original data presented and discussed later in this thesis.

A. 1.1.1 Maximal GLU Release

For a direct comparison between FM 2-10 dye and GLU release assays it was necessary that the stimuli employed in this thesis produced a maximal level of GLU release. In order to determine this, synaptosomes were treated with the three stimuli (HK, ION and 4AP) – see material and methods for further details – in the presence of a range of extracellular Ca^{2+} concentrations ($[\text{Ca}^{2+}]_e$) (Fig A1). It can be observed that 5 mM $[\text{Ca}^{2+}]_e$ produced maximal GLU release for all stimuli, and a further increase in $[\text{Ca}^{2+}]_e$ to 10 mM had no effect on HK evoked GLU release (Fig A1 A), and possibly decreased GLU release with ION and 4AP (Fig A1 B-C). For all experiments in this study a concentration of 5 mM $[\text{Ca}^{2+}]_e$ was therefore used with each of the three stimuli to maximally release GLU from synaptosomes.

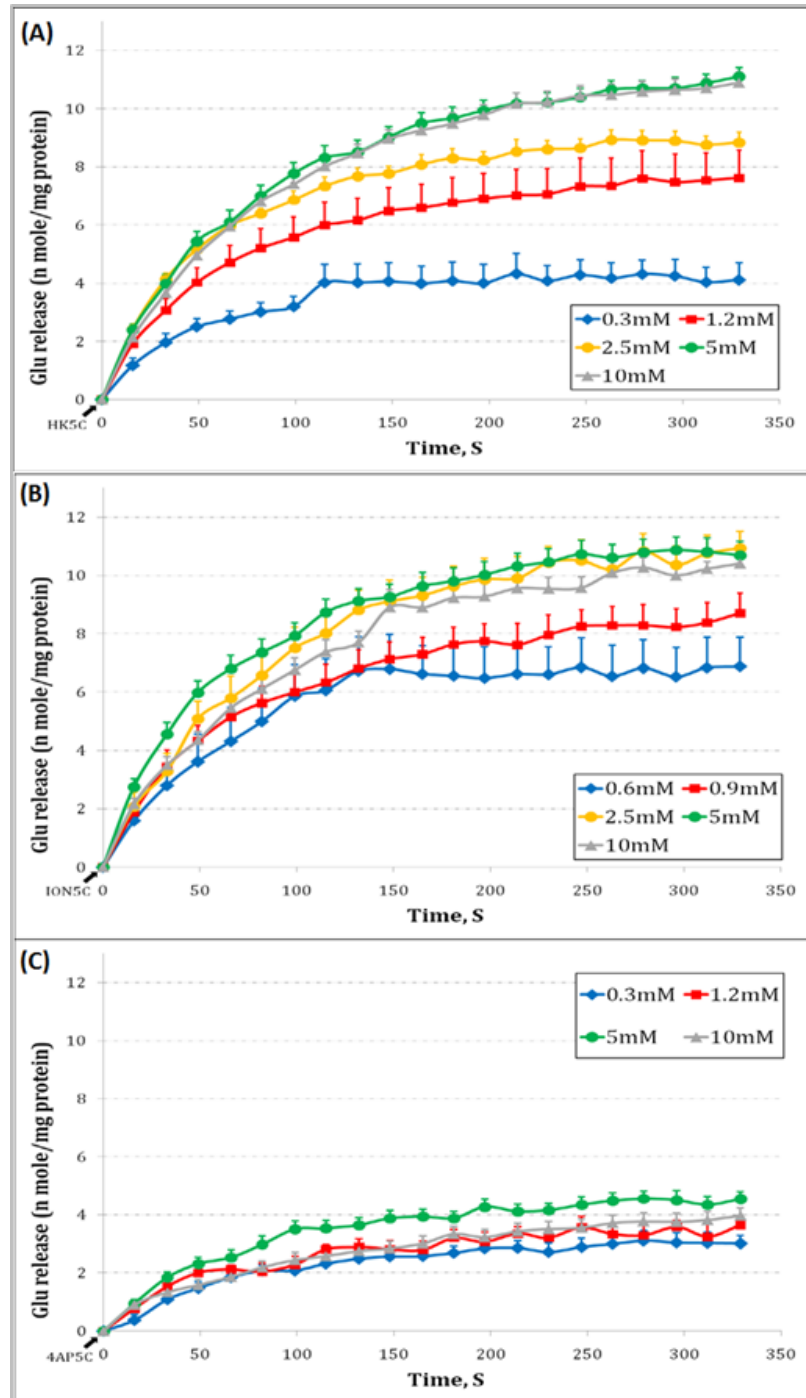


Figure A1: Effect of a Range of $[Ca^{2+}]_e$ upon Evoked GLU Release

Stimulation in the presence of 5 mM $[Ca^{2+}]_e$ induces maximal GLU release for HK (A), ION (B) and 4AP (C). Values represented are the mean plus S.E.M. from 4 independent experiments.

Stimulation with 4AP5C produced a lower maximal GLU release (4.5 moles/mg of protein) (Fig A1 C) compared to HK5C (10.8 moles/mg of protein) ($p < 0.05$) (Fig A1 A) or ION5C (11 moles/mg of protein) ($p < 0.05$) (Figure A1 B) with 5 mM $[Ca^{2+}]_e$. An explanation for this can be found when looking at the different changes in $[Ca^{2+}]_i$ produced by each stimuli (Fig A2). 4AP5C produces a lower, more gradual change in $[Ca^{2+}]_i$ (180 ± 20 nM Ca^{2+}) than either HK5C or ION5C (370 ± 25 nM Ca^{2+}) ($p < 0.05$), which is interpreted as 4AP5C only being able to release the RRP of SVs whilst HK5C and ION5C can release both the RRP and the RP of SVs.

Though HK5C and ION5C achieved an equivalent level of $[Ca^{2+}]_i$, in this figure, this is mediated by different kinetics (Fig A2). HK5C produced much of the $[Ca^{2+}]_i$ increase upon the application of stimulation, plateauing rapidly (< 10 sec), potentially due to VGCC desensitisation (Bähring & Covarrubias, 2011); whilst ION5C produced a more gradual increase in $[Ca^{2+}]_i$ which plateaus later (~ 40 sec) (Figure A2). This speed of achieving maximum increase in $[Ca^{2+}]_i$ applies in every experiment that has been performed in this thesis and over 10 years of research. However, it would appear that distinct batches of ionomycin may achieve higher maximum $\Delta[Ca^{2+}]_i$ than HK5C although maximum release is not altered (see throughout body of text).

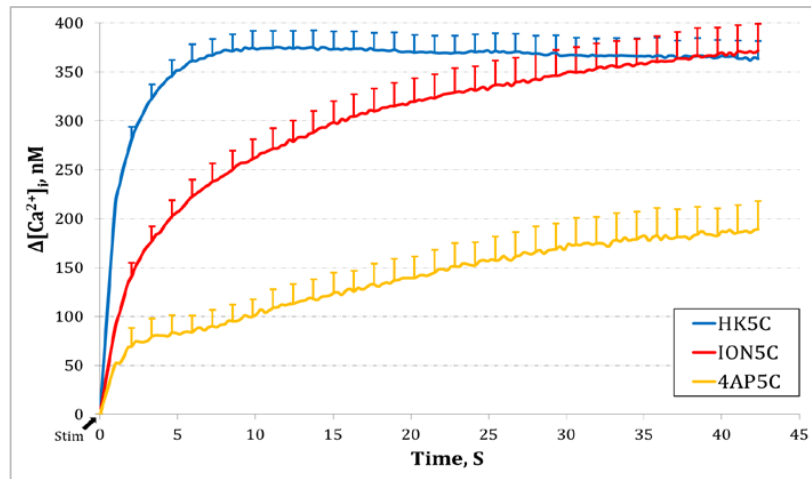


Figure A2: Effect of Stimuli upon Cytosolic free Calcium [Ca²⁺]_i

All three stimuli employed in this study produce a change in [Ca²⁺]_i via different kinetics. 4AP5C evokes a significantly lower [Ca²⁺]_i change than HK5C or ION5C ($p < 0.05$). No significant difference was observed between HK5C and ION5C ($p > 0.05$) in this set of experiments. Values represented are the mean plus S.E.M. from 3 independent experiments. Note in the other experiment reported in the main body of the thesis, ION5C can induce a higher maximal [Ca²⁺]_i than HK5C

A. 1.2 A Single Round of Exocytosis

Due to the kinetics of the FM 2-10 dye and GLU release assays, synaptosomes in this study are subject to long stimulation periods (between 60-300 sec). Due to this long duration of stimulation there is a possibility that SVs could undergo multiple rounds of recycling, refilling with and re-release GLU, leading to an erroneous interpretation of GLU release. Further, it is possible that a SV releasing via KR could retain its FM 2-10 dye label while undergoing several round of KR recycling, or SV could lose its FM 2-10 dye and release additional GLU without a link to dye fluorescence. In order to accurately compare GLU and FM 2-10 dye release, it is essential to establish that SVs are only undergoing one round of release during the stimulation and measurement period.

In order to ensure recycling was not occurring during stimulation and measurement, synaptosomes were acutely treated with 1 μ M of the selective vacuolar H⁺ ATPase (V-ATPase) inhibitor Bafilomycin A1. The V-ATPase pump is a complex found on SVs that is responsible for re-acidification of the vesicular lumen after endocytosis, which is vital in order for SVs to be re-filled with GLU (Cotter *et al*, 2015). Such acute bafilomycin A1 treatment has no effect upon the GLU content of non-exocytosed SVs, and does not impede their release upon stimulation (Ikeda and Bekkers, 2008). An acute treatment of 1 μ M Bafilomycin A1 did not significantly affect GLU release compared with untreated controls, regardless of stimulation (Fig A3) ($p>0.05$). If SVs were undergoing multiple rounds of recycling, the level of GLU release would be expected to decrease with the Bafilomycin A1 treatment.

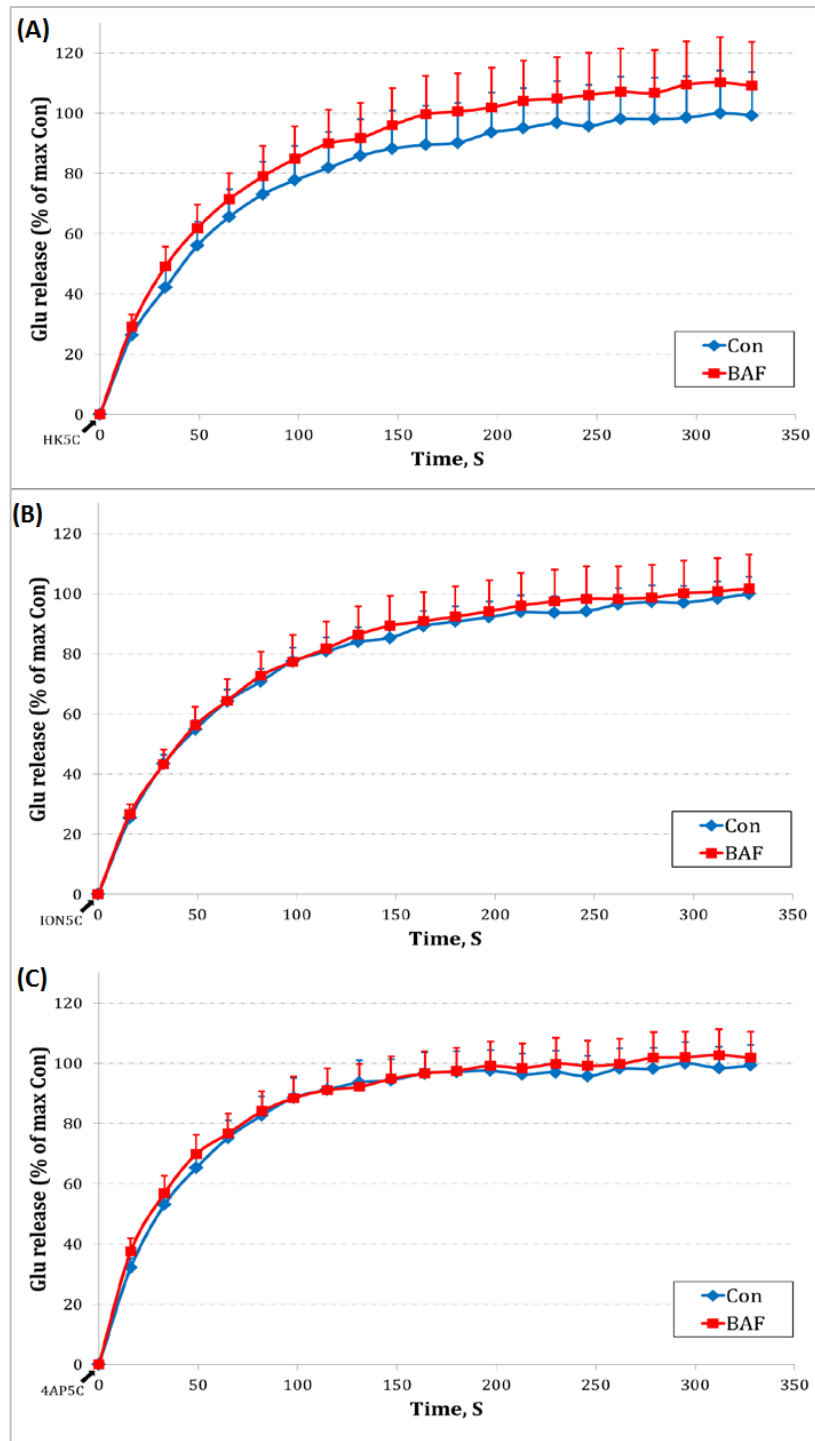


Figure A3: Effect of 1 μ M Bafilomycin A1 upon Evoked GLU release

Treatment with 1 μ M Bafilomycin A1 does not significantly affect GLU release when stimulated with HK5C (A), ION5C (B) or 4AP5C (C) compared to untreated controls ($p > 0.05$ for all). Values represented are the mean plus S.E.M. from 4 independent experiments.

A. 1.3 Maximal Labelling of SVs with FM 2-10 Dye

Styryl dyes, such as FM 2-10, have been used extensively to label lipid membranes and in particular vesicular trafficking and recycling. In all experiments a concentration of 100 μM FM 2-10 dye was utilised, as many researchers have employed the same concentration (Baldwin *et al*, 2003; Cheung *et al*, 2010). Clayton and Cousin (2008) however, have previously suggested that the labelling of SVs, especially via bulk endocytosis, is dependent upon the concentration of FM 2-10 dye, and 1 mM but not 100 μM will fully label all SVs (Clayton and Cousin, 2008).

In order to ensure that all SVs are fully labelled with FM 2-10 dye, synaptosomes were incubated with 1 mM or 100 μM and evoke to release during a drug treatment (160 μM Dynasore) which has been observed to increase exocytosis via FF (Fig A4). In this model system there was no significant difference in FM 2-10 dye release seen between synaptosomes loaded with 1 mM or 100 μM ($p>0.05$), and drug treatment had no significant impact upon labelling or release of SVs ($p>0.05$). If 100 μM FM 2-10 dye had been failing to label all releasable SVs, then a reduced amount of dye would be released.

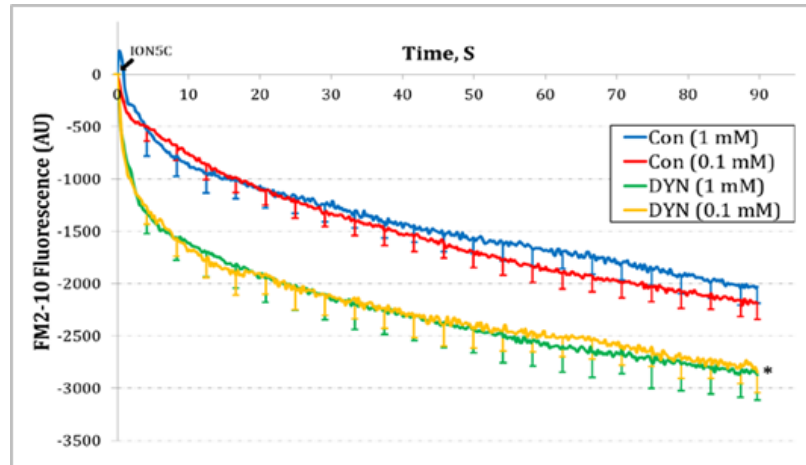


Figure A4: Difference between SVs Loaded with 1 mM or 100 μ M FM 2-10 Dye

SVs loaded with 1 mM (Blue) or 100 μ M (Red) release equivalent levels of FM 2-10 dye following stimulation ($p>0.05$). Drug treatment, 160 μ M Dynasore, increases FM 2-10 dye release by a corresponding amount, regardless of amount of FM 2-10 dye loaded, following stimulation (Green vs Yellow) ($p>0.05$). Values represented are the mean minus S.E.M from 4 independent experiments.

A. 1.4 The Mode of Exocytosis is Stimulation Dependent

Each of the stimuli used in this thesis have been shown to evoke release through distinct $[Ca^{2+}]_i$ kinetics (Fig A2), and changes in $[Ca^{2+}]_i$ have been linked to regulating the mode of exocytosis of distinct pools (Alés *et al*, 1999), therefore each stimuli could evoke release of SVs pools via unique modes. As the RRP is suggested to be released within 2 sec of stimulation (Rizzoli and Betz, 2005), this time period was studied during FM 2-10 dye release for all stimuli (Fig A5 A).

Interestingly HK5C and ION5C did not cause any significantly release of FM 2-10 dye in this period ($p>0.05$), unlike 4AP5C (Fig A5 A) ($p<0.05$). It could be argued that this indicates no SVs are being release during this time period, however when the experiment was repeated with a pre-treatment of 0.8 μ M OA (Fig A5 B), an inhibitor of protein phosphatase 1 and 2A which is known to convert all RRP SVs to FF (Ashton *et al*, 2011),

an increase in FM 2-10 dye release was noted for all stimuli, that was not significantly different between stimuli at 2 sec ($p>0.05$). Comparison of these results are interpreted as HK5C and ION5C releasing the RRP via KR under control conditions, while 4AP5C releases roughly half the RRP via KR and half by FF. All three stimuli release an equivalent amount of FM 2-10 dye with OA during this period (2 sec), suggesting it is the RRP being released.

In order to determine the exocytotic mode of the RRP and RP, the fluorescence value of FM 2-10 dye release during control conditions was subtracted from the fluorescence value achieved during OA treatment (Fig A6). HK5C stimulation caused all RRP SVs to undergo KR in the first 2 sec (Fig A6 A), and all RP SVs to release via FF (after 2 sec; Fig A6 B). Stimulation with 4AP5C releases all RRP SVs some via KR and some by FF, with fluorescence subtraction demonstrating that both modes contribute equally (Fig A6 C). RP SVs do not release when synaptosomes are stimulated with 4AP5C, as this stimuli induced a lower average $[Ca^{2+}]_i$ compared to HK5C and ION5C, and this is unable to drive RP fusion (see Fig A1 C and Fig A2).

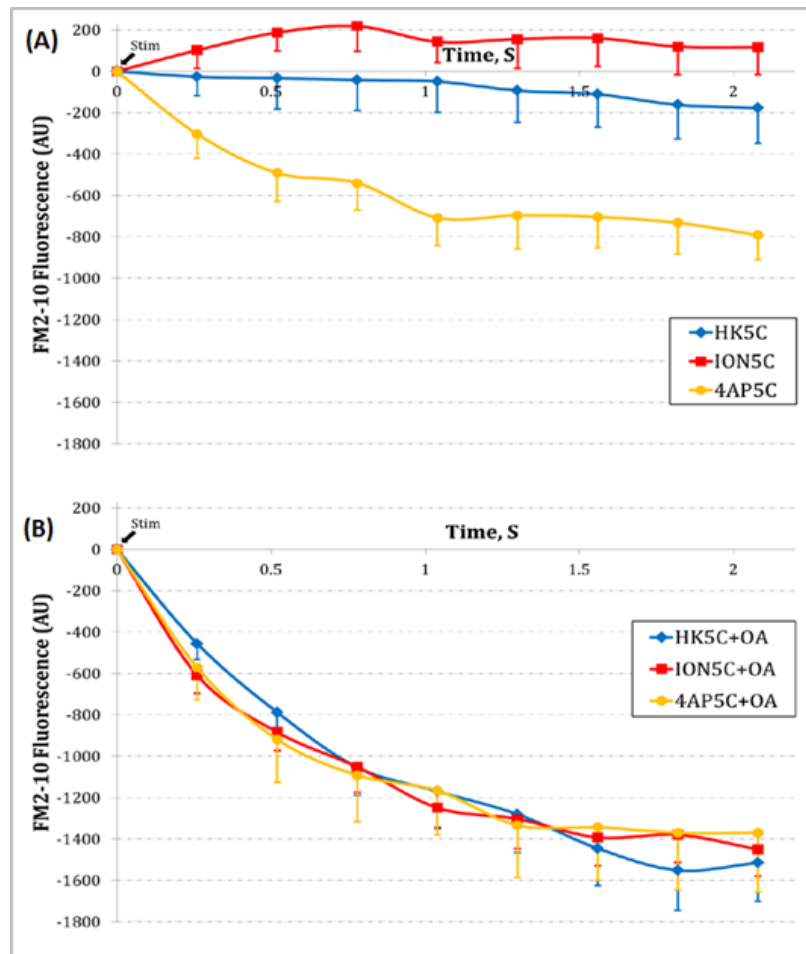


Figure A5: Mode of RRP Release during Control and 0.8 μ M OA Treatment

(A) Measurement of control levels of FM 2-10 dye release after stimulation during first 2 sec. Only 4AP5C releases a significant amount of dye ($p < 0.05$). (B) Treatment with OA induces equivalent release of FM 2-10 dye regardless of stimulation over first 2 sec ($p > 0.05$). Values represented are the mean plus S.E.M. from 3 independent experiments.

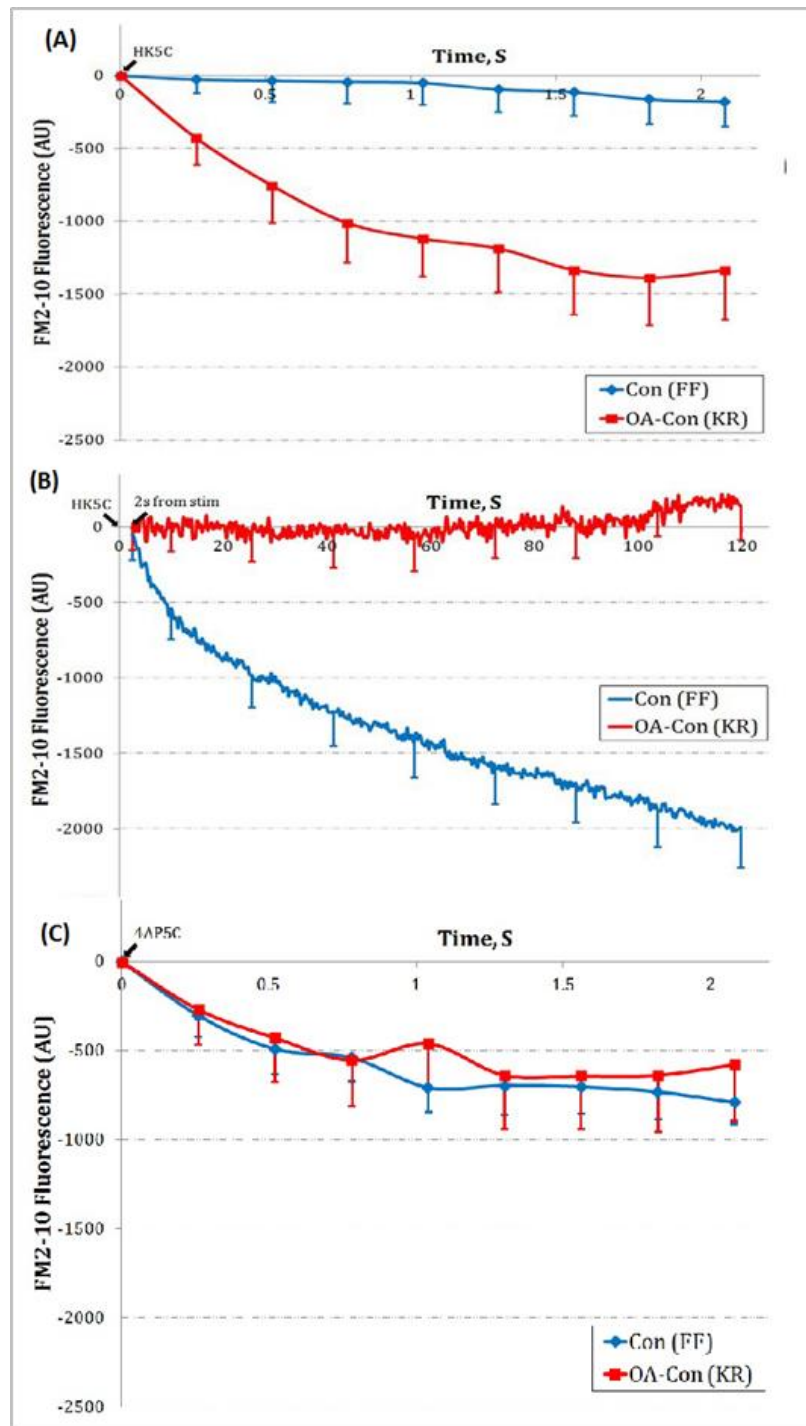


Figure A6: Mode of RRP and RP Release during Control and 0.8 μ M OA Treatment

When FM 2-10 dye fluorescence of control was subtracted from OA conditions, it was found that all SVs release via KR during initial 2 sec of HK5C stimulation (A), and remaining SVs are released via FF after 2 sec (B). During 4AP5C stimulation (C), all SVs are released by a combination of KR and FF for initial 2 sec. Values are average of 3 experiments plus S.E.M, taken from (Bhuva, 2015, p. 62) with permission.

A. 1.5 Presynaptic Proteins Regulating Exocytosis

Dyn I could have a role in modulating the mode of exocytosis at the FP. Previous research undertaken by Ashton group has demonstrated that inhibition of Dyn I GTPase activity with 160 μ M Dynasore did not perturb GLU release with any stimuli (Fig A7 A-C) ($p>0.05$), but significantly increased FM 2-10 dye release with ION5C and 4AP5C (Fig A7 E-F) ($p<0.05$). These results were interpreted as ION5C and 4AP5C having a Dyn I dependence to release the RRP via KR, while HK5C was able to release the RRP independent of Dyn I (Fig A7 D).

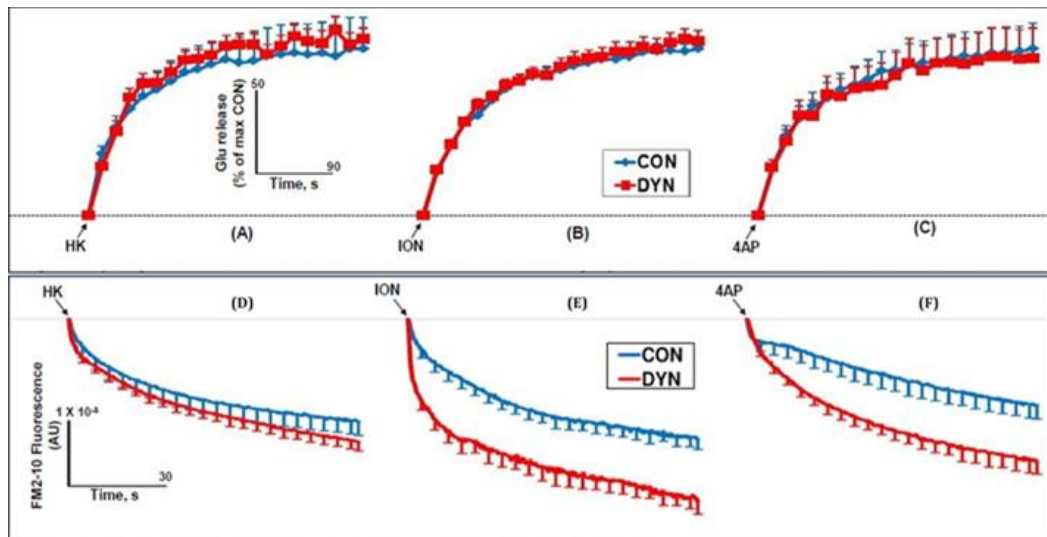


Figure A7: Effect of 160 μ M Dynasore vs Control upon Evoked GLU and FM 2-10 Dye Release

Treatment with 160 μ M Dynasore does not perturb GLU release evoked by HK5C (A), ION5C (B) or 4AP5C (C) ($p>0.05$). 160 μ M Dynasore had no significant effect of HK5C evoked FM dye release (D) ($p=0.508$), but increased ION5C (E) ($p=0.014$) and 4AP5C evoked FM dye release (F) ($p=0.034$). Values are mean plus SEM from 4 experiments. Figure taken with permission from a manuscript prepared by A. Ashton.

NM-II has also been implicated in regulating the mode of exocytosis at the FP (Chan *et al*, 2010; Berberian *et al*, 2009; Neco *et al*, 2008). Since no change in FM 2-10 dye release was observed when Dyn I was inhibited with Dynasore during HK5C stimulation (Fig A7 D), it was theorised NM-II could be responsible for regulating the FP during this mode of exocytosis. Thus NM-II was blocked with 50 μ M Blebbistatin, a selective, high affinity small molecule which blocks NM-II by inhibiting ATPase activity (Shu *et al*, 2005; Kovacs *et al*, 2004). A treatment of 50 μ M Blebbistatin did not perturb GLU release with any stimuli ($p>0.05$) (Fig A8), but did significantly increase FM 2-10 dye release with HK5C stimulation only ($p<0.05$) (Fig A9 A). These data may suggest that NM-II is able to close the FP during HK5C stimulation, when the $[Ca^{2+}]_i$ level at the AZ is high (Fig A2), as Ca^{2+} is required to regulate NM-II phosphorylation and activation (Martinsen *et al*, 2014). These data may also suggest that the $[Ca^{2+}]_i$ level achieved at the AZ during ION5C and 4AP5C stimulation may not be high enough to activate NM-II (Fig A9 B-C), but satisfactory to activate Dyn I to regulate the exocytosing FP (Fig A7 E-F).

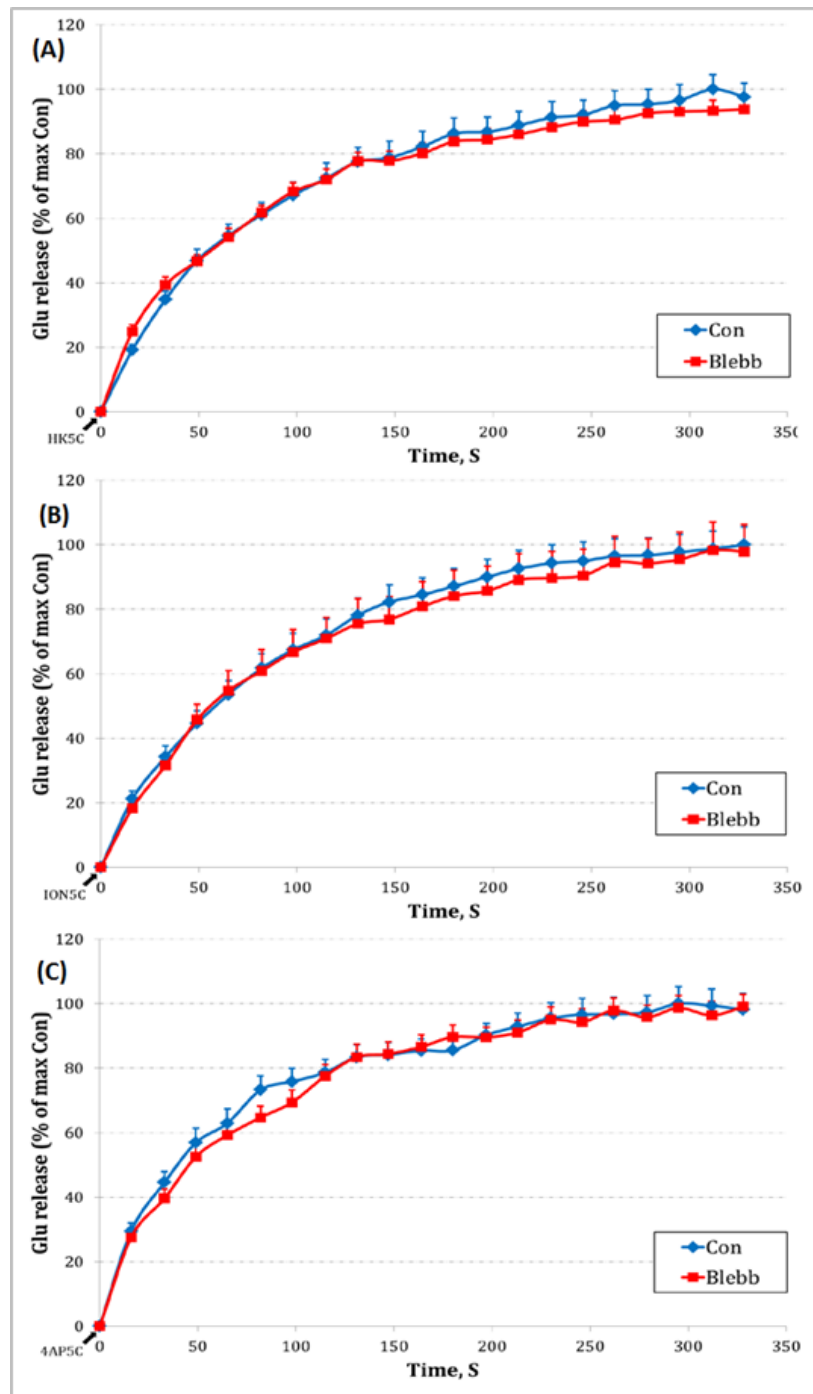


Figure A8: Effect of 50 μ M Blebbistatin upon Evoked GLU Release

Treatment with 50 μ M Blebbistatin did not significantly affect GLU release when stimulated with HK5C (A), ION5C (B) or 4AP5C (C) ($p > 0.05$). Values represented are the mean plus S.E.M. from 4 independent experiments.

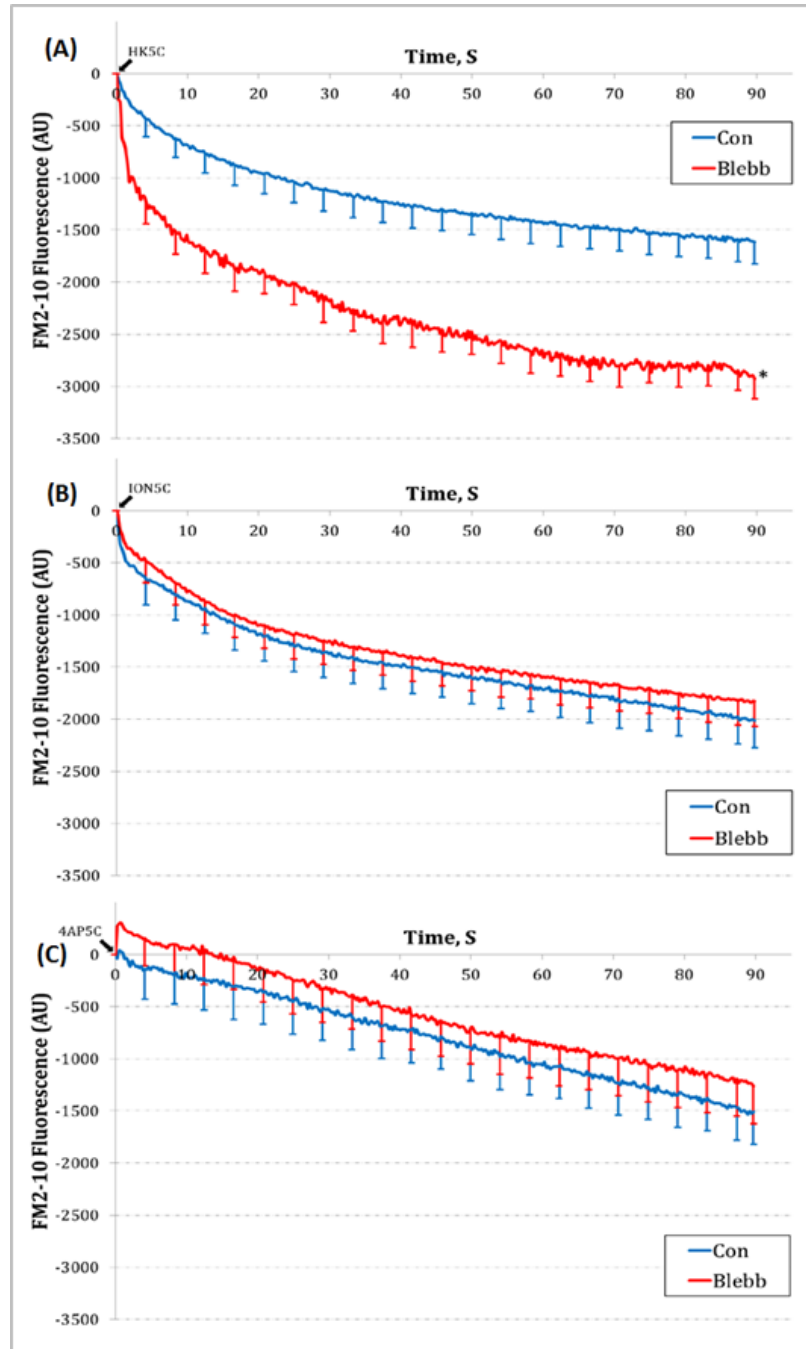


Figure A9: Effect of 50 μ M Blebbistatin upon Evoked FM 2-10 Dye Release

Treatment with 50 μ M Blebbistatin significantly increased FM 2-10 dye release when stimulated with HK5C (A) ($p < 0.05$), but had no effect when stimulated with ION5C (B) ($p = 0.716$) or 4AP5C (C) ($p = 0.642$). Values represented are the mean plus S.E.M. from 3 independent experiments.

The Ca^{2+} -dependent phosphatase calcineurin may also have a role in regulating proteins which participate in exocytosis, as calcineurin rapidly dephosphorylates many presynaptic proteins upon terminal depolarisation (Robinson *et al*, 1994). Inhibition of calcineurin with 1 μM Cyclosporine A (Cys A) did not significantly affect GLU release (Fig A10 A-C) ($p>0.05$), but significantly decreased FM 2-10 dye release when stimulated with HK5C and ION5C (Fig A10 D-E, respectively) ($p<0.05$). This differs with some studies that have shown Cys A treatment increases GLU release (Gaydukov *et al*, 2013), but in the context of this model this further indicates maximal GLU release is being observed under these conditions already (i.e. with 5 mM $[\text{Ca}^{2+}]_e$ Fig A1). When the effects of calcineurin inhibition with 1 μM Cys A were investigated upon $[\text{Ca}^{2+}]_i$ levels, a significant increase was noted with all three stimuli (Fig A10 G-I) ($p<0.05$). These data are interpreted as the inhibition of calcineurin causing more SVs to release via a KR mode of exocytosis, which could be due to the increased $[\text{Ca}^{2+}]_i$ level attained during Cys A treatment (Fig A10 G-I). The lack of effect upon 4AP5C evoked GLU and FM 2-10 dye, even during an increase in $[\text{Ca}^{2+}]_i$ could suggest calcineurin inhibition only affects the RP, since 4AP5C does not release the RP (Fig A1 C, and Fig A2), and the RRP is already releasing via KR with both HK5C and ION5C stimuli (Fig A5 A).

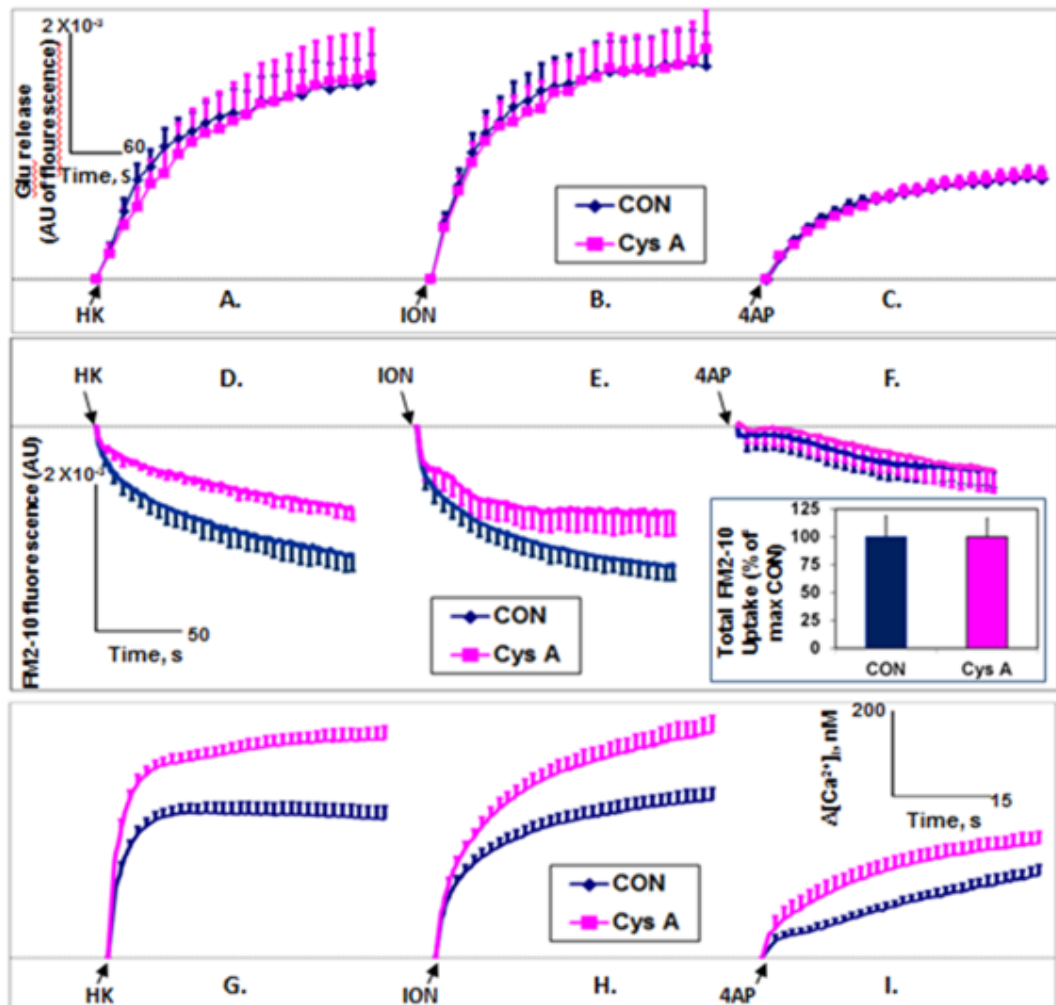


Figure A10: Effect of 1 μM Cys A upon Evoked GLU and FM 2-10 Dye Release

1 μM Cys A did not perturb Glu release evoked by HK5C (A), ION5C (B) or 4AP5C (C) ($p > 0.05$ for all). 1 μM Cys A significantly decreased HK5C (D) ($p < 0.025$) and ION5C (E) ($p < 0.023$) evoked FM 2-10 dye release, but had no effect upon 4AP5C (F) ($p = 0.985$) evoked FM 2-10 dye release. 1 μM Cys A significantly increased $[\text{Ca}^{2+}]_i$ levels with HK5C (G) ($p < 0.001$), ION5C (H) ($p < 0.044$) and 4AP5C (I) ($p < 0.049$) stimulation, compared to controls. Values represented are the mean plus S.E.M. from 4 experiments. Figure taken from a manuscript prepared by A. Ashton.

A.1.1.5.1 Switching of HK5C evoked SV exocytosis from NM-II dependent KR to Dyn dependent KR

Ashton and colleagues have deciphered that HK5C activates PKCs that inactivate Dyn 1 but that activate NM-II. Thus, one can make HK5C action switch from the NM-II pathway to the Dyn dependent pathway by inhibiting PKCs with Go 6983. Neither pre-treatment with Go 6983 followed by the addition of Blebbistatin (Fig A11A) or Dynasore (Fig A11B) perturbed the HK5C evoked GLU release indicating that these conditions did not perturb SV from exocytosing and releasing their NT.

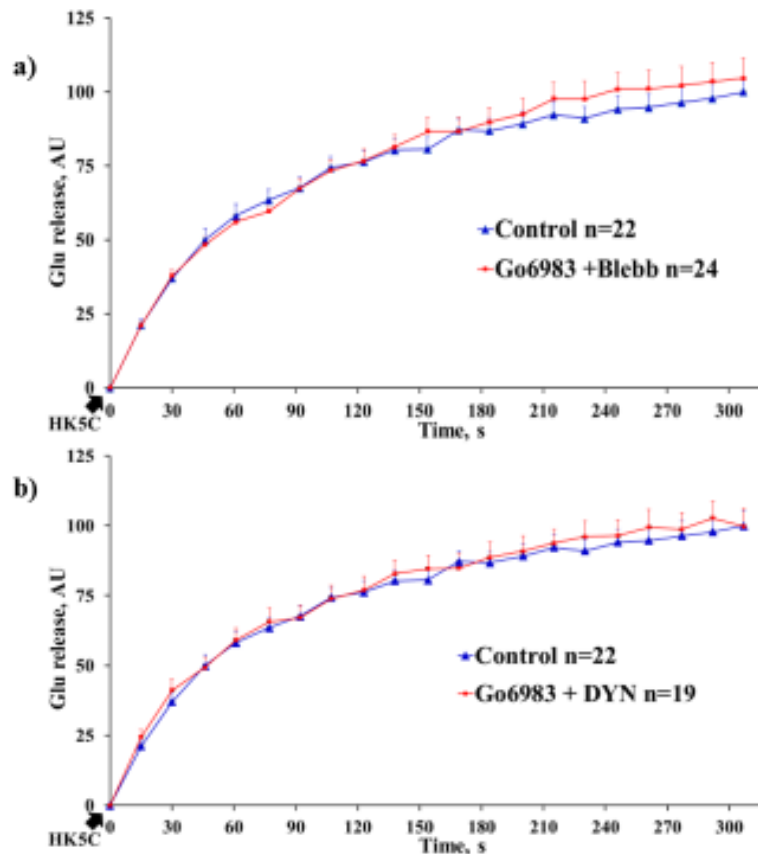


Figure A11. HK5C evoked GLU release in a) non-drug treated control or Go 6983 plus Blebbistatin treatment b) non-drug treated control or Go 6983 plus Dynasore treatment.

The experiment was done N=4 independent times. There is no significant difference between the control and the drug treated samples.

However, following pre-treatment with Go 6983, Blebbistatin no longer switched the HK5C evoked RRP SVs to a FF mode as there was not an increase in FM dye release compared to the control (Fig A12 A). Remarkably, such Go 6983 treatment now allowed Dynasore to act on the HK5C evoked RRP SVs and these did switch to a FF mode (Fig A12 B).

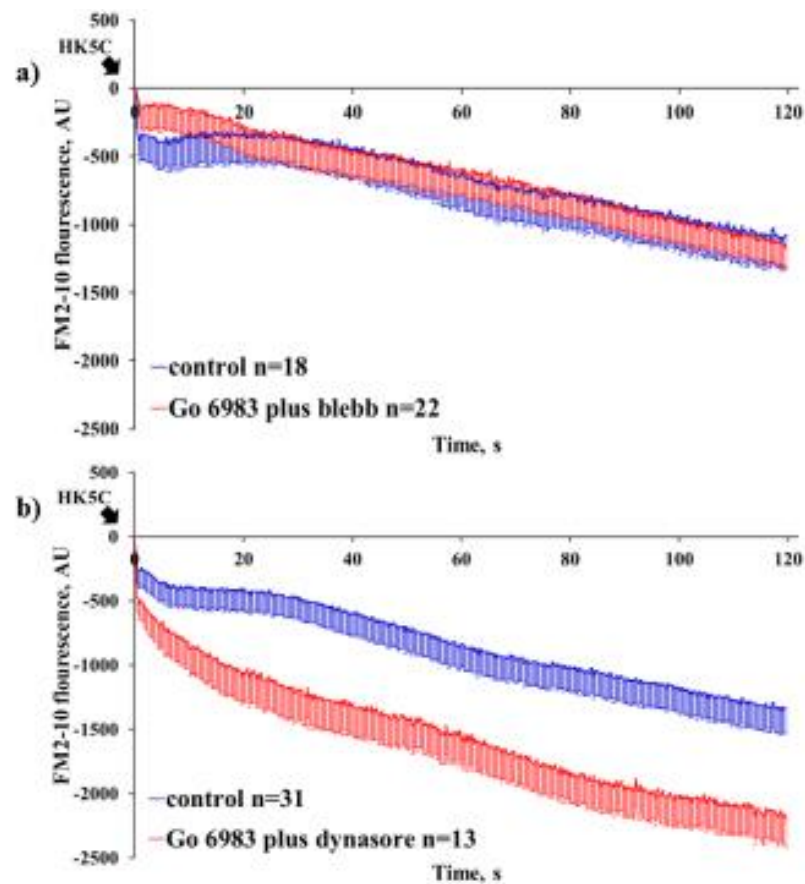


Figure A12. HK5C evoked FM2-10 dye release in a) non-drug treated control or Go 6983 plus Blebbistatin treatment b) non-drug treated control or Go 6983 plus dynasore treatment. The experiment was done N=3 independent times. There is no significant difference between the control and Go 6983 plus Blebbistatin but there is a significant difference between control and Go 6983 plus Dynasore.

A.1.1.5.2 Switching of ION5C evoked SV exocytosis from dynamin dependent KR to NM-II dependent KR

Not only can one switch the HK5C stimulus to act on the Dyn dependent KR but one can also switched the ION5C stimulus to act through the NM-II dependent pathways. This is achieved by using a low concentration of 40 nM PMA (an active phorbol esters) that can activate certain PKCs within the synaptosomes. Note that this concentration does not switch the RRP SV KR mode to FF alone although a higher concentration (1 μ M PMA) does. However, neither 40 nM PMA plus Blebbistatin (Fig A13 A) treatment nor 40 nM plus Dynasore (Fig A 13B) treatment perturbs the ION5C evoked GLU release. This indicates that the RRP and RP SVs are still undergoing exocytoses and releasing their transmitter content.

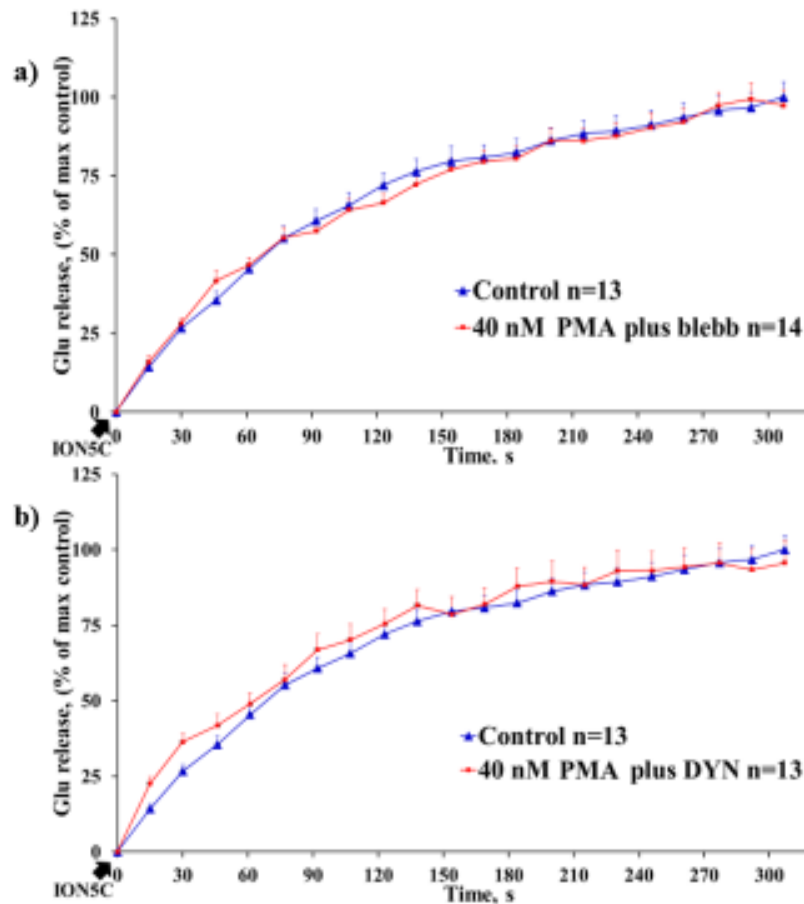


Figure A13: ION5C evoked GLU release in a) non-drug treated control or Go 6983 plus Blebbistatin treatment b) non-drug treated control or Go 6983 plus Dynasore treatment.

The experiment was done N=3 independent times. There is no significant difference between the control and the drug treated samples.

However, following pre-treatment with 40 nM PMA, Blebbistatin was able to switch the ION5C evoked RRP SVs to a FF mode as there was now an increase in FM dye release compared to the control (Fig A14 A). Remarkably, such 40 nM PMA treatment now prevented Dynasore acting on the ION5C evoked RRP SVs and these remained undergoing a KR mode such that there was no extra FM dye release (Fig A14 B).

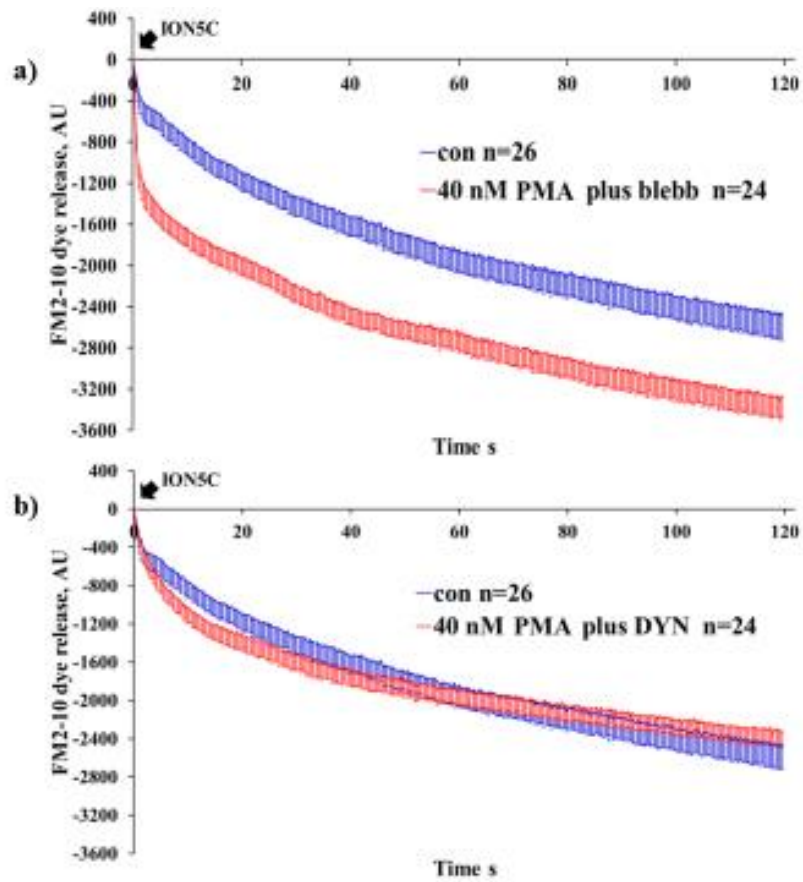
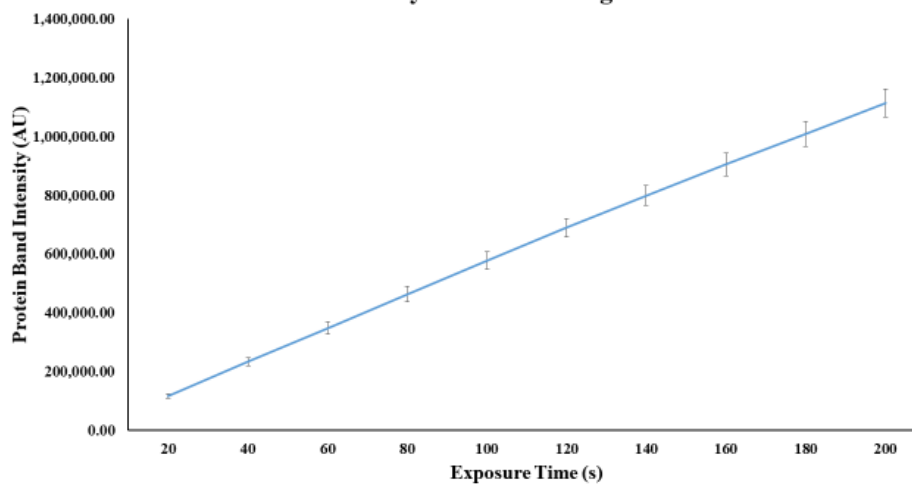


Figure A14: ION5C evoked FM2-10 dye release in a) non-drug treated control or 40 nM PMA plus Blebbistatin treatment b) non-drug treated control or 40 nM plus Dynasore treatment.

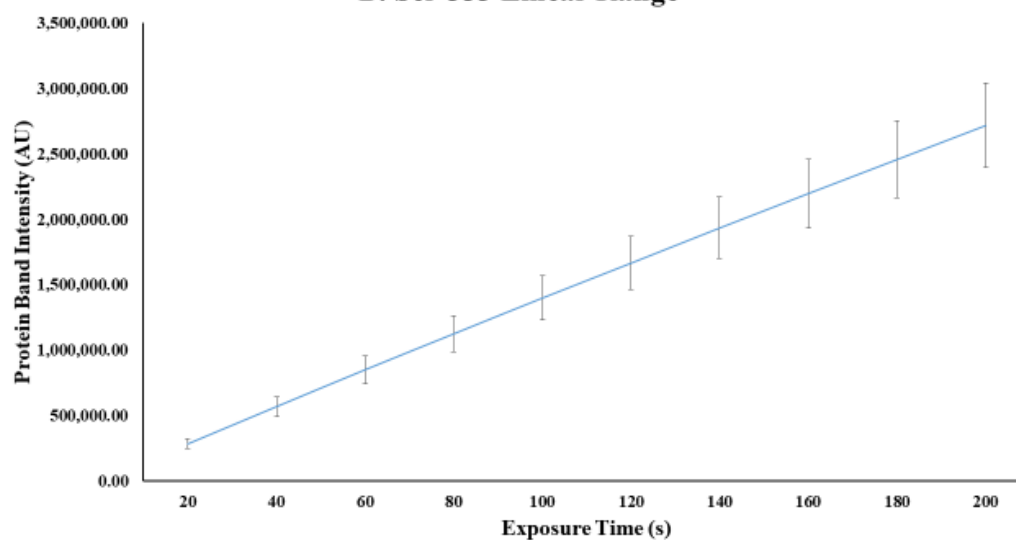
The experiment was done N=4 independent times. There is a significant difference between the control and Go 6983 plus Blebbistatin but there is no significant difference between control and Go 6983 plus Dynasore.

Appendix 2

A. Pan-Syn-I Linear Range



B. Ser-553 Linear Range



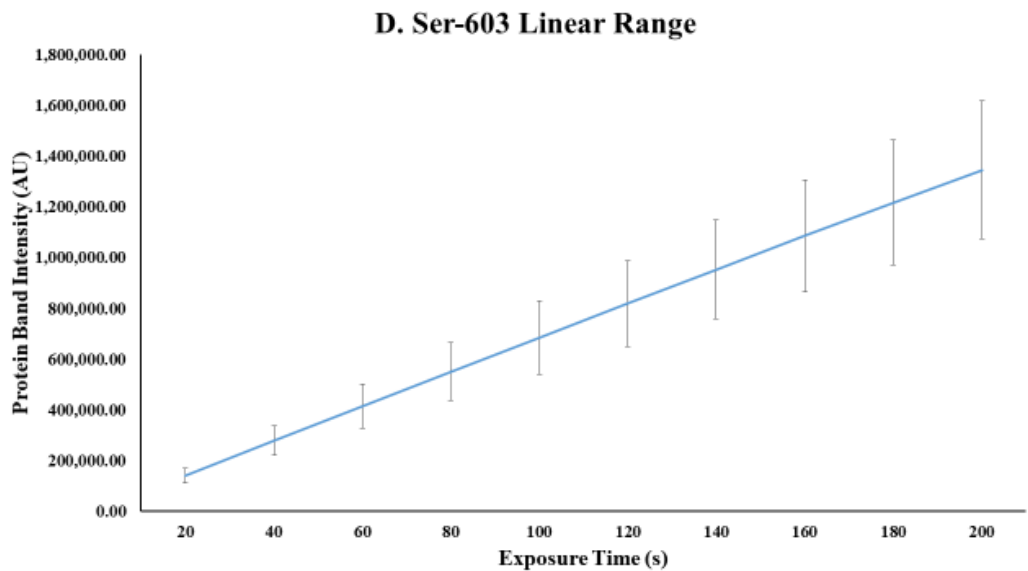
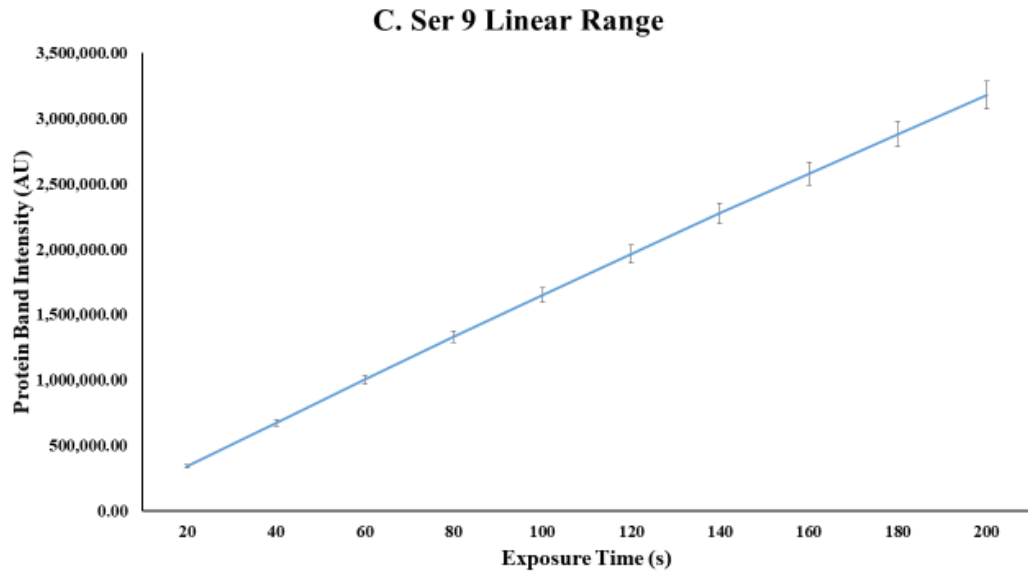


Fig A15. Detection of total Syn I (A), phospho-Ser553 in Syn I (B), phospho-Ser-9 in Syn 1 (C), or phospho-Ser-603 in Syn I (D) using specific antibodies. These bound antibodies were detected using a specific secondary antibody conjugated to HRP. This enzyme reacts with chemiluminescence substrate and light is produced. Such western blots were exposed for different exposure times and the intensity of the detected band determined. These graphs enable one to choose exposure times that are in the linear range of the detection system.

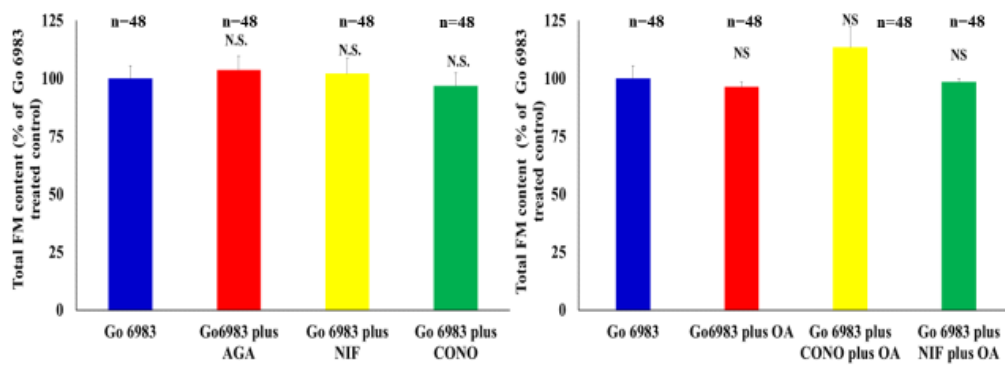
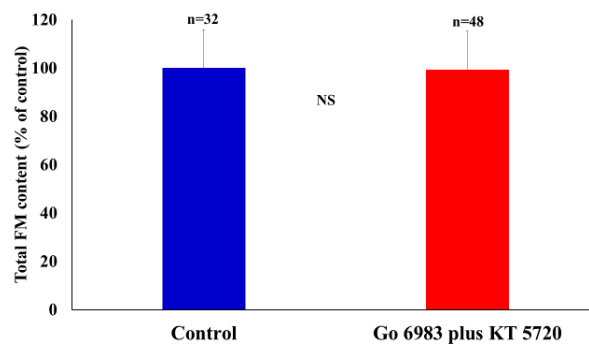
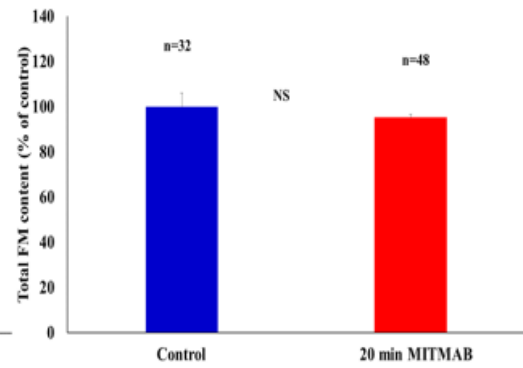
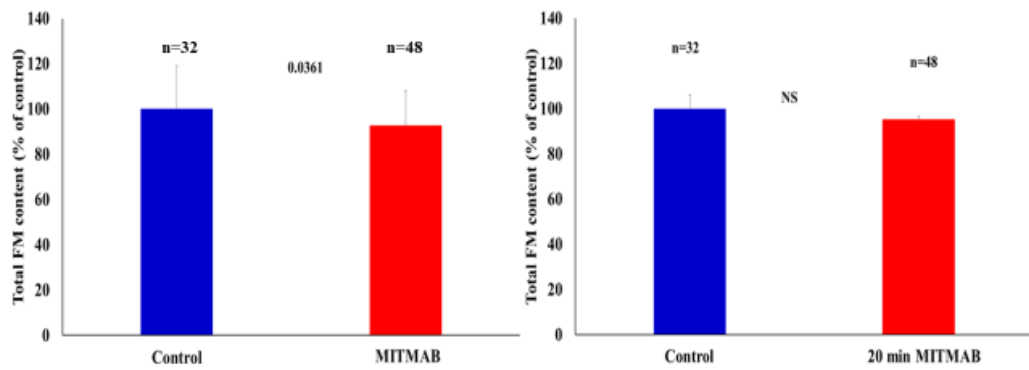
Appendix 3

Total FM2-10 Dye Content at the beginning of Measurements

In order for key interpretations drawn in this thesis to be accurate, it is important to ascertain if any of the drug treatment employed perturbs the amount of FM 2-10 dye being loaded into the nerve terminals. Without this information, comparisons between the FM 2-10 dye release and GLU assays would lead to incorrect assumptions. The fluorescence of the FM 2-10 dye was measured prior to stimulation (time 0) and compared with the control utilised in each assay. MITMAB incubated for 5 min had minor significant difference but this was unlikely to have affected the result. All the other drugs employed herein have had no significant (N.S) impact upon the total FM 2-10 dye uptake ($p > 0.05$).

Bar charts presented below represents the average nerve terminal fluorescence before stimulation began, error bars are plus S.E.M.

Appendix 3 (Continued)



Appendix 3 (Continued)

